AN EVOLUTIONARILY CONSERVED REGULATORY MECHANISM FOR ENDOSOMAL MEMBRANE TRAFFICKING

A thesis submitted to the
FACULTY OF BIOMEDICAL AND LIFE SCIENCES

For the degree of
DOCTOR OF PHILOSOPHY

by
Marion Symington Struthers

Division of Molecular and Cellular Biology
Faculty of Biomedical and Life Sciences
University of Glasgow

September 2009

Abstract

Membrane fusion in all eukaryotic cells is facilitated by the formation of SNARE (soluble N-ethylmaleimide-sensitive factor attachment protein receptor) complexes; a process that is regulated by Sec1p/Munc18 (SM) proteins. Membrane fusion has been conserved through evolution and hence a lot or our knowledge about the molecular mechanism that regulates membrane traffic has come from experimentally tractable model organisms such as *Saccharomyces cerevisiae*. The work presented in this thesis demonstrates that the mammalian SNARE protein, syntaxin 16 (Sx16), is a functional homologue of the yeast SNARE protein, Tlg2p, as expression of Sx16 in *tlg2Δ* cells, fully complements trafficking defects displayed by these cells. This finding is supported by experiments demonstrating that Sx16 interacts both physically and functionally with the SM protein of Tlg2p, Vps45p, both *in vivo* and *in vitro*. Vps45p regulates Sx16 in a manner similar to the way that it regulates Tlg2p; controlling entry into functional SNARE complexes and regulating cellular levels. A model, in which Vps45p is required for regulating membrane fusion and regulating the cellular levels of Tlg2p, is also presented and discussed in this thesis.

Table of Contents

Abbreviations……..11

Chapter 1 – Introduction.....14
1.1 Type 2 Diabetes.....15
1.1.1 Insulin signaling.....15
1.1.2 GLUT4.....16
1.1.3 A model for GLUT4 trafficking.....17
1.2 Trafficking and Transport in Eukaryotic cells.....18
1.2.1 SNARE proteins.....18
1.2.2 The SNARE hypothesis.....19
1.2.3 Syntaxins.....20
1.2.4 Syntaxin 16 (Sx16).....22
1.2.5 Sx16 has been implicated in the trafficking of GLUT4.....25
1.2.6 Trafficking in yeast and mammalian cells.....29
1.2.7 Identification and characterisation of the yeast t-SNARE, Tlg2p.....29
1.3 Overview of Membrane Fusion.....31
1.3.1 SM Proteins.....32
1.3.2 SM proteins regulate membrane fusion.....33
1.3.3 CPY trafficking and the identification of VPS genes.....38
1.3.4 Identification and characterisation of the SM protein, Vps45p.....40
1.3.5 Characterisation of the interaction between Vps45p and Tlg2p.....41
1.4 Cellular levels of syntaxins are regulated by their cognate SM protein.....43
1.4.1 Post-translational modifications of Tlg2p?.....44
1.5 Aims.....47

Chapter 2 – Materials and Methods.....49
2.1 Materials.....50
2.1.1 Reagents and Enzymes.....50
2.1.2 Bacterial and Yeast Strains.....50
2.1.3 Media.....50
2.1.4 Antibodies.....51
2.2 Methods.....52
2.2.1 Isolation of yeast chromosomal DNA.....52
2.2.2 Purification of plasmid DNA from bacteria.....53
2.2.3 Molecular Cloning.....53
2.2.4 TA cloning.....55
2.2.5 Plasmid Construction.....56
2.2.6 DNA sequencing.....60
2.2.7 Transformation of E. coli and S. cerevisiae.....60
2.2.8 Rescue of plasmid DNA from S. cerevisiae.....61
2.2.9 Electrophoretic separation of proteins.....61
2.2.10 Immunoblot Analysis.....62
2.2.11 Antibody purification.....63
2.2.12 Preparation of yeast whole cell lysates for immunoblot analysis.....64
2.2.13 Testing copper toxicity and osmotic sensitivity.....64
2.2.14 Trichloroacetic Acid (TCA) precipitation of secreted proteins.....65
2.2.15 Ste3p receptor endocytosis assay.....65
2.2.16 FM4-64 and Vacuolar labelling.....66
2.2.17 Immunofluorescence.....66

2.2.18 Immunoprecipitation from yeast cell lysates 67
2.2.19 Pulse-Chase Experiments.....68
2.2.20 Recombinant Protein Expression and Purification 69
2.2.21 Pull-down assays.....71
2.2.22 Functional assay for degradation of Tlg2p 72
2.2.23 Hydroxylamine Treatment 72
2.2.24 Bradford protein assay 73

Chapter 3 – Sx16 is a functional homologue of the yeast t-SNARE, Tlg2p 79
3.1 Introduction.....80
3.2 Heterologous expression of mammalian syntaxins, 16 and 4 in yeast.....81
3.3 Comparison of the expression of HA-tagged Tlg2p and endogenous Tlg2p.....87
3.4 Copper toxicity.....92
3.5 Functional analysis.....93
3.5.1 Osmotic sensitivity.....93
3.5.2 Trafficking of intracellular proteins – CPY 94
3.5.3 Ste3p receptor endocytosis.....96
3.5.4 FM4-64, vacuolar labelling.....98
3.5.5 Immunofluorescence analysis of syntaxin localisation.....100
3.6 Discussion 102

Chapter 4 – Sx16 is regulated by Vps45p when expressed in yeast 103
4.1 Introduction.....104
4.2 Sx16 and Tlg2p share the same mode of interaction with the SM protein, Vps45p 104
4.2.1 Yeast Vps45p binds Sx16 via Mode 2 binding.....104
4.2.2 Vps45p binds Sx16-containing cis-SNARE complexes in yeast.....107
4.3 Levels of Tlg2p and Sx16 are greatly reduced in yeast cells lacking Vps45p...109
4.3.1 Levels of Tlg2p are greatly reduced in yeast cells lacking Vps45p.....109
4.3.2 Levels of Sx16 are also greatly reduced in yeast cells lacking Vps45p.....110
4.4 A truncated version of Tlg2p/Sx16 can bypass the requirement for Vps45p 111
4.5 Discussion 113

Chapter 5 – Regulation of Tlg2p levels in the cell.....118
5.1 Introduction.....119
5.2 Steady-state levels of Tlg2p are mediated by the vacuole 119
5.3 Tlg2p is ubiquitinated in wild-type and *vps45Δ* cells 127
5.4 Mapping the ubiquitination sites of Tlg2p.....133
5.5 Cellular levels of Tlg2p are regulated by Mode 2 binding 142
5.6 Other factors that may be involved in regulating levels of Tlg2p in the cell.....145
5.6.1 Palmitoylation of Tlg2p 145
5.7 Discussion 148

Chapter 6 - Final Discussion 152
6.1 Sx16 is a functional homologue of the yeast t-SNARE, Tlg2p 153
6.2 Sx16 is regulated by the Tlg2p-binding SM protein, Vps45p 154
6.3 Regulation of Tlg2p levels in the cell 158
6.4 Future Work 161

Bibliography 163

Publications.....177

List of Tables

Table 2.1 - *E. coli* and *S. cerevisiae* strains used in this study.....74

Table 2.2 - Oligonucleotides used in this study.....75

Table 2.3 - Plasmids used in this study.....77

List of Figures

Chapter 1

Figure 1.1 – A model for insulin-stimulated GLUT4 trafficking. 18

Figure 1.2 – Schematic and graphical diagrams of Sx1a.....21

Figure 1.3 – A representative diagram displaying the two different conformations adopted by Sx1a.....22

Figure 1.4 – Conservation of vesicle targeting and fusion machinery from yeast to man...29

Figure 1.5 – A diagrammatic representation of the steps involved in membrane fusion.....32

Figure 1.6 – A ribbon representation of the Munc18a-Sx1a interaction; Mode 1 binding..34

Figure 1.7 – A graphical representation of the Sly1p-Sed5p interaction; Mode 2 binding. 36

Figure 1.8 – Two different interpretations of how Sec1p may interact with the SNARE complex.....37

Figure 1.9 – Sequence alignments of the first 33 amino acids of Pep12p, Tlg2p and Sx16. 41

Chapter 3

Figure 3.1 – Schematic diagram of the homologous recombination strategy used to create pMAZ002, pMAZ006, pMAZ007. 82

Figure 3.2 – Flow chart showing an overview of homologous recombination and the steps that follow 83

Figure 3.3 – Sx16 oligonucleotide primer sequences 84

Figure 3.4 – Screening co-transformed yeast for Sx16 expression.....84

Figure 3.5 – SDM oligonucleotide primer sequences used to introduce the HA-tag to Sx16. 85

Figure 3.6 - Screening yeast for HA-Sx16 expression.....86

Figure 3.7 – HA-Sx4 oligonucleotide primer sequences 86

Figure 3.8 – Screening of co-transformed yeast for HA-Sx4 expression. 87

Figure 3.9 – HA-*TLG2* oligonucleotide primer sequences 88

Figure 3.10 - Screening of co-transformed yeast for HA-Tlg2p expression.....88

Figure 3.11 - Copper titration to assess optional copper concentrations for syntaxin expression.....89

Figure 3.12 – A comparison of endogenous Tlg2p expression to that of HA-Tlg2p expression controlled by the yeast promoters *CUP1* and *ADH1*. 91

Figure 3.13 - Expression of HA-Tlg2p, HA-Sx16, HA-Sx4 in *tlg2*Δ cells. 92

Figure 3.14 – Testing for copper sensitivity 93

Figure 3.15 – Expression of human Sx16 complements the osmotic sensitivity phenotype of *tlg2Δ* mutant cells. 94

Figure 3.16 – Expression of human Sx16 complements the CPY trafficking defects of *tlg2*Δ mutant cells.....95

Figure 3.17 - Expression of Sx16 overcomes the block in Ste3p endocytosis observed in *tlg2*Δ cells.....98

Figure 3.18– Expression of Sx16 promotes efficient FM4-64, vacuolar labelling in *tlg2Δ* cells. 99

Figure 3.19– Sx16 co-localises with both endogenous Tlg2p and HA-Tlg2p.....101

Chapter 4

Figure 4.1 – Monomeric Sx16 and Tlg2p both interact with yeast Vps45p via Mode 2 binding. 106

Figure 4.2 – Sx16 and Tlg2p both interact with yeast Vps45p when present in the *cis*-SNARE complexes. 108

Figure 4.3 – Both the t-SNARE, Tlg2p and the v-SNARE, Snc2p are greatly reduced in *vps45Δ* cells.....110

Figure 4.4 – Sx16 and Tlg2p are both degraded in *vps45Δ* cells.....111

Figure 4.5 - A schematic diagram of full-length and truncated versions of syntaxins, Tlg2p (HA-Tlg2pΔHabc) and Sx16 (HA-Sx16ΔHabc). 112

Figure 4.6 – Expression of either truncated HA-Tlg2p or HA-Sx16 lacking the Habc domain results in the maturation of CPY in *vps45Δ* cells.....113

Figure 4.7 – Data taken from (Struthers et al., 2009) showing that SNARE-complex assembly is stimulated by both the deletion of the Habc domain from Tlg2p and also by Vps45p. 116

Chapter 5

Figure 5.1 – Cellular levels of Tlg2p are elevated in cells lacking vacuolar activity. 120

Figure 5.2 – Levels of HA-Tlg2p (expressed from pMAZ006) are elevated in wild-type cells lacking active vacuolar proteases. 121

Figure 5.3 – A comparison of steady-state levels of HA-Tlg2p in wild-type (WT) and *vps45Δ* cells containing active vacuolar proteases.....123

Figure 5.4 – A schematic diagram showing the proposed topology of Tlg2p. 124

Figure 5.5 - N- and C-terminally HA-tagged versions of Tlg2p display different patterns of degradation products in *vps45Δ* cells (containing active vacuolar proteases). 125

Figure 5.6 – A schematic diagram of full-length HA-tagged Tlg2p (HA-Tlg2p) and truncated HA-tagged Tlg2p (HA-Tlg2p(1-336)). 126

Figure 5.7 – Removal of the lumenal domain from Tlg2p does not increase the steady-state levels of Tlg2p, nor does it prevent the *PEP4*-dependent degradation of Tlg2p. 127

Figure 5.8 – SDS-PAGE quantification of the purified GST-fusion proteins 129

Figure 5.9 – No ubiquitinated Tlg2p is detected in wild-type or *vps45Δ* cells. 131

Figure 5.10 – HA-tagged Tlg2p is ubiquitinated in wild-type and *vps45Δ* cells. 132

Figure 5.11 – Tlg2p expressed from pMAZ001 is fully degraded in *vps45Δ* cells. 134

Figure 5.12 – Schematic diagram of the strategy used to develop a functional assay to monitor the degradation of Tlg2p in cells lacking endogenous Vps45p.....135

Figure 5.13 – Schematic diagram of the fusion protein encoded by pMAZ017.....136

Figure 5.14 – Expression of the Tlg2p-His3p fusion protein 137

Figure 5.15 – A Tlg2p-His3p fusion protein supports growth of 'wild-type' and *tlg2*Δ but not *vps45*Δ histidine auxotrophic cells on media lacking histidine. 138

Figure 5.16 – Sequence alignment of Sx16 and Tlg2p 140

Figure 5.17 – Analysis of lysine residues in Tlg2p.....141

Figure 5.18 - *vps45Δ* cells expressing $Vps45_{L117R}$ contain ~15% of Tlg2p that is found in wild-type cells. 143

Figure 5.19– Schematic diagram of the truncated fusion protein encoded by pMAZ029. 144

Figure 5.20 – Expression of the N-terminal peptide of Tlg2p (1-33aa) fused to full-length His3p allows the growth of *vps45Δ* histidine auxotrophic cells on media lacking histidine. 144

Figure 5.21 – Levels of HA-Tlg2p are reduced in wild-type and *vps45Δ* lysates treated with the compound, hydroxylamine.....146

Figure 5.22 - Levels of HA-Tlg2p are reduced in wild-type and *vps45Δ* lysates treated with the compound, hydroxylamine.....147

Acknowledgements

Firstly, I would like to thank my supervisor Dr. Nia J. Bryant for all the support, advice and encouragement that she has given me throughout my PhD.

I would also like to thank everyone in Lab 241, past and present, for their support. In particular I would like to thank my dear friends Becky, Veronica and Fiona.

I must also say a special thanks to Scott Shanks, who has greatly contributed to the work presented in this thesis and also a thank you must go to the other members of the Bryant lab for all their fun and support.

Finally, a heart-felt thanks must go to the members of my family, Mum (aka Wilma), Dad (aka Robert), Lizzie and Dougie and also my partner, Ross, who have all been a great support to me throughout my PhD.

Declaration

I declare that the work presented in this thesis has been carried out by me, unless otherwise stated. It is entirely of my own composition and has not, in whole, or in part been submitted for any other degree.

Marion S. Struthers

September 2009

Abbreviations

~	approximately
2µ	2 micron
aa	amino acid
ATP	adenosine triphosphate
APS	adaptor molecule containing PH and SH2 domains
AS160	Akt substrate of 160 kDa
bp	basepair
BFA	brefeldin A
BHK-21	baby hamster kidney-21
β-me	β-mercaptoethanol
BSA	bovine serum albumin
c-Cbl	casitas b-lineage lymphoma
CAP	c-Cbl associated protein
cat #	catalogue number
CBZ-pheleu	*N*-acetyl-DL-phenylalanine β-naphthyl ester
cDNA	complementary deoxyribonucleic acid
C. elegans	*Caenorhabditis elegans*
CEN	centromeric
CORVET	class C core vacuole/endosome tethering
COS	cells being CV-1 (simian) in origin carrying the SV40 genetic material
CPY	carboxypeptidase Y
$CuCl_2$	copper chloride
cyto	cytosolic
deGlc	2-Deoxy-D-glucose
dH_20	distilled water
DIC	differential interference contrast
DNA	deoxyribonucleic acid
dNTP	deoxyribonucleotide phosphate
D. melanogaster	*Drosophila melanogaster*
DMF	dimethylformamide
DTT	dethiothreitol
E1	ubiquitin activating enzyme
E2	ubiquitin conjugating enzyme
E3	ubiquitin ligase
E. coli	*Escheria coli*
ECL	enhanced chemiluminescence
EDTA	ethylenediaminetetraacetic acid
EDTA-Na	ethylenediaminetetraacetic acid disodium salt
ER	endoplasmic reticulum
ERAD	ER-associated degradation
EST	expressed sequence tag
FM4-64	N-(3-triethylammoniumpropyl)-4-(p-diethylaminophenyl-hexatrienyl) pyridium dibromide
g	gram
g	gravitational force
Gap1p	general amino acid permease
GFP	green fluorescent protein
GLUT4	glucose transporter 4
GS28	Golgi SNARE protein of 28 kDa

GST	glutathione S-tranferase
GSV	GLUT4 storage vesicle
HeLa	Henrietta lacking
HA	hemagglutinin
HAc	acetic acid
HCl	hydrochloric acid
HECT	homologous to the E6-AP carboxy terminus
HEPES	2-[4-(2-Hydroxyethyl)-1-piperazine]ethanesulfonic acid
HOPS	homotypic fusion and protein sorting
HRP	horseradish peroxidise
IgG	immunoglobin G
IRAP	insulin-responsive aminopeptidase
IRS	insulin receptor substrate
IPTG	isopropyl-β-galactosidopyranoside
K_2HPO_4	dipotassium hydrogen orthophosphate
kb	kilobase
k_BT	thermal energy (Boltzmann's constant x temperature)
KCl	potassium chloride
KH_2PO_4	potassium dihydroden orthophosphate
KOAc	potassium acetate
KOH	potassium hydroxide
L	litre
LCA	*lens culinaris agglutinin*
LSB	Laemmli sample buffer
µ	micro
µl	microlitre
µg	microgram
µM	micromolar
M	molar
mA	milliamp
mg	milligram
$MgCl_2$	magnesium chloride
$MgSO_4$	magnesium sulphate
min	minute
ml	millilitre
mM	millimolar
MVB	multivesicular body
mRNA	messenger RNA
n	nano
NaCl	sodium chloride
NaN_3	sodium azide
Na_2HPO_4	disodium hydrogen orthophosphate
NEM	N-ethylmaleimide
nm	nanometre
NMR	nuclear magnetic resonance
NSF	N-ethylmaleimide-sensitive factor
OD_{600}	optical density at 600 nm
ORF	open reading frame
PBS	phosphate buffered saline
PBS/T	0.1% Tween-20 in PBS
PCR	polymerase chain reaction
PDK1	phosphatidylinositol-dependent kinase 1
PFA	paraformaldehyde

PI3K	phosphatidylinositol 3-kinase
PIP_2	phosphatidylinositol-4,5-bisphosphate
PIP_3	phosphatidylinositol-3,4,5-trisphosphate
PI(3)P	phosphatidylinositol 3-phosphate
PIPES	1,4-Piperazinediethanesulfonic acid
PIKfyve	phosphoinositide kinase FYVE finger containing
PKB	protein kinase B
PKC	protein kinase C
PMSF	phenylmethylsulphonyl fluoride
PrA	protein A
PVC	prevacuolar compartment
RabGAP	Rab GTPase activating protein
RNA	ribonucleic acid
RING	really interesting gene
RS-ALP	retention sequence-alkaline phosphatase
S. cerevisiae	*Saccharomyces cerevisiae*
sec	second
SDM	site-directed mutagenesis
SDS	sodium dodecyl sulphate
SDS-PAGE	sodium dodecyl sulphate polyacrylamide gel electrophoresis
SH2	Src homology-2
SM	Sec1p/Munc18
SNAP	soluble NSF attachment protein
SNARE	soluble NSF attachment protein receptor
Sx	syntaxin
$t_{½}$	half-life
TAE	Tris-Acetic acid-EDTA
TBS	tris-buffered saline
TBS/T	0.1% in TBS
TCA	trichloroacetic acid
TE	Tris-EDTA
TEMED	N,N,N’,N’, - tetramethyl ethylene diamine
Tf	transferrin
TGN	*trans*-Golgi network
Tlg2p	t-SNARE of the late Golgi compartment 2
TM	transmembrane
Tm	melting temperature
Tris	2-Amino-2-(hydroxmethyl)-1,3-propanediol
t-SNARE	target SNARE
TST	tris-saline-tween
Ub	ubiquitin
UBA	ubiquitin associated
Ubl	ubiquitin-like
UTR	untranslated region
VAMP-2	vesicle associated membrane protein-2
v-SNARE	vesicle SNARE
VPS	vacuolar sorting protein
v/v	volume per volume
WHO	world health organisation
w/v	weight per volume
YPD	yeast peptone dextrose

Chapter 1 – Introduction

1.1 Type 2 Diabetes

Diabetes mellitus is characterised by hyperglycemia (high blood sugar) and is a result of defects in insulin secretion, action or both (Saltiel and Kahn, 2001, Zimmet et al., 2001). There are two main types of diabetes, Type 1 and Type 2 (Saltiel and Kahn, 2001, Zimmet et al., 2001). Type 1 is caused by the autoimmune destruction of the pancreatic β-cell islet, resulting in a block in insulin secretion (Saltiel and Kahn, 2001, Zimmet et al., 2001). Type 2 diabetes is characterised by insulin resistance caused by a deregulation of insulin action (Saltiel and Kahn, 2001, Zimmet et al., 2001).

Type 2 diabetes is by far the most prevalent type of diabetes, accounting for approximately 90-95% of those individuals suffering from diabetes (Zimmet et al., 2001). In 2008, the World Health Organisation (WHO) reported that more than 180 million people worldwide suffer from diabetes and have estimated that this number is likely to double by 2030.

1.1.1 Insulin signaling

Binding of insulin to its heterotetrameric receptor (α2β2) occurs via the extracellular alpha subunits of the receptor resulting in a conformational change which, in turn, activates the tyrosine-kinase domains present in the intracellular portion of the beta subunits of the receptor (reviewed in (Lee and Pilch, 1994)). This results in the activation of two signal transduction pathways, the phosphatidylinositol 3-kinase (PI3K) pathway and the casitas b-lineage lymphoma (c-Cbl) pathway, both of which result in the translocation of the glucose transporter 4 (GLUT4) receptor from its intracellular location to the plasma membrane, by a mechanism which is still unclear (Bryant et al., 2002, Leney and Tavare, 2009).

1.1.1.1 PI3K pathway

PI3K is recruited to the plasma membrane by tyrosine phosphorylation of the insulin receptor substrate (IRS 1/2) (Myers et al., 1993). PI3K phosphorylates phosphatitidylinositol-4,5-bisphosphate (PIP_2) to phosphatidylinositol-3,4,5-trisphosphate (PIP_3) (Tengholm and Meyer, 2002). This results in the recruitment of proteins containing the pleckstrin homology (PH) domain, in particular protein kinase B (PKB also known as Akt) and its upstream kinase phosphatidylinositol-dependent kinase 1 (PDK1) (Alessi et al., 1997, Stephens et al., 1998, Stokoe et al., 1997). It is thought that PKB/Akt may stimulate GLUT4 translocation through the Rab GTPase Activating protein (RabGAP)

domain of the Akt Substrate of 160 kDa (AS160) (Eguez et al., 2005, Larance et al., 2005, Sano et al., 2003) and/or through PIKfyve (phophoinositide kinase, FYVE finger containing) (Ikonomov et al., 2007, Ikonomov et al., 2002). Isoforms of protein kinase C (PKC), λ/ζ, have also been implicated in the translocation of GLUT4 to the plasma membrane however the mechanism of this is still unknown (Bandyopadhyay et al., 1997a, Bandyopadhyay et al., 1997b, Imamura et al., 2003, Liu et al., 2006, Lorenzo et al., 2002).

1.1.1.2 c-Cbl pathway

This pathway works independently of the PI3K pathway and involves the tyrosine phosphorylation of c-Cbl (Ribon and Saltiel, 1997). c-Cbl is recruited to the plasma membrane by two adaptor proteins; c-Cbl associated protein (CAP) and adaptor molecule containing PH and Src homology-2 (SH2) domains (APS) (Ribon et al., 1998). Tyrsoine-phosphorylated c-Cbl recruits CrkII, an adaptor protein, and C3G, a guanine exchange factor for the Rho-like GTPase TC10, into lipid rafts (Chiang et al., 2001, Gupte and Mora, 2006, Ribon et al., 1996, Ribon et al., 1998, Ribon and Saltiel, 1997). The activation of this pathway by insulin is thought to regulate the translocation of GLUT4 to the plasma membrane, possibly acting through several different processes such as cortical actin rearrangement (Kanzaki and Pessin, 2001), phosphatidylinositol 3-phosphate (PI(3)P) formation (Maffucci et al., 2003), recruitment of the exocyst complex to the plasma membrane (Inoue et al., 2003, Inoue et al., 2006) and/or the inactivation of the Rab protein, Rab31 (Lodhi et al., 2007).

1.1.2 GLUT4

In the 1950s it was first demonstrated that the hormone, insulin, stimulated the uptake of glucose into muscle and adipose tissue (Levine and Goldstein, 1958, Park and Johnson, 1955). However it was not until 1989 that the facilitative glucose transporter, GLUT4, was cloned and identified as the major isoform responsible for the uptake of glucose into these tissues in response to insulin (Birnbaum, 1989, Charron et al., 1989, Fukumoto et al., 1989, James et al., 1989, Kaestner et al., 1989). As discussed above, insulin stimulates the movement of GLUT4 from an intracellular membrane-bound pool to the plasma membrane (Bryant et al., 2002). This was demonstrated using subcellular fractionation (Deems et al., 1994, Marette et al., 1992, Pilch et al., 1993), electron and fluorescence microscopy (Voldstedlund et al., 1993), bis-mannose photolabelling of plasma membranes (Calderhead et al., 1990, Holman et al., 1990) and also epitope-tagged versions of GLUT4 (Bryant et

al., 2002, Czech et al., 1993, Dawson et al., 2001, Dobson et al., 1996, Kanai et al., 1993). At the surface of the cell, GLUT4 allows the transport of glucose out of the blood into the cell down a concentration gradient (Saltiel and Kahn, 2001). Glucose can then be stored as glycogen in the liver and skeletal muscle or as fat in adipose tissue (Saltiel and Kahn, 2001).

A substantial amount of work has been carried out to investigate the location of GLUT4 in the absence of insulin (under basal conditions) (reviewed in (Bryant et al., 2002, Leney and Tavare, 2009)). GLUT4 is associated with a variety of different intracellular compartments. These include the Golgi complex, *trans*-Golgi network (TGN), late endosomes and recycling endosomes (Ralston and Ploug, 1996), with the majority of GLUT4 found in a subset of vesicles known as the GLUT4 storage vesicles (GSVs), which are also enriched in insulin-responsive aminopeptidase (IRAP) and vesicle associated membrane protein-2 (VAMP-2) (Malide et al., 1997).

1.1.3 A model for GLUT4 trafficking

Understanding the intracellular trafficking of GLUT4 has proven difficult due to the fact that under basal conditions GLUT4 is localized to many different intracellular membrane-bound organelles (Bryant et al., 2002). A model that has been proposed to explain the multiple intracellular locations of GLUT4 suggests that GLUT4 exists in two interrelated endosomal pathways; a fast cycling pathway which functions to control trafficking between the plasma membrane and the early endosomes returning GLUT4 to an intracellular location in the absence of insulin and a slow cycling pathway which functions by trafficking GLUT4 from the recycling endosomes to the TGN and on to the GSVs (Bryant et al., 2002). According to this model, insulin binding to its receptor releases GLUT4 from these GSVs, by some unknown mechanism, which results in its trafficking to the plasma membrane (Bryant et al., 2002). It is unlikely that in the absence of insulin GLUT4 remains in a static pool of GSVs, as this would result in the depletion of GLUT4 from the other intracellular compartments in which it can be detected (Bryant et al., 2002). The GLUT4 trafficking model described here is summarised in the following diagram.

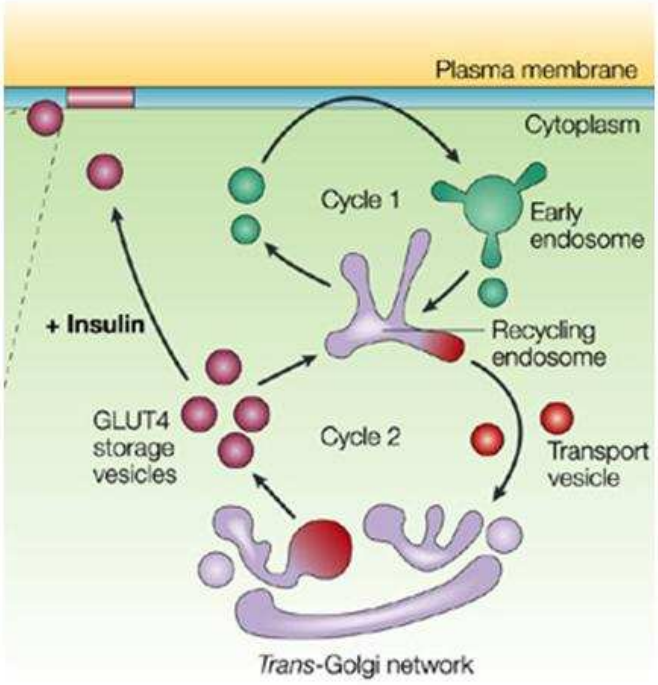

Figure 1.1 – A model for insulin-stimulated GLUT4 trafficking.
The fast and slow cycling pathways are labelled Cycle 1 and 2, respectively. This diagram is taken from (Bryant et al., 2002).

In order to understand how insulin alters the trafficking itinerary of GLUT4 to bring about its delivery to the cell surface, it is important to understand how membrane traffic is regulated in eukaryotic cells.

1.2 Trafficking and Transport in Eukaryotic cells

All eukaryotic cells are compartmentalised into numerous membrane-bound compartments or organelles. Exchange of materials between these organelles occurs by means of vesicular transport; a highly specific mechanism that ensures the correct delivery of molecules from one intracellular membrane bound compartment to another (Bonifacino and Glick, 2004, Palade, 1975). Efficient trafficking of molecules between organelles is essential, as the incorrect localisation of proteins could have disastrous, even fatal, consequences for the cell.

1.2.1 SNARE proteins

Soluble N-ethylmalemide (NEM) sensitive factor (NSF) attachment protein (SNAP) receptors (SNAREs) are a family of membrane proteins first identified in the neuronal

synapse by their ability to interact with NSF and its attachment protein α-SNAP during affinity purification (Sollner et al., 1993). Since then, a large number of SNARE proteins have been identified in yeast, plants and animals (Bennett, 1995, Linial, 1997, Rothman, 1994). These C-terminally anchored proteins play a critical role in membrane trafficking in all eukaryotic cells (Jahn and Sudhof, 1999). Members of the SNARE protein family share one feature in common, a weakly conserved 60-70 aa domain located in their C-terminal region, upstream of the transmembrane domain (Jahn and Sudhof, 1999). This motif known as the SNARE motif/domain is largely unstructured and is characterised by a heptad repeat of hydrophobic residues (Jahn and Sudhof, 1999). The association of four of these SNARE domains results in the formation of a highly structured and stable four helix bundle (Antonin et al., 2002, Poirier et al., 1998, Sutton et al., 1998) also known as the SNARE or core complex, formation of which is sufficient to catalyse the energetically unfavourable process of fusing two phosholipid bilayers (Jahn and Sudhof, 1999). Surface force measurements have demonstrated that the energy provided during the formation of a single SNARE complex is sufficient to catalyse hemifusion; the fusion of one leaflet of a lipid bilayer (Li et al., 2007). For complete lipid bilayer fusion (50-100k_BT) it is thought that 3 or more SNARE complexes (each providing 35k_BT of energy) are required (Cohen and Melikyan, 2004, Hua and Scheller, 2001, Li et al., 2007).

1.2.2 The SNARE hypothesis

In 1993, Rothman and colleagues proposed the SNARE hypothesis to explain the fidelity of membrane fusion (Sollner et al., 1993). That is, how the cell ensures that a transport vesicle docks and fuses only with the appropriate target membrane. According to the SNARE hypothesis transport vesicles carry v (vesicle) SNAREs bind, in a highly specific manner, to their cognate t (target) SNAREs located on the appropriate target membrane (Sollner et al., 1993). Only when a complex is formed between the appropriate set of SNARE proteins will membrane fusion proceed and thus the specificity of t- and v-SNARE interaction contributes to the specificity of membrane fusion (Sollner et al., 1993).

More recently the definition of typical t-SNAREs and v-SNAREs has become less clear cut (Jahn and Sudhof, 1999) for example during the homotypic fusion events of vacuolar, endoplasmic reticulum (ER) and Golgi membranes following cell division (Fasshauer et al., 1998). This along with the unexpected discovery of four hydrophilic (3 glutamine and 1 arginine) residues conserved at the zero layer of SNARE complexes has led to the reclassification of SNAREs as either Q- or R- SNAREs (Fasshauer et al., 1998) with a

functional SNARE complex containing three Q-SNAREs and one R-SNARE (Fasshauer et al., 1998). Q-SNAREs can be further subdivided into Qa-SNAREs (also known as syntaxins or t-SNARE heavy chain), Qb-SNAREs and Qc-SNAREs (both of which are also known as the t-SNARE light chains) (Bock et al., 2001). It should, however, be noted that the Q/R-SNARE classification does not encompass all SNARE proteins. There are several SNAREs that cannot be classified as either Q- or R- SNAREs, for example the yeast ER-Golgi v-SNARE Bet1p, contributes a serine (S) residue instead of an arginine (R) residue at the zero layer of the SNARE complex (Fasshauer et al., 1998). Similarly the mammalian t-SNARE, Vti1b, contributes an aspartate residue (D) at the zero layer of the SNARE complex in place of a glutamine (Q) (Zwilling et al., 2007).

1.2.3 Syntaxins

Syntaxins or Qa-SNAREs are a member of the superfamily of SNARE proteins. They possess a SNARE and a transmembrane (TM) domain as well as an additional Habc domain (Fernandez et al., 1998) (Figure 1.2A). The Habc domain is located in the N-terminal half of the syntaxin and is composed of three anti-parallel alpha helices that fold back on each other (Figure 1.2B) (Fernandez et al., 1998).

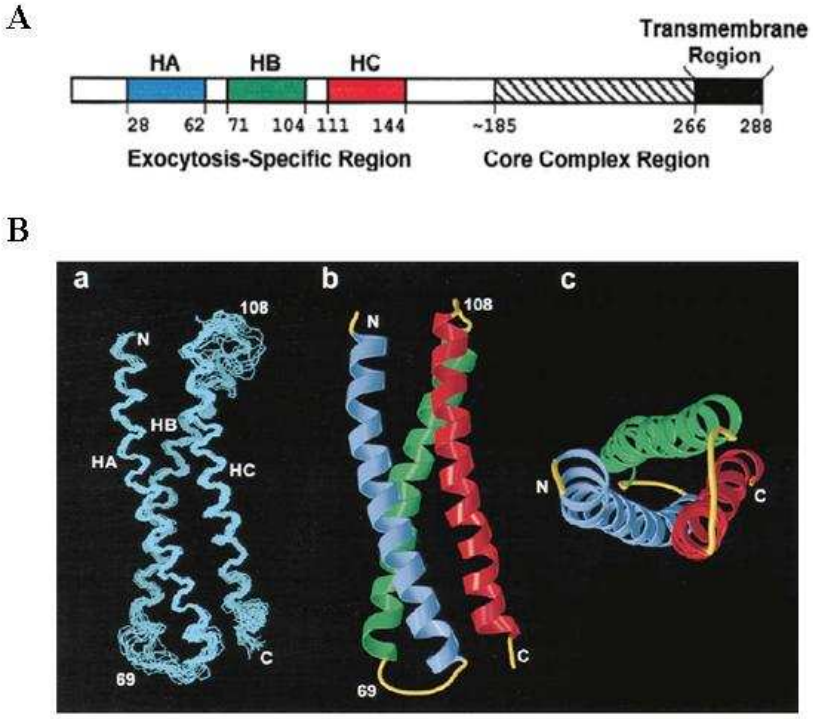

Figure 1.2 – Schematic and graphical diagrams of Sx1a
(A) A schematic diagram representing the key domains of syntaxins. The residue numbers are specific for syntaxin 1a (Sx1a) (Fernandez et al., 1998). (B) Graphical diagrams displaying the structure of the Habc domain as viewed in two different orientations. Those residues annotated are representative of Sx1a. Taken from (Fernandez et al., 1998).

Sequence alignment of the Habc domain from all syntaxins has shown a varying level of homology with the greatest number of similarities detected between syntaxins involved in neurotransmitter release (Fernandez et al., 1998).

Identification of the Habc domain has greatly enhanced our understanding of how membrane fusion may be regulated by Sec1/Munc18 (SM) proteins (discussed in more detail in Section 1.3.2). Structural and mutational studies have demonstrated that certain syntaxins, such as Sx1a and Sso1p, can exist in two different conformations, these are known as the closed and open conformations (Figure 1.3) (Dulubova et al., 1999, Misura et al., 2000, Munson et al., 2000).

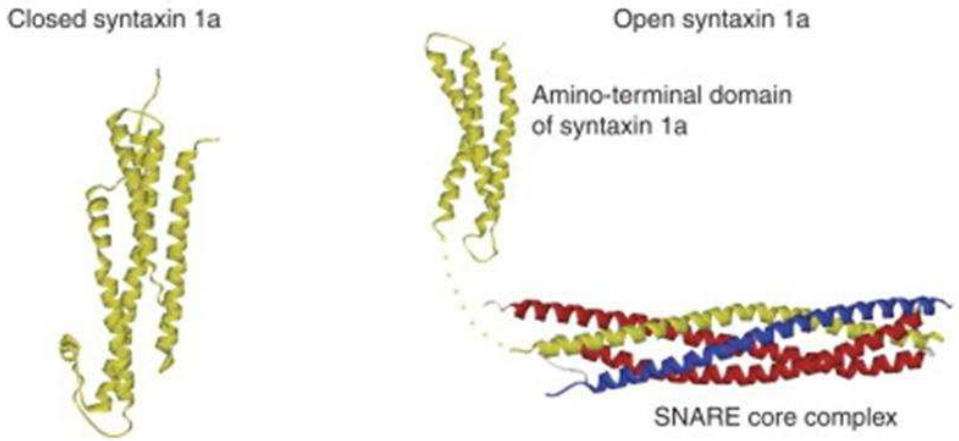

Figure 1.3 – A representative diagram displaying the two different conformations adopted by Sx1a.
The closed conformation is shown on the left hand side; in this conformation the Habc domain is folded back against the SNARE domain. The open conformation is shown on the right hand side; in this conformation the Habc domain (amino-terminal domain) has no contact with the SNARE domain. The two other SNARE proteins involved in the SNARE complex are show in red (SNAP-25) and blue (VAMP-2). Taken from (Burgoyne and Morgan, 2007).

In the closed conformation the Habc domain folds over and interacts with the SNARE domain and prevents any interaction with other SNARE domains; this is a fusion incompatible state as it is incompatible with SNARE complex assembly (Dulubova et al., 1999). In the open conformation the Habc domain has no contact with the SNARE domain which therefore is free to interact with other SNARE domains to form a functional SNARE complex; this is a fusion compatible state (Dulubova et al., 1999).

1.2.4 Syntaxin 16 (Sx16)

Sx16 was first cloned and sequenced by Simonsen and colleagues (Simonsen et al., 1998). Sx16 was identified by searching the expressed sequence tag (EST) database for sequences which showed similarities to the C-termini of syntaxins (Simonsen et al., 1998). The authors subsequently designed PCR primers to one EST which contained a 246 bp region that showed homology to the syntaxin family. This allowed them to amplify full-length cDNA from HeLa and brain plasmid cDNA libraries. The two longest PCR products generated from the HeLa plasmid cDNA library, syntaxin 16A (Sx16A) and syntaxin 16C (Sx16C), were identical except Sx16A contained a 161 bp insertion and a 12 bp deletion (Simonsen et al., 1998). Sx16C also contains an in-frame stop codon in place of the Sx16A insertion, which results in the translation of a C-terminally truncated protein

lacking the SNARE and TM domain of Sx16A (Simonsen et al., 1998). The longest PCR product obtained from the brain cDNA plasmid library, Sx16B, was identical to Sx16A however it contained an additional 63 bp insertion (Simonsen et al., 1998).

Profile-database searches identified four hypothetical proteins to which Sx16B could be aligned (Simonsen et al., 1998). Two of these hypothetical proteins were from the plant, *Arabidopsis thaliana* (2P16.16 and T10M13.19), one from the nematode, *Caenorhabditis elegans* (ZC155.3) and one from the yeast, *Saccharomyces cerevisiae* (YOL018c). Sx16B shows a 27-34% identity and 52-58% similarity to these hypothetical proteins (Simonsen et al., 1998).

Testing the tissue distribution of Sx16, Simonsen and colleagues, probed a northern blot containing mRNAs from the human tissues, heart, brain, placenta, skeletal muscle, kidney and pancreas with a probe that would recognise all three splice variants of Sx16; however only one band, of approximately 5 kb was detectable in all of the tissues tested. The author's explanation for this was that the Sx16 mRNAs must contain large untranslated regions and suggest that the sizes of the mRNAs are too similar to be resolved. Further attempts to probe the northern blot specifically for Sx16B, using a probe specific to the 63 bp insert which is absent in both Sx16A and Sx16C was unsuccessful. They therefore conclude that it is unclear to what extent the splice variants are expressed in the same or different tissues.

Intracellular localisation of Sx16 was investigated using Myc-tagged versions of each of the Sx16 splice variants (A, B and C) expressed in baby hamster kidney-21 (BHK-21) cells (Simonsen et al., 1998). Sx16A and Sx16B were found at a juxtanuclear structure, whereas Sx16C was found in the cytosol (Simonsen et al., 1998). Confocal immunofluorescence microscopy, further demonstrated that Sx16A co-localises with the Golgi marker β-COP and also partially co-localises with the TGN marker, the mannose-6-phosphate receptor (Simonsen et al., 1998). Sx16A also showed a small amount of co-localisation with the ER marker, calreticulun, however treatment of cells with cycloheximide demonstrated that Sx16A is only initially associated with the ER membrane prior to reaching its final destination at the Golgi (Simonsen et al., 1998).

At a similar time a second group had also identified a novel syntaxin-like molecule from a human EST database, which they used as a probe in a human pancreas cDNA library (Tang et al., 1998). This EST had previously been numbered as human syntaxin 16H (Sx16H)

and the authors retained this name for their clone (Tang et al., 1998). Sx16H shows a high level of homology to those Sx16 genes already deposited by Simonsen and colleagues in GenBank (Sx16A, B and C). Sx16H is very similar to Sx16A and Sx16B, but not identical. The N-terminal region of Sx16H is identical to Sx16C; however, Sx16H encodes a full-length version of the syntaxin (307 amino acids in length) whereas Sx16C encodes a truncated version of the protein (116 amino acids in length) (Tang et al., 1998).

Testing the tissue distribution of Sx16H, Tang and colleagues probed a multiple tissue (heart, brain, placenta, lung, liver, skeletal muscle, kidney and pancreas) northern blot with full-length Sx16H. A single reactive band of approximately 6.5 kb was detected in all tissues tested, with slightly higher levels detected in the heart and pancreas. They concluded that the presence of a reactive band in all tissues suggests that the protein has a general function (Tang et al., 1998).

Intracellular localisation of Sx16H was investigated using an N-terminally Myc-tagged version of Sx16H expressed in cells being CV-1 (simian) in origin carrying the SV40 genetic material (COS cells). Confocal immunofluorescence microscopy demonstrated that Sx16H co-localises with the Golgi lectin marker *lens culinaris agglutinin* (LCA) as well as the Golgi SNARE protein of 28 kDa (GS28) and syntaxin 5 (Sx5). Further treatment of cells with the drug brefeldin A (BFA) showed Sx16H to be localised to the Golgi stack.

Following on from the data provided by those groups mentioned above, Dulubova and colleagues went on to characterise Sx16 (Dulubova et al., 2002). They describe the three longest splice variants of Sx16 (A, B and H) as differing in an alternatively spliced region present after the sequence encoding the first 27 residues of Sx16 but prior to sequence encoding the Habc domain. The shortest splice variant of Sx16, Sx16C, is identical to Sx16H, but has a stop codon present in the sequence encoding the second helix, Hb of the Habc domain. Dulubova and colleagues also identified a fourth splice variant of Sx16, syntaxin 16D (Sx16D), also identical to Sx16H, but with a stop codon located between the sequence encoding the Habc domain and the SNARE domain.

Testing the tissue distribution of Sx16, Dulubova and colleagues analysed equal amounts of homogenate from the mouse tissues; heart, brain, spleen, lung, liver, muscle, kidney and testis, for the presence of Sx16 using immunoblot analysis with an antibody specific to Sx16C (Dulubova et al., 2002). A single Sx16-immunoreactive band was detected in

brain, which was representative of full-length Sx16. Prolonged exposure demonstrated that Sx16 was present in all of the tissues tested but this was at much lower level than that seen in brain. The authors conclude that under normal conditions the shorter splice variants, Sx16C and Sx16D, are not present at steady-state levels.

In summary five different splice variants of Sx16 have been identified; Sx16A, Sx16B, Sx16C (Simonsen et al., 1998), Sx16H (Tang et al., 1998), Sx16D (Dulubova et al., 2002). The three longest splice variants Sx16A, Sx16B and Sx16H encode membrane bound proteins (Dulubova et al., 2002, Sollner et al., 1993, Tang et al., 1998) which differ from each other in the region between the first 27 amino acids and the Habc domain (Dulubova et al., 2002). Sx16C and Sx16D are identical to Sx16H, but encode truncated versions of the syntaxin, both of which lack a SNARE domain and transmembrane domain (Dulubova et al., 2002, Simonsen et al., 1998). Sx16 was detected in all of the tissues tested, with slightly elevated levels detectable in human heart and pancreatic tissues (Simonsen et al., 1998, Tang et al., 1998) and also in brain tissue prepared from mice (Dulubova et al., 2002). As only full-length Sx16 was detectable in these tissues, it was suggested that under normal conditions the shorter splice-variants are not present at steady-state levels (Dulubova et al., 2002). Sx16A and B localise to a juxtanuclear structure with Sx16A co-localising with the Golgi marker β-COP and also partially co-localising with the mannose-6-phosphate receptor (Simonsen et al., 1998). Sx16H co-localises with the Golgi lectin marker, LCA, as well as GS28 and Sx5 (Tang et al., 1998). Further treatment of cells with the drug, BFA, showed Sx16H to be localised to the Golgi stack (Tang et al., 1998).

1.2.5 Sx16 has been implicated in the trafficking of GLUT4

Sx16, the syntaxin of interest in this study, and its binding partner, syntaxin 6 (Sx6) (Kreykenbohm et al., 2002, Mallard et al., 2002, Perera et al., 2003) have been implicated as playing an important role in insulin-regulated GLUT4 trafficking (Perera et al., 2003, Proctor et al., 2006, Shewan et al., 2003).

In 2003, Shewan and colleagues provided the first link between these three proteins using confocal immunofluorescence microscopy which demonstrated that GLUT4 co-localises with Sx16 and Sx6 in a subdomain of the TGN that is morphologically distinct from the TGN38 compartment (Shewan et al., 2003). This was further confirmed by the presence of Sx16 and Sx6 in immunoisolated GLUT4 vesicles (Shewan et al., 2003). In order to determine whether or not Sx16 and Sx6, like GLUT4, are present in an insulin-responsive

compartment, Shewan and colleagues utilised subcellular fractionation and immunoblot analysis to determine the location of Sx16 and Sx6 following insulin-stimulation (Shewan et al., 2003). Their results confirmed that Sx16 and Sx6 are present in an insulin-responsive compartment, as unlike TGN resident proteins, they are transported to the plasma membrane in response to insulin (Shewan et al., 2003). This finding was further supported using a plasma membrane assay (Robinson et al., 1992) which demonstrated that Sx16 and Sx6 are present at higher levels at the plasma membrane of insulin treated cells compared to those cells under basal conditions (Shewan et al., 2003). The kinetics at which Sx6 was delivered to the plasma membrane in response to insulin was identical to that of GLUT4, suggesting that these molecules are transported in the same population of vesicles (Shewan et al., 2003).

Further evidence that Sx16 and Sx6 play a role in the trafficking of GLUT4, came from a second study performed by Perera and colleagues (Perera et al., 2003). In this study the authors focused primarily on Sx6. Initially, they utilised subcellular fractionation to demonstrate that Sx6, like GLUT4 and IRAP, is translocated to the plasma membrane in response to insulin in 3T3-L1 adipocytes. Quantification of this data indicated that similar amounts of these three proteins are delivered to the plasma membrane following insulin-stimulation. Furthermore, immunoblot analysis of immunoisolated GLUT4-containing vesicles demonstrated that ~85% of cellular Sx6 is present in GLUT4-containing vesicles.

To determine the functional role that Sx6 plays in adipocytes, Perera and colleagues utilised a recombinant adenovirus to overexpress a cytosolic version of Sx6 lacking its transmembrane domain (referred to as Sx6-cyto hereafter) (Perera et al., 2003). This truncated version of Sx6 acts as an inhibitor of membrane fusion as it forms non-functional SNARE complexes (this has previously been demonstrated in studies utilising the syntaxin, Sx4 (Olson et al., 1997, Tellam et al., 1997b, Volchuk et al., 1996). In order to monitor the trafficking of GLUT4 in those cells overexpressing Sx6-cyto, the authors utilised a glucose transport assay, which measures the uptake of radiolabelled 2-Deoxy-D-glucose (deGlc) in insulin treated and untreated cells. Their results showed that although there was no change in the uptake of deGlc in insulin treated cells overexpressing Sx6-cyto, there was a significant increase in the rate of deGlc uptake under basal conditions. To explain these findings the authors proposed that GLUT4 trafficking from the endosomal system into its insulin-sensitive storage compartment was impaired in cells overexpressing Sx6-cyto, they further hypothesised that this would result in an increased level of GLUT4 in recycling endosomes and thus at the plasma membrane. To test their hypothesis, the authors utilised

the glucose transport assay described above to measure the rate of deGlc transport following insulin withdrawal in those cells overexpressing Sx6-cyto. In agreement with their hypothesis they detected a decrease in the rate of deGlc transport to return to that of basal levels following insulin withdrawal. The authors describe this effect as being due to a decrease in either the rate of GLUT4 endocytosis or the rate at which GLUT4 is sequestered from the recycling endosomes. In order to investigate this, the authors analysed the distribution of GLUT4 within these cells at set time points following insulin withdrawal. Their results showed an apparent decrease in the rate of GLUT4 endocytosis and sequestration from recycling endosomes; further implying that Sx6 does plays an important role in GLUT4 trafficking. To further investigate whether or not Sx6 is involved in the trafficking of GLUT4 between the endosomal system/TGN and GSVs, the authors used iodixanol gradients. These gradients can be used to separate GLUT4 that is present in the TGN/endosomes from that which is present in the GSVs (Hashiramoto and James, 2000, Maier and Gould, 2000). Their results suggest that Sx6 is involved in the sorting of GLUT4 into GSVs (Perera et al., 2003).

Perera and colleagues also set about identifying other proteins present in adipocytes which interact with Sx6 and hence may also be involved in the trafficking of GLUT4 (Perera et al., 2003). In particular the authors identified Sx16, which co-immunoprecipitates with Sx6. Further investigation of the relationship between Sx16 and GLUT4 demonstrated that like Sx6, >85% of Sx16 is found in GLUT4 vesicles isolated by immunoadsorption. In addition to this, Sx16, unlike Sx6, was found to be present in higher levels in the GSV fraction rather than the TGN/endosomal fraction of iodixanol gradients prepared from adipocytes. Finally the authors investigated the phosphorylation of Sx6 and Sx16 in insulin treated and untreated adipocytes. The authors demonstrate that only Sx16 is subject to phosphorylation and that this phosphorylation is decreased approximately 50% following insulin treatment.

Following on from the data provided in those studies described above, Proctor and colleagues went on to further investigate the role of Sx16 in the trafficking of GLUT4 (Proctor et al., 2006). Like Perera and colleagues, Proctor and colleagues utilised a recombinant adenovirus to overexpress an inhibitory version of Sx16 (Sx16-cyto) which lacks its transmembrane domain (discussed above for Sx6). Similar to those results obtained for Sx6-cyto, overexpression of Sx16-cyto decreased the rate at which deGlc transport was returned to that of basal levels following insulin withdrawal. To further confirm these results, Proctor and colleagues utilised morpholino antisense

oligonucleotides to knock-down the levels of Sx16 in 3T3-L1 adipocytes and subsequently utilised these cells to analyse the rate of deGlc transport following insulin withdrawal. Consistent with their previous findings, they detected a decrease in the rate at which deGlc transport was returned to that of basal conditions, following insulin withdrawal. However, they also noticed a decrease in the rate of insulin-stimulated deGlc transport and further demonstrated that this effect was specific to the trafficking of GLUT4 as the endocytic trafficking of the Transferrin receptor (TfR) was unaffected. Interestingly, the authors also noticed that the levels of GLUT4 were reduced by ~30% in these cells. From these data, Proctor and colleagues hypothesise, that by knocking-down the levels of Sx16, the levels of GLUT4 present in the GSVs will also be reduced which in turn will result in a decrease in the amount of deGlc transported into the cell following insulin-stimulation and also an over-all decrease in the levels of GLUT4 present within these cell. They further confirmed their hypothesis by demonstrating that there was a decrease in insulin-stimulated translocation of GLUT4 as well as a decreased level of GLUT4 present in these cells with levels being particularly depleted in those membrane fractions normally enriched in GLUT4 (eg GSVs).

The three studies described above all support a common model in which Sx6 and Sx16 play a role in the intracellular trafficking of GLUT4, functioning to control the entry of GLUT4 into the slow cycling pathway and also its entry into GSVs and hence suggest that these syntaxins function to regulate the insulin responsiveness of adipocytes (Perera et al., 2003, Proctor et al., 2006, Shewan et al., 2003). Consistent with this model, the discovery that Sx16 is a phosphoprotein which is dephosphorylated in response to insulin (Perera et al., 2003), makes Sx16 an extremely attractive candidate as a regulatory node of insulin-regulated GLUT4 trafficking.

Although, it is clear that the three studies described above have provided strong evidence for the involvement of Sx16 in insulin-regulated GLUT4 trafficking it has proven hard to gain molecular insight into the regulation of this, due to the experimental intractability of terminally differentiated insulin-sensitive cells. As with many areas of cell biology a lot of our knowledge about the molecular mechanism that regulates membrane traffic has come from model systems such as yeast, worms and flies (Calakos and Scheller, 1996).

1.2.6 Trafficking in yeast and mammalian cells

The molecular machinery that controls membrane trafficking has been highly conserved during evolution from yeast to mammalian cells (Ferro-Novick and Jahn, 1994). This was demonstrated by the observation that the yeast *SEC18* gene product can replace mammalian NSF in a cell free assay that reconstitutes membrane transport (Wilson et al., 1989). The striking similarities between yeast and mammalian cells has been confirmed as identification of different components involved in synaptic vesicle release at nerve endings and protein transport in yeast using both biochemical and genetic studies have found many homologous proteins (Figure 1.4) (reviewed in (Ferro-Novick and Jahn, 1994)). Such studies have established yeast as a good model system to study membrane trafficking events.

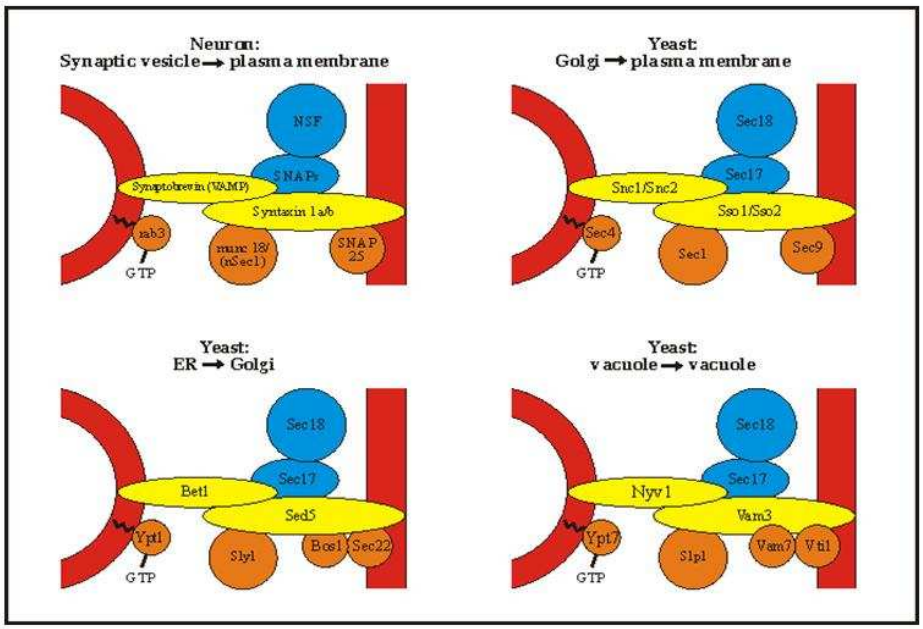

Figure 1.4 – Conservation of vesicle targeting and fusion machinery from yeast to man. Taken from (Ferro-Novick and Jahn, 1994).

1.2.7 Identification and characterisation of the yeast t-SNARE, Tlg2p

As discussed above (see Section 1.2.4), *in silico* analysis has identified Sx16 as being homologous to one hypothetical protein from the yeast strain, *S. cerevisiae* encoded by YOL018c present on chromosome XV (Simonsen et al., 1998).

In 1998, three independent groups characterised the protein encoded by YOL018c as the t-SNARE, Tlg2p (Abeliovich et al., 1998, Holthuis et al., 1998, Seron et al., 1998). Tlg2p is a 396 amino acid protein with a domain structure typical of syntaxins (Dulubova et al., 2002). It has a Habc (residues 70-187), a SNARE domain (residues 253-307) and a transmembrane domain (residues 317-334) (Dulubova et al., 2002). In addition and unusual for a SNARE protein, Tlg2p also possesses a further 63 residues at its C-terminus (predicted to be lumenal) (Dulubova et al., 2002) which are not required for its function (Abeliovich et al., 1998).

Tlg2p is localised to the TGN, co-localising and co-fractionating with the TGN markers, Kex2p and DPAP A (Holthuis et al., 1998) and also to the endosomal system, demonstrated by the exaggerated endosomal compartment that accumulated in Class E vacuolar protein sorting (vps) mutants (Abeliovich et al., 1998).

Cells lacking Tlg2p (*tlg2Δ*) are viable, however they display a variety of different phenotypes representative of defects in endocytosis (Abeliovich et al., 1998, Holthuis et al., 1998, Seron et al., 1998). These include delayed turnover of the phermone receptors, Ste2p and Ste3p by the vacuole (Abeliovich et al., 1998, Holthuis et al., 1998, Seron et al., 1998); defects in sorting of vacuolar proteases, such as carboxypeptidase Y (CPY), with approximately 15-20% of total CPY secreted in the late Golgi (p2) form (Abeliovich et al., 1998); and defects in the retrieval of TGN resident proteins such as Kex2p (Abeliovich et al., 1998, Holthuis et al., 1998) and less significantly DPAP A (Holthuis et al., 1998). Tlg2p is also required for the recycling of the SNARE protein, Snc1p, through the early endosomes (Lewis et al., 2000); the delivery of the protein aminopeptidase I to the vacuole via the cytoplasm to vacuole (CVT) pathway (Abeliovich et al., 1999); and TGN homotypic fusion (Brickner et al., 2001). *tlg2Δ* cells are also sensitive to osmotic stress (Abeliovich et al., 1998) and have a fragmented vacuolar morphology (Abeliovich et al., 1998, Seron et al., 1998).

It should be noted that cells lacking the t-SNARE, Tlg1p or the v-SNARE, Vti1p display some of those defects seen in *tlg2Δ* cells (Coe et al., 1999, Holthuis et al., 1998) and both co-immunoprecipitate with Tlg2p (Coe et al., 1999, Holthuis et al., 1998) indicating that these SNARE proteins participate in the same SNARE complex as Tlg2p. Similarly the functionally redundant, v-SNAREs, Snc1p and Snc2p, were also found to co-immunoprecipitate with Tlg2p (Abeliovich et al., 1998, Holthuis et al., 1998). Reconstitution of Tlg2p, Tlg1p, Vti1p (acting as t-SNAREs) and Snc1p or Snc2p (acting as

the v-SNARE) into two independent populations of liposomes allowed fusion via an *in vitro* liposome fusion assay, demonstrating that these SNARE proteins (Tlg2p/Tlg1p/Vti1p/Snc(1p or 2p)) can form functional SNARE complexes *in vitro* (Paumet et al., 2001). The entry of Tlg2p into functional SNARE complexes, like many other SNARE proteins, is regulated by phosphorylation (Gurunathan et al., 2002). This was demonstrated by the restoration of endocytosis in *snc* cells expressing a mutant version of Tlg2p (S90A) in which the serine residue targeted for PKA phosphorylation had been mutated to an alanine residue (Gurunathan et al., 2002).

Consistent with *in silico* analysis which identified Sx16 as homologous to Tlg2p (Simonsen et al., 1998), the mammalian SNAREs Sx6 and Vti1a, have also been identified as the putative mammalian homologues of Tlg1p and Vti1p, respectively (Coe et al., 1999, Fischer von Mollard and Stevens, 1998). These SNAREs are also involved in trafficking at the TGN in mammalian cells (Bassham et al., 2000, Mallard et al., 2002). It should also be noted that Sx16, like Tlg2p, is a phosphoprotein which, intriguingly, is dephosphorylated upon insulin binding to its receptor (Perera et al., 2003).

1.3 Overview of Membrane Fusion

In vitro fusion assays (Weber et al., 1998)s and more recently the fusion of cells by flipped SNAREs (Hu et al., 2003) has provided substantial evidence to suggest that SNARE proteins are necessary and sufficient to catalyse membrane fusion (Hu et al., 2003, Weber et al., 1998). However the rate at which fusion occurs *in vitro* is significantly slower than that observed *in vivo*, hence it is clear that other proteins are required to enhance the rate of fusion as well as regulate the process. In fact, many other molecules are required for tethering, docking and fusing membranes (Figure 1.5) (reviewed in (Bonifacino and Glick, 2004, Toonen and Verhage, 2003)).

Membrane fusion is a multistep process that commences with the priming of SNAREs on both the target and the vesicular membrane (Toonen and Verhage, 2003). This is an adenosine triphosphate (ATP) requiring process catalysed by NSF and α-SNAP (Mayer et al., 1996), which releases the SNARE proteins from their *cis*-SNARE complexes and promotes their interaction with cognate SNAREs present on the opposing membranes. Tethering follows the process of priming and is an important step involved in initiating membrane fusion as it holds the two membranes in close proximity (Toonen and Verhage, 2003). Tethering requires tethering complexes and the action of Rab proteins, a family of

small GTPases (Dunn et al., 1993, Novick and Brennwald, 1993, Zerial and McBride, 2001). Once the two membranes are in close proximity a proof reading mechanism is thought to act to ensure the correct pairing/association of a vesicle and target membrane before the committed step of docking (Bryant and James, 2003). Finally, the transition of the *trans*-SNARE complex to the *cis*-SNARE complex (Lin and Scheller, 1997, Sutton et al., 1998) is a result of the fusion of the two phospholipid bilayers and the delivery of the vesicular content to the target organelle. The associated SNARE proteins are then recycled via the action of NSF and its attachment protein, α-SNAP (Mayer et al., 1996). The steps involved in membrane fusion are summarised in the following diagram.

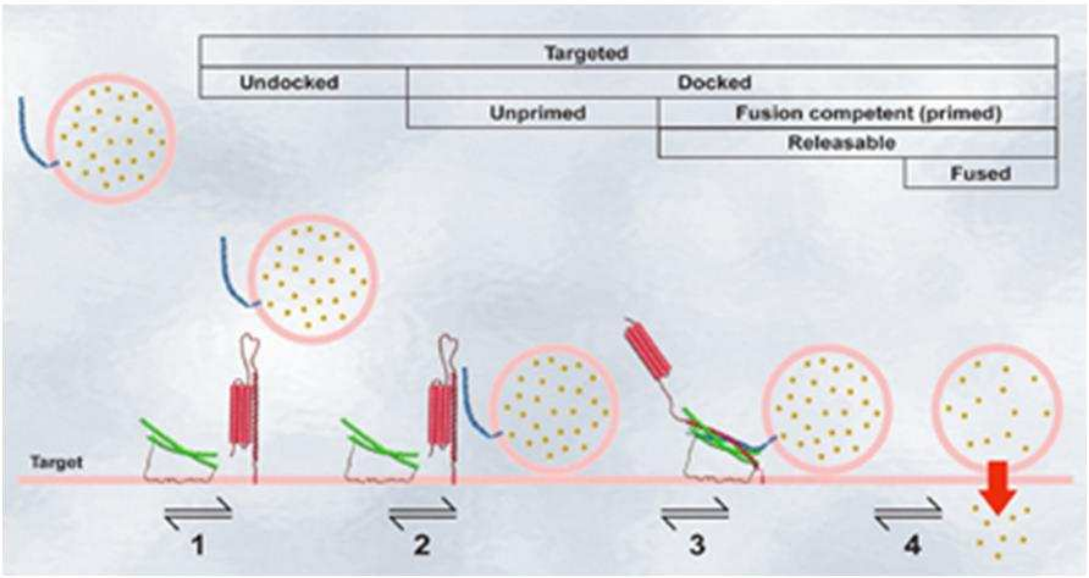

Figure 1.5 – A diagrammatic representation of the steps involved in membrane fusion. Sx1a is shown in red, SNAP25 is shown in green and synaptobrevin is shown in blue. (1) Priming - Vesicles are recruited to the target membrane and the SNARE proteins present in the target membrane are released from *cis*-SNARE complexes. (2) Tethering and docking – this step holds the vesicular and target membranes in close proximity (3) Formation of SNARE complexes – as a result of tethering and docking a *trans*-SNARE complex is formed this is subsequently changed to a *cis*-SNARE complex as a result of membrane fusion between the vesicular and target phospholipid bilayers and hence the delivery of the vesicular content shown in (4). Taken from (Toonen and Verhage, 2003).

1.3.1 SM Proteins

One family of proteins that are required for SNARE-mediated membrane fusion *in vivo* are the SM proteins (Jahn, 2000, Toonen and Verhage, 2003). There are four SM proteins found in yeast (Vps45p, Vps33p, Sly1p, Sec1p) and seven found in mammalian cells (Munc18a, Munc18b, Munc18c, mVps45, mVps33a, mVps33b, Sly1) (Dulubova et al.,

2002). SM proteins are arch-shaped peripheral membrane proteins of approximately 60-70 kDa, which display a high level of homology along their entire length (Jahn, 2000). The first SM protein identified, Unc18, was discovered genetically in *C. elegans* (Brenner, 1974). The mammalian homologue of Unc18, Munc18a, was later discovered in brain tissue by its ability to bind with high affinity to syntaxin (Hata et al., 1993) and was later cloned by homology screening based on its similarity to Unc18 and the Drosophila homologue, Rop (Garcia et al., 1994, Pevsner et al., 1994b). Munc18a is an essential factor, involved in the release of neurotransmitters throughout the brain (Verhage et al., 2000). Mutation of Munc18a (also known as n-Sec1 or rb-Sec1) in mice results in paralysis and although deletion of Munc18a does not affect the development of neuronal tissue in null mutant embryos they die immediately after birth due to their inability to breath (Verhage et al., 2000). SM proteins also play an essential role in yeast, as loss of function of any of the four SM proteins results in a block in membrane traffic (Cowles et al., 1994, Novick and Schekman, 1979, Ossig et al., 1991, Robinson et al., 1988, Wada et al., 1990).

1.3.2 SM proteins regulate membrane fusion

Most SM proteins bind to the syntaxin that is involved in the same transport step and since, SM proteins display a high level of homology along their entire length (Jahn, 2000) it is reasonable to assume that SM proteins would display a conserved mode of interaction with their cognate syntaxin(s) (Toonen and Verhage, 2003). However to date at least three distinct modes of direct interaction between an SM protein and its cognate syntaxin have been identified (Burgoyne and Morgan, 2007, Toonen and Verhage, 2003). Mode 1 – binding of an SM protein to its cognate syntaxin when it exists in a closed conformation; Mode 2 - binding of an SM protein to the extreme N-terminus of its cognate syntaxin; Mode 3 - Binding of an SM protein to its cognate syntaxin when it is in a complexed state. It should be noted that Mode 3 binding is not as well defined as Modes 1 and 2 as it has yet to be characterised structurally (Burgoyne and Morgan, 2007).

1.3.2.1 Mode 1 binding

The first example of an SM protein binding to its cognate syntaxin via Mode 1 binding was Munc18a binding to Sx1a (Misura et al., 2000). This SM protein functions at the plasma membrane where it plays an important role in exocytosis (Pevsner et al., 1994b). Munc18a binds to Sx1a within its arched shaped cavity, a process that requires Sx1a to be in a closed

conformation (Misura et al., 2000). Both the Habc domain and the SNARE domain of Sx1a participate in Munc18a binding, with approximately half of the interacting residues coming from the Habc domain (Figure 1.6) (Misura et al., 2000). As Munc18a binds to Sx1a when it is in a closed conformation (see Section 1.2.3) it was thought to play an inhibitory role in membrane fusion by preventing Sx1a from forming SNARE complexes (Dulubova et al., 1999, Misura et al., 2000, Pevsner et al., 1994a). However, the deletion of Munc18a does not result in constitutive membrane fusion and, in fact, causes a block in vesicular transport (Verhage et al., 2000).

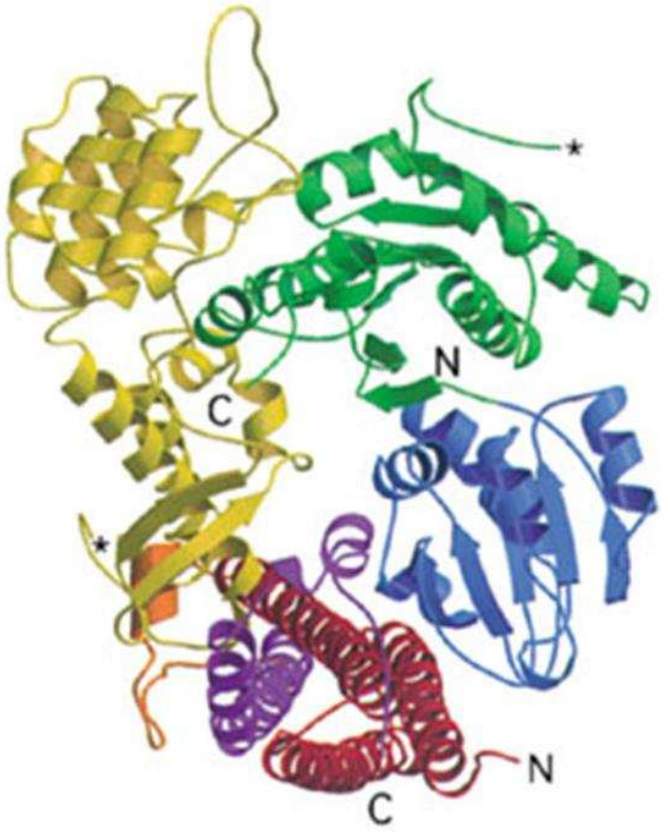

Figure 1.6 – A ribbon representation of the Munc18a-Sx1a interaction; Mode 1 binding. Domains 1, 2 and 3 of the SM protein, Munc18c are shown in blue, green and yellow, respectively. The N-terminal region of Sx1a, containing the Habc domain, is shown in red and the C-terminal portion of Sx1a containing the SNARE domain is shown in purple. Taken from (Misura et al., 2000).

1.3.2.2 Mode 2 binding

An example of an SM protein which binds to its cognate syntaxin via Mode 2 binding is Sly1p (Bracher and Weissenhorn, 2002). This SM protein functions at the ER and the Golgi apparatus and has two binding partners, Ufe1p and Sed5p (Bracher and

Weissenhorn, 2002, Yamaguchi et al., 2002). Mutational and structural studies of the Sed5p-Sly1p complex demonstrated that the N-terminal 20 amino acids of Sed5p are sufficient for Sly1p binding (Bracher and Weissenhorn, 2002, Yamaguchi et al., 2002). In fact, the first ten amino acids of Sed5p are conserved amongst all of its homologues (Yamaguchi et al., 2002). One residue that appears to play a critical role in the binding of Sed5p to Sly1p is a phenylalanine at residue number 10 (Yamaguchi et al., 2002). The crystal structure of Sly1p in complex with the N-terminal 45 residues of Sed5p revealed that Phe10 of Sed5p interacts with Sly1p via a hydrophobic pocket on the surface of domain I of the SM protein, Sly1p (Figure 1.7) (Bracher and Weissenhorn, 2002); its mutation to an alanine residue completely abolishes their interaction (Yamaguchi et al., 2002). This phenylalanine residue is also conserved in the other binding partner of Sly1p, Ufe1p (however it is present at residue 9 rather than 10) (Yamaguchi et al., 2002) and also in the syntaxin Tlg2p/Sx16, which also adopts a similar mode of interaction with their cognate SM protein Vps45p/mVps45 (Carpp et al., 2006, Dulubova et al., 2002) (This is discussed in detail later). In a reciprocal experiment, the substitution of any of the hydrophobic residues (L137, L140, A141, I153 and V156) present in the binding pocket on the outer surface of domain I of the SM protein, Sly1p, which surround F10 of Sed5p, to a lysine or arginine residue, also abolishes the interaction between Sed5p and Sly1p (Peng and Gallwitz, 2004). Interestingly, abrogation of Mode 2 binding between Sly1p and Sed5p or Vps45p and Tlg2p does not appear to affect membrane trafficking in yeast (Carpp et al., 2006, Peng and Gallwitz, 2004). This is in contrast to those studies which have been performed in mammalian systems where competing peptides blocking Mode 2 binding between Sly1 and Sx5 have been demonstrated to disrupt Golgi morphology (Dulubova et al., 2003, Yamaguchi et al., 2002). It should, however, be noted that this effect appears to be cell type specific (Williams et al., 2004). Hence it is clear that further work is required to fully understand the role of Mode 2 binding.

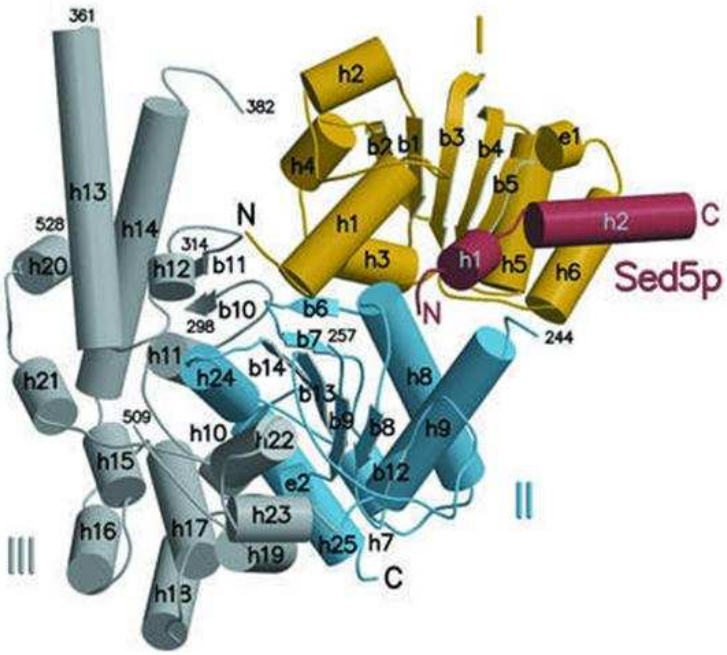

Figure 1.7 – A graphical representation of the Sly1p-Sed5p interaction; Mode 2 binding. Domains 1, 2 and 3 (I, II and III) are shown in yellow, blue and grey respectively. The N-terminal peptide of Sed5p is show in red. α-helices are represented by cylinders and β-sheets are represented by arrows. Taken from (Bracher and Weissenhorn, 2002).

1.3.2.3 Mode 3 binding

An example of an SM protein which binds to its cognate syntaxin, Sso1p, via Mode 3 binding is Sec1p (Carr et al., 1999). In contrast to both of the interactions described above, the SM protein, Sec1p does not associate with the monomeric syntaxin but is thought to preferentially bind to Sso1p when it is preassembled in the SNARE complex (Carr et al., 1999). Although there is no structural data, as yet, to confirm this, there is sufficient experimental evidence to support this hypothesis (Carr et al., 1999, Munson et al., 2000, Scott et al., 2004a). It has been demonstrated that Sec1p co-precipitates all three of the SNARE proteins involved in exocytosis (Sso1p, Sec9p and Sncp) in a ratio resembling that found in the SNARE complex (Carr et al., 1999). Furthermore, the utilisation of temperature sensitive mutants displaying defects in key enzymes (*sec4-8* and *sec18-1*) involved in the cycle of membrane fusion allowing the accumulation of either the monomeric syntaxin (*sec4-8*) or SNARE complex intermediates (*sec18-1*) result in an increase in Sso1p co-precipitating with complexed Sec1p only (Carr et al., 1999). These data were further enhanced by *in vitro* binding experiments which confirmed what had previously been found, that Sec1p binds strongly to preassembled t-SNARE complex

(Sso1p/Sec9p) as well as the v-t-SNARE complex (Sso1p/Sec9p; Snc2p) (Scott et al., 2004a).

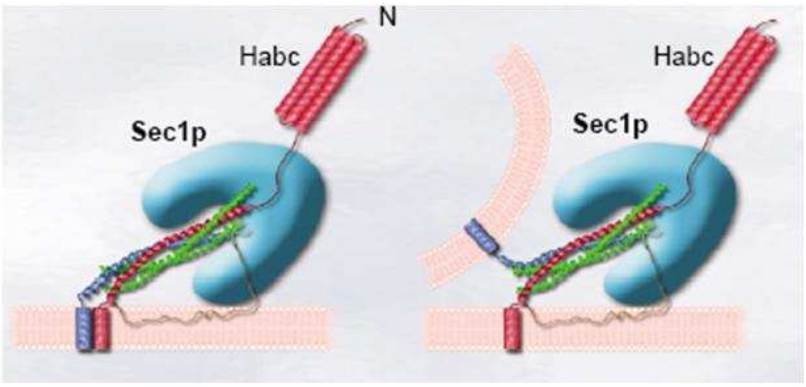

Figure 1.8 – Two different interpretations of how Sec1p may interact with the SNARE complex.
Sso1p is shown in red, Snc2p is shown in dark blue, Sec9p is shown in green and the SM protein, Sec1p is shown in light blue. Taken from (Toonen and Verhage, 2003).

1.3.2.4 Other modes of binding

SM proteins can also associate with their cognate syntaxins indirectly; an example of an SM protein which binds to its cognate syntaxin, Vps33p, via so-called 'bridging' proteins, is Vam3p (Sato et al., 2000). In yeast the Vps-C complexes (class C core vacuole/endosome tethering (CORVET) complex and homotypic fusion and protein sorting (HOPS) complex) function at the late endosomes and vacuole (Nickerson et al., 2009). The Vps-C core complex present in both HOPS and CORVET is composed of the four different proteins Vps11p, Vps16p, Vps18p and Vps33p (Sato et al., 2000). One of these components, the SM protein Vps33p, is thought to interact with the syntaxin Vam3p (Sato et al., 2000). Vam3p plays an essential role in all forms of vacuolar fusion (Nichols et al., 1997, Sato et al., 2000, Wickner and Haas, 2000). Vps33p can only interact with monomeric Vam3p when it is itself in a complexed state (Sato et al., 2000). In 2000 Sato and colleagues reported the preferential binding of the Vps-C core complex to monomeric Vam3p, with no association occurring when Vam3p is involved in the trans-SNARE complex (Vam3p-Vti1p-Vam7p) (Sato et al., 2000).

More recently it has become apparent that SM proteins may utilise more than one mode of binding to interact with their cognate syntaxin depending on the stage of fusion (Burgoyne

and Morgan, 2007, Toonen and Verhage, 2003). For example, it has recently been demonstrated that the SM protein, Munc18a, can utilise Mode1 and Mode 2 binding to interact with Sx1a at different stages in membrane fusion (Burkhardt et al., 2008, Dulubova et al., 2007, Rickman et al., 2007, Shen et al., 2007). This is also the case for other SM proteins, such as Vps45p (discussed in detail later) (Carpp et al., 2006).

1.3.2.5 SM proteins and non-syntaxin SNAREs

SM proteins can also interact directly with non-syntaxin SNAREs (Carpp et al., 2006, Peng and Gallwitz, 2004). This was first demonstrated in pull-down experiments, by the ability of wild-type Sly1p and a 'pocket-filled' mutant version of Sly1p (Sly1pL140K) to pull-down the non-syntaxin SNAREs Bet1p, Bos1p, Sft1p and Gos1p (Peng and Gallwitz, 2004). The non-syntaxin SNARE, Ykt6p was also pulled-down however much higher quantities of Ykt6p were found to bind to the mutant version of Sly1p (Sly1pL140K) when compared to wild-type Sly1p (Peng and Gallwitz, 2004). Further investigation of the interaction between Sly1p and these non-syntaxins demonstrated that the SNARE motif was essential for Sly1p binding and as demonstrated in the initial experiments this interaction does not require the hydrophobic pocket on the surface of Sly1p which is involved in Mode 2 binding (Peng and Gallwitz, 2004). The interaction between Sly1p and the non-syntaxin SNAREs appears to affect their assembly into SNARE complexes as increasing the concentration of Sly1pL140K present in pull-down experiments reduces the amount of Bet1p and Bos1p that is pulled-down by Sed5p (Peng and Gallwitz, 2004). The association of an SM proteins with a non-syntaxin SNARE has also been reported for the SM protein, Vps45p, which can bind directly to the SNARE domain of Snc2p, but cannot bind directly to Vti1p or Tlg1p (Carpp et al., 2006). Like Sly1p, Vps45p binding to the non-syntaxin SNARE, Snc2p, occurs through a mode distinct from that used by the SM protein to interact with its cognate syntaxin, Tlg2p (Carpp et al., 2006).

1.3.3 CPY trafficking and the identification of VPS genes

1.3.3.1 CPY trafficking

CPY is synthesised as an inactive precursor (preproCPY) on ER-bound ribosomes and is translocated across the ER membrane courtesy of its N-terminal ER signal peptide (Valls et al., 1987). Upon delivery of preproCPY into the ER lumen the signal peptide is cleaved and the resultant proCPY molecule undergoes N-linked glycosylation; this 67 kDa ER-

modified form of proCPY is referred to as p1CPY (Blachly-Dyson and Stevens, 1987, Hasilik and Tanner, 1978b, Johnson et al., 1987). From the ER, p1CPY is transported to the Golgi apparatus where it undergoes further oligosaccharide modifications, resulting in a 69 kDa Golgi-modified form of proCPY known as p2CPY (Stevens et al., 1982, Trimble et al., 1983). At the late Golgi, p2CPY is sorted away from soluble proteins destined for secretion via the secretory pathway by its receptor, Vps10p (Marcusson et al., 1994). Vps10p and p2CPY are trafficked to the prevacuolar compartment (PVC) where they dissociate from each other (Deloche and Schekman, 2002, Hasilik and Tanner, 1978a, Seaman et al., 1997). Vps10p is then recycled back to the late Golgi and p2CPY is transported to the vacuole where it is cleaved into its mature, active form (mCPY) by vacuolar proteases (Deloche and Schekman, 2002, Hasilik and Tanner, 1978a).

The CPY trafficking pathway has been well characterised which has made it a good tool for studying those proteins involved in vacuolar sorting (Johnson et al., 1987, Stevens et al., 1982).

1.3.3.2 Identification of the *VPS* genes

The *VPS* genes were first identified utilising two independent screens which looked for mutants that were unable to efficiently delivery proteins to the vacuole (Bankaitis et al., 1986, Jones, 1984, Rothman and Stevens, 1986). The first of these screens used a hybrid protein which incorporated the N-terminal 433 amino acids of proCPY fused to an N-terminally truncated version of the enzyme invertase, CPY-Inv433 (Bankaitis et al., 1986). Under normal conditions the enzyme invertase is trafficked via the secretory pathway where it functions by catabolising the fermentable carbon source, sucrose (Esmon et al., 1987). However the fusion protein used in this screen lacked the N-terminal peptide signal required for secretion of invertase and instead was trafficked to the vacuole courtesy of the signal peptide at the N-terminus of CPY (Bankaitis et al., 1986). The screen was performed in yeast strains lacking an endogenous copy of the gene for invertase (*SUC2*) and hence mutants defective in the vacuolar delivery of the hybrid protein were the only strains able to grow in media containing sucrose as the sole fermentable carbon source (Bankaitis et al., 1986).

The second screen also identified those mutants which missorted the vacuolar hydrolase, CPY. Secreted pro-CPY is enzymatically active, even in those cells lacking active vacuolar proteases (*pep4*), and hence is capable of cleaving the ‘blocked’ dipeptide N-

CBZ-phenylalanyl-L-leucine (Kuhn et al., 1974). The screen was performed in leucine auxotrophs lacking active vacuolar proteases (*leu2 pep4-3*) overproducing proCPY. Only those mutants defective in vacuolar delivery of proCPY were able to grow well on media containing CBZ-pheleu, as the sole source of leucine, by virtue of their missorted CPY (Jones, 1984, Rothman and Stevens, 1986).

Over 40 complementation groups were identified from these studies, which have subsequently been divided into six classes (A-F) corresponding to their vacuolar morphology (Banta et al., 1988, Robinson et al., 1988). Class A *vps* mutants display wild-type vacuolar morphology; Class B *vps* mutants have fragmented vacuoles; Class C *vps* mutants lack any identifiable vacuolar structures; Class D *vps* mutants are similar to Class A but display a large, single vacuolar structure and also have a defect in mother-to-daughter cell vacuolar inheritance; Class E *vps* mutants contain novel endosome-like compartment in addition to normal vacuoles; Class F *vps* mutants contain a single large vacuolar structure that is encircled by smaller, fragmented structures (Banta et al., 1988, Robinson et al., 1988).

1.3.4 Identification and characterisation of the SM protein, Vps45p

The gene encoding Vps45p (*VPS45*) was cloned by two independent groups in 1994 by its ability to complement the CPY sorting defect (Piper et al., 1994) and the temperature-conditional growth (Cowles et al., 1994) phenotype of strains containing *vps45* alleles (Cowles et al., 1994, Piper et al., 1994). Vps45p is a hydrophilic protein of 67 kDa, which displays homology to the SM family of proteins (Cowles et al., 1994, Piper et al., 1994). Cells lacking Vps45p (*vps45Δ*) are viable but missort multiple vacuolar hydrolases such as CPY (approximately 75-85% of the Golgi-modified p2CPY); are temperature sensitive for growth and display a vacuolar morphology typical of that of the Class D *vps* mutants i.e. they have a large, single vacuolar structure and exhibit defects in mother-to-daughter cell inheritance (Cowles et al., 1994, Piper et al., 1994). Approximately 65% of Vps45p is localised to the Golgi, co-fractionating with the Golgi marker protein, Kex2p (Cowles et al., 1994, Piper et al., 1994). It has also been suggested that Vps45p associates with the endosomal compartments; however this could not be verified due to the lack of known marker proteins specifically associated with these structures (Cowles et al., 1994, Piper et al., 1994).

Two syntaxins, Tlg2p and Pep12p, both interact genetically and biochemically with Vps45p (Abeliovich et al., 1999, Brickner et al., 2001, Bryant and James, 2001, Burd et al., 1997, Carpp et al., 2006, Dulubova et al., 2002, Nichols et al., 1998, Webb et al., 1997, Yamaguchi et al., 2002). Vps45p is involved in transport at the early endosome, the TGN and the late endosome (Cowles et al., 1994, Piper et al., 1994). Transport at the late endosomal compartment/PVC also requires the syntaxin Pep12p (Becherer et al., 1996). Unlike, Tlg2p, Pep12p does not bind directly to Vps45p; this was demonstrated through pull-down experiments utilising GST-tagged versions of Tlg2p and Pep12p (Bryant and James, 2001).

1.3.5 Characterisation of the interaction between Vps45p and Tlg2p

Initially the region of Tlg2p responsible for interacting with Vps45p was shown to exist in the first 230 amino acids of Tlg2p (Bryant and James, 2001); demonstrated by the inability of a truncated version of Tlg2p lacking the first 230 residues to recruit Vps45p to membranes (Bryant and James, 2001). More recently, Dulubova and colleagues demonstrated that the first 33 amino acids of Tlg2p are necessary and sufficient to capture Vps45p *in vitro* (Dulubova et al., 2002). Sequence alignment of Tlg2p and Sx16 (which has been shown to interact with the putative mammalian homologue of Vps45p, mVps45 (Tellam et al., 1997a, Yamaguchi et al., 2002)) revealed several conserved residues that play an important role in the binding of Vps45p/mVps45 (shown in bold in Figure 1.9). These residues are similar to those present in the N-terminal peptide of Sed5p and Ufe1p which are involved in their binding to Sly1p (discussed in Section 1.3.2.2), in particular the phenylalanine residue at position 9 and 10 of Tlg2p and Sx16, respectively (Yamaguchi et al., 2002).

```
Tlg2p  -     MF**R**DRTNL**FL**SY**R**RTFPH**N**ITFSSGKAPLGDDQ
Sx16   -    MAT**R**RLTDA**FL**LL**R**NNSIQ**N**RQLLA-EQELDELA
```

Figure 1.9 – Sequence alignments of the first 33 amino acids of Tlg2p and Sx16. Those residues conserved between Tlg2p and Sx16 are shown in bold. This is an adaptation of the data provided in (Dulubova et al., 2002).

The interaction between Vps45p/mVps45 and Tlg2p/Sx16 can be abolished through mutation of the N-terminal peptide of Tlg2p/Sx16 (Dulubova et al., 2002) in a manner

similar to that required to abolish the interaction between Sly1p and Sed5p (Yamaguchi et al., 2002). These findings suggested that Tlg2p, utilises the putative hydrophobic pocket identified in domain I of Vps45p (Carpp et al., 2006) binding in a mode analogous to the 'pocket-mode' of binding (Mode 2) captured in the Sly1p/Sed5p crystal structure, where the N-terminal peptide of the syntaxin inserts into a hydrophobic pocket on the outer surface of the SM protein (Bracher and Weissenhorn, 2002). The analogy between Sly1p/Sed5p and Vps45p/Tlg2p binding was further confirmed utilising a 'pocket-filled' mutant version of Vps45p (Vps45pL117R), in which a leucine residue present in the hydrophobic binding pocket had been replaced by an arginine residue (Carpp et al., 2006). This mutant version of Vps45p is no longer capable of binding a Protein A (PrA) tagged version of Tlg2p and fails to co-precipitate with Tlg2p from yeast cells (Carpp et al., 2006).

As mentioned previously (Section 1.3.2.4), Vps45p utilises two different modes of binding to interact with its cognate syntaxin, Tlg2p, at two different stages in the SNARE complex assembly/disassembly cycle (Bryant and James, 2003, Carpp et al., 2006). As discussed above, Vps45p binds to monomeric Tlg2p (Bryant and James, 2003, Carpp et al., 2006, Dulubova et al., 2002) using Mode 2 binding (Carpp et al., 2006, Dulubova et al., 2002); however Vps45p also binds to Tlg2p containing *cis*-SNARE complexes (Bryant and James, 2003) using Mode 3 binding (Carpp et al., 2006). Mode 3 binding of Vps45p to *cis*-SNARE complexes was demonstrated using a double mutant version of Vps45p (Vps45pW244R/L117R) that can no longer bind to monomeric Tlg2p but can bind to assembled SNARE complexes (Carpp et al., 2006). Mutation of the tryptophan residue at position 244 of Vps45p to an arginine residue produces a dominant-negative version of Vps45p (Vps45pW244R) that is capable of binding to monomeric Tlg2p via Mode 2 binding and assembled SNARE complexes via Mode 2 and Mode 3 binding, however unlike wild-type Vps45p, this mutant version of Vps45p does not allow the SNARE complex assembly/disassembly cycle to proceed (Carpp et al., 2006). Introduction of the 'pocket-filling' mutation to this dominant-negative version of Vps45p, generates a double mutant version of Vps45p (Vps45pW224R/L117R) that is no longer capable of bind to monomeric Tlg2p via Mode 2 binding, but is capable of associating with assembled SNARE complexes via Mode 3 binding (Carpp et al., 2006). Interestingly the introduction of the 'pocket-filling' mutation to the dominant negative version of Vps45p prevents it from exerting its dominant negative effect (Carpp et al., 2006). This was an interesting finding as under normal circumstances abrogation of Mode 2 binding does not appear to affect membrane trafficking in yeast (Carpp et al., 2006, Peng and Gallwitz, 2004).

It has also been suggested that Vps45p may interact with Tlg2p using a mode analogous to that of Munc18a binding to Sx1a; Mode 1 binding (Bryant and James, 2001). This requires Tlg2p to adopt a closed conformation akin to that of Sx1a (Bryant and James, 2001). However this is controversial and evidence for and against a closed conformation of Tlg2p exists (Bryant and James, 2001, Dulubova et al., 2002). Evidence that Tlg2p can form a closed conformation was provided by the ability of a truncated version of Tlg2p, lacking its Habc domain (Tlg2ΔHabc) to partially complement the CPY trafficking defects observed in *vps45Δ* cells (Bryant and James, 2001). Evidence against a closed conformation of Tlg2p comes from nuclear magnetic resonance (NMR) data which suggests that a bacterially produced construct of Tlg2p (residues 60-283) is unlikely to form a closed conformation (Dulubova et al., 2002).

1.4 Cellular levels of syntaxins are regulated by their cognate SM protein

As discussed above (see Section 1.3.2), SM proteins function to regulate membrane fusion by interacting with their cognate syntaxin. More recently, it has also been suggested that SM proteins may regulate membrane fusion via an indirect mechanism, acting as chaperone-like molecules (Bryant and James, 2001, Toonen et al., 2005). It has been demonstrated that the deletion of *VPS45* results in the destabilisation of Tlg2p, resulting in a decrease of the cellular levels of Tlg2p by ~90% as assessed by immunoblot analysis (Bryant and James, 2001). Tlg2p is degraded by the proteasome in *vps45Δ* cells (Bryant and James, 2001). This conclusion was reached since, in contrast to *vps45Δ* cells containing proteasomal activity, *vps45Δ* cells in which proteasomal activity has been abolished (through mutation of either the catalytic subunits, Pre1p and Pre2p (*pre1-1*, *pre2-2*) or the regulatory domain, Cim3p (*cim3-1*) (Heinemeyer et al., 1993, Heinemeyer et al., 1991, Ghislain et al., 1993)) contain levels of Tlg2p that can easily be detected through immunoblot analysis (Bryant and James, 2001). Inactivation of vacuolar proteases through the *pep4-3* mutation, on the other hand, did not restore Tlg2p levels in *vps45Δ* cells (Bryant and James, 2001). It should also be noted that this phenomenon is not specialised to yeast, for example it has been reported that levels of Sx1a are reduced in neuronal cells of Munc18a knockout mice (Verhage et al., 2000).

Several explanations as to the role that SM proteins play in protecting their cognate syntaxin from degradation have been provided (Toonen and Verhage, 2003). For example

it has been suggested that SM proteins may be required for the correct synthesis and targeting of their cognate syntaxin (Rowe et al., 2001, Rowe et al., 1999). Evidence for this comes from systems in which the syntaxin, Sx1a, is overexpressed resulting in aberrant membrane protrusions as a result of premature membrane fusions (Rowe et al., 2001, Rowe et al., 1999). However it is thought that this may be an artefact of overexpression as a similar phenomenon is not detected in cells lacking Munc18a, Unc18 or Sec1p (Novick and Schekman, 1979, Verhage et al., 2000). Similarly, the stabilisation of the syntaxin, Tlg2p in *vps45Δ* cells did not affect the localisation of Tlg2p, demonstrated using subcellular fractionation and fluorescence microscopy (Bryant and James, 2001). Hence it has been suggested that a more likely explanation is that the reduced levels of the syntaxin present in cells lacking their cognate SM protein are a result of impaired stability at the site of action (Toonen and Verhage, 2003). This later explanation is supported by the recent findings that the SM protein, Sly1p, protects the ER-localised syntaxin, Ufe1p, from ER-associated degradation (ERAD) (Braun and Jentsch, 2007). However these findings also support the previous suggestion that SM proteins may stabilise their cognate syntaxin shortly after synthesis. Hence further work is required to fully understand the role that SM proteins play in protecting their cognate syntaxin from degradation.

1.4.1 Post-translational modifications of Tlg2p?

1.4.1.1 Ubiquitination

Ubiquitin is a highly conserved, 76 amino acid protein found ubiquitously in all eukaryotic cells (Hicke and Dunn, 2003). Ubiquitination is the process, by which, Ubiquitin becomes covalently attached to a protein (Hicke and Dunn, 2003). Ubiquitin is linked to its target protein via an isopeptide bond, connecting the carboxy group of the C-terminal glycine residue of ubiquitin to the ε-amino group of a lysine residue in the target protein (Hicke and Dunn, 2003).

The addition of ubiquitin to a target protein requires the action of three enzymes; E1, a ubiquitin-activating enzyme; E2, a ubiquitin-conjugating enzyme; and E3, a ubiquitin ligase (Hicke and Dunn, 2003, Schwartz and Hochstrasser, 2003, Weissman, 2001). E1 initiates ubiquitination by adenylating the carboxy terminus of ubiquitin (Hicke and Dunn, 2003, Schwartz and Hochstrasser, 2003, Weissman, 2001). This is ATP-dependent step, primes ubiquitin for the formation of a thiolester bond with a cysteine side-chain at the

active site of the E1 enzyme. The E1 enzyme then tranfers ubiquitin to a cysteine residue in an E2 enzyme, a process known as transthiolation (Hicke and Dunn, 2003, Schwartz and Hochstrasser, 2003, Weissman, 2001). The ubiquitin moiety is finally transferred to the side chain of a lysine residue in the target protein, via the action of an E3 enzyme (Hicke and Dunn, 2003, Schwartz and Hochstrasser, 2003, Weissman, 2001). An E3 enzyme can catalyse this final step, either directly, by forming a thioester bond with ubiquitin before transferring it to the substrate or indirectly by forming a bridge between the substrate and the activated E2 enzyme (Hicke and Dunn, 2003, Schwartz and Hochstrasser, 2003, Weissman, 2001). This is dependent on whether or not the E3 enzyme contains a HECT (homologous to the E6-AP carboxy terminus) domain or a RING (really interesting new gene) domain, respectively (Hicke and Dunn, 2003, Schwartz and Hochstrasser, 2003, Weissman, 2001). E3 enzymes are thought of as the key regulatory determinant of ubiquitination as they largely determine the substrate specificity and the timing of the process (Hicke and Dunn, 2003).

Ubiquitination was first characterised as the signal for degradation of a protein by the proteasome; however ubiquitination can also have a variety of different effects within the cell (Hicke and Dunn, 2003). These include endocytosis of membrane receptors and targeting of proteins for entry into multi-vesicular bodies (MVBs) for degradation via the vacuole/lysosome (Katzmann et al., 2002). The outcome of a ubiquitinated substrate is dependent on whether a single ubiquitin moiety (monoubiquitination) or a chain of ubiquitin moieties (polyubiquitination) becomes covalently attached to the substrate protein and also the lysine residue in the ubiquitin moiety by which it is linked to subsequent ubiquitin moiety/moieties (Hicke and Dunn, 2003). Polyubiquitination involves three key lysine residues within ubiquitin, Lysines 29, 48, 63 (Hicke and Dunn, 2003). Lys-48 linked polyubiquitination targets nuclear, cytosolic and ER membrane proteins for degradation by the large barrel-shaped multicatalytic protease complex known as the 26S proteasome (Chau et al., 1989, Hershko and Ciechanover, 1998, Thrower et al., 2000). Di- or tri-ubiquitin chains linked via Lys-63 are thought to regulate the endocytosis of some plasma membrane proteins (Fisk and Yaffe, 1999, Galan and Haguenauer-Tsapis, 1997, Hoege et al., 2002). Monoubiquitination functions to regulate proteins through the late secretory and endocytic pathways (Hicke, 2001, Hoege et al., 2002, Piper and Luzio, 2007, Salghetti et al., 2001).

As discussed previously in this section, proteins destined for proteasomal degradation generally undergo Lys-48 linked polyubiquitination (Thrower et al., 2000). As levels of

Tlg2p are regulated by the proteasome in *vps45Δ* cells (Bryant and James, 2001) this would suggest that Tlg2p is subject to polyubiquitination.

1.4.1.2 Palmitoylation

Members of the SNARE protein family are known substrates for palmitoylation. For example SNAP-25 and Ykt6p, which both lack a transmembrane domain, require lipid modification for membrane association (Fukasawa et al., 2004, Veit et al., 1996). However palmitoylation is not restricted to those proteins lacking a transmembrane domain. Lipid modification of transmembrane proteins occurs in the cytosolic portion of a protein and generally occurs adjacent or within the transmembrane domain; it should be noted that no signalling sequence appears to be required for palmitoylation (Yik and Weigel, 2002). The significance of the lipid modification of proteins containing a transmembrane domain is unknown, however it has been suggested that this may affect the trafficking of proteins (Bijlmakers and Marsh, 2003).

The SNARE partners of Tlg2p, the t-SNARE Tlg1p and the v-SNARE Snc2p, are modified by palmitoylation (Couve et al., 1995, Valdez-Taubas and Pelham, 2005). This was demonstrated using the compound hydroxylamine which selectively removes thioester-linked palmitates (Chamberlain and Burgoyne, 1998). The palmitoyltransferase responsible for the palmitoylation of Tlg2p, Snc2p and Snc1p was identified to be Swf1p (Valdez-Taubas and Pelham, 2005). Swf1p belongs to a family of proteins that contain a DHCC cysteine-rich domain of 50 residues in length, which have been suggested to play a general role in palmitoylation (Putilina et al., 1999). Palmitoylation has been proposed to increase the stability of proteins *in vivo*; this was demonstrated by the reduced half-life of a mutant version of epitope-tagged Snc1p, in which the target cysteine for palmitoylation had been mutated to a serine residue (Couve et al., 1995). A similar trend was reported for the levels of Snc1p present in *swf1Δ* cells (Valdez-Taubas and Pelham, 2005). Expression of a green fluorescent protein (GFP)-tagged version of Tlg1p in *swf1Δ* cells displayed a different intracellular location than that seen in wild-type cells; fluorescence of the GFP-tag was mostly detected inside the vacuole instead of at the TGN/endosomal compartment as seen in wild-type cells (Valdez-Taubas and Pelham, 2005). Confirmation that this effect was due to the non-palmitoylation of Tlg1p was demonstrated by mutating the cysteine residues that undergo palmitoylation to serine residues (Valdez-Taubas and Pelham, 2005). This non-palmitoylated version of Tlg1p no longer localises to the TGN of wild-type cells, but instead localises to the interior of the vacuole (Valdez-Taubas and Pelham, 2005).

Further investigation of this demonstrated that non-palmitoylated Tlg1p is ubiquitinated; represented by the higher molecular weight bands detectable by both anti-Tlg1p and anti-ubiquitin antibodies during immunoblot analysis of Tlg1p-immunoprecipitates from *swf1Δ* cells which were either absent or at reduced levels in wild-type cells (Valdez-Taubas and Pelham, 2005). Furthermore this ubiquitination requires the ubiquitin ligase Tul1p, as removal of Tul1p prevents the mislocalisation and degradation of GFP-tagged Tlg1p in *swf1Δ* cells (Valdez-Taubas and Pelham, 2005). Tul1p is a RING domain ubiquitin ligase that recognises polar TM domains and targets them for degradation (Reggiori and Pelham, 2002). From these results, it was concluded that palmitoylated Tlg1p is protected from ubiquitination by Tul1p, which subsequently prevents its entry in MVBs and subsequent degradation by the vacuole (Valdez-Taubas and Pelham, 2005).

It should be noted that two potential sites of palmitoylation have been identified for Tlg2p (Valdez-Taubas and Pelham, 2005).

1.5 Aims

1) *In silico* analysis has demonstrated that Sx16 is homologous to Tlg2p (Simonsen et al., 1998), however it has yet to be demonstrated whether or not these syntaxins are also functionally homologous. Hence, the first aim of my work was to investigate whether or not Sx16 is a functional homologue of the yeast t-SNARE, Tlg2p. This is an important question as it opens up the possibility of using the experimentally tractable yeast strain *S. cerevisiae* as a model organism to further investigate the role of mammalian Sx16 (for example the functional consequences of Sx16 phosphorylation).

2) Sx16 can interact with yeast Vps45p, *in vitro* (Dulubova et al., 2002), however it has yet to be confirmed whether or not they interact *in vivo*. Hence, the second aim of my work was to investigate whether or not Sx16 interacts with Vps45p *in vivo*. This will provide further confirmation as to whether or not Sx16 is a functional homologue of Tlg2p (outlined in aim 1) by demonstrating whether or not Sx16 utilises the same molecular machinery as Tlg2p when expressed in yeast.

3) SM proteins are thought to act as chaperone-like molecules (Toonen et al., 2005). Cells lacking Vps45p (*vps45Δ*) have reduced levels of Tlg2p (Bryant and James, 2001). Hence the third aim of my work was to further investigate the regulation of steady-state levels of

Tlg2p in wild-type and *vps45Δ* cells, in the hope that this would give some in-sight into the mechanism by which the levels of Tlg2p are regulated by the SM protein, Vps45p.

Chapter 2 – Materials and Methods

2.1 Materials

2.1.1 Reagents and Enzymes

Chemical and any other reagents not mentioned below were purchased from Sigma-Aldrich (Poole, UK), VWR (Poole, UK) or Fisher Scientific (Leicester, UK). Ingredients used to synthesise media were purchased from both Melford Laboratories Ltd. (Suffolk, UK) and FORMEDIUM (Norwich, UK). Yeast lytic enzyme was obtained from MP Biomedicals (Aurora, USA).

DNA restriction enzymes, *Taq*® polymerase, *Pfu*® polymerase, T4 DNA ligase, dNTPs, 1 kb ladder and 6 x loading dye were obtained from either Promega (Southampton, UK) or New England Biolabs (Hitchin, UK). Platinum *Pfx*® polymerase was obtained from Invitrogen (Paisley, UK). Agarose MP was purchased from Roche Diagnostics (Mannheim, Germany) and Ethidium Bromide from Gene Choice (Maryland, USA). Gel extraction was performed using the QIAquick® Gel Extraction Kit from QIAGEN (Hilden, Germany) and DNA purification performed using the Wizard® Plus SV Miniprep DNA Purification System manufactured by Promega (Southampton, UK).

Protein gels were synthesized using a 30% acrylamide-bisacrylamide mixture (37.5:1 ratio) purchased from Severn Biotech Ltd (Kidderminter, UK). Broad range protein markers were purchased from Bio-Rad (Hertfordshire, UK). Nitrocellulose transfer membrane was obtained from Whatman (Dassel, Germany). Enhanced chemiluminescence (ECL) solutions and secondary antibodies used in immunoblot analysis were purchased from GE Healthcare (Buckinghamshire, UK).

2.1.2 Bacterial and Yeast Strains

The bacterial (*E. coli*) and yeast (*S. cerevisiae*) strains used in this study are listed in Table 2.1.

2.1.3 Media

Bacterial cells were grown in 2xYT (1.6% (w/v) Tryptone, 1% (w/v) Yeast Extract, 0.5% (w/v) NaCl). Solid media was generated by the addition of 2% (w/v) micro agar. Plasmid

selection was achieved by adding the antibiotic, Ampicillin, to the media at a final concentration of 100 µg/ml.

Yeast cells were grown in YPD (1% (w/v) Yeast Extract, 2% (w/v) Peptone, 2% (w/v) Glucose). Solid media was generated by the addition of 2% (w/v) micro agar. Plasmid selection was achieved using minimal synthetic defined (selective) medium, SD (0.675% (w/v) Yeast Nitrogen Base without amino acid, 2% (w/v) Glucose) lacking specific amino acids –ura-met (0.185% (w/v) synthetic drop out: -ura-met); –ura-leu (0.183% (w/v) synthetic drop out: -ura-leu); -his (0.193% (w/v) synthetic drop out: -his). Again, solid media was generated by the addition of 2% (w/v) mico agar.

2.1.4 Antibodies

2.1.4.1 Primary Antibodies

Rat monoclonal antibodies (clone 3F10; 100 µg/ml; catalogue number (cat #) 11867423001) that specifically recognise the epitope YPYDVPDYA (derived from the human influenza hemagglutinin (HA) protein) were purchased from Roche (Mannheim). 10 µl of this was utilized in immunoprecipitation experiments (see Section 2.2.18) and a 1:50 dilution was used in immunofluorescence experiments (see Section 2.2.17). Polyclonal antibodies against Tlg2p were raised in rabbits immunised with peptides corresponding to residues 272-287 and 381-396 (this was performed by Eurogentec). Antibodies present in the antiserum were affinity purified using PrA-agarose (see Section 2.2.11.1; ~0.4 mg/ml) and were generally used at a 1:100 dilution in immunoblot analysis. 1:50 dilution of purified anti-Tlg2p antiserum was utilised in immunofluorescence experiments. Polyclonal antibodies against Vps45p were raised in rabbits immunised with peptides corresponding to residues 14-28 and 563-577 (this was performed by Eurogentec). Antibodies specific to residues 563-577 of Vps45p were affinity purified from the rabbit antiserum using a SulfoLink Kit (Pierce Biotechnology, cat # 44895; see Section 2.2.11.2). Purified anti-Vps45p antibodies (~0.6 mg/ml) were used at a 1:500-1:1000 dilution for immunoblot analysis. Polyclonal antibodies against Snc2p were raised in rabbits immunised with peptides corresponding to residues 11-25 and 72-86 (this was performed by Eurogentec). Antibodies specific to residues 11-25 were affinity purified from the rabbit antiserum by Eurogentec. Purified anti-Snc2p antibodies (~0.7 mg/ml) were used at a 1:1000 dilution for immunoblot analysis. Mouse monoclonal anti-CPY antibodies (clone 10A5; 20 µg/ml) have previously been described in (Roeder and Shaw, 1996) and were

used at a 1:50 dilution for immunoblot analysis. 15 µl of a 1:10 dilution of rabbit polyclonal anti-CPY antiserum previously described in (Bryant and James, 2001) was used in pulse-chase experiments. The following antibodies were used solely for immunoblot analysis. Mouse monoclonal anti-HA antibodies (HA.11, clone 16B12; 2-3 mg/ml; cat # MMS-101R) were purchased from Covance (Cambridge Bioscience Ltd, UK) and were generally used at a 1:2000 dilution. Rabbit polyclonal anti-Vti1p antiserum has previously been described in (Coe et al., 1999) and was used at a 1:1000 dilution. Mouse monoclonal anti-Vph1p antibodies (10D7-A7-B2; 250 µg/ml; cat # A-6427) were purchased from Molecular Probes® (Eugene, Oregon) and were used at a dilution of 1:1000. Living Colours A.v mouse monoclonal antibodies (JL-8; cat # 632381) against *Aequorea Victoria* Green Fluorescent Protein (GFP; 1 mg/ml) was purchased from Clonetech Laboratories Inc (California, USA) and used at a dilution of 1:3000. Mouse monoclonal antibodies (clone 9E10, cat # 5546) that specifically recognise the epitope EQKLISEEDL (derived from the human $p62^{c\text{-}Myc}$ protein) were purchased from Sigma-Aldrich (Poole, UK) and were used at a dilution of 1:100. Rabbit polyclonal anti-Pgk1p antiserum has previously been described in (Piper et al., 1994) and was used at a 1:20000 dilution.

2.1.4.2 Secondary Antibodies

All secondary antibodies used in immunoblot analysis were conjugated to horseradish peroxidise (HRP) and were purchased from GE Healthcare (Buckinghamshire, UK). Anti-rabbit IgG, HRP-linked antibodies (cat # NA934) were used at a dilution of 1:5000; anti-mouse IgG, HRP-linked antibodies (cat # NA931) were used at a dilution of 1:2000; anti-rat IgG, HRP-linked antibodies (cat # 5546) were used at a dilution of 1:1000. Secondary antibodies used in immunofluorescence experiments, Alexa Fluor® 488 donkey anti-rat IgG (2 mg/ml; cat # A21208) and Alexa Fluor® 594 donkey anti-rabbit IgG (2 mg/ml; cat # A21207), were purchased from Molecular Probes (Oregon, USA) and used at a 1:500 dilution.

2.2 Methods

2.2.1 Isolation of yeast chromosomal DNA

Yeast cells were grown overnight in the rich media, YPD. The following morning the cells were harvested by centrifugation at 931 *g* for 2 mins and washed in 1.0 M Sorbitol, 0.1 M EDTA (pH 7.5). The resultant cell pellet was resuspended in 0.4 ml of 1.0 M Sorbitol,

0.1 M EDTA (pH 7.5). 15 µl of yeast lytic enzyme (15 mg/ml) was added to the cells prior to incubating at 37°C for 30 mins. The resultant spheroplasts were harvested by centrifugation at 3610 *g* for 2 mins and resuspended in 500 µl of Tris-EDTA (TE) buffer (10 mM Tris-HCl pH 8, 1 mM EDTA pH 8). 90 µl of freshly made lysis buffer (0.25 M EDTA, 0.4 M Tris, 2% (w/v) SDS, pH 8) was added to the spheroplasts and the cells lysed at 65°C for 30 mins. 80 µl of 5 M potassium acetate (KOAc) was added to the lysed cells prior to a 2 hour incubation on ice. Precipitated proteins and cell debris was removed using centrifugation at 16160 *g* for 15 mins at 4°C. The supernatant was transferred to a fresh tube to which 1 ml of ice-cold ethanol was added. The resultant precipitated DNA was then collected by centrifugation at 16160 *g* for 15 mins. The pellet was washed with 70% (v/v) ethanol and subsequently dried. Finally the pellet was resuspended in 100 µl of TE. 1 µl of this was used as a template for PCR amplification (Section 2.2.3.1).

2.2.2 Purification of plasmid DNA from bacteria

Plasmid DNA was routinely obtained from bacterial cultures using the Promega Wizard® Plus SV Miniprep kit by Promega (Southampton, UK). 1 µl of a 1:10 dilution of purified plasmid DNA (~1 mg/ml) was used as a template for polymerase chain reaction (PCR) amplification and 50 ng used for site-directed mutagenesis (SDM) (see Section 2.2.3.1 and 2.2.3.2).

2.2.3 Molecular Cloning

The oligonucleotides used in PCR amplification or SDM are listed in Table 2.2. These were synthesized either by Yorskshire Bioscience Ltd (York, UK) or Vhbio Ltd (Gateshead, UK) and were resuspended in nuclease free water to a final concentration of 50 pmol/µl.

2.2.3.1 Polymerase Chain Reaction (PCR)

PCR recipe:

10 mM dNTPs	5 µl
50 mM $MgSO_4$	5 µl
10x *Pfx*® buffer	5 µl
Enhancer	5 µl
dH_20	26 µl
Forward primer (50 pmol/µl stock)	1 µl
Reverse primer (50 pmol/µl stock)	1 µl
Template DNA	1 µl
Pfx® DNA polymerase	1 µl

Programme:

Step 1 = 95ºC 1 min

Step 2 = 94ºC 1 min

Step 3 = 55ºC 1 min *

Step 4 = 68ºC (1 min/kb)

Step 5 = 68ºC 10 mins

Step 6 = 4ºC hold

Steps 2-4 were repeated for 30 cycles.

* the annealing temperature varied between different PCR reactions depending on the melting temperature (Tm) of the primers used.

DNA fragments were routinely resolved electrophoretically through 0.6-1.0% (w/v) agarose gels, typically 0.8% (w/v) in Tris-acetate (TAE) buffer (0.04 M Tris-acetate, 0.001 M EDTA). Gel extraction was performed using the QIAquick® Gel Extraction Kit from QIAGEN (Hilden, Germany).

2.2.3.2 Site-Directed Mutagenesis (SDM)

SDM recipe:

10 mM dNTPs	1 µl
10x *Pfu*® buffer	5 µl
dH_2O (to a final volume of)	50 µl
Forward primer (50pmol/µl stock)	125 ng
Reverse primer (50pmol/µl stock)	125 ng
Template DNA	50 ng
Pfu® polymerase	1 µl

Programme:

Step 1 = 95ºC 1 min

Step 2 = 95ºC 50 secs

Step 3 = 60ºC 50 secs *

Step 4 = 68ºC (2 mins/kb)

Step 5 = 68ºC 7 mins

Step 6 = 4ºC hold

Steps 2-4 are repeated for 18 cycles.

* the annealing temperature was increased to 68ºC in certain SDM reactions in order to decrease the occurrence of false positives and to improve mutagenesis efficiency.

1 µl (10 units) of the restriction enzyme, *Dpn*I, was added to the SDM reaction mixture after completion. A further incubation of 1 hour at 37ºC was performed to catalyse *Dpn*I digestion of the methylated parental DNA. 5 µl of the *Dpn*I treated SDM reaction mixture was transformed into the *E. coli* host strain XL-1 Blue (see Section 2.2.7.1).

2.2.4 TA cloning

PCR products (generated as described above in Section 2.2.3.1) to be cloned into pCR®2.1 - TOPO®, which has 3' thymine overhangs, were treated with *Taq*® polymerase to generate 3' adenosine overhangs.

Recipe:

PCR product	10 µl
10x *Taq*® buffer	1 µl
25 mM $MgCl_2$	0.6 µl
Taq® polymerase	1 µl
dNTPs	0.5 µl

The reaction was performed at 72°C for 20 mins.

TA cloning could then be performed using the TA Cloning® kit (Invitrogen). 4 µl of *Taq*® treated PCR product was added to 0.5 µl of pCR®2.1 - TOPO® vector in a sterile eppendorf tube. The 3' thymine overhangs on the vector and the 3' adenosine overhangs on the *Taq*® treated PCR product were allowed to anneal at room temperature for 5 mins. The reaction was terminated by adding 0.5 µl of salt solution. The whole reaction mixture was transformed into TOP10 cells (see Section 2.2.7.1). The transformants were plated onto 2 x YT containing Ampicillin (100 µg/ml), which had been pre-treated with 40 µl of X-Gal (from a stock solution of 20 mg/ml in Dimethylformamide (DMF)) and incubated overnight at 37°C. The following day white colonies were selected as these represent those cells successfully transformed with pCR®2.1 - TOPO® containing the gene of interest.

2.2.5 Plasmid Construction

The oligonucleotides and plasmids used in this study are listed in Tables 2.2 and 2.3, respectively.

pNB701 (constructed by Dr. Nia J. Bryant, University of Glasgow, UK) was created using SDM to remove a *Sal*I site present in the polylinker region of a plasmid ((provided by Rob Piper, University of Iowa, IA) which contains the coding sequence for RS-ALP (retention sequence-Alkaline phosphatase) under the control of the *CUP1* promoter (Bryant et al., 1998) in pRS316 (Sikorski and Hieter, 1989)). The significance of this was that the majority of the *PHO8* ORF was removed from the plasmid, pNB701, when it was digested with the restriction enzymes, *Xho*I and *Sal*I. Homologous recombination could then be used to introduce a coding sequence of interest immediately after the *CUP1* promoter. This was achieved by transforming PCR products (containing the gene of interest flanked by sequences homologous to the 3' end of the *CUP1* promoter and the proximal end of the

3’ UTR of *PHO8*) and *Xho*1/*Sal*1 digested pNB701 into the yeast strain, SF838-9D (see Figure 3.1).

pMSS001 was constructed by amplifying the human Sx16A Open Reading Frame (ORF; accession number AAB69282) from cDNA kindly provided by Prof. Gwyn Gould (University of Glasgow, U.K.) by PCR using the oligonucleotide primers 105 and 106 (detailed in Table 2.2). The resultant PCR product consisting of the Sx16A ORF flanked by sequences homologous to the 3’ end of the *CUP1* promoter and the proximal end of the 3’ UTR of *PHO8* was then used to repair gapped (*Xho*I/*Sal*I digested) pNB701 by homologous recombination.

pMAZ002 was constructed by introducing sequence encoding the HA-tag (YPYDVPDYA) between the *CUP1* promoter and 5’-hSx16A sequence of pMSS001, by SDM using the oligonucleotides 258 and 259 (detailed in Table 2.2).

pMAZ006 was constructed by amplifying the *TLG2* ORF from yeast chromosomal DNA (prepared from SF838-9D) by PCR using the oligonucleotide primers, 314 and 311 (detailed in Table 2.2). The resultant PCR product containing sequence encoding Tlg2p with a HA-tag immediately after the initiating methionine, flanked by sequences homologous to the 3’ end of the *CUP1* promoter and the proximal end of 3’ UTR of *PHO8*, was then used to repair gapped (*Xho*I/*Sal*I digested) pNB701 by homologous recombination.

pMAZ007 was constructed in a manner similar to that employed to make pMAZ006. The murine syntaxin 4 (Sx4) ORF (accession number P70452) was amplified from the plasmid pQE30-Syntaxin 4 (provided by Luke Chamberlain, University of Edinburgh, U.K.) using the oligonucleotide primers 315 and 313 (detailed in Table 2.2). The resultant PCR product containing sequence encoding Sx4 with a HA-tag immediately after the initiating methionine, flanked by the sequences homologous to the 3’end of the *CUP1* promoter and the proximal end of the 3’ UTR of *PHO8*, was then used to repair gapped (*Xho*I/*Sal*I digested) pNB701 by homologous recombination.

pMAZ001 was constructed by amplifying the *TLG2* ORF from yeast chromosomal DNA (prepared from SF838-9D) by PCR using the oligonucleotide primers 267 and 268 (detailed in Table 2.2). Chromosomal DNA from SF838-9D was utilized as template DNA for PCR amplification and the oligonucleotides primers synthesized so they would anneal

to a segment of DNA 500 kb upstream of the initiating ATG and 300 kb downstream as a means to incorporate the endogenous promoter and 3' UTR. The resultant PCR product was TA cloned into pCR®2.1-TOPO® and further subcloned into the *Xho*I-*Xba*I sites of pRS416 (Sikorski and Hieter, 1989) to generate pMAZ001.

pMAZ017 was constructed by introducing a *Bam*HI and *Sal*I sites after the first 99 bp of the *TLG2* ORF in pMAZ001. This was achieved by SDM using the oligonucleotides 316 and 317 (detailed in Table 2.2) and generated the intermediate plasmid, pMAZ016. The *HIS3* coding sequence was subsequently amplified by PCR using the oligonucleotide primers 269 and 270 (detailed in Table 2.2). The resultant PCR product was TA cloned into pCR®2.1-TOPO® and further subcloned into the *Bam*HI-*Sal*I sites of pMAZ016, to generate pMAZ017.

pMAZ027 was constructed by using SDM to introduce a *Bam*HI site prior to the initiating ATG of the *TLG2* ORF in pMAZ017 using the oligonucleotides 397 and 398 (detailed in Table 2.2). The first 99 bp of the *TLG2* ORF were removed by digesting with *Bam*HI (taking advantage of the newly introduced *Bam*HI site and that already present after the first 99 bp in pMAZ017). Two stop codons were subsequently introduced after the *HIS3* ORF by SDM using the oligonucleotides 395 and 396 (detailed in Table 2.2)

pMAZ028 (K26R), pMAZ030 (5KR) and pMAZ033 (3KR) were constructed by SDM, using pMAZ017 as template DNA and the oligonucleotides 214 and 215; 333, 334, 335 and 336; 407 and 408 (detailed in Table 2.2), respectively.

pMAZ029 was constructed by introducing two stop codons immediately after the *HIS3* ORF in pMAZ017 by SDM using the oligonucleotides 395 and 396 (detailed in Table 2.2).

pMAZ038 was constructed using SDM to introduce two stop codons directly after the sequence encoding the transmembrane domain in the *TLG2* ORF present in pMAZ006 using the oligonucleotides 380 and 381 (detailed in Table 2.2).

Plasmids pSGS025, pSGS036, pSGS043 and pSGS044 were constructed by Dr Scott G. Shanks (University of Glasgow, UK.). pSGS025 and pSGS036 were created by amplifying sequence encoding HA-tagged Sx16A and HA-tagged murine Sx4 from pMAZ002 and pMAZ007 by PCR using the oligonucleotide primers 301 and 303; 308 and

310, respectively. The resultant PCR product flanked by *Xba*I and *Xho*I restriction sites was ligated into the *Xba*I-*Xho*I sites of pVT102u (Vernet et al., 1987).

pSGS043 and pSGS044 were created by amplifying sequence encoding residues 231-396 of Tlg2p and 206-303 of Sx16A from the plasmids pHA-Tlg2 (Seron et al., 1998) and pSGS025 by PCR using oligonucleotides 383 and 384; 382 and 303, respectively. The resultant PCR products flanked by *Xba*I and *Xho*I restriction sites were subsequently ligated into the *Xba*I-*Xho*I sites of pVT102u (Vernet et al., 1987).

pALA001 was constructed by Alicja Drozdowska (University of Glasgow, UK). The human Sx16A ORF (accession number AAB69282) was amplified from a cDNA kindly provided by Prof. Gwyn Gould (University of Glasgow, U.K.) by PCR using the oligonucleotide primers 286 and 287 (detailed in Table 2.2). The resultant PCR product was TA cloned into pCR®2.1-TOPO® and further subcloned into the *Nde*I-*Xho*I sites of pCOG022 (Carpp et al., 2006), generating pALA001.

pCOG039 was constructed by Dr. Lindsay N. Carpp (University of Glasgow, UK). A C-terminally HA-tagged version of Tlg2p was amplified from a yeast chromosomal preparation of SF838-9D by PCR using the oligonucleotide primers 63 and 66 (detailed in Table 2.2). This resultant PCR product containing sequence encoding Tlg2p with an HA-tag immediately before the terminating stop codon, flanked by sequence homologous to the 3'end of the *CUP1* promoter and the proximal end of 3' UTR of *PHO8*, was then used to repair gapped (*Xho*I/*Sal*I digested) pNB701 by homologous recombination.

pCAL1 was constructed by Christopher Antony Lamb (PhD student, University of Glasgow, UK). SDM was used to mutate the sequence encoding methionine 342 and phenylalanine 344 in the *DSK2* ORF in pGEX-DSK2$_{UBA}$ to sequence encoding an arginine and alanine, respectively, using the oligonucleotides 352 and 353 (detailed in Table 2.2).

All constructs generated during the course of this study were sequenced to ensure that no errors had been introduced during cloning.

2.2.6 DNA sequencing

DNA sequencing was performed by The Sequencing Service (School of Life Sciences, University of Dundee, Scotland) using Applied Biosystems Big-Dye Ver 3.1 chemistry on an Applied Biosystems model 3730 automated capillary DNA sequencer.

2.2.7 Transformation of E. coli and S. cerevisiae

2.2.7.1 E. coli

Competent *E. coli* cells were prepared as follows. A 5 ml overnight culture of *E. coli* grown in the rich media, 2xYT, was used to inoculate 500 ml of the same media. Cells were then grown at 37ºC with constant shaking until they reached mid-log phase (an Optical Density at 600 nm (OD_{600}) of 0.4-0.6). Cells were harvested using centrifugation at 2095 *g* for 10 mins at 4ºC. The resultant cell pellet was resuspended in 50 ml of ice-cold 0.1 M $CaCl_2$ and left on ice for 1 hour. Cells were repelleted by centrifugation at 2095 *g* for 10 mins at 4ºC, before resuspension in 20 ml of ice-cold storage buffer (0.1 M $CaCl_2$/15% Glycerol). Competent cells were divided into 50 µl aliquots and stored at -80°C.

Competent *E. coli* cells were transformed as follows. 2 µl of plasmid DNA was added to 50 µl of XL-1 Blue competent cells (generated above) in 1.5 ml eppendorf tubes. Tubes were inverted to ensure proper mixing, and left on ice for 30 mins. The cells were heat shocked for 45 secs at 42^{o}C before adding 900 µl of 2xYT. The competent bacterial cells were allowed to recover for 1 hour at 37^{o}C, before harvesting by centrifugation at 16160 *g* for 5 mins and resuspension in 150 µl 2xYT. The cells were finally plated onto 2xYT containing Ampicillin (100 µg/ml) and incubated overnight at 37^{o}C.

2.2.7.2 S. cerevisiae

Competent yeast cells were prepared as follows. An overnight culture was used to inoculate 50 ml of the rich media, YPD, at an OD_{600} of 0.2. Cells were grown at 30ºC with constant shaking until they reached mid-log phase (OD_{600} of 0.5-1.0) at which point they were harvested by centrifugation at 3610 *g* for 2 mins. The cell pellet was washed in approximately 10 ml of LiTE-Sorb (0.1 M LiOAc, 10 mM Tris-HCl pH 7.6, 1 mM EDTA, 1.2 M Sorbitol) before being incubated for 1 hour at 30ºC with constant shaking in 1 ml of

LiTE-Sorb. The competent cells were rested on ice for 20 mins prior to transformation with DNA.

Competent yeast cells were transformed as follows. 200 µl of 70% (w/v) PEG-3350 was added to 200 µl of competent yeast cells in 1.5 ml eppendorf tubes, which were inverted to ensure proper mixing. 10 µl of DNA was added and again the tubes were mixed by inversion. No vortexing was performed, as this would have damaged the fragile, competent cells. The cells were incubated at 30^{o}C with shaking for 30-45 mins. After this incubation step the cells were heat shocked for 20 mins at 42^{o}C, before harvesting in a microcentrifuge at 3610 *g* for 2 mins. The resultant cell pellet was resuspended in 100 µl of sterile distilled water (dH_2O), plated onto selective media and incubated for 2-4 days at 30^{o}C. The selective media, on which the cells were plated, was dependent on the genotype of the yeast strain and the selective marker of the plasmid.

2.2.8 Rescue of plasmid DNA from S. cerevisiae

A volume of cells equivalent to an OD_{600} of 5 was harvested by centrifugation at 3610 *g* for 2 mins at room temperature. The supernatant was discarded and the resultant cell pellet resuspended in 500 µl of buffer S (100 mM K_2PO_4 pH 7.2, 10 mM EDTA, 50 mM β-mercaptoethanol, 50 µg/ml zymolyase). These cells were incubated at 37^{o}C for 30 mins before lysing by vortexing briefly in the presence of 100 µl of lysis buffer (25 mM Tris, pH 7.5, 25 mM EDTA, 2.5% (w/v) SDS) and incubating for 30 mins at 65^{o}C. 166 µl of 3 M KOAC was added prior to incubating on ice for 10 mins. The precipitated proteins were pelleted using micorcentrifugation at 16160 *g* for 10 mins at 4^{o}C. The supernatant, containing DNA, was collected and 0.8 ml of ice-cold ethanol added. The samples were then left on ice for 10 mins. The precipitated DNA was then collected using centrifugation at 16160 *g* and subsequently washed with 70% ethanol (v/v), air dried and resuspended in 40 µl of dH_20. 20 µl of the DNA was generally used to transform competent XL-1 Blue cells (see Section 2.2.7.1).

2.2.9 Electrophoretic separation of proteins

Electrophoretic separation of proteins was achieved using discontinuous SDS polyacrylamide gel electrophoresis (SDS-PAGE) as outlined by (Laemmli, 1970). Gels were composed of a stacking region (5% (v/v) acrylamide, 0.25 M Tris-HCl pH 6.8, 0.2% (w/v) SDS) and separating region (7.5-14.5% (v/v) (generally 10%) acrylamide, 0.75 M

Tris-HCl pH 8.8, 0. 2% (w/v) SDS). Gels were run in a tris-glycine electrophoresis buffer (25 mM Tris-HCl, 250 mM glycine, 0.1% (w/v) SDS). Protein samples analysed by SDS-PAGE were generally denatured by heating for 5 mins at either 65°C (for detection of polytopic membrane proteins, such as Ste3p and Gap1p) or 95ºC, in 2 x LSB (100 mM Tris-HCl pH 6.8, 4% (w/v) SDS, 20% (v/v) glycerol, 0.2% (w/v) bromophenol blue, 10% (v/v) β-Mercaptoethanol).

Protein separation was visualised by incubating the gel in Coomassie Brilliant Blue solution (0.25 g Coomassie Brilliant Blue R250 in methanol:d$H_2$0:glacial acetic acid (4.5:4.5:1 v/v/v)) for 1 hour, followed by destaining in destain solution (5% (v/v) methanol, 10% (v/v) glacial acetic acid) until bands were clearly visible.

2.2.10 Immunoblot Analysis

A Bio-Rad Trans-Blot® SD cell was used to transfer proteins from polyacrylamide gels to nitrocellulose membranes (Whatman Protran, 0.45 μ pore size). The gel, nitrocellulose membrane and 6 pieces of Whatman 3 mm paper were all presoaked in semi-dry transfer buffer (50 mM Tris-HCl, 40 mM glycine, 0.037% (w/v) SDS, 10% (v/v) methanol). The gel and nitrocellulose membrane were then sandwiched between the 6 sheets of Whatman paper and any air bubbles removed. A constant current of 180 mA was applied for 30 mins (for one gel) up to 60 mins (for four gels). After the proteins were transferred onto the nitrocellulose membrane, the membrane was blocked in 5% (w/v) non-fat dried milk in PBS/T (140 mM NaCl, 3 mM KCl, 1.5 mM KH_2PO_4, 8 mM Na_2HPO_4, 0.1% (v/v) Tween) for at least 30 mins. This step prevents the non-specific association of antibodies to the nitrocellulose. Alternatively, membranes probed with anti-CPY antibody were incubated with 5% (w/v) non-fat dried milk in TBS/T (20 mM Tris-HCl pH 7.5, 500 mM NaCl, 0.1% (v/v) Tween). The blocked membrane was then incubated with primary antibody diluted in 1-5% (w/v) non-fat dried milk in either PBS/T or TBS/T for 2 hours. The percentage of non-fat dried milk used was dependent on the purity/specificity of the primary antibody. Non-specifically bound primary antibody was subsequently washed off, leaving only the antibody specifically bound to the protein of interest, by washing the membrane for 6 times with 5 mins intervals between each wash. Again, the buffer used for washing was dependent on the primary antibody, either PBS/T or TBS/T. Next, the membrane was exposed to the appropriate secondary antibody diluted in 5% (w/v) non-fat dried milk in either PBS/T or TBS/T for 1 hour. Following another 6 x 5 mins washes, protein bands were visualised using enhanced chemiluminescence (ECL).

2.2.11 Antibody purification

2.2.11.1 IgG Affinity Purification

2 ml of 50% PrA-agarose slurry (Sigma-Aldrich) was allowed to settle before being washed with 10 ml of PBS (140 mM NaCl, 3 mM KCl, 1.5 mM KH_2PO_4, 8 mM Na_2HPO_4). 500 µl of PBS was added to 500 µl of sera and the diluted sera filtered through a 0.22 µm filter. The filtered serum was added to the agarose and incubated at 4ºC for 1 hour with constant rotation. The agarose was subsequently washed three times with 10 ml of PBS. At this stage the agarose was either incubated with more sera or eluted. Elution was achieved by adding 6 times 0.5 ml of elution buffer (50 mM Glycine pH 2.5). The six elution fractions collected were treated as follows: the first elution fraction was neutralized with 25 µl of 1 M Tris pH 10 and fractions 2-6 were neutralized with 70 µl of 1 M Tris pH 10. The fractions with the highest protein concentration (measured by their absorbance at 280 nm) were pooled and dialysed overnight against 5 L of PBS.

2.2.11.2 Peptide Affinity Purification

Peptide affinity purification was performed using the Sulfolink® kit (Pierce Biotechnology; cat # 44895).

First the peptide (supplied by Eurogentec) was coupled to the SulfoLink® Coupling gel column. This was achieved by equilibrating the column with 8 ml of coupling buffer (50 mM Tris, 5 mM EDTA-Na, pH 8.5). 15.5 mg of the hydrogenated peptide was rehydrated in 2-3 ml of coupling buffer and added to the column. The immobolised peptide was incubated with end-over-end rotation at room temperature for 15 mins, followed by an additional 30 mins without mixing at room temperature. The column was drained and subsequently washed with 6 ml of coupling buffer. Non-specific binding sites on the matrix were blocked to prevent non-specific association with the column; this can occur when the column becomes exposed to proteins which contain free sulfhydryl groups. Blocking of the matrix was achieved by applying a 0.05 M cysteine solution to the column, followed by a 15 min incubation with end-over-end rotation and a static 30 min incubation at room temperature. Subsequently the column was drained and washed with 12 ml of wash solution (1.0 M NaCl, 0.05% (w/v) NaN_3) followed by 4 ml of degassed PBS containing 0.05% (w/v) NaN_3. 2 ml PBS containing 0.05% (w/v) NaN_3 was further applied to the column once the bottom cap was replaced and a porous disc added to the top

of the column to within 1 mm of the gel bed, this prevents the column from drying out as well as the resuspension of the packed gel bed. At this stage the column was ready to utilise in the purification of antibodies from the immunised sera. Purification was performed under static conditions.

The purification protocol involved equilibrating the column with 6 ml of Sample Buffer (PBS). Next, 1.5 ml of sera was added to the column and allowed to enter the matrix completely; this was followed by the addition of 0.2 ml of Sample Buffer. The bottom cap was replaced on the column and a further 0.5 ml of Sample Buffer applied. The top cap was subsequently replaced and the column incubated at room temperature for 1 hour. The matrix was washed with 12 ml of Sample Buffer (PBS) and the bound antibodies eluted using 8 ml of Elution Buffer (100 mM Glycine, pH 2.5-3.0). 1 ml fractions were collected and neutralized by the addition of 100 µl of 1 M Tris, pH 7.5. Elutions were monitored by measuring the absorbance at 280 nm, and those fractions with the largest value of absorbance, pooled and dialysed at 4ºC, overnight, against 5 L PBS.

2.2.12 Preparation of yeast whole cell lysates for immunoblot analysis

To assess the steady-state levels of protein in yeast whole cell lysates, cells grown to mid-log phase (OD_{600} of 0.5-1.0) were harvested by centrifugation at 3610 *g* for 2 mins. The resultant cell pellets were washed in distilled water (dH_20) and resuspended at 100 OD_{600} units/ml in Twirl Buffer (50 mM Tris pH 6.8, 5% (w/v) SDS, 8 M Urea, 10% (v/v) Glycerol, 0.2% (w/v) Bromophenol Blue, 10% (v/v) β-mercaptoethanol). Whole cell lysates were generated by incubating for 10 mins at 65ºC, followed by brief vortexing. The denatured proteins contained within 10 µl of whole cell lysate were separated by SDS-PAGE prior to immnoblot analysis.

2.2.13 Testing copper toxicity and osmotic sensitivity

Yeast cells transformed with the appropriate plasmids were grown to mid-log phase ($O.D_{600}$ 0.6-1.0) in the selective media, SD-ura-met containing 50 µM $CuCl_2$. Cells were harvested by centrifugation at 3610 *g* for 2 mins and the resultant cell pellet was resuspended at an OD_{600} of 0.8 in sterile dH_2O. Subsequent dilutions of this culture were performed generating cultures with a final OD_{600} of 0.8, 0.08, 0.008, 0.0008. 5 µl of each culture was spotted onto the appropriate media; SD-ura-met, SD-ura-met containing

50 µM $CuCl_2$ (to investigate copper toxicity) or SD-ura-met containing both 50 µM $CuCl_2$ and 1.5 M KCl (to investigate osmotic sensitivity).

2.2.14 Trichloroacetic Acid (TCA) precipitation of secreted proteins

Yeast cells transformed with the appropriate plasmids were grown to an OD_{600} of 1.0 in 20 ml of the selective media, SD-ura-met, containing 50 µM $CuCl_2$. Cells were harvested by centrifugation at 931 *g* for 2 mins and 18 ml of the supernatant collected. Ice-cold TCA (50% (w/v)) was added to a final concentration of 10% (v/v) and the samples incubated on ice for a minimum of 30 mins. The precipitated proteins were collected by centrifugation at 16160 *g* for 10 mins at 4°C. The resultant pellets were washed with ice-cold acetone and re-pelleted at 16160 *g* for 10 mins at 4°C before being left to air dry at room temperature. The precipitated proteins were finally resuspended in LSB (500 µM Tris pH 6.8, 10% (v/v) glycerol, 5% (w/v) SDS, 0.2% (w/v) Bromophenol Blue, 10% (v/v) β-mercaptoethanol), vortexed and incubated at 95ºC for 5 mins. 5 µl of a saturated Tris-HCl solution at pH 8.0 was added to any samples that had turned yellow in colouration (resulting from a low pH). The precipitated proteins were separated using SDS-PAGE and the amount of CPY secreted assessed using immunoblot analysis with an antibody specific to CPY.

2.2.15 Ste3p receptor endocytosis assay

Yeast cells transformed with the appropriate plasmids were grown for one generation (i.e. until they reached an OD_{600} of 0.4-0.6) in 50 ml of the selective media, S-Raf/Gal-ura-leu (0.675% (w/v) Yeast Nitrogen Base without amino acid, 0.183% (w/v) synthetic complete drop-out: -ura-leu, 2% (w/v) raffinose, 2% (w/v) galactose) before adding glucose at a final concentration of 3% (v/v). The addition of glucose switches off the expression of Myc-tagged Ste3p from the *GAL1* promoter allowing the degradation of Ste3p-Myc to be monitored. Cells were collected immediately after the addition of glucose (time-point 0) and again after a 20, 40 and 60 min incubation at 30ºC. Further degradation of Ste3p was prevented by incubating the cells on ice in the presence of 15 mM NaN_3. Cells collected at the 0, 20, 40 and 60 min time-points were harvested by centrifugation at 3610 *g* for 2 mins and lysed by the resuspending in Twirl Buffer (5% (w/v) SDS, 8 M Urea, 10% (v/v) Glycerol, 500 µM Tris pH 6.8, 0.2% (w/v) Bromophenol Blue, 10% (v/v)

β-mercaptoethanol) at a volume equivalent to 100 OD_{600}/ml and incubating for 10 mins at 65 ºC. The denatured proteins present in whole cell lysates were separated by SDS-PAGE and the amount of Ste3p-Myc at time-points 0, 20, 40 and 60 min was assessed using immunoblot analysis with an antibody specific to the Myc-tag.

2.2.16 FM4-64 and Vacuolar labelling

Vacuolar membrane morphology and endocytosis dynamics were monitored using the lipophilic styryl dye, N-(3-triethylammoniumpropyl)-4-(p-diethylaminophenylhexatrienyl) pyridium dibromide (FM4-64). The method used was similar to that described in detail in (Vida and Emr, 1995).

Yeast cells transformed with the appropriate plasmids were grown in the selective media, SD-ura-met, containing 50 µM $CuCl_2$ until they reached mid-log phase (OD_{600} of 0.8-1.0). The cells were harvested by centrifugation at 3610 *g* for 2 mins and resuspended in chilled media, SD-ura-met, to a final concentration of 20-40 OD_{600}/ml. FM4-64 was added to the culture at a final concentration of 30 µM from a stock solution of 1 mM in Dimethyl Sulfoxide (DMSO). Henceforth the cells were kept in the dark. They were incubated with FM4-64 for 30 mins at 0^{o}C before being harvested by centrifugation at 3610 *g* for 2 mins at 0^{o}C. The chase period was initiated by resuspending the cells in fresh pre-warmed media, SD-ura-met, at a concentration of 10-20 OD_{600}/ml. Cells were collected after 10 and 45 mins and NaN_3 added to the cells at a final concentration of 15 mM to terminate the chase period. Cells were kept on ice until they were visualized using fluorescence and differential interference contrast (DIC) microscopy.

2.2.17 Immunofluorescence

Yeast cells transformed with the appropriate plasmids were grown in 10 ml of the selective media, SD-ura-met, containing 50 µM $CuCl_2$ until they reached mid-log phase ($O.D._{600}$ 0.6-1.0). Pre-fixing of the cells was achieved by incubation at room temperature for 1 hour in the presence of 3.7% (v/v) formaldehyde. Fixation was performed by resuspending the pre-fixed cells in 2 ml of fixative (45 µM NaOH, 4% (w/v) paraformaldehyde, 0.1 M KH_2PO_4) and leaving at room temperature overnight (16 hours) with constant agitation. The following day the fixed cells were harvested by centrifugation at 3610 *g* for 2 mins, resuspended in 750 µl TEβ (200 mM Tris pH 8, 20 mM EDTA, 1% (v/v) β-mercaptoethanol) and incubated for 10 mins at 37ºC. Fixed cells were subsequently

spheroplasted by resuspending in 1 ml of spheroplasting buffer (1.2 M Sorbitol, 50 mM KPi pH 7.3, 1 mM $MgCl_2$, 15 µl of 15 mg/ml yeast lytic enzyme) and incubating at 30ºC for 45 mins. The spheroplasts were permeabilised at room temperature for 5 mins in the presence of 2.5% (w/v) SDS in 1.2 M Sorbitol. The permeabilised cells were washed once with 1 ml Sorbitol, and resuspended in 400 µl of 1.2 M Sorbitol.

Permeabilised cells contained within 40 µl of cells prepared as described above were allowed to adhere to Poly-L Lysine coated mutliwell slides (40 µl of cells were added to each well) for 15 mins. The liquid was removed from the wells before washing twice with PBS-BSA (PBS + 5 mg/ml BSA). Non-specific binding sites on the cells were blocked by incubating for an hour in a humid container in the presence of 30 µl of a 1:100 dilution of donkey sera made up in PBS-BSA. The blocking solution was removed and 30 µl of the primary antibody solution containing anti-HA and anti-Tlg2p (both at a 1:50 dilution; see Section 2.1.4.2) was added to the wells and left to incubate at room temperature for 2 hours. Subsequently the wells were washed seven times with PBS-BSA before the secondary antibodies were added (Alexa Fluor® 488 donkey anti-rat IgG and Alexa Fluor® donkey anti-rabbit IgG at a 1:50 dilution; see Section 2.1.4.2). The cells were left for a further hour in a dark humid environment. Again the cells were washed with PBS-BSA nine times. The mounting solution, Immu-mount (Thermo Electron Corperation, Pittsburgh), was added to the wells and coverslips fixed and sealed. Cells were visualised using a 100x oil immersion objective on a Zeiss LSM410 laser confocal imaging system. Image sets were processed and overlaid using Adobe Photoshop™.

2.2.18 Immunoprecipitation from yeast cell lysates

Yeast cells transformed with the appropriate plasmids were grown at 25°C for one generation (OD_{600} 0.4-0.6) in 500 ml of SD-ura-met containing 50 µM $CuCl_2$. For temperature sensitive experiments only, cells were either left at 25°C or transferred to the non-permissive temperature of 37°C for 30 mins. Cells were harvested by centrifugation at 931 *g* for 2 mins and the resultant cell pellets washed in 10 ml of YPD-Sorb (50% (v/v) YPD, 50% (v/v) 2.4 M sorbitol) before spheroplasting for 1 hour in the presence of 5 ml YPD-Sorb to which 15 µl β-mercaptoethanol and 50 µl Yeast Lytic Enzyme (15 mg/ml) had been added. Spheroplasts were lysed by resuspending in 5 ml of lysis buffer (200 mM sorbitol, 100 mM KoAc, 1% (v/v) Triton-X, 50 mM KCl, 20 mM Tris-HCl pH 6.8) and incubating for 1 hour at 4ºC. The lysates were collected by pelleting the cell debris using centrifugation at 2095 *g* for 5 mins. 1.2 ml of cleared lysate was incubated on ice for

15 mins with 50 µl of PrA-agarose to remove those proteins that non-specifically bind to the agarose. 1.1 ml of lysate was collected after pelleting the PrA-agarose using centrifugation at 7370 *g* for 5 mins and incubated with 10 µl of anti-HA antibody for 2 hours at 4°C. 50 µl of PrA-agarose was subsequently added and the samples left incubating for a further 1 hour at 4°C with constant agitation. The PrA-agarose was then washed three times with 1 ml of lysis buffer and the bound proteins eluted by heating at 100°C for 5 mins in the presence of 30 µl LSB. The eluted proteins were analysed using SDS-PAGE immunoblot analysis with antibodies specific to Vps45p and the HA-tag.

2.2.19 Pulse-Chase Experiments

Yeast cells transformed with the appropriate plasmids were grown to mid-log phase (not exceeding an OD_{600} of 1.0) in the selective media, SD-ura-met, containing 50 µM $CuCl_2$, at which point a volume of cells equivalent to an OD_{600} of 1.0 was harvested by centrifugation at 3610 *g* for 2 mins. The resultant cell pellets were resuspended in labelling media (SD-met, 50 µM $CuCl_2$, 50 mM Kphos pH 5.7, 2 mg/ml BSA) to which 20 µl of label, Promix L-[^{35}S] *in vivo* cell labeling mix SJQ0079 (Amersham) was added and incubated for 10 mins at 30ºC. 100 µl of chase (5 mg/ml cysteine/methionine) was added to the cells and a 500 µl sample collected immediately (time-point 0) with another being collected following a 30 mins incubation at 30ºC. 20 µl of 1 M NaN_3 was added to each sample immediately, following its collection, to prevent any subsequent trafficking of CPY. Cells collected at time point 0 and after 30 mins were harvested by centrifugation at 3610 *g* for 2 mins. The supernatant was removed into a fresh tube and 100 µl of 10 x IP Buffer (0.9 M Tris pH 8.0, 1% (w/v) SDS, 1% (v/v) Triton X-100, 0.02 M EDTA pH 8.0) was added. The samples were then incubated at 100ºC for 5 mins. The cell pellets were spheroplasted by resuspending in 150 µl Spheroplasting Buffer (1.4 M Sorbitol, 50 mM Tris pH 7.4, 2 mM $MgCl_2$ 10 mM NaN_3 to which 3 µl of β-mercaptoethanol and 15 µl of lyticase per ml were added immediately before use) followed by an incubation of 1 hour at 30ºC. At this stage 50 µl of 2% (v/v) SDS was added to the spheroplasts which were subsequently boiled at 100ºC for 5 mins. Generally, at this stage, the samples were stored overnight at -20°C. The following day, 100 µl of 10 x IP-SDS (0.9 M Tris pH 8.0, 1% (v/v) Triton X-100, 0.02 M EDTA pH 8.0), 700 µl dH_20 and 50 µl of ZYSORBIN (ZEMED® Laboratories, Invitrogen) were added to the spheroplasts and 400 µl dH_20 and 50 µl ZYSORBIN added to the supernatant. Samples were then incubated on ice for 15 mins before pelleting the ZYSORBIN and associated proteins by microcentifuging at 16160 *g* for 5 mins. This step removed those proteins which bind non-specifically to the

ZYSORBIN. The resultant supernatants were transferred to fresh tubes containing 15 µl of a 1:10 dilution of anti-CPY antiserum (see Section 2.1.4.1) and the solution vortexed briefly before reincubating on ice for 90 mins. 50 µl of ZYSORBIN was then added to each tube and the solutions left on ice for a further 45 mins. The ZYSORBIN was pelleted by centrifugation at 16160 *g* for 1 min, and the resultant pellet washed twice with 1 ml IP Buffer (0.09 M Tris pH 8.0, 0.1% (w/v) SDS, 0.1% (v/v) Triton X-100, 0.002 M EDTA pH 8.0) before eluting in 15 µl of 2 x LSB at 100°C for 5 mins. The ZYSORBIN was separated from the eluted proteins using microcentrifugation at 16160 *g* for 1 min and 10 µl of the eluted proteins separated by SDS-PAGE (7.5% (v/v) polyacrylamide gel). The resultant gel was fixed by incubating in fixative (25% (v/v) Methanol, 10% (v/v) Acetic Acid) for 30 mins. The fixative was removed by washing the gel in dH_2O. The gel was subsequently incubated for a further 30 mins in the presence of the water soluble fluor Sodium Salicylate (at a final concentration of 1 M), washed in dH_20, dried down and a piece of Medical X-ray film (Kodak) placed on the gel and left for 2-3 days at -80ºC.

2.2.20 Recombinant Protein Expression and Purification

Chemically competent BL21 Star™ (DE3) cells (Invitrogen) were transformed with plasmids, pCOG025 (Carpp et al., 2006), pALA001, pFB09/1, pGEX-DSK2$_{UBA}$ or pCAL1 driving the expression of the appropriate fusion proteins (Tlg2$_{cyto}$-PrA, Sx16A$_{cyto}$-PrA, Sx4$_{cyto}$–PrA, GST-UBA and GST-mutUBA, respectively). 5 ml overnight cultures of transformed cells were used to inoculate 500 ml of Terrific Broth medium containing 100 µg/ml of the antibiotic Ampicillin. Cells were grown at 37ºC with constant rotation until they reached mid-log phase (O.D.$_{600}$ 0.5-0.7) before protein expression was induced by the addition of Isopropyl-β-D-1-thiogalactopyranoside (IPTG), at a final concentration of 1 mM, for 4 hours. Cells were harvested using centrifugation at 3273 *g* for 20 mins. Cell pellets were washed in 20 ml of PBS and stored at -20ºC. Frozen cell pellets were thawed on ice and resuspended in 20 ml of PBS. Lysis was then performed by incubating the cells on ice in the presence of Lysozyme at a final concentration of 1 mg/ml for 30 mins, followed by 6 times 20-sec bursts of sonication (Sanyo Soniprep 150) with intervals of 20 secs rests on ice. Lysed cells were clarified by centrifugation at 48400 *g* for 25 mins at 4ºC.

2.2.20.1 Purification of PrA-tagged proteins

500 µl of settled IgG Sepharose™ 6 Fast Flow (GE Healthcare) was equilibrated by washing in 2 ml of TST (Tris-saline Tween 20 (TST); 50 mM Tris-HCl pH 7.6, 150 mM NaCl and 0.05% Tween 20) followed by 1 ml of HAc pH 3.4 (0.5 M acetic acid adjusted to pH 3.4 with ammonium acetate), 1 ml of TST, 1 ml of HAc pH 3.4 and 2 ml of TST. The equilibrated Sepharose was then incubated with clarified *E. coli* lysate (prepared as described above in Section 2.2.20) for 2 hours at 4ºC with rotation. Unbound proteins were removed by centrifugation at 70 *g* for 2 mins and the pelleted sepharose washed 8 times with TST. Proteins bound to the IgG Sepharose were assessed by eluting a small fraction of beads (20 µl) using 0.5 M HAc pH 3.4. An equivalent volume of 2 x LSB was then added prior to incubation at 95ºC for 5 mins. 5 µl of a saturated Tris-HCl solution at pH 8.0 was added to each of the samples to increase their pH. The Sepharose was then pelleted by centrifugation at 70 *g* for 2 mins and the proteins present in the eluate separated by SDS-PAGE. The amount and purity of purified proteins were assessed by Coomassie staining the gel.

2.2.20.2 Purification of GST-tagged proteins

600 µl of glutathione-Sepharose™ 4B (GE Healthcare) suspension was washed 3 times with 1 ml PBS, resuspended in 0.5 ml of PBS and added to a cleared *E. coli* lysate (prepared as described above in Section 2.2.20). The Sepharose was incubated with the lysate for 1 hour at 4ºC with constant rotation. At the end of this incubation the Sepharose was washed a further 3 times with 1 ml PBS. Finally, the beads were resuspended in a volume of PBS (supplemented with protease inhibitors (1 tablet of complete protease inhibitors (Roche)/50 ml PBS)) equivalent to the volume of settled beads. The levels of recombinant proteins associated with the sepharose was analysed by diluting a sample of the sepharose (5 µl) 1:5 with LSB. Proteins were eluted from the sepharose by heating at 65ºC for 10 mins and separated from the Sepharose by centrifugation at 70 *g* for 1 min. The recombinant proteins that were associated with the beads were compared to purified GST (as a means to monitor whether or not the fusion proteins had degraded) as well as BSA standards of known protein content. Comparison was performed by separating the eluted proteins by SDS-PAGE and Coomassie staining the resultant gel.

2.2.21 Pull-down assays

2.2.21.1 Vps45p pull-downs from yeast lysates

Yeast cells transformed with the appropriate plasmids were grown to mid-log phase (OD_{600} of 0.6-1.0) in 100 ml of the selective media, SD-ura-met. The cells were then pelleted at 931 *g* for 2 mins, before resuspending in 100 µl of binding buffer (40 mM Hepes.KOH pH 7.4, 150 mM KCl, 1 mM DTT, 1 mM EDTA, 0.5% NP-40) per OD_{600}. A volume of glass beads equivalent to half the volume of resuspended cells was added and the cells lysed by vortexing four times for 30 sec each time with 1 min intervals on ice. Unlysed cells and the glass beads were pelleted by centrifugation at 70 *g* for 5 mins. A sample of lysate was saved for later analysis. Lysates were then added to Sepharose pre-bound by Tlg2-PrA, Sx16-PrA or Sx4-PrA (see Section 2.2.20.1) and the beads incubated overnight at 4ºC mixing end-over-end. The beads were then harvested, the supernatant removed and the Sepharose washed three times with TST. Finally, proteins bound to the beads were eluted by the addition of 40 µl HAc pH 3.4; 20µl of the eluate was removed and incubated at 95ºC for 5 mins in the presence of 20 µl of 2 x LSB. 5 µl of a saturated Tris-HCl solution at pH 8.0 was added to each of the samples to increase their pH. The eluted proteins were separated by SDS-PAGE prior to immunoblot analysis with an antibody specific to the HA-tag.

2.2.21.2 Ubiquitin pull-downs from yeast lysates

Yeast cells transformed with the appropriate plasmids were grown in 50 ml of the selective media, SD-ura-met, containing 100 µM $CuCl_2$, until they reached mid-log phase (OD_{600} of 0.6-1.0). They were then harvested at 931 *g* for 2 mins and spheroplasted by incubating at 30°C for 1 hour in the presence of 5 ml YPD-Sorb (50% (w/v) YPD, 50% (w/v) 2.4 M sorbitol) containing 15 µl of β-mercaptoethanol and 50 µl of Yeast Lytic Enzyme. Spheroplasts were collected by centrifugation at 2095 *g* for 5 mins and subsequently lysed in 250 µl lysis buffer (200 mM Sorbitol, 100 mM KoAc, 1% (v/v) Triton-X, 50 mM KCl, 20 mM Pipes pH 6.8, 3 mM NEM, 1 tablet of complete protease inhibitors (Roche)/50 ml PBS) for 1 hour at 4°C, mixing end-over-end. The cell lysates were cleared by centrifugation at 12470 *g* for 15 mins at 4ºC. 10 µl of the lysate was collected and treated by adding 10 µl of 2 x LSB, followed by 15 mins incubation at 65°C (this sample is representative of the yeast cell lysate). 100 µl of the cleared lysate was added to 10 µl of glutathione-Sepharose 4B pre-bound with either GST-UBA or GST-mutUBA (see Section

2.2.20.1) and rotated at 4°C for 2 hours. Beads were subsequently washed 3 times with 1 ml of PBS. Proteins were eluted from the beads by the addition of 20 µl of LSB followed by a 15 min incubation at 65ºC. The eluted proteins were separated from the Sepharose by centrifugation at 70 *g* for 1 min and analysed using SDS-PAGE and immunoblot analysis with antibodies specific to Tlg2p, the HA-tag or the GFP-tag.

2.2.22 Functional assay for degradation of Tlg2p

Yeast cells transformed with the appropriate plasmids were grown to mid-log phase ($O.D_{600}$ 0.6-1.0) in the selective media, SD-ura-met. Cells were subsequently harvested by centrifugation at 3610 *g* for 2 mins. The resultant cell pellets were resuspended in sterile dH_2O at an OD_{600} of 0.8. Subsequent dilutions of this culture were performed generating cultures with a final OD_{600} of 0.8, 0.08, 0.008, 0.0008. 5 µl of each culture was spotted onto SD-ura-met and SD-his.

2.2.23 Hydroxylamine Treatment

The method used was similar to that described in detail in (Valdez-Taubas and Pelham, 2005).

Yeast cells transformed with the appropriate plasmids were grown to mid-log phase (OD_{600} of 0.6-1.0) in 50 ml of the selective media, SD-ura-met, containing 100 µM $CuCl_2$. Cells were harvested using centrifugation at 931 *g* for 2 mins and the resultant cell pellets resuspended in 5 ml of YPD-Sorb (50% (v/v) YPD, 50% (v/v) 2.4 M sorbitol), to which 15 µl of β-mercaptoethanol and 50 µl of yeast lytic enzyme were added and incubated at 30°C for 1 hour. The spheroplasts were then collected by centrifugation at 2,095 *g* for 5 mins and lysed by resuspending in 250 µl of lysis buffer (200 mM Sorbitol, 100 mM KoAc, 1% (v/v) Triton-X, 50 mM KCl, 20 mM Pipes pH 6.8, 3 mM NEM, 1 tablet of complete protease inhibitors (Roche)/50 ml PBS) and incubating for 1 hour at 4°C, mixing end-over-end. The cell lysates were cleared by centrifugation at 12470 *g* for 15 mins at 4ºC. The protein concentration of the cell lysates was estimated using the Bradford protein assay (see Section 2.2.24), 100 µg of protein extract, in a volume no greater than 50 µl, was then incubated with either 600 µl of 1 M Hydroxylamine-HCl pH 7.4 or 600 µl of 1 M Tris-HCl for 1 hour at room temperature. A mixture of chloroform-methanol (650 µl chloroform, 150 µl methanol) was added to each reaction mixture and the samples vortexed. Centrifugation at 16160 *g* was performed on the samples for 2 mins and the

upper phase removed carefully without disturbing the proteins present in the interphase. 450 µl methanol (100% (v/v)) was added, the samples vortexed and proteins pelleted using centrifugation at 16160 *g* for 2 mins. The pelleted proteins were air dried before resuspending in 100 µl of LSB (lacking the reducing agent β-mercaptoethanol) prior to incubation at 65ºC for 15 mins. 20 µl of these precipitated proteins were separated using SDS-PAGE prior to immunoblot analysis with antibodies specific to the HA-tag.

2.2.24 Bradford protein assay

Protein concentration was estimated using the Bradford protein assay. A 1 mg/ml stock of bovine serum albumin (BSA) dissolved in dH_2O was used to generate standards of known protein concentration (0.1, 0.2, 0.3, 0.4, 0.5, 0.6, 0.7, 0.8, 0.9, 1.0 mg/ml) by diluting in dH_2O. 20 µl of each of the standards and 20 µl of a 1:100 dilution of protein extract(s) (diluted in dH_20) were mixed in separate 1 cm pathlength disposable cuvettes with 1 ml of Quick Start™ Bradford Dye Reagent (Bio-Rad Laboratories, Inc.). The absorbance of each solution was measured at 595 nm and a graph constructed of the absorbance at 595 nm against protein concentration for the protein standards. The Bradford protein assay gives a hyperbolic curve, which at low protein concentrations gives a relatively straight line. The equation of the linear range of this graph was utilised to calculate the concentration of proteins present in the protein extract(s).

Table 2.1 - *E. coli* and *S. cerevisiae* strains used in this study

***E. coli* strains used in this study:**			
Strain	**Genotype**		**Source**
BL-21 Star™ (DE3)	F^- *ompT* *hsd*$S_B(r_B^-m_B^-)$ *gal dcm rne131* (DE3)		Invitrogen
TOP10	F^- *mcrA* Δ(*mrr-hsd*RMS-*mrc*BC) ϕ80*lac*ZΔM15 Δ*lac*X74 *rec*A1 *ara*D139 Δ(*ara-leu*)7697 *gal*K *rps*L (Str^R) *end*A1 *nup*G		Invitrogen
XL1 Competent Blues	*recA1 endA1 gyrA96 thi-1 hsdR17 supE44 relA1 lac* [F´ *proAB lacI*qZΔ*M15* Tn*10* (Tetr)].		Invitrogen
***S. cerevisiae* strains used in this study:**			
Strain	Genotype	Construction	Reference
RPY10	*MAT*α *ura3-52 leu2-3, 112 his4-519 ade6 gal2*		(Piper et al., 1994)
SF838-9D	*MAT*α *ura3-52 leu2-3, 112 his4-519 ade6 gal2 pep4-3*		(Rothman and Stevens, 1986)
SEY6210	*MAT*α *ura3-52 his3-Δ200 lue2-3, 112 lys2-801 trp1-Δ901 suc2-Δ9 ade2-101*		(Robinson et al., 1988)
RMY8	*MAT*α *ura3-52 his3-Δ200 lue2-3, 112 lys2-801 trp1-Δ901 suc2-Δ9 ade2-101 pep4-3*	*Eco*RI digested pPLO2010 (Nothwehr et al., 1995) was used to disrupt *PEP4* in SEY6210	Constructed by Dr. Rebecca K. McCann (This study)
NOzY4	*MAT*α *ura3-52 leu2-3, 112 his4-519 ade6 gal2 tlg2Δ::Kan^r*		(Bryant and James, 2001)
NOzY2	*MAT*α *ura3-52 leu2-3, 112 his4-519 ade6 gal2 vps45Δ::Kan^r*		(Bryant and James, 2001)
NOzY3	*MAT*α *ura3-52 leu2-3, 112 his4-519 ade6 gal2 pep4-3 tlg2Δ::Kan^r*		(Bryant and James, 2001)
NOzY1	*MAT*α *ura3-52 leu2-3, 112 his4-519 ade6 gal2 pep4-3 vps45Δ::Kan^r*		(Bryant and James, 2001)
MSY001	*MAT*α *ura3-52 his3-Δ200 lue2-3, 112 lys2-801 trp1-Δ901 suc2-Δ9 ade2-101 tlg2Δ::Kan^r*	*Not*I digested pUG7 (Seron et al., 1998) used to disrupt *TLG2* in SEY6210	(Seron et al., 1998)
LCY007	*MAT*α *ura3-52 his3-Δ200 lue2-3, 112 lys2-801 trp1-Δ901 suc2-Δ9 ade2-101 vps45Δ::Kan^r*	*Sma*I/*Sph*I digested pNOz13 (Bryant and James, 2001) used to disrupt *VPS45* in SEY6210	Constructed by Dr Lindsay N. Carpp (This study)
LCY011	*MAT*α *ura3-52 leu2-3, 112 sec18-1 tlg2Δ::Kan^r*	*Not*I digested pUG7 (Seron et al., 1998) used to disrupt *TLG2* in SEY5186 (Emr et al., 1984)	Constructed by Dr. Lindsay N. Carpp (This study)

Table 2.2 - Oligonucleotides used in this study

Oligo	Description	Sequence
105	***CUP1****SX16A*	**GATATTAAGAAAAACAAACTGTACAATCAATC AATCAATCATCACATACC**ATGGCCACCAGGCG TTTAACCGAC
106	***3'UTR****SX16A*	**ATTATAACGTATTAAATAATATGTGAAAAAAG AGGGAGAGTTAGATAGGA**TTATCGAGACTTCA CGCCAACGAG
258	***CUP1HA****SX16A*	**AATCAATCATCACATAAAATGTACCCATACGA TGTTCCGGATTACGCT**GCCACCAGGCGTTTAAC C
259	reverse complement of 258	GGTTAAACGCCTGGTGGC**AGCGTAATCCGGAA CATCGTATGGGTACATTTTATGTGATGATTGA TT**
314	***CUP1HA****TLG2*	**GATATTAAGAAAAACAAACTGTACAATCAATC AATCAATCATCACATAAAATGTACCCATACGA TGTTCCGGATTACGCT**TTTAGAGATAGAACTA ATTTATTTTT
311	***3'UTR****TLG2*	**ATTATAACGTATTAAATAATATGTGAAAAAAG AGGGAGAGTTAGATAGGA**TCAAAGTAGGTCAT CCAAAGCAT
315	***CUP1HA****SX4*	**GATATTAAGAAAAACAAACTGTACAATCAATC AATCAATCATCACATAAAATGTACCCATACGA TGTTCCGGATTACGCT**CGCGACAGGACCCACG AGTTG
313	***3'UTR****SX4*	**ATTATAACGTATTAAATAATATGTGAAAAAAG AGGGAGAGTTAGATAGGA**TTATCCAACGGTTA TGGTGATGC
63	***CUP1****TLG2*	**GATATTAAGAAACTGTACAATCAATCAATCAA TCATCACATAAA**ATGTTTAGAGATAGAACTAAT TA
66	***3'UTRHA****TLG2*	**ATTATAACGTATTAAATAATATGTGAAAAAAG AGGGAGAGTTAGATAGGATCAAGCGTAATCC GGAACATCGTATGGGTA**AAGTAGGTCATCCAA
301	*XbaI**HA**SX16A*	AATCTAG**ATGTACCCATACGATGTTCCG**
303	*XhoISX16A*	AACTCGAGTTATCGAGACTTCACGCC
308	*XbaI**HA**SX4*	AAATCTAG**ATGTACCCATACGATGTTCCGGAT TACGCT**CGCGACAGGACCCACGAGTTG
310	*XhoISX4*	AAACTCGAGTTATCCAACGGTTATGGTGATGCC
383	*XbaI**HA**TLG2(Δ2-230)*	AATCTAG**ATGTACCCATACGGATGTTCCGGAT TACGCT**ACGTTGCAGAGACAGCAACAG
384	*XhoITLG2*	AACTCGAGTCAAAGTAGGTCATCCAAAGC
382	*XbaI**HA**SX16A(Δ2-205)*	AATCTAG**ATGTACCCATACGGATGTTCCGGAT TACGCT**TTAGTTCTGGTGGACCAGAAC
286	*NdeISX16A(1-278)*	CATATGGCCACCAGGCGTTTAACC
287	*XhoISX16A(1-278)*	CTCGAGCTTCCGATTCTTCTTTTGATACTG
267	*XhoITLG2*	GGCTCGAGTCAACTGACCCCTTCTTTTTACC
268	*XbaITLG2*	CGTCTAGACAAAACAAAAACTTGCCCCGAGC
269	*BamHIHIS3*	CGGGATCCATGACAGAGCAGAAAGCCCTAG
270	*SalIHIS3*	ACGTCGACCATAAGAACACCTTTGGTGGAGG
316	*TLG2BamHISalITLG2*	TTGGGCGATGATCAAGGATCCAAAGTCGACGAT ATTGAAATGGGTAC

317	reverse complement of 316	TACCCATTTCAATATCGTCGACTTTGGATCCTTG ATCATCGCCCAAG
214	*TLG2**K26R**TLG2*	ACTTTCTCATCTGG**GAG**AGCACCCTTGGGCG
215	reverse complement of 214	CGCCCAAGGGTGC**TCT**CCCAGATGAGAAAGT
333	*TLG2**K189R, K193R, K198R**TLG2*	TTGAAATTCTTGAAC**AGA**GATGATTTG**AGA**CCT ATCCGCAAT**AGA**GCCAGTGCAGAGAAC
334	reverse complement of 334	GTTGTGTGCACTGGC**TCT**ATTGCGGATAGG**TCT** CAAATCATC**TCT**GTTCAAGAATTTCAA
335	*TLG2**K218R, K229R**TLG2*	GAGGCAGCAAGAGAG**AGA**AGAGAGGGCCTCGA TATTGAAGACTATTCA**AGA**AGGACGTTGCAGAG A
336	reverse complement of 335	TCTCTGCAACGTCCT**TCT**TGAATAGTCTTCAATA TCGAGGCCCTCTCT**TCT**CTCTCTTGCTGCCTC
352	*DSK2**M342R, F344A**DSK2*	GACAACTAAACGAC**AGG**GGC**GCC**TTCGATTTCG ATAGAAAC
353	reverse complement of 352	GTTTCTATCGAAATCGAA**GGC**GCC**CCT**GTCGTT TATTGGTC
407	*TLG2**K305R, K311R, K315R**TLG2*	GCAACACACTACCAGAGAAGAACTCAAAGATGT AGAGTCATTTTATTACTAACA
408	reverse complement of 407	TGTTAGTAATAAAATGACTCTACATCTACATCTT TGAGTTCTTCTCTGGTAGTGTGTTGC
380	*TLG2ΔC**STOP, STOP3'UTR***	TTCTTTGTTATGTTGAAA**TGATGA**CCACATGGCG GTGGC
381	reverse complement of 380	GCCACCGCCATGTGG**TCATCA**TTTCAACATAAC AAAGAA
397	*BamHITLG2*	GGCAGTCGTTACAAACGGATCCATGTTTAGAGA TAGAAG
398	reverse complement of 397	CTTCTATCTCTAAACATGGATCCGTTTGTAACGA CTGCC
395	*HIS3**STOP, STOP**TLG2*	CCAAAGGTGTTCTTATG**TAGTAG**GATTATTGAA ATGGGTAC
396	reverse complement of 395	GTACCCATTTCAATATC**CTACTA**CATAAGAACA CCTTTGG

Table 2.3 - Plasmids used in this study

Plasmid	Description	Reference
pLO2010	*pep4-3-ΔH3* in pRS306	(Nothwehr et al., 1995)
pVT102u	Yeast expression plasmid (*2μ*, *URA3*)	(Vernet et al., 1987)
pSGS025	Yeast expression plasmid (*2μ*, *URA3*) encoding a HA-tagged version of human Sx16A from the *ADH1* promoter	Constructed by Dr. Scott G. Shanks (This study)
pSGS036	Yeast expression plasmid (*2μ*, *URA3*) encoding a HA-tagged version of human Sx4 from the *ADH1* promoter	Constructed by Dr. Scott G. Shanks (This study)
pHA-Tlg2	Yeast expression plasmid (*2μ*, *URA3*) encoding a HA-tagged version of yeast syntaxin, Tlg2p from the *ADH1* promoter	(Seron et al., 1998)
pSGS043	Yeast expression plasmid (*2μ*, *URA3*) encoding a HA-tagged truncated version of the yeast syntaxin, Tlg2p, lacking the first 230 residues.	Constructed by Dr. Scott G. Shanks (This study)
pSGS044	Yeast expression plasmid (*2μ*, *URA3*) encoding a HA-tagged truncated version of the human syntaxin, Sx16A, lacking the first 205 residues.	Constructed by Dr. Scott G. Shanks (This study)
pNB701	Yeast expression plasmid (*CEN*, *URA3*) encoding Pho8p from the *CUP1* promoter	Constructed by Dr. Nia J. Bryant (This study)
pMAZ002	Yeast expression plasmid (*CEN*, *URA3*) encoding a HA-tagged version of human Sx16A from the *CUP1* promoter	This study
pMAZ006	Yeast expression plasmid (*CEN*, *URA3*) encoding a HA-tagged version of yeast syntaxin, Tlg2p from the *CUP1* promoter	This study
pMAZ007	Yeast expression plasmid (*CEN*, *URA3*) encoding a HA-tagged version of mouse Sx4 from the *CUP1* promoter	This study
pSL2099	Yeast expression plasmid (*CEN*, *LEU2*) encoding a Myc-tagged version of yeast Ste3p from the *GAL1* promoter	(Davis et al., 1993)
pNB706	Yeast expression plasmid (*CEN*, *URA3*) encoding wild-type HA-Vps45p	(Carpp et al., 2006)
pNB708	As pNB706 encoding HA-Vps45pL117R	(Carpp et al., 2006)
pET-Duet™-1	ColE1 *ori* Ampr *lacI*; *E. coli* expression vector	Novagen
pCOG022	*E. coli* expression plasmid encoding two synthetic repeats of the IgG binding domains of *S. aureus* protein A	(Carpp et al., 2006)
pCOG025	*E. coli* expression plasmid encoding a C-terminally PrA-tagged truncated version of Tlg2p (cytosolic residues 1-318)	(Carpp et al., 2006)
pALA001	*E. coli* expression plasmid encoding a C-terminally PrA-tagged truncated version of Sx16A (cytosolic residues 1-269).	Constructed by Alicja Drozdowska (This study)
pFB09/1	*E. coli* expression plasmid encoding a C-terminally PrA-tagged truncated version of Sx4 (cytosolic residues 1-273).	Constructed by Dr. Fiona Brandie (This study)

pCOG070	Yeast expression plasmid (*2μ*, *URA3*) encoding a HA-tagged version of the yeast SM protein Vps45p from the *VPS45* promoter	(Carpp et al., 2006)
pCOG071	Yeast expression plasmid (*2μ*, *URA3*) encoding a HA-tagged mutant version of the yeast SM protein Vps45p (L117R) from the *VPS45* promoter	(Carpp et al., 2006)
pCOG039	Yeast expression plasmid (*CEN*, *URA3*) encoding a C-terminally HA-tagged version of the yeast syntaxin Tlg2p from the *CUP1* promoter	Constructed by Dr. Lindsay N. Carpp (This study)
pMAZ038	Yeast expression plasmid (*CEN*, *URA3*) encoding a HA-tagged truncated version of Tlg2p (residues 1-336)	This study
pGEX-$DSK2_{UBA}$	*E. coli* expression plasmid encoding a GST-tagged version of the Ubiquitin associated domain (residues 328-373 of the yeast adaptor protein Dsk2p)	(Funakoshi et al., 2002)
pCAL1	*E. coli* expression plasmid encoding a GST-tagged mutant version of the Ubiquitin associated domain (M324R and F344A)	Constructed by Christopher A. Lamb (This study)
P2313	Yeast expression plasmid (*CEN*, *URA3*) encoding C-terminally GFP-tagged Gap1p from the *CUP1* promoter	(Scott et al., 2004b)
pRS416	Yeast expression plasmid (*CEN*, *URA3*)	(Sikorski and Hieter, 1989)
pMAZ004	2148 bp fragment encoding the yeast syntaxin, Tlg2p under the control of its own promoter and 3' UTR flanked by *Xho*I and *Xba*I sites in pCR2.1®-TOPO®.	This study
pMAZ001	Yeast expression plasmid (*CEN*, *URA3*) encoding the yeast syntaxin Tlg2p from the *TLG2* promoter.	This study
pMAZ005	663 bp fragment encoding the yeast enzyme Imidazoleglycerol-phosphate dehydratase, His3p flanked by *BamH*I and *Sal*I sites in pCR2.1®-TOPO®.	This study
pMAZ016	As pMAZ001, but with a *BamH*I and *Sal*I site introduced after codon 33 of *TLG2*.	This study
pMAZ017	Yeast expression plasmid (*CEN*, *URA3*) encoding a fusion protein incorporating the yeast syntaxin Tlg2p and the enzyme Imidazoleglycerol-phosphate dehydratase, His3p	This study
pMAZ027	As pMAZ017, but encoding the enzyme Imidazoleglycerol-phosphate dehydratase, His3p under the control of the *TLG2* promoter and *3'UTR*	This study
pMAZ028	As pMAZ017, but with the lysine at position 26 mutated to an arginine residue (K26R)	This study
pMAZ029	As pMAZ017, but encoding the first 33 amino acids of Tlg2p fused to full length His3p under the control of the *TLG2* promoter and *3'UTR*	This study
pMAZ030	As pMAZ017, but with the five lysines at positions 190, 194, 199, 219 and 230 mutated to arginine residues (5KR)	This study
pMAZ033	As pMAZ017, but with three lysines mutated at positions 306, 312 and 316 mutated to arginine residues (3KR)	This study
pCR®2.1 - TOPO®	ColE *ori* Amp^r Kan^r *lacZα*, TA cloning vector	Invitrogen

Chapter 3 – Sx16 is a functional homologue of the yeast t-SNARE, Tlg2p

The work presented in this chapter has been published in (Struthers et al., 2009)

3.1 Introduction

In silico analysis has previously identified Tlg2p as being homologous to the mammalian protein, Sx16 (Simonsen et al., 1998). This chapter describes experiments directed towards investigating whether Sx16 and Tlg2p are also functional homologues. This was an important question to ask since, if the two syntaxins are functional homologues, it would open up the possibility of using yeast as a model system to study the role of mammalian Sx16. Using yeast as a model system to study the function of Sx16 offers a number of advantages over studying the syntaxin in mammalian cells alone, since yeast cells are much more experimentally tractable. There are a number of precedences for this type of approach in the literature, since the molecular machinery that regulates membrane traffic in eukaryotic cells is conserved from yeast to humans (Ferro-Novick and Jahn, 1994).

In order to address whether Sx16 is a functional homologue of Tlg2p, I chose to express the mammalian syntaxin in yeast cells lacking endogenous Tlg2p and ask whether it could complement for the loss of the yeast syntaxin. There are five different splice variants of Sx16: Sx16A, Sx16B, Sx16C (Simonsen et al., 1998), Sx16H (Tang et al., 1998) and Sx16D (Dulubova et al., 2002) (see Section 1.2.4). In this study I selected the splice variant Sx16A to investigate whether or not Sx16 and Tlg2p are functional homologues. This splice variant has previously been used to study the trafficking of GLUT4 in 3T3-L1 adipocytes (Proctor et al., 2006). Yeast cells lacking Tlg2p (*tlg2Δ* mutant cells) display multiple phenotypes as a result of impaired traffic through the endosomal system (Abeliovich et al., 1998, Holthuis et al., 1998, Seron et al., 1998). Phenotypes of *tlg2Δ* cells include osmotic sensitivity (Abeliovich et al., 1998); incorrect trafficking of vacuolar proteases (Abeliovich et al., 1998); abnormal vacuolar morphology (Abeliovich et al., 1998, Seron et al., 1998) and impaired delivery of endocytosed material to the vacuole (Holthuis et al., 1998, Abeliovich et al., 1998, Seron et al., 1998). For my studies it was important that expression of Sx16 was not grossly elevated compared to the levels of Tlg2p normally found in yeast. This was important because SNARE proteins contain a large amount of coiled-coil sequence which makes them notoriously ‘sticky’, i.e. they are prone to interact with non *bona fide* partners under non-physiological conditions, such as overexpression or *in vitro* binding studies (Fasshauer et al., 1999, Tsui and Banfield, 2000, Yang et al., 1999). Indeed it has previously been reported, in yeast, that the overexpression of the vacuolar syntaxin, Vam3p, can compensate for loss of the endosomal SNARE Pep12p and *vice versa* (Darsow et al., 1997, Gotte and Gallwitz, 1997). This is unlikely to

be due to the formation of a *bona fide* SNARE complex since this effect is not observed if Vam3p or Pep12p are expressed at, or close to, endogenous levels (Gotte and Gallwitz, 1997). For this reason, it was also important to include a second mammalian syntaxin in my study, so that I could ensure that any observed complementation of *tlg2Δ* phenotypes by Sx16 was specific to the Tlg2p *in silico* homologue. For this purpose I chose mammalian syntaxin 4 (Sx4).

This chapter describes the construction of vectors that drive expression of the mammalian syntaxins Sx16 and Sx4 in yeast cells. Also documented here is the ability of Sx16 to complement multiple endocytic trafficking defects displayed by *tlg2Δ* mutant yeast cells.

3.2 Heterologous expression of mammalian syntaxins, 16 and 4 in yeast

In order to heterologously express mammalian syntaxins in yeast, it was necessary to place the ORFs encoding the proteins downstream of a yeast promoter. Initially the syntaxins were cloned into the plasmids pVT102u (Vernet et al., 1987), under the control of the *ADH1* promoter. *ADH1* encodes the fermentative isozyme, alcohol dehydrogenase, which is responsible for the last step of the glycolytic pathway; the reduction of acetaldehyde to ethanol (Dickinson et al., 2003, Lutstorf and Megnet, 1968). The cloning of the syntaxins into pVT102u was performed by Dr Scott Shanks (University of Glasgow, UK) generating pSGS025 (encoding HA-Sx16) and pSGS036 (encoding HA-Sx4). A similar vector encoding HA-Tlg2p, pHA-Tlg2 (Seron et al., 1998) was also used in the complementation experiments. However, expression from the *ADH1* promoter is constitutive and strong, and it was a concern that this might lead to expression of the syntaxins at grossly elevated levels when compared to that of endogenous Tlg2p. To address this concern, I constructed a second set of vectors, utilising the inducible *CUP1* promoter. *CUP1* encodes the copper methallothionen protein which aids in the process of metal ion detoxification by tightly chelating copper ions (Butt et al., 1984). The higher the concentration of copper ions in the media, the greater the amount of the protein produced from the *CUP1* promoter (Mascorro-Gallardo et al., 1996). This feature of the *CUP1* promoter makes it an extremely useful tool for regulating the expression of heterologous proteins in yeast, since the level of expression of an ORF placed downstream of the *CUP1* promoter can be controlled by the regulating the concentration of copper ions present in the media in which cells are grown (Mascorro-Gallardo et al., 1996). DNA encoding either HA-tagged

versions of Tlg2p, Sx16, or Sx4 was placed under control of the *CUP1* promoter using the "gap-repair" strategy outlined in Figure 3.1.

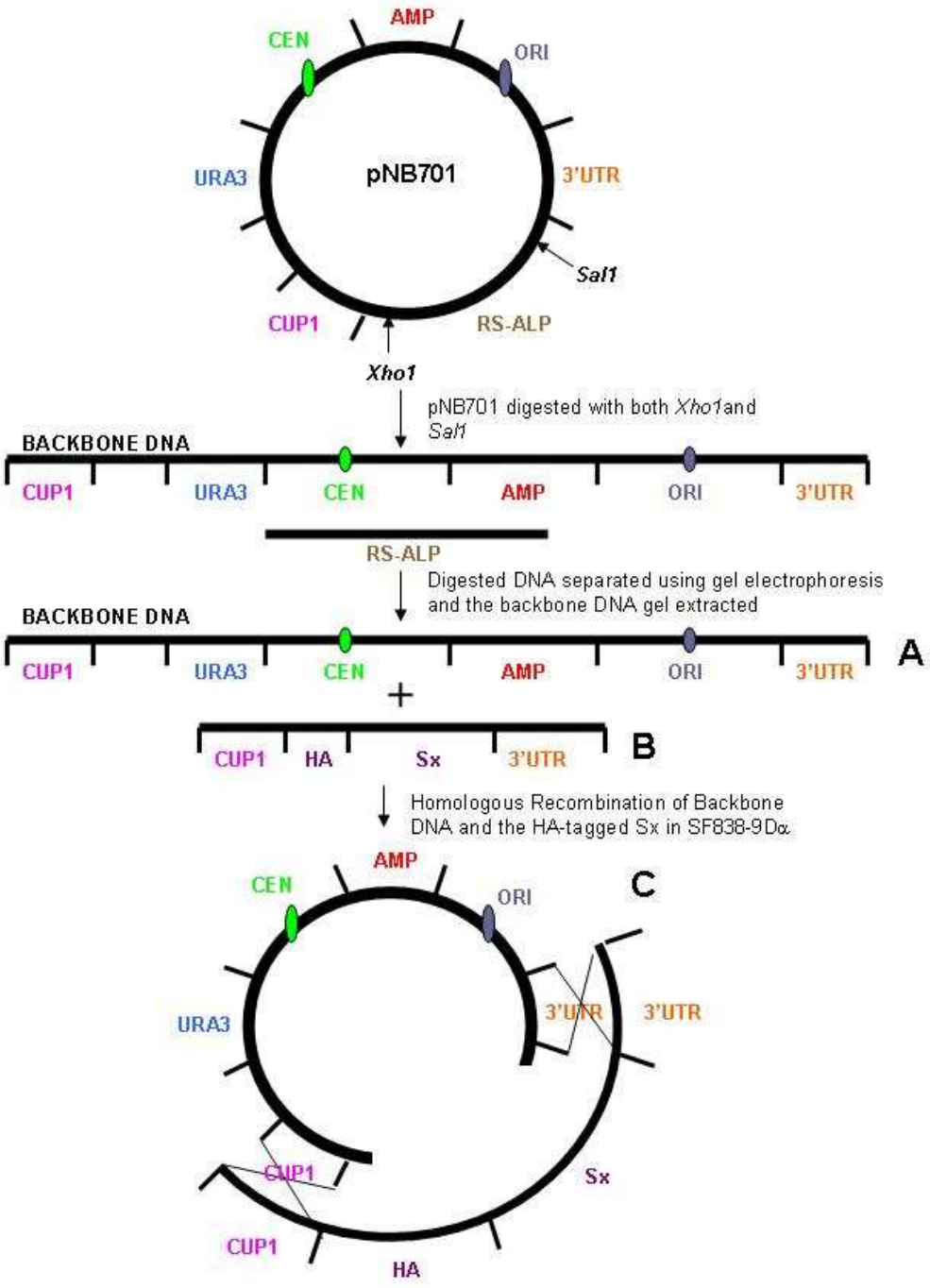

Figure 3.1 – Schematic diagram of the homologous recombination strategy used to create pMAZ002, pMAZ006, pMAZ007 (please see following text for details).

Initially, the plasmid pNB701 was digested with the restriction enzymes *Xho*I and *Sal*I to remove most of the coding sequence for RS-ALP (retention sequence-alkaline phosphatase) (Bryant et al., 1998). The resultant "gapped plasmid" (A in Figure 3.1) and PCR products (B in Figure 3.1), which encode the desired syntaxin flanked by sequences

homologous to the 3' end of the *CUP1* promoter and the 5' end of the 3' UTR of *PHO8*, were co-transformed into yeast (strain SF838-9D). "Gap-repair" of pNB701 (C in Figure 3.1) was performed in yeast through homologous recombination and the transformants selected by their ability to grow on media lacking uracil (SD-ura-met). To ensure that homologous recombination had been successful, expression of the desired syntaxin was screened using immunoblot analysis. Finally the plasmid was rescued from yeast identified as producing the desired syntaxin, and sequenced (as described in Sections 2.2.8 and 2.2.6). The overall procedure is summarised below in Figure 3.2.

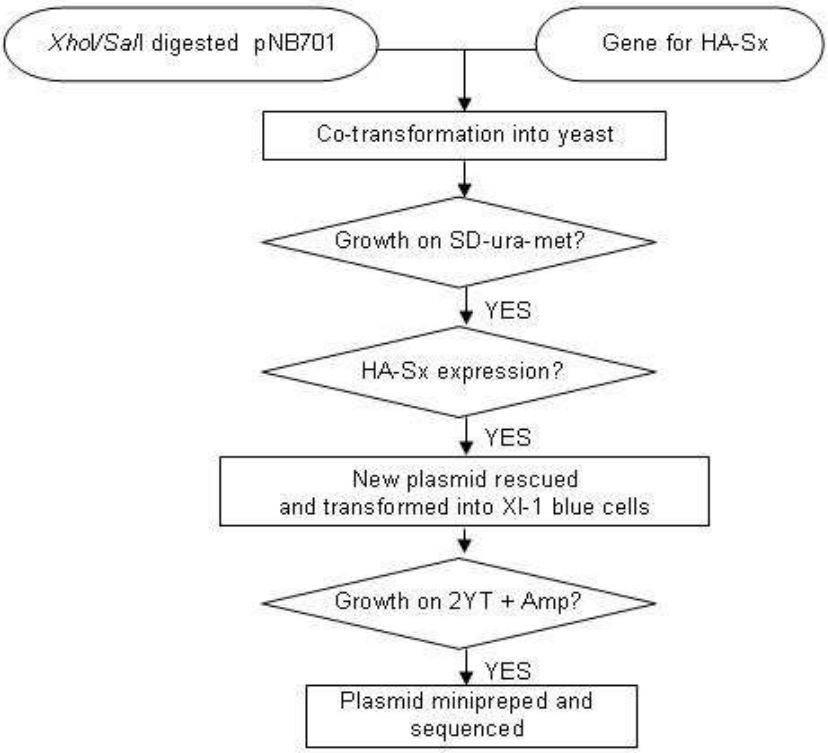

Figure 3.2 – Flow chart showing an overview of homologous recombination and the steps that follow

A more detailed description of how plasmids pMAZ002 (encoding HA-Sx16) and pMAZ007 (encoding HA-Sx4) were generated is described below.

For pMAZ002 the human Sx16A ORF (accession number AAB69282) was amplified from a cDNA kindly provided by Prof. Gwyn Gould (University of Glasgow, U.K.) by PCR using the oligonucleotide primers shown in Figure 3.3.

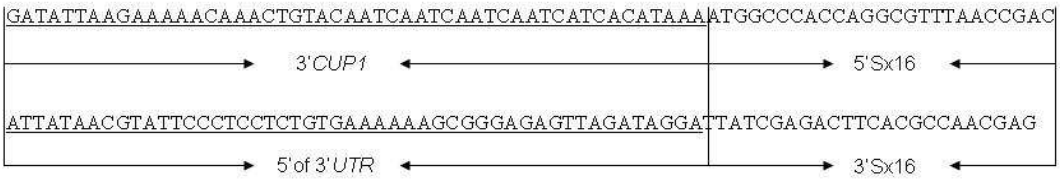

Figure 3.3 – Sx16 oligonucleotide primer sequences

This generated PCR product containing the Sx16 ORF flanked by sequences homologous to the 3' end of the *CUP1* promoter and the proximal end of the 3' UTR of *PHO8* (both underlined in Figure 3.3). This fragment was then used to repair the gapped plasmid, pNB701, by co-transforming yeast (strain SF838-9D) with *Xho*I/*Sal*I digested pNB701 and PCR product. Seven transformants capable of growing on selective media lacking uracil (SD-ura-met) were screened for the expression of Sx16 using immunoblot analysis with an antibody specific to Sx16 (Figure 3.4). Expression of Sx16 from the *CUP1* promoter was induced by the addition of 200 μM $CuCl_2$ to the media in which these transformants were grown.

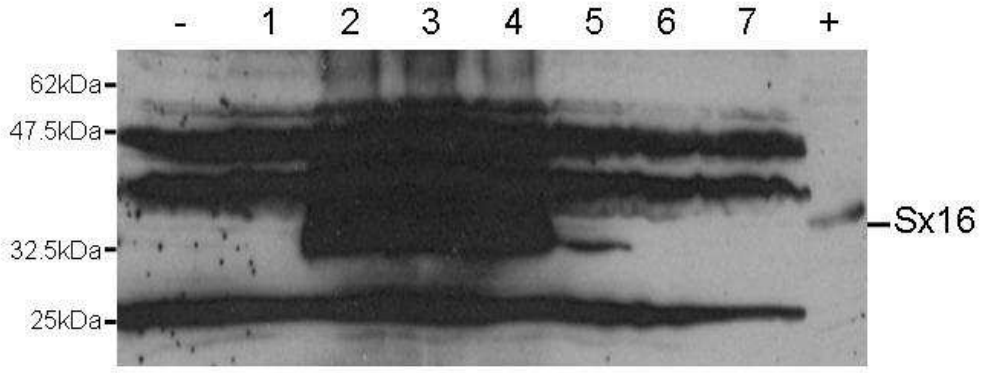

Figure 3.4 – Screening co-transformed yeast for Sx16 expression
Whole cell lysates prepared from equal numbers of yeast (SF838-9D) cells (1 OD_{600} equivalents) co-transformed with PCR product (Sx16 ORF flanked by sequences homologous to the 3' end of the *CUP1* promoter and the proximal end of the 3' UTR of *PHO8*) and *Xho*I/*Sal*I digested pNB701 were screened for Sx16 expression using immunoblot analysis with an antibody specific to Sx16. A whole cell lysate prepared from 1 OD_{600} equivalents of SF838-9D cells transformed with the empty vector, pNB701, was included in the immunoblot analysis as a negative control (-) and a whole cell lysate prepared from adipocytes (kindly provided by Dr Kirsty Proctor, University of Glasgow, UK) was included as a positive control (+). Expression of Sx16 from the *CUP1* promoter was induced by the addition of 200 μM $CuCl_2$ to the selective media (SD-ura-met) in which these transformants were grown.

Three of the seven transformants screened expressed Sx16 (lanes 2, 3 and 4 of Figure 3.4). These transformants were selected and the plasmids encoding Sx16 rescued and sequenced (as described in Section 2.2.8 and 2.2.6). Following DNA sequencing to confirm the constructs, one plasmid was selected and named pMSS001.

To create pMAZ002 sequence encoding the HA-tag was introduced immediately after the initiating methionine of Sx16 in pMSS001 using SDM with the oligonucleotide primers shown in Figure 3.5.

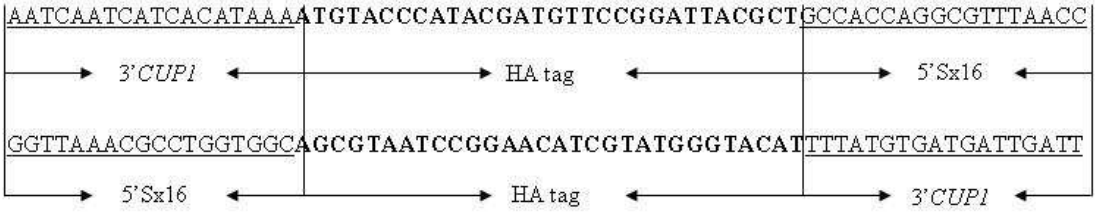

Figure 3.5 – SDM oligonucleotide primer sequences used to introduce the HA-tag to Sx16.

To ensure that the HA-tag had been successful introduced, five plasmids generated during the SDM of pMSS001 were transformed into the yeast strain, SF838-9D. The transformants were then screened for the expression of HA-tagged Sx16 using immunoblot analysis with an antibody specific to the HA-tag. Expression from the *CUP1* promoter was induced by the addition of 200 μM $CuCl_2$ to the selective media, SD-ura-met, in which these transformants were grown.

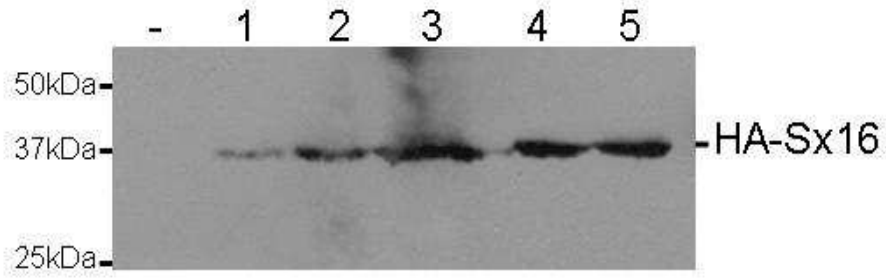

Figure 3.6 - Screening yeast for HA-Sx16 expression
Whole cell lysates prepared from equal numbers of yeast (SF838-9D) cells (1 OD_{600} equivalents) transformed with plasmids generated during the SDM reaction were screened for expression of HA-Sx16 using immunoblot analysis with an antibody specific to the HA-tag. A whole cell lysate prepared from 1 OD_{600} equivalents of SF838-9D cells transformed with the empty vector, pNB701, was also included in the immunoblot analysis as a negative control (-). Expression of HA-Sx16 from the *CUP1* promoter was induced by the addition of 200 µM $CuCl_2$ to the selective media, SD-ura-met, in which these transformants were grown.

Each of the five plasmids transformed into the yeast strain, SF838-9D, expressed an HA-tagged version of Sx16, confirming that the SDM treatment had been successful (Figure 3.6). To ensure that no errors had been introduced during the SDM reaction, the coding sequences in these newly synthesised plasmids were checked by DNA sequencing. One plasmid was subsequently selected and named pMAZ002.

pMAZ007 was constructed in a manner similar to that of pMAZ002. The murine Sx4 ORF (accession number P70452) was amplified from the plasmid pQE30-Sx4 (provided by Luke Chamberlain, University of Edinburgh, U.K.) using the oligonucleotide primers shown in Figure 3.7. The resulting PCR product, containing sequence encoding Sx4 with an HA-tag immediately after the initiating methionine (encoded by the bold sequence in Figure 3.7) flanked by sequences homologous to the 3' end of the *CUP1* promoter and the proximal end of the 3' UTR of *PHO8* (underlined in Figure 3.7), was then used to repair gapped pNB701 as outlined in Figures 3.1 and 3.2.

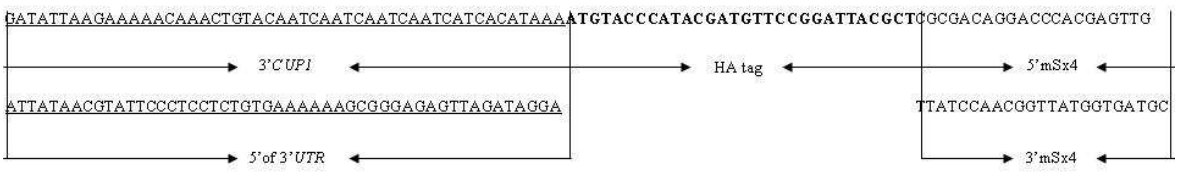

Figure 3.7 – HA-Sx4 oligonucleotide primer sequences

Co-transformed yeast (SF838-9D) capable of growing on the selective media, SD-ura-met, were screened to identify those expressing HA-tagged Sx4. This was achieved using immunoblot analysis with an antibody specific to the HA-tag (Figure 3.8).

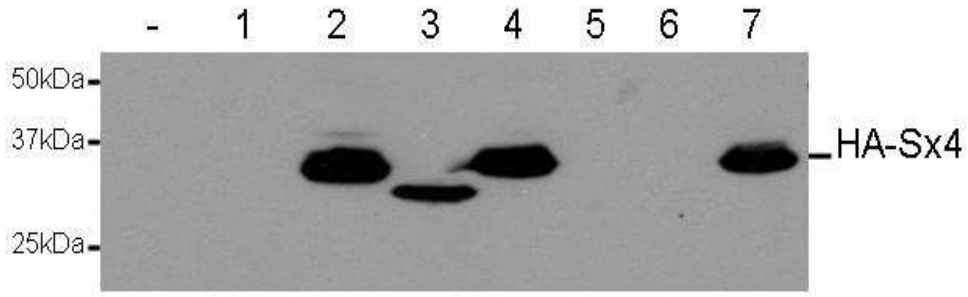

Figure 3.8 – Screening of co-transformed yeast for HA-Sx4 expression.
Whole cell lysates prepared from equal numbers of yeast (SF838-9D) cells (1 OD_{600} equivalents) co-transformed with PCR product (HA-Sx4 ORF flanked by sequences homologous to the 3' end of the *CUP1* promoter and the proximal end of the 3' UTR of *PHO8*) and *Xho*I/*Sal*I digested pNB701 were screened for HA-Sx4 expression using immunoblot analysis with an antibody specific to the HA-tag. A whole cell lysate prepared from 1 OD_{600} equivalents of SF838-9D cells transformed with the empty vector, pNB701, was also included in the immunoblot analysis as a negative control (-). Expression of HA-Sx4 from the *CUP1* promoter was induced by the addition of 200 µM $CuCl_2$ to the selective media, SD-ura-met, in which these transformants were grown.

Of the seven transformants screened, four expressed proteins recognisable by the anti-HA antibody. These four transformants were selected (lanes 2, 3, 4 and 7 in Figure 3.8) and the plasmids rescued (as described in Section 2.2.8). Each of the coding sequences in the newly synthesised plasmids was checked by DNA sequencing. This was necessary as homologous recombination can, in some cases result in the expression of truncated proteins (lane 3 in Figure 3.8). Following DNA sequencing one plasmid was selected and named pMAZ007.

3.3 Comparison of the expression of HA-tagged Tlg2p and endogenous Tlg2p

As mentioned above (in Section 3.1) an important consideration for this study was to express the mammalian syntaxins at similar levels to those at which Tlg2p is found in wild-type yeast cells. This was to address the concern that overexpression of syntaxins may force incorrect SNARE partnering and complex formation (Darsow et al., 1997, Gotte and Gallwitz, 1997). In order to compare the levels of the heterologously expressed mammalian syntaxins to that of endogenous Tlg2p, I constructed a vector similar to

pMAZ002 and pMAZ007 expressing HA-Tlg2p from the *CUP1* promoter; pMAZ006. This was achieved using PCR to amplify the *TLG2* ORF from yeast chromosomal DNA, using the oligonucleotides shown in Figure 3.9. The resulting PCR product, containing sequence encoding Tlg2p with an HA-tag immediately after the initiating methionine (encoded by the bold sequence shown in Figure 3.9) flanked by the sequences homologous to the 3'end of the *CUP1* promoter and the proximal end of the 3' UTR of *PHO8* (underlined in Figure 3.9), was then used to repair gapped pNB701 (outlined in Figure 3.1 and 3.2).

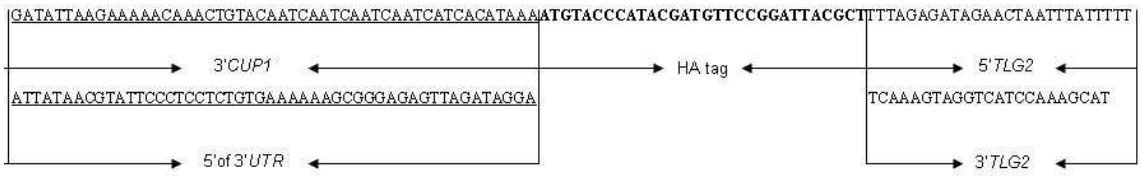

Figure 3.9 – HA-*TLG2* oligonucleotide primer sequences

As described above (in Section 3.2) yeast (SFS838-9D) co-transformed with PCR product and *Xho*I/*Sal*I digested pNB701 were screened for HA-Tlg2p expression using immunoblot analysis with an antibody specific to the HA-tag (Figure 3.10) and the plasmid encoding HA-Tlg2p isolated using the procedure detailed in Figure 3.2.

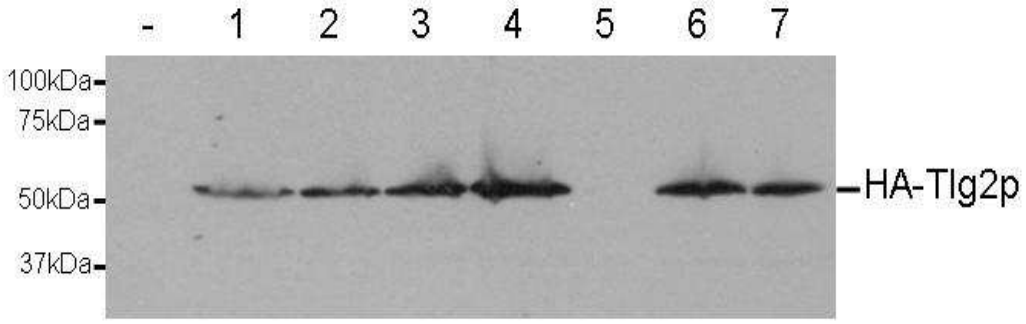

Figure 3.10 - Screening of co-transformed yeast for HA-Tlg2p expression.
Whole cell lysates prepared from equal numbers of yeast (SF838-9D) cells (1 OD_{600} equivalents) co-transformed with PCR product (HA-*TLG2* ORF flanked by sequences homologous to the 3' end of the *CUP1* promoter and the proximal end of the 3' UTR of *PHO8*) and *Xho*I/*Sal*I digested pNB701 were screened for HA-Tlg2p expression using immunoblot analysis with an antibody specific to the HA-tag. A whole cell lysate prepared from 1 OD_{600} equivalents of SF838-9D transformed with the empty vector, pNB701, was included in the immunoblot analysis as a negative control (-). Expression of HA-Tlg2p from the *CUP1* promoter was induced by the addition of 200 µM $CuCl_2$ to the selective media (SD-ura-met) in which these transformants were grown.

It was important to decide the concentration of copper that should be used express the three syntaxins. In order to do this, I carried out a copper titration; cells lacking endogenous Tlg2p (NOzY3; SF838-9D *tlg2Δ*) were transformed with pMAZ002 (encoding HA-Sx16), pMAZ006 (encoding HA-Tlg2p) or pMAZ007 (encoding HA-Sx4). These transformants were then grown in selective media (SD-ura-met) containing different concentrations of copper ions (0, 25, 50, 75, 100 or 150 µM $CuCl_2$). Proteins contained within whole cell lysates prepared from equal numbers of these transformants (1 OD_{600} equivalents) were separated by SDS-PAGE. The levels of the individual syntaxins were then assessed using immunoblot analysis with an antibody specific to the HA-tag.

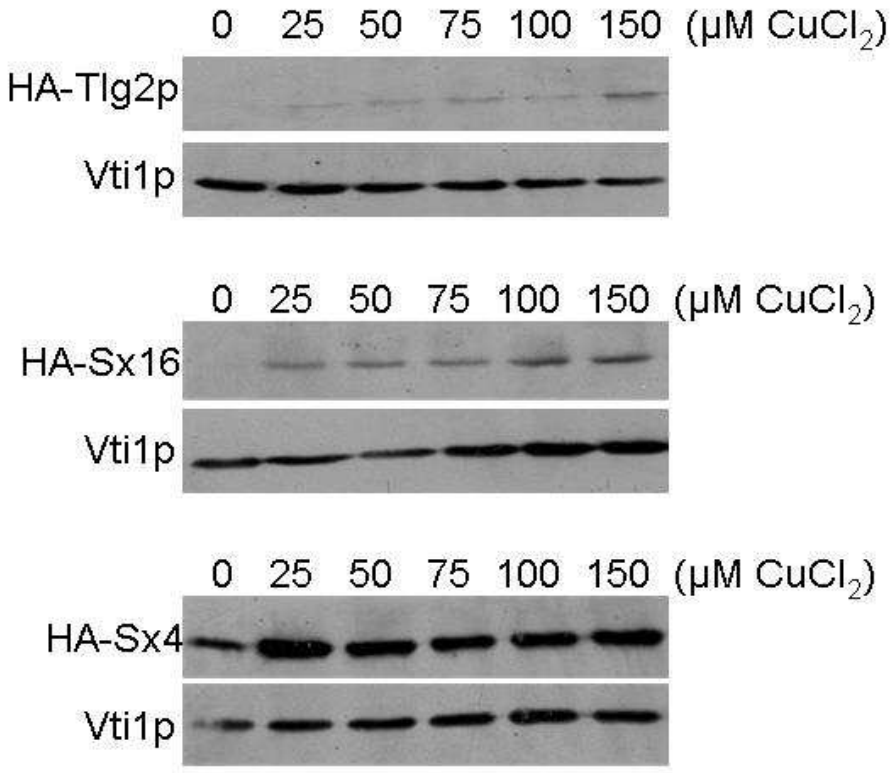

Figure 3.11 - Copper titration to assess optional copper concentrations for syntaxin expression.
NOzY3 (SF838-9D *tlg2Δ*) cells transformed with the plasmids pMAZ006 (encoding HA-Tlg2p), pMAZ002 (encoding HA-Sx16) or pMAZ007(encoding HA-Sx4) were grown in selective media containing different concentrations of $CuCl_2$, namely 0, 25, 50, 75, 100 and 150µM. Whole cell lysates prepared from equal numbers of these transformants (1 OD_{600} equivalents) were prepared and analysed using immunoblot analysis with an antibody specific to the HA-tag. Levels of the v-SNARE, Vti1p, were also assessed using immunoblot analysis to control for equal loading.

The expression of HA-Tlg2p and HA-Sx16 increases with copper concentration. However HA-Sx4 seems to be expressed at maximal level at all of the copper concentrations tested

(Figure 3.11). 50 µM $CuCl_2$ was selected as the concentration of copper to be added to the media to drive the expression of Tlg2p, Sx16 and Sx4. This concentration is not high enough to introduce any of the toxic effects of copper (Kagi et al., 1979, Macreadie et al., 1989), but is sufficient to give an easily detectable amount of the syntaxins.

I next went on to compare the levels of HA-Tlg2p expressed from pMAZ006 (in the presence of 50 µM $CuCl_2$) to that of endogenous Tlg2p. Cells lacking endogenous Tlg2p (NOzY3; SF838-9D *tlg2Δ*) were transformed with either pNB701 (empty vector) or pMAZ006 (encoding HA-Tlg2p). Transformants were then grown in selective media containing 50 µM $CuCl_2$ to induce the expression of HA-Tlg2p. Whole cell lysates prepared from equal numbers of these transformants (1 OD_{600} equivalents) were run alongside a whole cell lysates prepared from an equivalent number (1 OD_{600} equivalents) of wild-type (SF838-9D; containing Tlg2p at normal, endogenous levels) and *tlg2Δ* (NOzY3; SF838-9D *tlg2Δ*) cells transformed with the empty vector, pNB701, which were also grown under the same conditions. The levels of Tlg2p present in these whole cell lysates was then assessed using immunoblot analysis with an antiserum that specifically recognise Tlg2p (Figure 3.12a). Expression of HA-Tlg2p from the vector pHA-Tlg2 (Seron et al., 1998) was also screened at the same time as a means to compare the expression from the endogenous promoter, the inducible promoter (*CUP1*) and the constitutive promoter (*ADH1*) (Figure 3.12b).

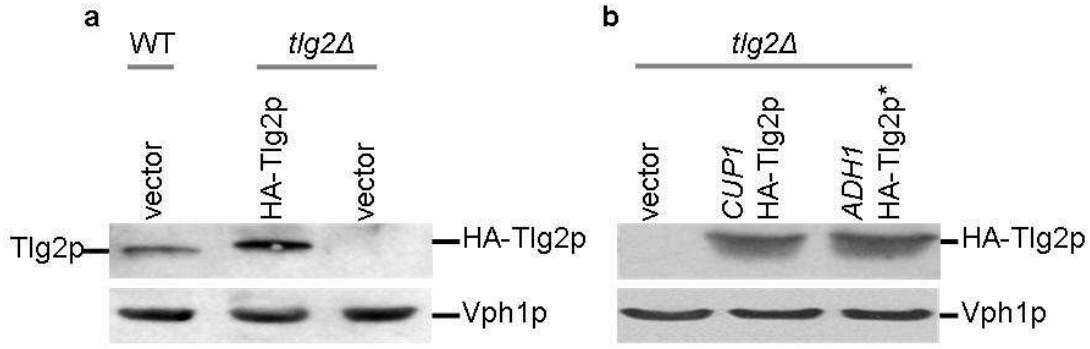

Figure 3.12 – A comparison of endogenous Tlg2p expression and HA-Tlg2p expression controlled by the yeast promoters *CUP1* and *ADH1*.
a) Wild-type cells (WT; SF838-9D) transformed with pNB701 (empty vector) and *tlg2Δ* cells (NOzY3; SF838-9D *tlg2Δ*) cells transformed with either pNB701 (empty vector) or pMAZ006 (encoding HA-Tlg2p) were grown to mid-log phase in the selective media, SD-ura-met, containing 50 µM $CuCl_2$. Levels of Tlg2p present in whole cell lysates prepared from equal numbers of these transformants (1 OD_{600} equivalents) were analysed using immunoblot analysis with an antiserum specific to Tlg2p. Levels of the vacuolar ATPase subunit, Vph1p, were also assessed using immunoblot analysis to control for equal loading. b) *tlg2Δ* cells (NOzY3; SF838-9D *tlg2Δ*) transformed with pVT102u (empty vector), pMAZ006 (driving HA-Tlg2p expression from the *CUP1* promoter) or pHA-Tlg2 (driving HA-Tlg2p* expression from the control of the *ADH1* promoter) were grown to mid-log phase in the selective media, SD-ura-met, containing 50 µM $CuCl_2$. Levels of Tlg2p present in whole cell lysates prepared from equal numbers of these transformants (1 OD_{600} equivalents) were analysed using immunoblot analysis with an antiserum specific to Tlg2p. Levels of the vacuolar ATPase subunit, Vph1p, were also assessed using immunoblot analysis to control for equal loading.

Figure 3.12 demonstrates that Tlg2p expression from the inducible *CUP1* promoter (at 50 µM $CuCl_2$) and the constitutive *ADH1* promoter does not differ greatly from the expression achieved by the endogenous promoter. Hence it is apparent that either expression system could be utilised in complementation experiments.

In order to compare the levels of Sx16 and Sx4 expression from the plasmids pMAZ002 and pMAZ007 to that of Tlg2p from pMAZ006, the HA-tag was utilised. This enabled me to use immunoblot analysis to directly compare the levels of protein expressed from the three constructs. This would not be possible using antibodies against the three different proteins as there would be no way of controlling for any differences in the affinity that the different antibodies would have for their syntaxins. Thus, cells lacking endogenous Tlg2p (NOzY3; SF838-9D *tlg2Δ*) were transformed with pNB701 (empty vector), pMAZ006 (encoding HA-Tlg2p), pMAZ002 (encoding HA-Sx16) or pMAZ007 (encoding HA-Sx4). Expression was induced by the addition of 50 µM $CuCl_2$ to the selective media, SD-ura-met, in which these transformants were grown. Proteins contained within whole cell lysates prepared from equal numbers of these transformants (1 OD_{600} equivalents) were

separated by SDS-PAGE and the levels of the syntaxins compared using immunoblot analysis with an antibody specific to the HA-tag.

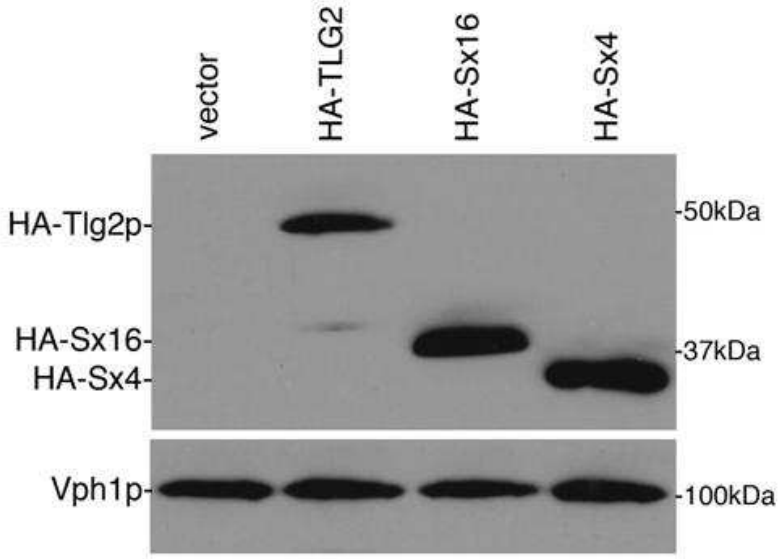

Figure 3.13 - Expression of HA-Tlg2p, HA-Sx16, HA-Sx4 in *tlg2*Δ cells.
Cells lacking endogenous Tlg2p (NozY3; SF838-9D *tlg2Δ*) were transformed with pNB701 (empty vector), pMAZ006 (encoding HA-Tlg2p), pMAZ002 (encoding HA-Sx16) or pMAZ007 (encoding HA-Sx4). Expression was induced by the addition of 50 µM $CuCl_2$ to the selective media, SD-ura-met, in which these transformants were grown. Proteins contained within whole cell lysates prepared from equal numbers of these transformants (1 OD_{600} equivalents) were separated by SDS-PAGE prior to immunoblot analysis with an antibody specific to the HA-tag. Levels of the vacuolar ATPase subunit, Vph1p, were also assessed using immunoblot analysis to control for equal loading.

Both HA-Sx4 and HA-Sx16 are expressed at levels which exceeds that of HA-Tlg2p (Figure 3.13). Although HA-Sx4 and HA-Sx16 appear to be somewhat overexpressed, as long as HA-Sx4 does not complement the function of Tlg2p then the possibility of the overexpression of HA-Sx16 being responsible for complementation can be ruled out.

3.4 Copper toxicity

Heavy metal ions, such as copper, are known to be toxic to yeast at high levels (Kagi et al., 1979). It has previously been reported that copper resistant strains can grow in the presence of greater than 0.3 mM $CuSO_4$; where as copper sensitive strains cannot (Macreadie et al., 1989). As a means of investigating whether or not the chosen copper chloride concentration (50 µM $CuCl_2$) would be toxic to the cells, I monitored the growth

of NOzY3 (SF838-9D *tlg2*Δ) cells expressing the HA-tagged syntaxins on selective plates (SD-ura-met) with and without copper chloride.

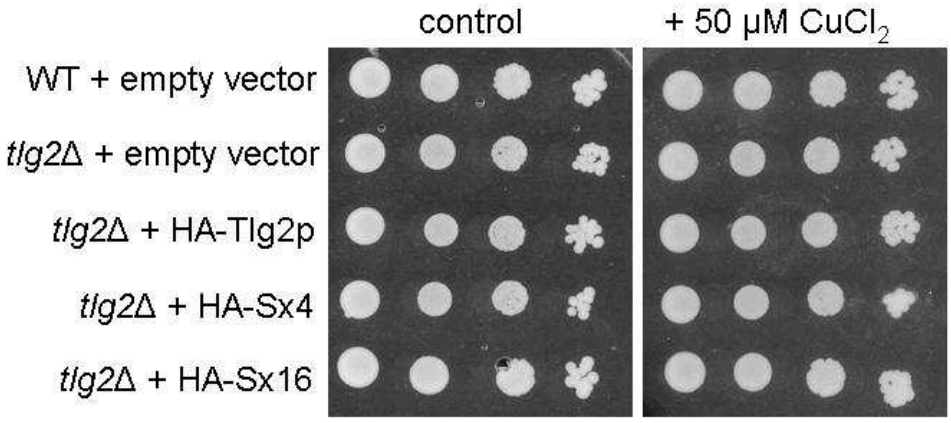

Figure 3.14 – Testing for copper sensitivity
Wild-type cells (WT; SF838-9D) transformed with pNB701 (empty vector) and cells lacking endogenous Tlg2p (*tlg2Δ*; NOzY3; SFS838-9D *tlg2Δ*) transformed with either pNB701 (empty vector), pMAZ006 (encoding HA-Tlg2p), pMAZ007 (encoding HA-Sx4) or pMAZ002 (encoding HA-Sx16) were grown to mid-log phase in the selective media, SD-ura-met, containing 50 µM $CuCl_2$. Cells were then harvested and resuspended at an OD_{600} of 0.8 in sterile dH_2O; subsequent serial dilutions were performed, generating cultures with an OD_{600} of 0.8, 0.08, 0.008 and 0.0008. 5 µl of each of these cultures was then spotted onto SD-ura-met (control) and SD-ura-met + 50 µM $CuCl_2$ and their growth monitored over several days at 30ºC.

It is evident that the presence of 50µM $CuCl_2$ in the media does not have any effect on the growth of the cells, hence copper toxicity can be ruled out as a limiting factor in the experiments which follow.

3.5 Functional analysis

3.5.1 Osmotic sensitivity

Yeast defective in vacuolar and/or endocytic trafficking often show sensitivity to osmotic stress (Banta et al., 1988). Cells lacking endogenous Tlg2p show a decreased growth rate on media containing abnormally high concentrations of salt (Abeliovich et al., 1998). In order to investigate whether or not Sx16 would complement the function of Tlg2p, yeast cells lacking endogenous Tlg2p (NOzY3; SF838-9D *tlg2Δ*) transformed with pMAZ006 (encoding HA-Tlg2p), pMAZ002 (encoding HA-Sx16) or pMAZ007 (encoding HA-Sx4) were grown to mid-log phase in the presence of 50 µM $CuCl_2$ before spotting onto selective media (SD-ura-met + 50 µM $CuCl_2$) containing high concentrations of the salt potassium chloride (KCl).

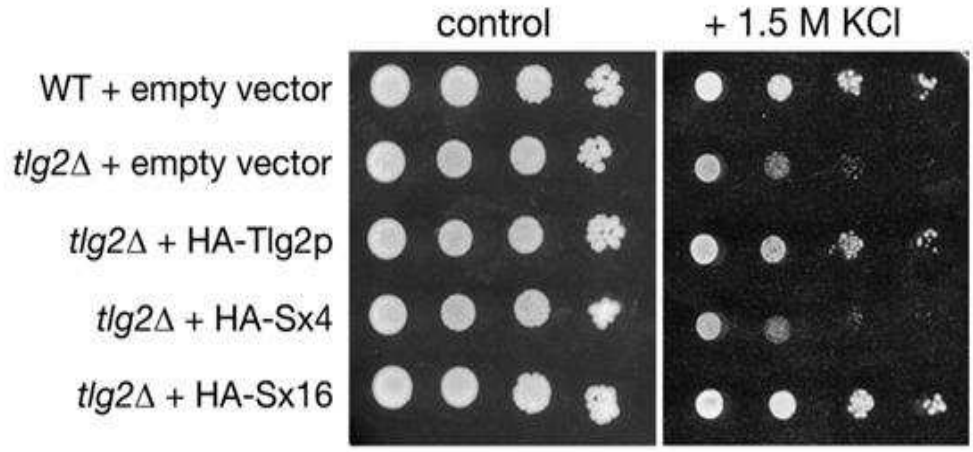

Figure 3.15 – Expression of human Sx16 complements the osmotic sensitivity phenotype of *tlg2Δ* mutant cells.
Wild-type cells (WT; SF838-9D) transformed with pNB701 (empty vector) and cells lacking endogenous Tlg2p (*tlg2Δ*; NOzY3; SFS838-9D *tlg2Δ*) transformed with either pNB701 (empty vector), pMAZ006 (encoding HA-Tlg2p), pMAZ007 (encoding HA-Sx4) or pMAZ002 (encoding HA-Sx16) were grown to mid-log phase in the selective media, SD-ura-met, containing 50 µM $CuCl_2$. Cells were then harvested and resuspended at an OD_{600} of 0.8 in sterile dH_2O; subsequent serial dilutions were performed, generating cultures with an OD_{600} of 0.8, 0.08, 0.008 and 0.0008. 5 µl of each of these cultures was then spotted onto SD-ura-met + 50 µM $CuCl_2$ (control) and SD-ura-met + 50 µM $CuCl_2$ + 1.5 M KCl (+ 1.5 M KCl) and their growth monitored over several days at 30ºC.

Cells lacking endogenous Tlg2p (*tlg2Δ*), but expressing either HA-Tlg2p or HA-Sx16, have a similar growth rate to that seen for wild-type cells (WT + pNB701). In comparison, cells lacking endogenous Tlg2p (*tlg2Δ*) but expressing HA-Sx4 show a reduced growth rate similar to that of *tlg2Δ* cells harbouring the empty vector (*tlg2Δ* + pNB701). Hence in this assay the expression of human Sx16 complements the osmotic sensitivity phenotype of *tlg2Δ* mutant cells in a manner indistinguishable from Tlg2p; in contrast Sx4 does not.

3.5.2 Trafficking of intracellular proteins – CPY

The vacuolar protease, CPY, is synthesised at the ER where it undergoes N-linked glycosylation; generating a 67 kDa ER-modified form of proCPY referred to as p1CPY (Blachly-Dyson and Stevens, 1987, Hasilik and Tanner, 1978b, Johnson et al., 1987). p1CPY is then trafficked from the ER to the Golgi apparatus where it undergoes further oligosaccharide modifications, resulting in a 69 kDa Golgi-modified form of proCPY known as p2CPY (Stevens et al., 1982, Trimble et al., 1983). At the late Golgi, p2CPY is sorted away from the secretory pathway by its receptor Vps10p (Marcusson et al., 1994). p2CPY and Vps10p are trafficked to the PVC, where they dissociate and Vps10p is recycled to the late Golgi (Deloche and Schekman, 2002, Hasilik and Tanner, 1978a,

Seaman et al., 1997). p2CPY is subsequently delivered to the vacuole where it is cleaved by vacuolar proteases into a 61 kDa active form of CPY, known as mature CPY (mCPY) (Deloche and Schekman, 2002, Hasilik and Tanner, 1978a).

Cells lacking endogenous Tlg2p are unable to correctly sort CPY and as a result secrete a small amount of the Golgi-modified form of CPY, p2CPY, from the cell (Abeliovich et al., 1998). In order to investigate whether or not Sx16 would complement this CPY trafficking defect, the CPY secreted from wild-type cells (SF838-9D) transformed with empty vector (pVT102u) was compared to that of cells lacking endogenous Tlg2p (NOzY3; SFS838-9D *tlg2Δ*) transformed with either empty vector (pVT102u) or plasmids driving the expression of HA-Sx16 (pSGS025), HA-Sx4 (pSGS036) or HA-Tlg2p (pHA-Tlg2). TCA precipitation was used to collect the secreted proteins from the media in which these cells had grown (see Section 2.2.14) and the presence of secreted CPY was then assessed using immunoblot analysis with an antibody specific to CPY.

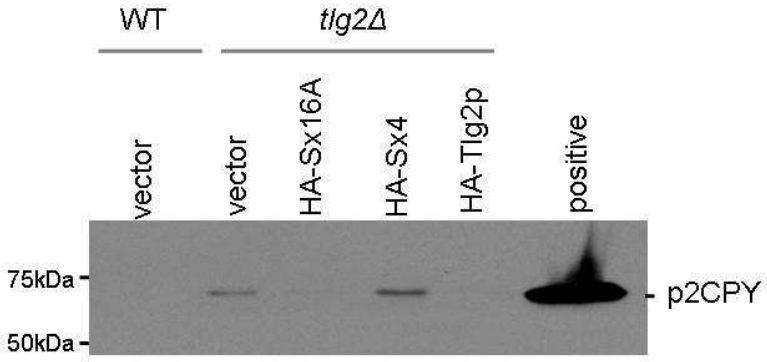

Figure 3.16 – Expression of human Sx16 complements the CPY trafficking defects of *tlg2*Δ mutant cells
Wild-type (WT; SF838-9D) cells transformed with pVT102u (empty vector) and *tlg2*Δ cells transformed with pVT102u (empty vector), pSGS025 (encoding HA-Sx16), pSGS036 (encoding HA-Sx4) or pHA-Tlg2 (encoding HA-Tlg2p) were grown to mid-log phase in the selective media, SD-ura-met. Equal numbers (18 OD_{600} equivalents) of these cells were then harvested and the proteins present in the resulting supernatant precipitated by the addition of TCA at a final concentration of 10% (v/v). The precipitated proteins were then separated using SDS-PAGE and the secretion of CPY assessed using immunoblot analysis with an antibody specific to CPY. A whole cell lysate prepared from 1 OD_{600} equivalents of SF838-9D cells transformed with the empty vector, pNB701, was also included in the immunoblot analysis as a positive control.

It is evident from Figure 3.16 that there is no detectable secretion of CPY from wild-type cells (WT) when compared to cells lacking endogenous Tlg2p (*tlg2Δ*). The expression of HA-Tlg2p or HA-Sx16 reduces CPY secretion of *tlg2Δ* cells to levels similar to that seen with wild-type cells. In contrast expression of HA-Sx4 in *tlg2Δ* cells did not prevent the

incorrect sorting and secretion of CPY. Hence, human Sx16 complements for the loss of Tlg2p with respect to trafficking of the vacuolar protease CPY, whereas Sx4 does not.

3.5.3 Ste3p receptor endocytosis

Mating haploid yeast cells secrete two different types of pheromone known as **a** and α factor (Davis et al., 1993). Haploid yeast cells secreting **a**-factor are known as **a** type and those secreting α factor are known as α type (Davis et al., 1993). Each type of haploid cell expresses the opposite type of receptor on its cell surface, for example an **a** type haploid cell will express an α receptor and vice versa (Davis et al., 1993). Binding of pheromone to its receptor allows mating to occur between two haploid cells (Herskowitz, 1989). Phermone receptors belong to the G-protein coupled receptor family (Naider and Becker, 2004). The α-factor receptor is more commonly known as Ste2p and the **a**-factor receptor as Ste3p (Naider and Becker, 2004). Ste2p and Ste3p are both subject to two different modes of endocytosis; ligand-dependent mode and ligand-independent constitutive mode (Davis et al., 1993). Upon internalisation the pheromone receptors are trafficked to the vacuole for degradation (Davis et al., 1993).

It has previously been shown that cells lacking Tlg2p have a defective vacuolar endocytic pathway, one consequence of this is an inability of proteins endocytosed from the plasma membrane, such as Ste2p and Ste3p, to reach the vacuole and be degraded (Holthuis et al., 1998, Abeliovich et al., 1998, Seron et al., 1998). Ste3p endocytosis can be followed by measuring the rate at which the receptor is degraded by vacuolar proteases (Davis et al., 1993). In wild-type cells Ste3p turnover is rapid, with a half-life of approximately 20 mins, however cells lacking endogenous Tlg2p show a reduced rate of Ste3p trunover, with a half-life of approximately 45 mins (Abeliovich et al., 1998).

In order to measure the turnover of Ste3p, expression must be controlled in such a way that it could be switched off to follow the degradation from a defined time-point. This strategy removes any confusion that would arise from the equilibrium between degradation and synthesis. Previously Ste3p turnover has been measured using different techniques such as radiolabelled pulse-chase (Abeliovich et al., 1998, Davis et al., 1993, Seron et al., 1998) and glucose repression (Davis et al., 1993), the kinetics of both parallel each other (Davis et al., 1993). In the experiments described below glucose repression was used to measure the turnover of Ste3p in wild-type and *tlg2Δ* cells. This involved using the plasmid pSL2099 (Davis et al., 1993) (based on pRS315 (Sikorski and Hieter, 1989)). pSL0299

expresses a Myc-tagged version of Ste3p under the control of the *GAL1* promoter. In the presence of media containing the sugar galactose (S-Raf/Gal-ura-leu), the *GAL1* promoter is switched on and hence promotes the expression of Ste3p-Myc. However upon the addition of a more favourable sugar source, such as glucose to the media, the *GAL1* promoter becomes switched off and Ste3p-Myc degradation from the time-point of glucose addition can be monitored using immunoblot analysis with an antibody specific to the Myc-tag. The expression of a Myc-tagged version of Ste3p makes it possible to distinguish between endogenously expressed Ste3p and that controlled by the *GAL1* promoter. This is important as otherwise, it would be impossible to monitor the degradation of Ste3p in those cells containing the wild-type gene (*STE3*).

Ligand-independent endocytosis and degradation of Ste3p-Myc was monitored using the *MATα* strain RPY10 and its isogenic *tlg2Δ* derivative NOzY4 (RPY10 *tlg2Δ*). NOzY4 (RPY10 *tlg2Δ*) cells were co-transformed with plasmids expressing Ste3p-Myc (pSL2099) and the desired syntaxin (HA-Sx16 from pSGS025, HA-Sx4 from pSGS036, HA-Tlg2p from pHA-Tlg2). As a means of a positive and negative control for this experiment both RPY10 and NOzY4 (RPY10 *tlg2Δ*) cells were co-transformed with pSL0299 (Ste3p-Myc) and pVT102u (empty vector). Selection of co-transformed plasmids was achieved using the selective media, SD-ura-leu. Co-transformed cells were then grown on selective media containing galactose and raffinose (S-Raf/Gal-ura-leu) for one generation (i.e. until the Optical Density at 600 nm doubles) before adding glucose. The point of glucose addition was taken as time-point zero, after which cells were collected every 20 mins and the levels of Ste3p-Myc monitored by preparing whole cell lysates, upon which immunoblot analyses were performed. This work was done in collaboration with Dr Scott Shanks (University of Glasgow, UK).

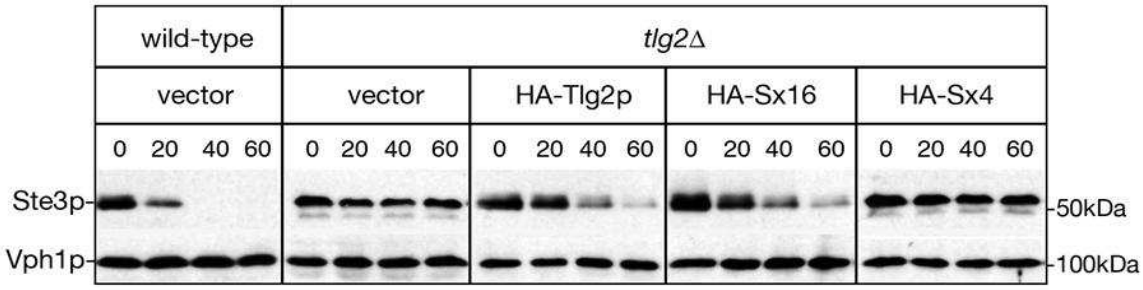

Figure 3.17 - Expression of Sx16 overcomes the block in Ste3p endocytosis observed in *tlg2*Δ cells.
Ste3p degradation in wild-type cells co-transformed with pSL2099 (Ste3p-Myc) and the empty vector (pVT102u) was compared to that of cells lacking endogenous Tlg2p (*tlg2Δ*) co-transformed with pSL2099 (Ste3p-Myc) and either pVT102u (empty vector), pHA-Tlg2 (HA-Tlg2p), pSGS025 (HA-Sx16) or pSGS036 (HA-Sx4). Co-transformed cells were grown on selective media containing galactose and raffinose (S-Raf/Gal-ura-leu) for one generation (i.e. until the Optical Density at 600 nm doubles) before adding glucose. Cells were collected immediately after glucose addition (time-point 0) and again after 20, 40 and 60 mins. Further degradation of Ste3p-Myc was prevented by the addition of NaN_3 to a final concentration of 15 mM. Equal numbers (1 OD_{600} equivalents) of these cells were then analysed using immunoblot analysis with an antibody specific to the Myc-tag. Levels of the vacuolar ATPase subunit, Vph1p, were also assessed using immunoblot analysis to control for equal loading.

As mentioned above, the half-life of Ste3p is approximately 20 mins and 45 mins in wild-type and *tlg2Δ* cells, respectively (Davis et al., 1993, Abeliovich et al., 1998). This is in agreement with the data presented in Figure 3.17. The introduction of HA-Tlg2p and HA-Sx16 to *tlg2Δ* cells increases the rate of Ste3p degradation to a rate comparable to that seen in wild-type cells; in contrast the introduction of HA-Sx4 has no effect. From this, I conclude that Sx16 complements the function of Tlg2p, with respect to the endocytic trafficking of the **a**-factor receptor, Ste3p, whereas Sx4 does not.

3.5.4 FM4-64, vacuolar labelling

Another technique which can be utilised to follow endocytic trafficking to the vacuole in yeast is to follow delivery of the lipophillic styryl dye, *N*-(3-triethylammoniumpropyl)-4-(*p*-diethylaminophenylhexatrinyl) more commonly known as FM4-64, from the plasma membrane to the vacuole (Vida and Emr, 1995). One of the main advantages of using FM4-64 apposed to other dyes is that FM4-64 is specifically trafficked to the vacuolar membrane via the endocytic pathway (Vida and Emr, 1995).

FM4-64 was used to investigate whether Sx16 would complement the function of Tlg2p by permitting efficient FM4-64 labelling of the vacuolar membrane. FM4-64 trafficking in

wild-type cells (RPY10) transformed with empty vector (pVT102u) was compared to that of cells lacking endogenous Tlg2p (NOzY4; RPY10 *tlg2Δ*) transformed with either empty vector (pVT102u) or plasmids driving the expression of HA-Tlg2p (pHA-Tlg2), HA-Sx16 (pSGS025) or HA-Sx4 (pSGS036). Transformants grown to mid-log phase were labelled with FM4-64 at 0ºC for 30 mins. The dye was subsequently removed and a chase period initiated by resuspending the cells in fresh prewarmed media (SD-ura-met) lacking FM4-64. Cells were incubated for 10 mins and 45 mins at 30ºC after which time the chase period was terminated by the addition of NaN_3. Cells were then kept on ice until they were visualised using fluorescence and DIC microscopy. This work was done in collaboration with Dr Scott Shanks (University of Glasgow, UK).

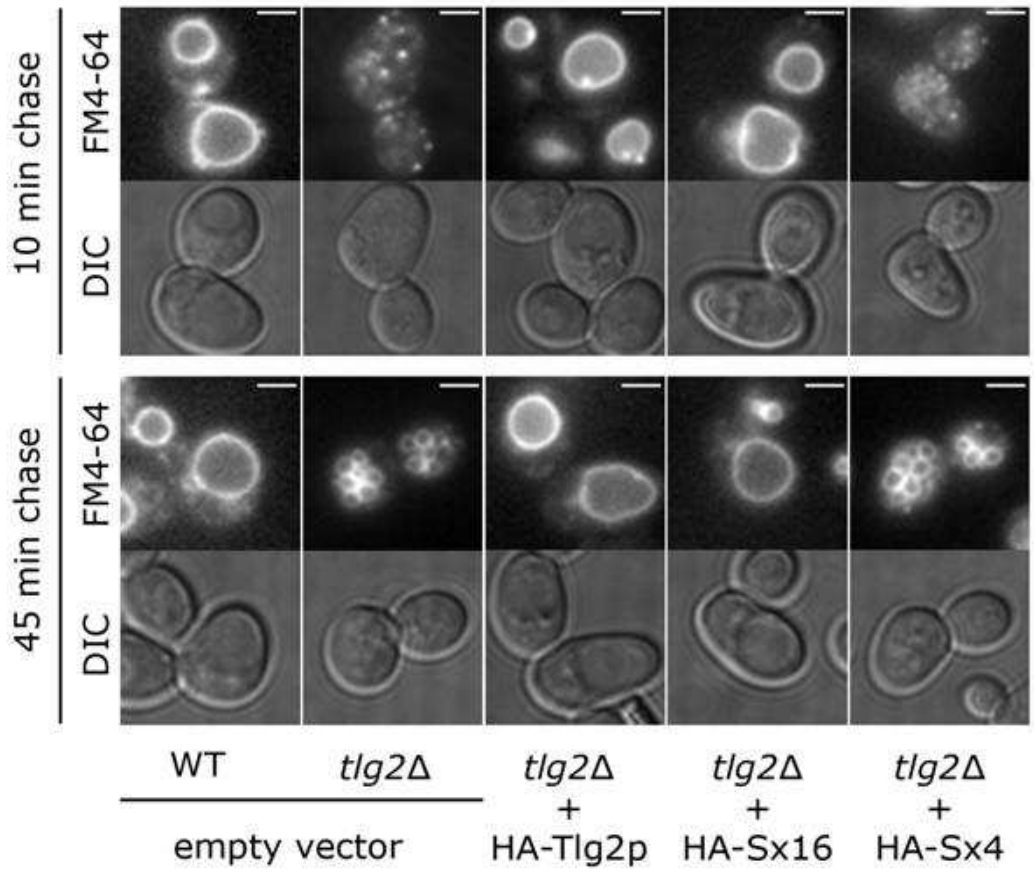

Figure 3.18– Expression of Sx16 promotes efficient FM4-64, vacuolar labelling in *tlg2Δ* cells. Trafficking of the lipophillic styryl dye, FM4-64, in wild-type cells (WT; RPY10) transformed with pVT102u (empty vector) was compared to that of *tlg2Δ* cells (NOzY4; RPY10 *tlg2Δ*) transformed with pVT102u (empty vector), pHA-Tlg2 (encoding HA-Tlg2p), pSGS025 (encoding HA-Sx16) or pSGS036 (encoding HA-Sx4). Transformants were grown to mid-log phase in SD-ura-met, before harvesting and resuspending in the rich media, YPD. FM4-64 was then added to these cultures at final concentration of 30 µM and the cells incubated at 0ºC for 30 mins. The dye was subsequently removed and a chase period initiated by resuspending the cells in fresh prewarmed media (SD-ura-met) lacking FM4-64. Cells were incubated for 10 mins and 45 mins at 30ºC after which time the chase period was terminated by the addition of NaN_3 at a final concentration of 15 mM. Cells were then kept on ice until they were visualised by fluorescent and DIC microscopy. The scale bars displayed in the top right corner of each of the fluorescent images represents 2 µm.

Figure 3.18 demonstrates that after a 10 min chase, the lipophillic styryl dye, FM4-64 clearly labels the vacuolar membrane of wild-type cells, as previously reported in (Vida and Emr, 1995). Clear vacuolar labelling is also displayed in *tlg2Δ* cells expressing HA-Tlg2p and HA-Sx16. In contrast, FM4-64 does not reach the vacuole in *tlg2Δ* cells containing empty vector or expressing HA-Sx4 and instead appears to concentrate in small cytosolic puncta within the cell (Figure 3.18). This is similar to the phenotype of that seen in wild-type cells incubated at 15ºC (Vida and Emr, 1995) in which FM4-64 is trapped in an endocytic compartment to which GFP-Tlg2p co-localises (Abeliovich et al., 1998). These results demonstrate that trafficking of FM4-64 to the vacuole is impaired in *tlg2Δ* cells and uncorrected by the expression of HA-Sx4. Although FM4-64 successfully labels the vacuolar membrane within *tlg2Δ* cells after a 45 min chase, the labelled vacuole appears to be more fragmented than that of wild-type cells; a phenotype which has previously been described for *tlg2Δ* cells (Seron et al., 1998). It should however be noted that *tlg2Δ* cells expressing either HA-Tlg2p or HA-Sx16 (but not those expressing HA-Sx4) have a vacuolar morphology similar to that of wild-type cells (Figure 3.18).

These data demonstrate a delayed trafficking of FM4-64 to the vacuolar membrane of *tlg2Δ* cells as well as describing the fragmented vacuolar morphology of these cells. The replacement of Tlg2p or the introduction of Sx16 to *tlg2Δ* cells complements both of these phenotypes whereas Sx4 does not. These findings support those previously found when investigating Ste3p endocytosis and hence support the hypothesis that Sx16 is a functional homologue of the yeast t-SNARE, Tlg2p.

3.5.5 Immunofluorescence analysis of syntaxin localisation

The syntaxins Tlg2p and Sx16 are both localised to the Golgi apparatus in yeast and mammalian cells, respectively (Holthuis et al., 1998, Simonsen et al., 1998, Tang et al., 1998). Tlg2p co-localises and co-fractionates with the yeast TGN markers Kex2p and DPAP A (Holthuis et al., 1998) and Sx16 co-localises with the mammalian Golgi marker β-COP and also partially co-localises with the TGN marker, the mannose-6-phosphate receptor (Simonsen et al., 1998). If Sx16 and Tlg2p are functional homologues they will likely co-localise to the same region within yeast cells. In order to investigate whether or not heterologously expressed Sx16 co-localises with endogenous Tlg2p immunofluorescene was used. Wild-type cells (SF838-9D) transformed with the plasmids, pMAZ002 (HA-Sx16) or pMAZ006 (HA-Tlg2p) were grown in media (SD-ura-met) containing 50 µM $CuCl_2$ for 3 hours before fixing (see Section 2.5.5). Fixed cells were

then spheroplasted and permeabilised. These cells were then attached to Poly-L-Lysine coated slides and double labelled with the primary antibodies, anti-Tlg2p and anti-HA, before incubating with the secondary antibodies, Alex Fluor® 594 donkey anti-rat (which binds to the primary anti-HA antibody and has an excitation/emission maxima of ~590 nm/617 nm (orange-red)) and Alex Fluor® 488 donkey anti-rabbit (which binds to the primary anti-Tlg2p antibody and has excitation/emission maxima of ~495 nm/519 nm (cyan-green)). The localisation of Tlg2p, HA-Tlg2p and HA-Sx16 was then visualised using confocal microscopy.

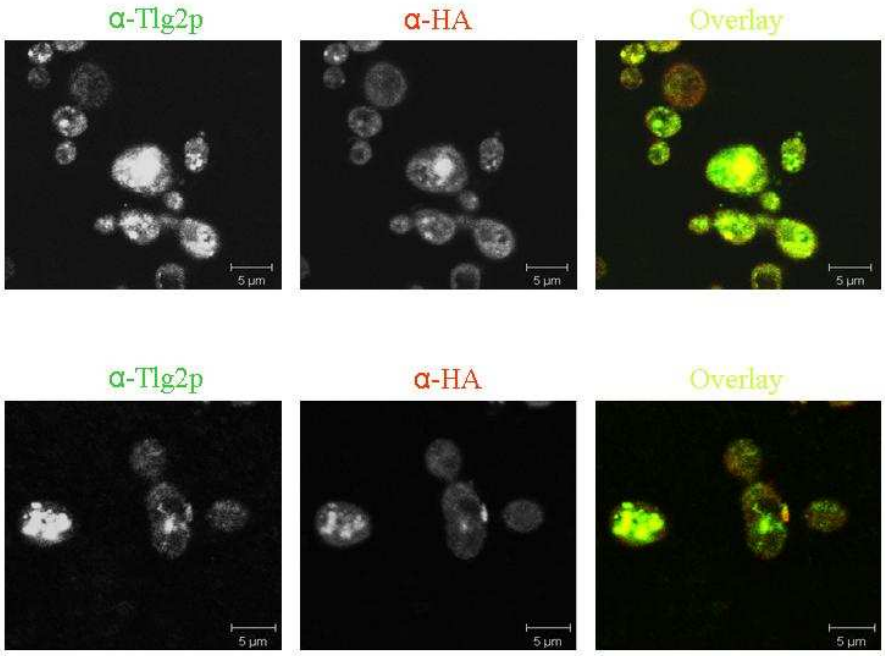

Figure 3.19– Sx16 co-localises with both endogenous Tlg2p and HA-Tlg2p. Localisation of HA-Sx16 and HA-Tlg2p was compared to that of endogenous Tlg2p in wild-type cells transformed with pMAZ002 (HA-Sx16) or pMAZ006 (HA-Tlg2p). Transformants were grown in the selective media SD-ura-met containing 50 µM $CuCl_2$, fixed and treated with the primary antibodies (anti-Tlg2p and anti-HA). Rabbit anti-Tlg2p was visualised with the secondary antibody, Alex Fluor® 488 donkey anti-rabbit, and the rat anti-HA antibody visualised using Alex Fluor® 594 donkey anti-rat. The images captured were overlaid to look for co-localisation of HA-Sx16 with endogenous Tlg2p (lower panel) and also the co-localisation of HA-Tlg2p with endogenous Tlg2p (upper panel).

Figure 3.19 indicates that both HA-Sx16 and HA-Tlg2p co-localise with endogenous Tlg2p. However further work is required to reduce the background staining detected with the anti-Tlg2p antibody possibly by introducing further washing or a higher dilution factor. Control experiments should also be performed to confirm that binding of the antibodies is specific to the proteins of interest. Sx4 was not included in this experiment as it has

previously been shown, in this chapter, that Sx4 does not complement the function of Tlg2p.

3.6 Discussion

The experiments performed in this chapter support the hypothesis that Sx16 is a functional homologue of the yeast t-SNARE, Tlg2p. This was demonstrated by the ability of the heterologous expressed splice variant of human Sx16, Sx16A, to complement for the loss of Tlg2p, by correcting the trafficking defects displayed in *tlg2Δ* mutant cells. These include osmotic sensitivity (Figure 3.15), incorrect trafficking of vacuolar proteases such as CPY (Figure 3.16), impaired endocytosis (Figure 3.17 and 3.18) and vacuolar morphology (Figure 3.18). Preliminary data also suggests that Sx16 co-localises with endogenous Tlg2p (Figure 3.19) however further work is required to provide conclusive evidence of this.

Chapter 4 – Sx16 is regulated by Vps45p when expressed in yeast

The work presented in this chapter has been published in (Struthers et al, 2009)

4.1 Introduction

SNARE proteins represent the minimal machinery required for membrane fusion *in vitro* (Hu et al., 2003, Weber et al., 1998); however, it is clear that there are a number of other factors required *in vivo*. A family of proteins, essential for SNARE-mediated membrane fusion *in vivo*, are the SM proteins. Loss of function mutations in SM genes results in a block in membrane fusion as demonstrated in the organisms *S. cerevisiae* (Cowles et al., 1994, Novick and Schekman, 1979, Ossig et al., 1991, Robinson et al., 1988, Wada et al., 1990), *D. melanogaster* (Harrison et al., 1994) and *C. elegans* (Hosono et al., 1992). SM proteins are arched-shaped peripheral membrane proteins of approximately 60-70 kDa (Bracher and Weissenhorn, 2002, Jahn, 2000, Misura et al., 2000). There are four SM proteins found in yeast (Vps45p, Vps33p, Sly1p, Sec1p) and seven found in mammalian cells (Munc18a, Munc18b, Munc18c, mVps45, mVps33a, mVps33b, Sly1) (Dulubova et al., 2002). The primary effectors of SM proteins are syntaxins (Jahn, 2000, Toonen and Verhage, 2003).

The SM protein Vps45p binds with high affinity to Tlg2p (Bryant and James, 2001) and regulates the entry of the syntaxin into SNARE complexes *in vivo* (Bryant and James, 2001). This chapter builds upon the findings presented in Chapter 3 that established Sx16 as a functional homologue of Tlg2p, and demonstrates that Sx16 utilises Vps45p when expressed in yeast.

4.2 Sx16 and Tlg2p share the same mode of interaction with the SM protein, Vps45p

4.2.1 Yeast Vps45p binds Sx16 via Mode 2 binding

The SM protein Vps45p binds with high affinity to Tlg2p (Bryant and James, 2001, Carpp et al., 2006, Dulubova et al., 2002), using a mode of binding analogous to that captured by the Sly1p/Sed5p crystal structure (Bracher and Weissenhorn, 2002) with the N-terminus of the syntaxin inserting into a putative hydrophobic pocket on the outer surface of the SM protein (Carpp et al., 2006, Dulubova et al., 2002).

In Chapter 3, I provided evidence to demonstrate that Sx16 is a functional homologue of the yeast syntaxin, Tlg2p. To extend this finding, I set out to ascertain whether Sx16

utilises the same molecular machinery as Tlg2p when expressed in yeast. Tlg2p-mediated membrane fusion requires the function of the SM protein Vps45p (Bryant and James, 2001) which binds the syntaxin with high affinity using at least two modes of binding (Mode 2 and Mode 3; see Section 1.3.2) (Carpp et al., 2006, Dulubova et al., 2002). Consistent with its identification as a homologue of Tlg2p, Sx16 has previously been shown to bind to the mammalian homologue of Vps45p (mVps45) and also to yeast Vps45p *in vitro* (Dulubova et al., 2002). The interaction between Vps45p/mVps45 and Sx16 can be abolished through mutation of the N-terminal peptide of Sx16 (Dulubova et al., 2002). This suggests that Sx16, like Tlg2p, utilises the putative hydrophobic pocket identified in domain 1 of Vps45p (Carpp et al., 2006). Binding in a mode analogous to the 'pocket-mode' of binding (Mode 2) captured in the Sly1p/Sed5p crystal structure, where the N-terminal peptide of the syntaxin inserts into a hydrophobic pocket on the outer surface of the SM protein (Bracher and Weissenhorn, 2002). This interaction can also be abolished through a mutation in the SM protein, Vps45p (L117R) which disrupts the hydrophobic pocket by introducing an arginine residue that is not only larger than leucine, but is also positively charged (Carpp et al., 2006). To ask whether this mutation also abolishes the binding of Vps45p to Sx16, a pull-down approach using proteins produced in *E. coli* was undertaken.

Plasmids pCOG025 (Carpp et al., 2006), pALA001 and pFB09/1 encoding the cytosolic domains of either Tlg2p, Sx16 or Sx4 fused in-frame to two IgG-binding domains from *Staphylococcus aureus* PrA at their C-terminus (Tlg2-PrA, Sx16-PrA and Sx4-PrA, respectively) were used to transform BL21 Star™ (DE3) cells (an *E. coli* strain which is utilised to improve expression of proteins in a T7 promoter based expression system (Invitrogen)). 5 ml of the transformants were grown to mid log-phase in 500 ml of Terrific Broth containing ampicillin (100 µg/ml). Protein expression was induced by the addition of IPTG (at a final concentration of 1 mM) and the cultures returned to 37°C for 4 hours with continuous shaking. Cells were harvested by centrifugation and subsequently lysed by sonication (see Section 2.2.20 for details). The proteins of interest were then purified on IgG Sepharose and the bound proteins analysed using SDS-PAGE (Figure 4.1).

The ability of these proteins to capture Vps45p, provided by yeast lysates, was then investigated. This was achieved by incubating the immobilised PrA-fusion proteins with whole cell lysates prepared from equal numbers (15 OD_{600} equivalents) of NOzY1 (SF838-9D *vps45Δ*) cells expressing HA-tagged versions of either wild-type Vps45p or a version harbouring the L117R mutation from the plasmids pCOG070 (HA-Vps45p) and pCOG071

(HA-Vps45pL117R), respectively (Carpp et al., 2006). As a control, the SM protein, Munc18c, was also incorporated in the pull-down experiment. Munc18c binds specifically to Sx4 and was included as a means of checking that the Sx4-PrA fusion protein had folded properly. The ability of Sx4-PrA to bind to Munc18c, but not Vps45p would also indicate that the interaction between Vps45p and Tlg2p/Sx16 is specific. Purified Munc18c was kindly donated by Dr Veronica Aran (University of Glasgow, UK). Following incubation with the purified SM proteins the bound material was washed and eluted (as described in Section 2.2.21.1). Proteins contained in the eluates were separated using SDS-PAGE and subsequently immunoblotted with antibodies specific to the HA-tag and Munc18c.

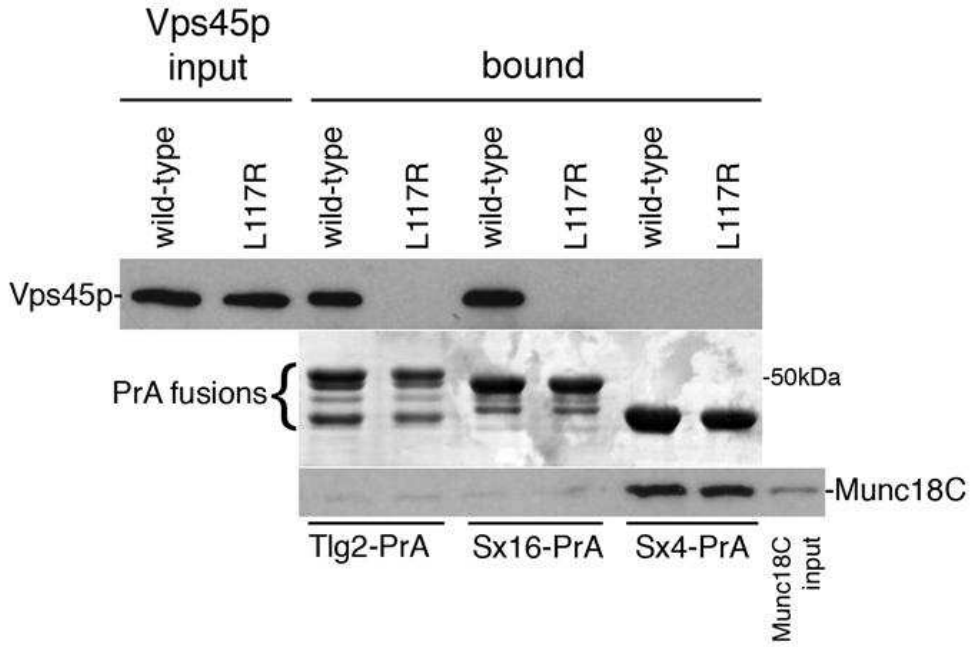

Figure 4.1 – Monomeric Sx16 and Tlg2p both interact with yeast Vps45p via Mode 2 binding. Equal amounts of each of the immobilised PrA-fusion proteins (Tlg2p-PrA, Sx16-PrA and Sx4-PrA) were incubated overnight at 4ºC with whole cell lysates prepared from 15 OD_{600} equivalents of NOzY1 (SF838-9D *vps45Δ*) cells transformed with either pCOG070 (wild-type HA-Vps45p) or pCOG071 (HA-Vps45pL117R). As a control equal amounts of the immobilised PrA-fusion proteins (Tlg2p-PrA, Sx16-PrA and Sx4-PrA) were also incubated with purified Munc18c (kindly provided by Dr Veronica Aran, University of Glasgow, UK). Proteins contained in the eluates were separated using SDS-PAGE prior to immunoblot analysis with antibodies specific to the HA-tag and Munc18c. 10% of the yeast lysate and 2% of the purified Munc18c were also included in the immunoblot analysis. Please note that this work was done in collaboration with Dr Scott Shanks (University of Glasgow, UK).

Figure 4.1 clearly shows that both C-terminally PrA-tagged cytosolic versions of Tlg2p and Sx16 (Tlg2-PrA and Sx16-PrA) efficiently capture HA-tagged wild-type Vps45p from the yeast lysate, whereas C-terminally PrA-tagged Sx4 (Sx4-PrA) does not. In contrast neither Tlg2p nor Sx16 bind the HA-tagged pocket-filled mutant version of Vps45p (Vps45pL117R). These results support previous findings, that both yeast Tlg2p and

mammalian Sx16 interact with yeast Vps45p (Dulubova et al., 2002), and indicate that this is via the same mode of binding; Mode 2. Although Sx4 does not associate with either wild-type or mutant Vps45p it is capable of associating with its cognate mammalian SM protein Munc18c. In contrast neither Sx16 nor Tlg2p interact with mammalian Munc18c. This demonstrates the specificity between SM protein/syntaxin pairing and further supports the finding that Sx16 is a functional homologue of Tlg2p.

4.2.2 Vps45p binds Sx16-containing cis-SNARE complexes in yeast

Originally it was thought that SM proteins used distinct modes of binding to interact with their cognate syntaxins (reviewed in (Burgoyne and Morgan, 2007, Toonen and Verhage, 2003)). For example, the SM protein Munc18a was thought to interact with its cognate syntaxin, Sx1a, only via Mode 1 binding (Hata et al., 1993, Pevsner et al., 1994b). However it is now becoming increasingly apparent that SM proteins can utilise multiple modes of binding to interact with their cognate syntaxins. For example, the SM protein, Munc18a can interact with Sx1a using both Mode 1 and Mode 2 binding (Burkhardt et al., 2008, Dulubova et al., 2007, Rickman et al., 2007, Shen et al., 2007).

Vps45p also uses two different modes of binding to interact with its cognate syntaxin, Tlg2p, at two different stages in the SNARE complex assembly/disassembly cycle (Bryant and James, 2003, Carpp et al., 2006). Vps45p not only binds to the monomeric Tlg2p using Mode 2 binding but can also bind to assembled SNARE complexes using Mode 3 binding; both of these interactions can be detected *in vivo* and *in vitro* (Bryant and James, 2003, Carpp et al., 2006, Dulubova et al., 2002). *cis*-SNARE complexes can be accumulated by blocking the action of the AAA-ATPase that is ordinarily responsible for their dissociation (Rouiller et al., 2002). Thus, yeast cells harbouring the temperature sensitive allele of *SEC18* (*sec18-1*) accumulate *cis*-SNARE complexes following incubation at the restrictive temperature of 37°C (Grote et al., 2000).

In order to determine whether Vps45p also associates with Sx16-containing *cis*-SNARE complexes, I used *sec18-1* cells to accumulate *cis*-SNARE complexes containing Sx16 in place of Tlg2p. This was achieved by expressing Sx16 in yeast cells harbouring the *sec18-1* allele, but lacking endogenous Tlg2p (LCY011; SEY5186 *tlg2Δ, sec18-1*). LCY011 cells transformed with the plasmids pNB701 (empty vector), pMAZ002 (encoding HA-Sx16) or pMAZ006 (encoding HA-Tlg2p) were grown at 25ºC in the

selective media, SD-ura-met, containing 50 μM $CuCl_2$ for one generation (OD_{600} of 0.4-0.6). At this stage, cells were either kept at 25°C or transferred to the restrictive temperature of 37°C, for 90 mins. The mutant Sec18p is no longer functional at 37ºC, resulting in an accumulation of *cis*-SNARE complexes in these cells. Immunoprecipitation from yeast cell lysates (prepared from equal numbers of cells, 40 OD_{600} equivalents) was performed at 4ºC for 2 hours using an antibody specific to the HA-tag followed by an hour incubation with PrA agarose. Proteins contained in the immunoprecipitates were separated by SDS-PAGE prior to immunoblot analysis with antibodies specific to Vps45p and the HA-tag. It should be noted that the HA-specific antibodies used for immunoprecipitation and immunoblot analysis were raised in different hosts, rat and mouse respectively, to prevent the cross-reaction of the light and heavy chains of the antibodies, which would make analysis of the results problematic.

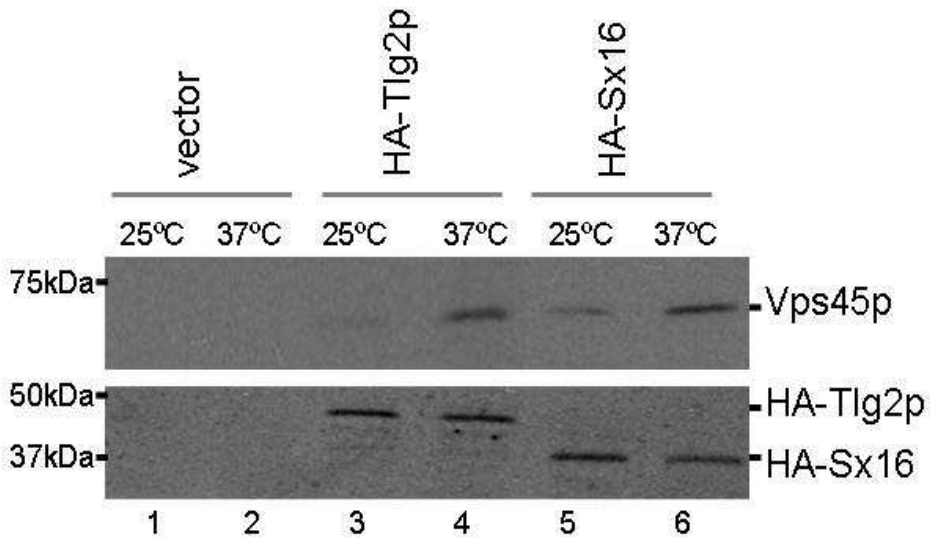

Figure 4.2 – Sx16 and Tlg2p both interact with yeast Vps45p when present in the *cis*-SNARE complexes.
LCY011 (SEY5186 *tlg2Δ, sec18-1*) cells transformed with pNB701 (empty vector), pMAZ002 (encoding HA-Sx16) or pMAZ006 (encoding HA-Tlg2p) were grown at 25ºC for one generation (OD_{600} of 0.4-0.6) in the selective media, SD-ura-met, containing 50μM $CuCl_2$. Cultures were either incubated at the non-permissive temperature (37ºC) or kept at the permissive temperature (25ºC) for a further 90 mins. Immunoprecipitation of yeast cell lysates (prepared from equal numbers of these cells (40 OD_{600} equivalents)) was performed at 4ºC for 2 hours in the presence of 10 μl of antibody specific to the HA-tag, followed by an hour incubation in the presence of 50 μl of settled PrA agarose. Following extensive washes (see Section 2.2.18) the agarose was eluted and the proteins contained in the eluates anlysed using SDS-PAGE and immunoblot analysis with antibodies specific to Vps45p and the HA-tag.

As previously observed (Bryant and James, 2003), Figure 4.2 demonstrates that incubation of *sec18-1* cells at the restrictive temperature leads to an increased association between Vps45p and Tlg2p (compare upper panel lanes 3 and 4; Figure 4.2), due to the association

of Vps45p with the accumulated *cis*-SNARE complexes (Bryant and James, 2003). Figure 4.2 also shows a similar increase of the association between Vps45p and Sx16 under these same conditions (compare lanes 5 and 6; Figure 4.2). Since this experiment was performed by immunoprecipitating Tlg2p/Sx16, rather than Tlg1p (as in (Bryant and James, 2003)) it is important to note that the co-precipitated Vps45p also represents that bound to monomeric Tlg2p/Sx16. Nevertheless, there is a marked increase in the amount of co-precipitated Vps45p upon the accumulation of *cis*-SNARE complexes indicating that, like Tlg2p-containing *cis*-SNARE complexes, Sx16-containing *cis*-SNARE complexes bind Vps45p *in vivo.*

4.3 Levels of Tlg2p and Sx16 are greatly reduced in yeast cells lacking Vps45p

4.3.1 Levels of Tlg2p are greatly reduced in yeast cells lacking Vps45p

It has previously been reported that the removal of the SM protein, Vps45p from the cell, results in the reduction of cellular levels of the syntaxin, Tlg2p, by greater than 90% when compared to wild-type cells (Bryant and James, 2001). To confirm this I analysed the levels of Tlg2p in wild-type (SF838-9D) and *vps45Δ* (NOzY1; SF838-9D *vps45Δ*) cells. This was achieved by preparing whole cell lysates from equal numbers (1 OD_{600} equivalents) of wild-type (SF838-9D) and *vps45Δ* (NOzY1; SF838-9D *vps45Δ*) cells grown to mid-log phase in the rich media, YPD. Immunoblot analysis was used to assess the levels of Tlg2p, and also the other individual components of the Tlg2p-containing SNARE complex, present in the lysates.

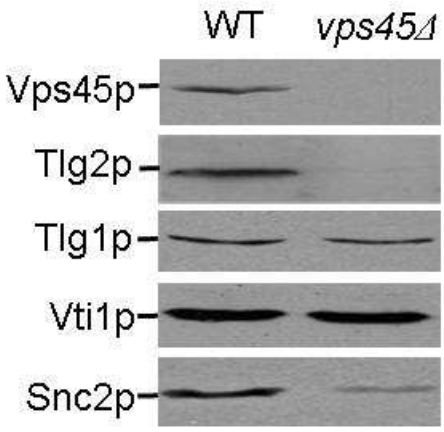

Figure 4.3 – Both the t-SNARE, Tlg2p and the v-SNARE, Snc2p are greatly reduced in *vps45Δ* cells.
Whole cell lysates prepared from equal numbers of wild-type (SF838-9D) and *vps45Δ* (NOzY1; SF838-9D *vps45Δ*) cells (1 OD_{600} equivalents) grown to mid-log phase in the rich media, YPD, were analysed using immunoblot analysis with antibodies specific to Vps45p, Tlg2p, Tlg1p, Vti1p and Snc2p.

Figure 4.3 confirms that endogenous levels of Tlg2p are greatly reduced in the absence of the SM protein, Vps45p (Bryant and James, 2001). In contrast the levels of the t-SNAREs, Tlg1p and Vti1p, are unaffected. It is interesting to note that the levels of the v-SNARE, Snc2p, are also reduced in cells lacking Vps45p. As well as binding Tlg2p, Vps45p also binds directly to Snc2p (Carpp et al., 2006). However no interaction between Vps45p and the t-SNAREs, Tlg1p or Vti1p, can be detected (Carpp et al., 2006). These results suggest that the SM protein, Vps45p, plays an important role in regulating the levels of the syntaxin, Tlg2p, and the v-SNARE, Snc2p, within the cell.

4.3.2 Levels of Sx16 are also greatly reduced in yeast cells lacking Vps45p

Considering the results already presented in this chapter which demonstrate that Sx16 interacts with Vps45p *in vitro* (Figure 4.1) and *in vivo* (Figure 4.2), I wondered if the levels of Sx16, like Tlg2p, may also be reduced in the absence of Vps45p. In order to investigate this, I compared the levels of Tlg2p, Sx16 and Sx4 in wild-type and *vps45Δ* cells. This was achieved by transforming wild-type (RPY10) and *vps45Δ* (NOzY2; RPY10 *vps45Δ*) cells with the plasmids pNB701 (empty vector), pMAZ002 (encoding HA-Sx16), pMAZ006 (encoding HA-Tlg2p) or pMAZ007 (encoding HA-Sx4). Transformants were grown to mid-log phase in the selective media, SD-ura-met, containing 50 µM $CuCl_2$ to induce the expression of the syntaxins. Whole cell lysates prepared from equal numbers of

these transformants (1 OD_{600} equivalents) were analysed using immunoblot analysis with an antibody specific to the HA-tag.

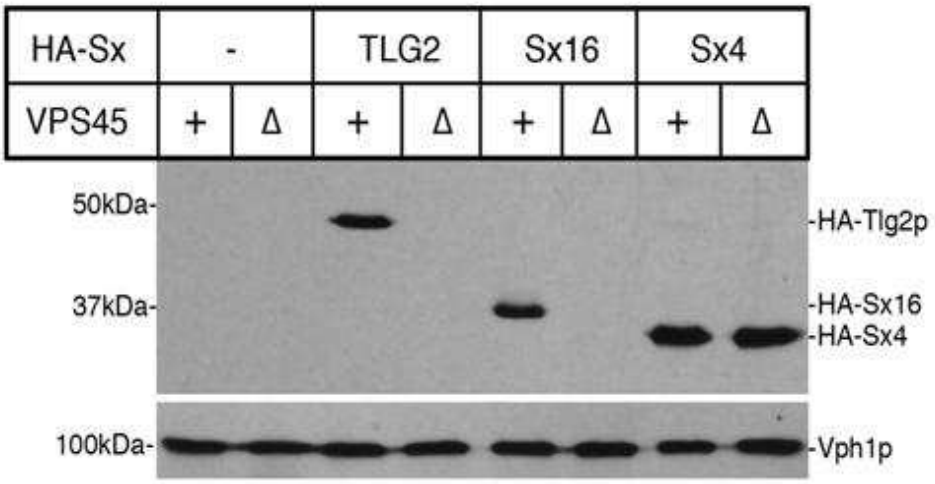

Figure 4.4 – Sx16 and Tlg2p are both degraded in *vps45Δ* cells.
Wild-type (VPS45+) and *vps45Δ* (VPS45Δ) cells transformed with the plasmids, pNB701 (empty vector (-)), pMAZ002 (encoding HA-Sx16), pMAZ006 (encoding HA-Tlg2p) or pMAZ007 (encoding HA-Sx4) were grown to mid-log phase in selective media, SD-ura-met, containing 50μM $CuCl_2$. Whole cell lysates prepared from equal numbers of these transformants (1 OD_{600} equivalents) were analysed using immunoblot analysis with an antibody specific to the HA-tag. The levels of the vacuolar ATPase, Vph1p, were also assessed using immunoblot analysis to control for equal loading.

Cells lacking endogenous Vps45p (VPS45Δ) expressing either HA-Tlg2p or HA-Sx16 have a reduced level of syntaxin when compared to wild-type cells (VPS45+) expressing either HA-Tlg2p or HA-Sx16 (Figure 4.4). However cellular levels of Sx4, which does not bind Vps45p (Figure 4.1), remain unaffected by the presence/absence of Vps45p. These results suggest that Sx16 is regulated in a manner similar to that of Tlg2p and further supports the hypothesis that Sx16 is a functional homologue of Tlg2p.

4.4 A truncated version of Tlg2p/Sx16 can bypass the requirement for Vps45p

It has previously been shown that, in contrast to the full-length syntaxin, a version of Tlg2p lacking its N-terminal 230 residues (Tlg2pΔHabc) is protected from downregulation in cells lacking Vps45p and is able to form SNARE complexes under these conditions (Bryant and James, 2001). Expression of this mutant version of Tlg2p suppresses trafficking defects displayed by yeast cells lacking Vps45p (*vps45Δ*) (Bryant and James, 2001). Like all *vps* mutants, *vps45*Δ mutant cells missort the vacuolar hydrolase

carboxypeptidase Y (CPY) (Cowles et al., 1994, Piper et al., 1994). In wild-type cells, proCPY (p2) is trafficked from the TGN to the vacuole where it is proteolytically processed into its active, mature form (m). *vps45Δ* mutant cells secrete ~75-85% of their CPY into the extracellular media (Cowles et al., 1994, Piper et al., 1994). The CPY which remains intracellular in *vps45Δ* mutant cells is in the p2 form indicating that it has been unable to reach the proteolytically active vacuole (Cowles et al., 1994, Piper et al., 1994). Expression of Tlg2pΔHabc in *vps45*Δ cells results in the internal CPY being processed to its mature form, demonstrating that the SNARE complexes formed by this mutant in the absence of Vps45p are functional (Bryant and James, 2001). As a means to investigate if a similar version of Sx16, lacking its Habc domain, could also suppress the trafficking defects of *vps45Δ* mutant cells, the plasmids pSGS043 (encoding HA-Tlg2pΔHabc) and pSGS044 (encoding HA-Sx16ΔHabc) were generated (a detailed description of how these plasmids were constructed is give in Section 2.2.5). A schematic diagram representing the differences between full-length and truncated version of the syntaxins is shown below.

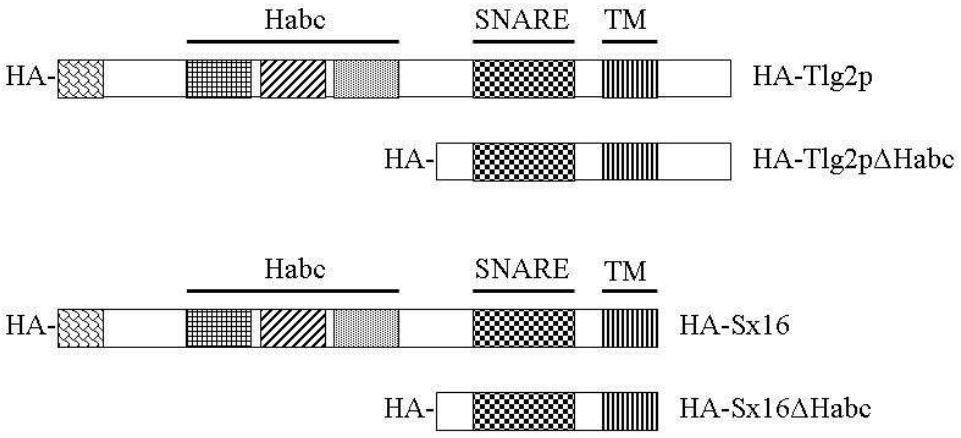

Figure 4.5 - A schematic diagram of full-length and truncated versions of syntaxins, Tlg2p (HA-Tlg2pΔHabc) and Sx16 (HA-Sx16ΔHabc).
The abbreviations in this diagram represent the HA-tag (HA), the Habc domain (Habc), the SNARE domain (SNARE) and the Transmembrane domain (TM).

In order to investigate whether or not this truncated version of Sx16, like Tlg2p, could bypass the requirement of Vps45p, maturation of CPY was monitored in NOzY2 (RPY10 *vps45Δ*) cells transformed with the plasmids, pVT102u (empty vector), pSGS043 (encoding HA-Tlg2pΔHabc) or pSGS044 (encoding HA-Sx16ΔHabc). Equal numbers of these cells (1 OD_{600} equivalent) grown to mid-log phase were labelled with [^{35}S]cysteine/methionine for 10 mins at 30ºC prior to the addition of an excess of unlabelled cysteine/methionine. Cells were collected immediately after the addition of

cysteine/methionine and again after 30 mins at 30ºC. CPY was immunoprecipitated from intracellular (I) and extracellular (E) fractions at the times indicated (0 and 30 mins) and the samples analysed using SDS-PAGE and fluorography (see Section 2.2.19). This work was done in collaboration with Dr. Nia J. Bryant (University of Glasgow, UK).

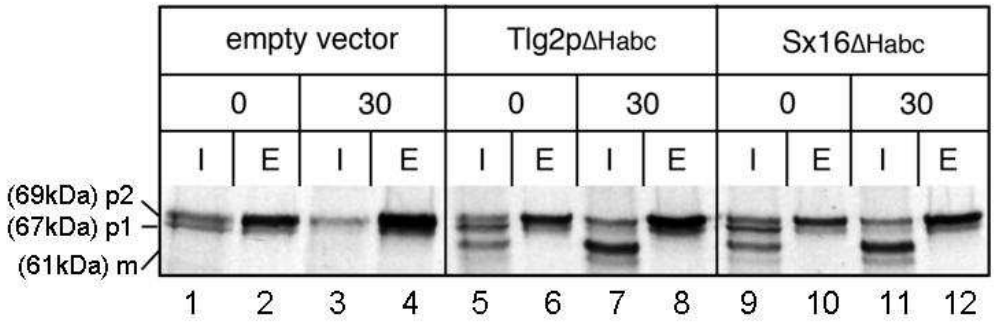

Figure 4.6 – Expression of either truncated HA-Tlg2p or HA-Sx16 lacking the Habc domain results in the maturation of CPY in *vps45Δ* cells.
NOzY2 (RPY10 *vps45Δ*) cells transformed with pVT102u (empty vector), pSGS043 (encoding HA-Tlg2pΔHabc) or pSGS044 (encoding HA-Sx16ΔHabc) were grown to mid-log phase in the selective media SD-ura-met. Equal numbers of these cells (1 OD_{600} equivalent) were then labelled with [^{35}S]cysteine/methionine for 10 mins at 30ºC prior to the addition of an excess of unlabelled cysteine/methionine. Cells were collected immediately after the addition of cysteine/methionine and again after 30 mins at 30ºC. CPY was immunoprecipitated from intracellular (I) and extracellular (E) fractions at the time-points indicated (0 and 30 mins). The resultant samples were analysed using SDS-PAGE and fluorography with the water-soluble fluor Sodium Salicylate.

As previously described CPY trafficking in *vps45Δ* cells is greatly impaired with ~75-85% of newly synthesised CPY being incorrectly secreted from the cell (Cowles et al., 1994, Piper et al., 1994), this is also reflected in these findings (Figure 4.6, compare lanes 1 and 2 and lanes 3 and 4). The fraction of CPY which accumulates intracellularly (I) is predominately in the p2 form, however upon the expression of truncated versions of the syntaxins Tlg2p (Tlg2pΔHabc) or Sx16 (Sx16ΔHabc) CPY successfully reaches maturation in the vacuole (Figure 4.6, lanes 5 and 7; 9 and 11, respectively).

4.5 Discussion

This chapter builds upon those findings presented in Chapter 3, which established Sx16 as a functional homologue of Tlg2p, by demonstrating that Sx16 utilises Vps45p when expressed in yeast. This was primarily demonstrated by the ability of Vps45p to interact with both monomeric Tlg2p and Sx16 *in vitro* using Mode 2 binding (Figure 4.1). Similarly Vps45p can also interact with Tlg2p and Sx16 containing *cis*-SNARE complexes

in vivo (Figure 4.2). Levels of Sx16, like Tlg2p, are also depleted in cells lacking Vps45p (Figure 4.4), further establishing the relationship between Sx16 and Vps45p. Lastly it was demonstrated that both a truncated version of Tlg2p (Tlg2pΔHabc) and Sx16 (Sx16ΔHabc) can bypass the requirement of the SM protein, Vps45p, and enable the vacuolar delivery of CPY (Figure 4.6). This finding supports the hypothesis that one function of Vps45p is to activate the syntaxin for entry into SNARE complexes by facilitating a transition from a closed to an open conformation (Bryant and James, 2001).

The following section further discusses the findings presented in Figure 4.6, which show that a truncated version of Tlg2p (HA-Tlg2pΔHabc) and Sx16 (HA-Sx16ΔHabc) can bypass the requirement of the SM protein, Vps45p. Truncation of the Habc domain from Tlg2p and Sx16 prevents these syntaxins from adopting a closed conformation analogous to that of Sx1a (Dulubova et al., 1999, Misura et al., 2000). The SM protein, Munc18a is required for the transition of Sx1a from a closed conformation to an open conformation (Dulubova et al., 1999, Misura et al., 2000). Hence the data presented here (Figure 4.6) and that previously presented (Bryant and James, 2001) would support a model in which Vps45p is required for the transition of Tlg2p and Sx16 from a closed conformation to an open conformation that is compatible with SNARE complex assembly. However this is contradictory to NMR data which indicates that a bacterially produced version of Tlg2p is unlikely to adopt a closed conformation (Dulubova et al., 2002). It should be noted that the construct used in these studies only spans residues 60-283 of Tlg2p and thus lacks 24 of the 54 residues that make up the SNARE motif (Dulubova et al., 2002). The authors chose this construct as it contains sequence involved in forming a closed conformation of Sx1a (Dulubova et al., 1999, Misura et al., 2000) and Sso1p (Fiebig et al., 1999, Munson et al., 2000). However, it is possible that this construct lacks residues required to stabilise a closed conformation of Tlg2p.

In order to explain how a truncated version of Tlg2p, Tlg2pΔHabc, forms functional SNARE complexes in the absence of Vps45p (Bryant and James, 2001) in light of their conclusion that Tlg2p does not adopt a closed conformation, Dulubova and colleagues suggest that some inhibitory factor might bind to the N-terminal portion of Tlg2p (possibly the Habc domain) and prevent SNARE complex formation (Dulubova et al., 2002). They postulated that Vps45p could be involved in releasing such an inhibition, and thus promote SNARE complex assembly. The truncated version of Tlg2p (Tlg2pΔHabc) would not be able to bind this inhibitory factor and thus would not be subject to the same regulation by Vps45p (Dulubova et al., 2002).

It is apparent that two different interpretations of the data presented in Figure 4.6 and (Bryant and James, 2001) exist. Although both of these interpretations agree that Vps45p promotes Tlg2p SNARE complex assembly, our group suggests that this is through the transition of Tlg2p from a closed conformation to an open conformation (Bryant and James, 2001) whereas Dulubova and colleagues suggest that Vps45p acts by releasing some inhibitory factor bound to the N-terminal portion of Tlg2p. In order to distinguish between these two different interpretations we further investigated the ability of Vps45p to promote SNARE complex formation by promoting the transition of Tlg2p from a closed to an open conformation. The following work (published in (Struthers et al., 2009)) was performed by Chris MacDonald, a PhD student in the lab.

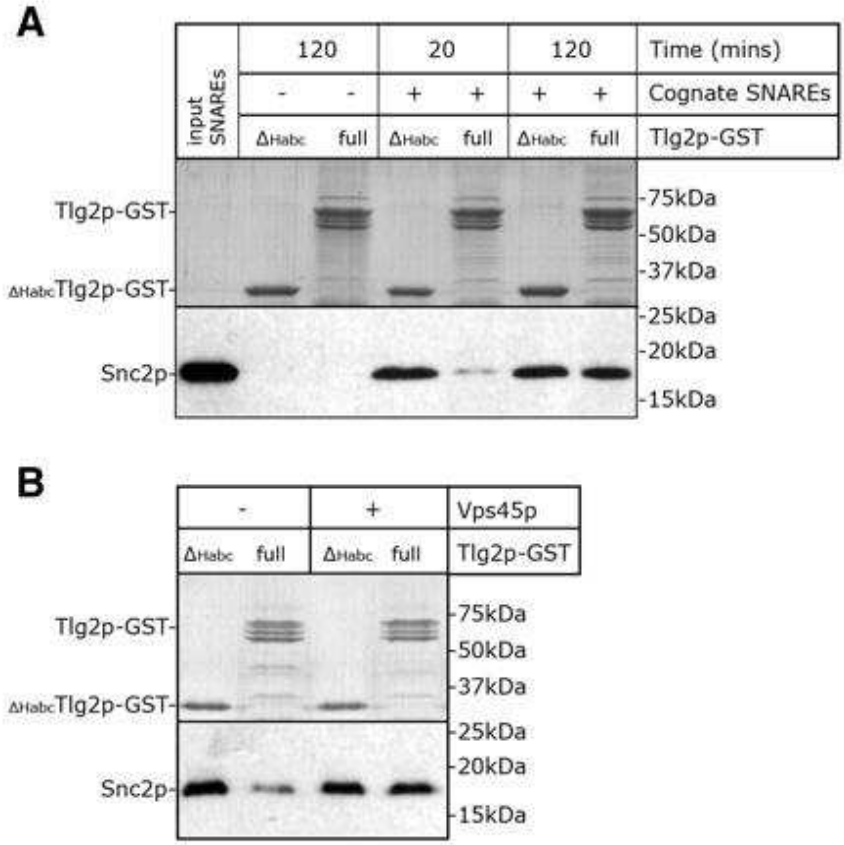

Figure 4.7 – Data taken from (Struthers et al., 2009) showing that SNARE-complex assembly is stimulated by both the deletion of the Habc domain from Tlg2p and also by Vps45p. (A) The ability of Tlg2p-GST, or a version lacking the Habc domain (Tlg2pΔHabc-GST), to form SNARE complexes *in vitro* was assessed by incubating the GST fusions (purified from *E. coli* and immobolised on glutathione-Sepharose) with tenfold molar excesses of His_6-tagged versions of Snc2p and Vti1p, and untagged Sx8-Tlg1p chimera. After incubation for 20 or 120 mins at 4ºC with continuous mixing. Sepharose beads were harvested by centrifugation at 1000g for 1 minute and washed extensively with binding buffer. Immunoblot analysis was used to assess the amount of Snc2p bound to the Tlg2p-GST fusions (lower panel; a sample of the input cognate SNAREs was included in this analysis). Upper panel shows a Coomassie-stained gel of the Tlg2p-GST fusions that were incubated either with (+) or without (-) the cognate SNARE-binding proteins. (B) The effect of adding purified His_6-tagged Vps45p on the ability of Tlg2p-GST and Tlg2pΔHabc-GST to form SNARE complexes *in vitro* during a 20 minute incubation was assessed by performing the experiments presented in A in the absence or presence of a tenfold molar excess of His_6-tagged Vps45p (over Tlg2p-GST and Tlg2pΔHabc-GST).

Chris used GST pull-down experiments to investigate the ability of full-length and truncated versions of Tlg2p to form SNARE complexes (Struthers et al., 2009). SNARE complex formation is assessed by the levels of Snc2p binding to full-length Tlg2p and truncated Tlg2p (Tlg2pΔHabc) after a 20 min and 120 min incubation in the presence of the SNARE components, Vti1p and the Sx8-Tlg1p chimera. After 20 mins, it is clear that the truncated version of Tlg2p, Tlg2pΔHabc, has formed more SNARE complexes than full-length Tlg2p (Figure 4.7A). However following a longer incubation of 120 mins,

similar amounts of SNARE complexes were formed by both truncated Tlg2p (Tlg2pΔHabc) and full-length Tlg2p (Figure 4.7A). These results indicate that Habc domain of Tlg2p inhibits the formation of SNARE complexes *in vitro*. To investigate whether or not Vps45p could alleviate this inhibition, Chris added purified Vps45p to his pull-down experiments. The addition of Vps45p resulted in similar amounts of Snc2p binding to both Tlg2pΔHabc and Tlg2p after a 20 min incubation (Figure 4.7B). Hence Vps45p does alleviate the inhibition caused by the Habc domain of Tlg2p.

It should be noted that these *in vitro* pull-down experiments used only bacterially produced proteins, hence the possibility of an inhibitory factor found *in vivo* binding to Tlg2p and preventing SNARE complex formation, could be ruled out. A more likely explanation would be that full-length Tlg2p adopts a closed conformation which requires the action of Vps45p to allow its transition to an open conformation compatible with SNARE complex assembly.

In addition to these findings (Figures 4.6 and 4.7; (Bryant and James, 2001)) it has recently been demonstrated using isothermal titration calorimetry (ITC) that fragments of Sx16 (residues 1-302, 1-279, 1-265) greater than the N-terminal peptide (residues 1-27) can bind mammalian Vps45 with a higher affinity that the N-terminal peptide alone (Burkhardt et al., 2008). The authors also identify an interaction between the C-terminal portion of the SNARE domain of Sx16 and Vps45p which is thought to be equivalent to the interaction between Sx1a and the central cavity of Munc18a (Burkhardt et al., 2008). Consistent with the finding that Tlg2p and Sx16 are functional homologues this would suggest that the Tlg2p construct (60-283) used in NMR studies (Dulubova et al., 2002) was lacking residues required to stabilise a closed conformation of Tlg2p (Dulubova et al., 2002).

In conclusion these results support our model that Vps45p is required for the transition of Tlg2p (and Sx16) from a closed conformation to an open conformation that is compatible with SNARE complex assembly.

Chapter 5 – Regulation of Tlg2p levels in the cell

5.1 Introduction

Cells lacking Vps45p (*vps45Δ*) have reduced levels of Tlg2p (Figure 4.3 and (Bryant and James, 2001)). *vps45Δ* cells synthesise Tlg2p to similar levels as wild-type cells, but the protein is turned over much more rapidly ($t_{½}$ of Tlg2p is 20 mins in *vps45Δ* cells, compared to > 2 hours in wild-type cells) resulting in low cellular levels of the syntaxin (Bryant and James, 2001). In order to further understand the mechanism by which Tlg2p is degraded in *vps45Δ* cells, I set out to investigate the regulation of steady-state levels of Tlg2p in wild-type and *vps45Δ* cells.

This chapter documents the vacuolar degradation of Tlg2p in wild-type cells; the ubiquitination and palmitoylation of Tlg2p in wild-type and *vps45Δ* cells, and also several attempts to identify the specific lysine(s) that is/are ubiquitinated.

5.2 Steady-state levels of Tlg2p are mediated by the vacuole

At steady-state levels, Tlg2p localises to the yeast TGN, co-localising and co-fractionating with the TGN markers Kex2p and DPAP A, respectively (Holthuis et al., 1998). Proteins localise to the yeast TGN by continually cycling through the proteolytically active endosomal system (Bryant and Stevens, 1997, Kornfeld, 1992, Piper et al., 1995), and thus it seemed plausible that vacuolar proteases may regulate the cellular levels of Tlg2p, just as the ER-associated degradative pathways function to regulate cellular levels of the ER-localised t-SNARE, Ufe1p (Braun and Jentsch, 2007). In order to investigate this I used immunoblot analysis to assess the steady-state levels of Tlg2p in wild-type cells containing vacuolar proteases (RPY10 and SEY6210) and those harbouring the *pep4-3* mutation (SF838-9D and RMY8). Mutation of the *PEP4* gene results in the loss of vacuolar activity; *PEP4* encodes an aspartyl protease that is required to activate vacuolar hydrolases (Woolford et al., 1986).

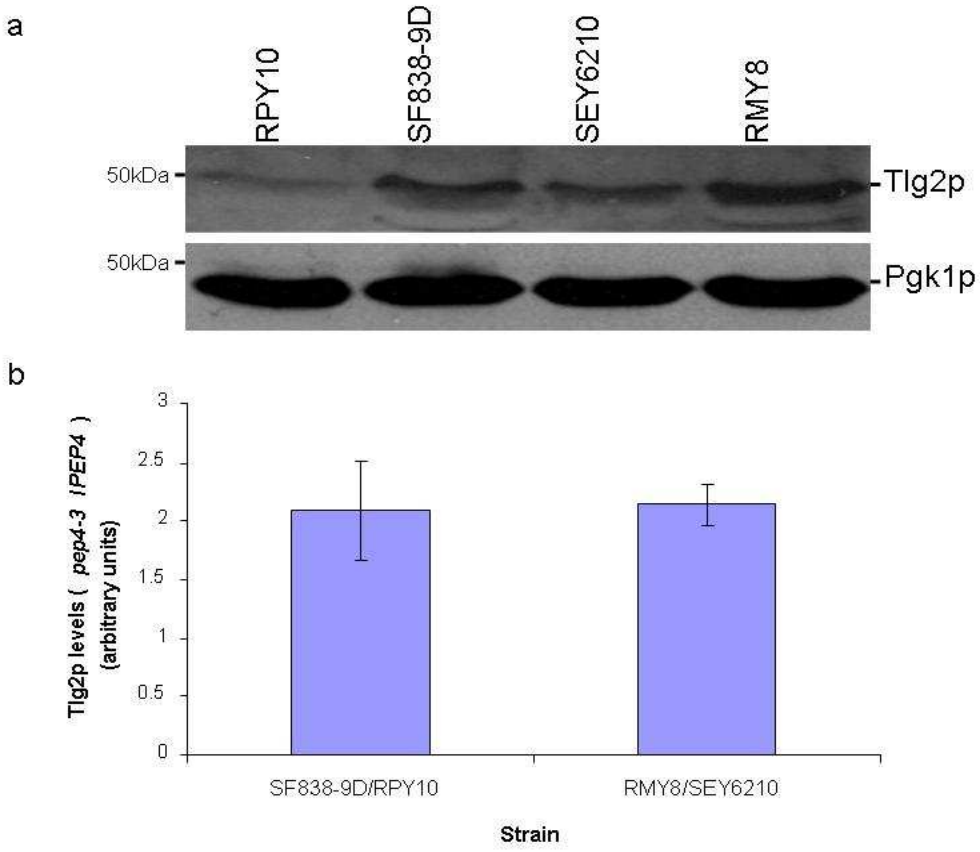

Figure 5.1 – Cellular levels of Tlg2p are elevated in cells lacking vacuolar activity. Immunoblot analysis was used to compare the steady-state levels of Tlg2p in wild-type cells containing active vacuolar proteases (RPY10 and SEY6210) and those lacking vacuolar proteases (SF838-9D and RMY8). (a) Proteins contained within whole cell lysates, prepared from 1 OD_{600} equivalents, were separated using SDS-PAGE prior to immunoblot analysis with an antiserum specific to Tlg2p. The same filter was probed for Pgk1p to control for equal loading. b) The levels of Tlg2p detected by immunoblot analysis were quantified using the computer software, Image Processing and Analysis in Java (Image J) and normalised to the loading control Pgk1p. The ratio of Tlg2p in cells lacking active vacuolar proteases (*pep4-3*) and those containing vacuolar proteases (*PEP4*) was then calculated (*pep4-3/PEP4*). Error bars are '+' and '-' standard deviations of the mean, n=3.

Figure 5.1 shows that steady-state levels of Tlg2p in wild-type cells lacking active vacuolar proteases are increased approximately 2 fold when compared to their isogenic strains containing active vacuolar protease (2.03 ± 0.43 fold greater in SF838-9D than RPY10 and 2.14 ± 0.18 fold greater in RMY8 than SEY6210). These data indicate that the vacuole does indeed play a role in regulating the levels of Tlg2p in wild-type cells.

To circumvent problems that arose with detecting endogenous Tlg2p using specific antiserum (which was in limited supply and not wholly reliable), the possibility of using the HA-tagged version of Tlg2p produced from pMAZ006 (described in Chapter 3) to study the regulation of cellular levels of Tlg2p was investigated. Initially I set out to

investigate if HA-Tlg2p (expressed from pMAZ006) was regulated in a similar manner to endogenous Tlg2p, i.e. if it would be degraded by vacuolar proteases. Wild-type cells containing active vacuolar proteases (RPY10 and SEY6210) and those harbouring the *pep4-3* mutation (SF838-9D and RMY8) were transformed with either pNB701 (empty vector) or pMAZ006 (encoding HA-Tlg2p). Expression from the *CUP1* promoter was induced by the addition of 50 µM $CuCl_2$ to the selective media, SD-ura-met, in which the transformants were grown. Proteins contained within whole cell lysates, prepared from equal numbers of these transformants (1 OD_{600} equivalents), were separated by SDS-PAGE prior to immunoblot analysis with an antibody specific to the HA-tag.

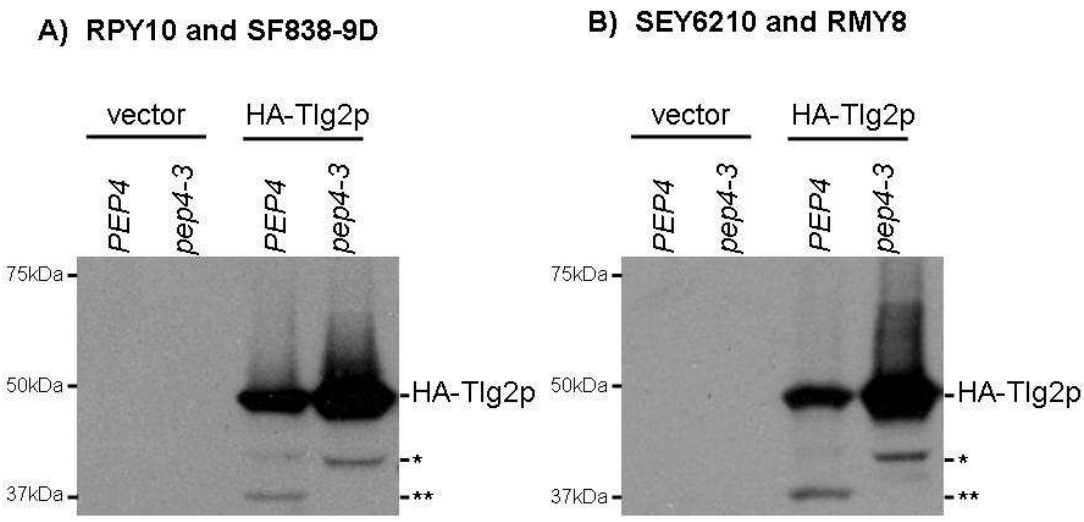

Figure 5.2 – Levels of HA-Tlg2p (expressed from pMAZ006) are elevated in wild-type cells lacking active vacuolar proteases.
Two independent yeast strains RPY10 and SEY6210 (both *PEP4*) and their isogenic *pep4-3* strains SF838-9D and RMY8, respectively, were transformed with either pNB701 (empty vector) or pMAZ006 (encoding HA-Tlg2p) and grown on the selective media, SD-ura-met, containing 50 µM $CuCl_2$. Levels of HA-Tlg2p present in whole cell lysates prepared from equal numbers of these transformants (1 OD_{600} equivalents) were assessed using immunoblot analysis with an antibody specific to the HA-tag.

Figure 5.2 demonstrates that levels of HA-Tlg2p expressed from pMAZ006 are regulated by vacuolar proteases in a similar manner to that observed for endogenous Tlg2p (Figure 5.1). A HA-immunoreactive band of approximately 37 kDa (**) is present in lysates prepared from HA-Tlg2p expressing cells containing vacuolar activity: this is likely a proteolytic product of HA-Tlg2p generated by vacuolar enzymes. It should also be noted a larger *PEP4*-independent degradation product (*) is present in lysates prepared from cells with and without active vacuolar proteases (this is particularly noticeable in those cells

lacking vacuolar activity) suggesting that (**) is generated from (*) (this is discussed in more detail later).

The finding that steady-state levels of Tlg2p are regulated by the vacuole (Figures 5.1 and 5.2) was intriguing since it has previously been reported that Tlg2p is degraded by the proteasome in *vps45Δ* cells (Bryant and James, 2001). This conclusion was reached since, in contrast to *vps45Δ* cells containing proteasomal activity, *vps45Δ* cells in which proteasomal activity has been abolished (through mutation of either the catalytic subunits, Pre1p and Pre2p (*pre1-1, pre2-2*) or the regulatory domain, Cim3p (*cim3-1*) (Heinemeyer et al., 1993, Heinemeyer et al., 1991, Ghislain et al., 1993)) contain levels of Tlg2p that can easily be detected through immunoblot analysis (Bryant and James, 2001). Inactivation of vacuolar proteases through the *pep4-3* mutation, on the other hand, did not restore Tlg2p levels in *vps45Δ* cells (Bryant and James, 2001).

Considering the data presented in Figures 5.1 and 5.2 and that from (Bryant and James, 2001), it would appear that both the proteasome and the vacuole are involved in mediating the levels of Tlg2p within the cell. One possibility is that more Tlg2p becomes exposed to vacuolar proteases in wild-type cells compared to *vps45Δ* cells, as Vps45p is required to allow the efficient delivery of proteins to the proteolytically active endosomal compartment (Bryant and Stevens, 1998, Cowles et al., 1994, Piper et al., 1994). Hence, the degradation of Tlg2p in wild-type cells would be dependent on both the vacuole and the proteasome, whereas the proteasome would be responsible for the degradation of Tlg2p in cells lacking Vps45p. This model would explain why levels of Tlg2p are not rescued in *vps45Δ pep4-3* cells (Bryant and James, 2001).

In order to investigate the possibility that Tlg2p does not enter the proteolytically active endosomal system in the absence of Vps45p, I decided to increase the production of HA-Tlg2p from pMAZ006 to a level at which it was still detectable in *vps45Δ* cells. As described in Chapter 3, expression of HA-Tlg2p from pMAZ006 is under the control of the regulatable *CUP1* promoter, and so by increasing the concentration of Cu^{2+} ions in the growth media it is possible to increase the production of HA-Tlg2p from pMAZ006. A copper concentration of 100 µM (twice that used in the complementation experiments discussed in Chapter 3) was selected. Increasing the production of HA-Tlg2p in *vps45Δ* cells would enabled me to investigate whether or not HA-Tlg2p is subject to vacuolar degradation in the absence of Vps45p, as it is in the presence of the SM protein (Figures 5.1 and 5.2). As previously mentioned a 37 kDa *PEP4*-dependent Tlg2p degradation

product is detectable in wild-type cells containing active vacuolar proteases, expressing HA-Tlg2p (** in Figure 5.2). If Tlg2p does not enter the proteolytically active endosomal system in the absence of Vps45p this *PEP4*-dependent Tlg2p degradation product should be absent or at least reduced. Two independent strains containing active vacuolar proteases (RPY10 and SEY6210) and their isogenic *vps45Δ* derivatives (NOzY2 and LCY007, respectively) were transformed with either pNB701 (empty vector) or pMAZ006 (encoding HA-Tlg2p). Expression from the *CUP1* promoter was induced by the addition of 100 µM $CuCl_2$ to the selective media in which the transformants were grown. Proteins contained within lysates, prepared from equal numbers of these cells (1 OD_{600} equivalents), were separated using SDS-PAGE prior to performing immunoblot analysis with an antibody specific to the HA-tag.

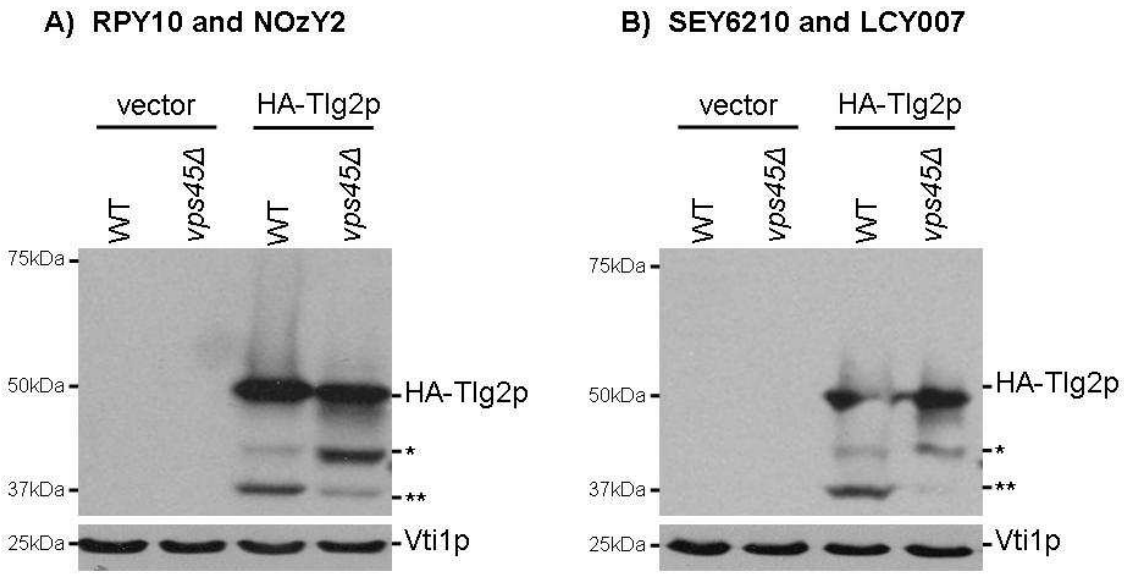

Figure 5.3 – A comparison of steady-state levels of HA-Tlg2p in wild-type (WT) and *vps45Δ* cells containing active vacuolar proteases.
Two independent yeast strains A) RPY10 and B) SEY6210 (both *PEP4*) and their isogenic *vps45*Δ derivatives NOzY2 and LCY007, respectively, were transformed with either pNB701 (empty vector) or pMAZ006 (encoding HA-Tlg2p). Transformants were grown on the selective media, SD-ura-met containing 100 µM $CuCl_2$. Proteins contained within whole cell lysates, prepared from equal numbers of these transformants (1 OD_{600} equivalents), were separated by SDS-PAGE prior to immunoblot analysis with an antibody specific to the HA-tag (and the SNARE protein, Vti1p, to control for equal loading).

It is evident from Figure 5.3 that a smaller fraction of HA-Tlg2p is processed by vacuolar proteases in cells lacking Vps45p. This is represented by the decreased levels of the 37 kDa (**) HA-immunoreactive reactive band detectable in lysates prepared from *vps45Δ* cells compared to those from wild-type cells. There is also a larger degradation product (*)

detected by the anti-HA antibody (also detected in Figure 5.2) which appears to be at elevated levels in lysates prepared from *vps45Δ* cells expressing HA-Tlg2p when compared to those from wild-type cells also expressing HA-Tlg2p (Figure 5.3). This larger degradative product (*) is also detected at elevated levels in lysates prepared from wild-type cells lacking active vacuolar proteases, expressing HA-Tlg2p (Figure 5.2). These results suggest that the levels of Tlg2p in *vps45Δ* cells are regulated in a manner independent of the vacuole and that this larger degradative product (*) is the substrate for the degradative process that generates the *PEP4*-dependent product (**). These observations are consistent with the hypothesis outlined above, which states that in the absence of Vps45p, Tlg2p does not enter the proteolytically active endosomal system.

The vacuolar dependent cleavage event(s) detected in Figures 5.2 and 5.3, must occur towards the C-terminus of the protein, as the product can be detected by HA antibodies and the HA-tag is at the extreme N-terminus of the protein (A in Figure 5.4). Thus product is lacking sequence from the C-terminus, the lumenal portion of Tlg2p. A schematic diagram of the proposed topology of Tlg2p is shown below.

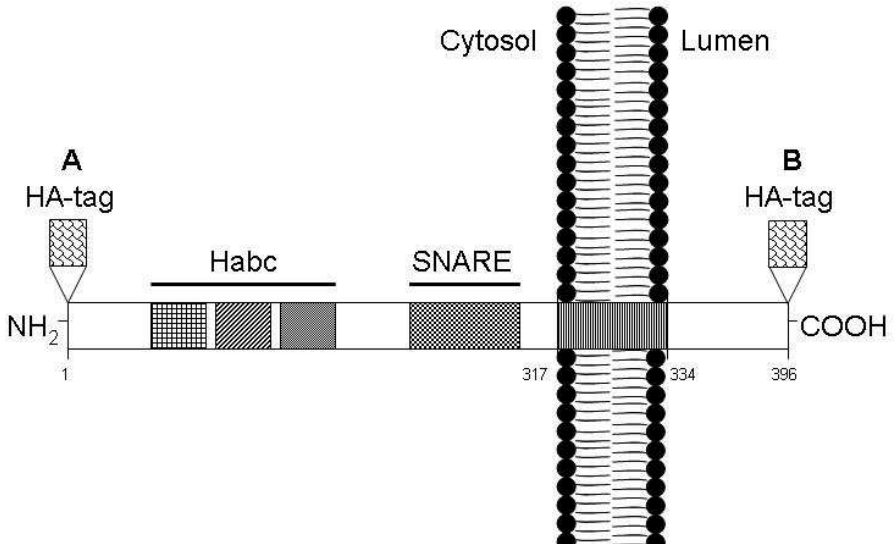

Figure 5.4 – A schematic diagram showing the proposed topology of Tlg2p. Residues 1-316 of the syntaxin, Tlg2p, represent the cytosolic domain which harbours the SNARE motif (SNARE) and the Habc domain (Habc). Residues 317-334 represent the Transmembrane domain which is buried within the phospholipid bilayer. Unlike other syntaxins, Tlg2p also contains an additional lumenal domain (residues 335-396) at its C-terminus. This diagram was constructed using the data provided in (Dulubova et al., 2002). A and B represent N- and C-terminally HA-tagged versions of Tlg2p, respectively.

In order to test this assumption, i.e. that the *PEP4*-dependent cleavage event(s) generating the HA-immunoreactive band of 37 kDa (** in Figures 5.2 and 5.3) is/are occurring

towards the C-terminus of the protein, I used immunoblot analysis to investigate whether or not I could detect any degradative products in cells expressing a C-terminally HA-tagged version of Tlg2p (Tlg2p-HA) (B in Figure 5.4). NOzY2 (RPY10 *vps45Δ*; *PEP4*) cells were transformed with the plasmids pNB701 (empty vector) pMAZ006 (encoding HA-Tlg2p) or pCOG039 (encoding Tlg2p-HA). Expression of these constructs (HA-Tlg2p and Tlg2p-HA) was under the control of the *CUP1* promoter and hence expression was driven by the addition of 100 µM $CuCl_2$ to the selective media, SD-ura-met, in which the transformants were grown. Proteins contained within whole cell lysates prepared from equal numbers of these transformants (1 OD_{600} equivalents) were separated using SDS-PAGE prior to immunoblot analysis with an antibody specific to the HA-tag.

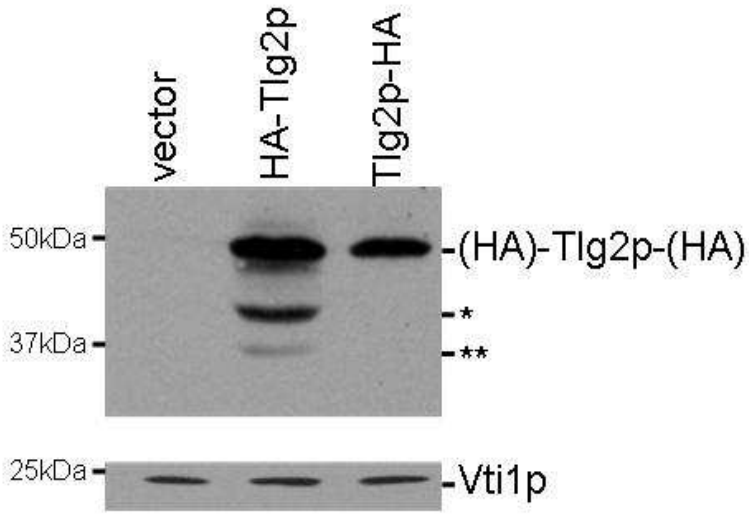

Figure 5.5 - N- and C-terminally HA-tagged versions of Tlg2p display different patterns of degradation products in *vps45Δ* cells (containing active vacuolar proteases).
Whole cell lysates prepared from NOzY2 (RPY10 *vps45Δ; PEP4*) cells transformed with the plasmids pNB701 (empty vector), pMAZ006 (encoding N-terminally tagged HA-Tlg2p) or pCOG039 (encoding C-terminally tagged Tlg2p-HA) were analysed using immunoblot analysis with an antibody specific to the HA-tag. Expression of the N- and C-terminally HA-tagged versions of Tlg2p from the *CUP1* promoter was induced by the addition of 100 µM $CuCl_2$ to the media in which the transformants were grown. Levels of Vti1p were also assessed using immunoblot analysis to control for equal loading.

In contrast to N-terminally HA-tagged Tlg2p (HA-Tlg2p), no HA-immunoreactive degradative products ((*) or (**)) are detectable in lysates prepared from *vps45Δ* cells containing active vacuolar proteases expressing C-terminally HA-tagged Tlg2p (Tlg2p-HA) (Figure 5.5). These data support the contention that the *PEP4*-dependent product of HA-Tlg2p is generated through cleavage of the C-terminus of Tlg2p.

It has been reported that Tlg2p expression in bacteria can be improved by removal of the lumenal domain (Paumet et al., 2005). Considering this and the data already provided in this chapter, it seemed plausible that the lumenal domain could also be involved in regulating the levels of Tlg2p *in vivo*. In order to investigate this I used SDM to introduce two stop codons immediately after the TM domain of the coding sequence for HA-Tlg2p (in pMAZ006) generating the plasmid pMAZ038 (encoding HA-Tlg2p(1-336)) (details of how this plasmid was generated are described in Section 2.2.5). A schematic diagram of full-length HA-tagged Tlg2p (HA-Tlg2p) and truncated HA-tagged Tlg2p (HA-Tlg2p(1-336)) is shown below.

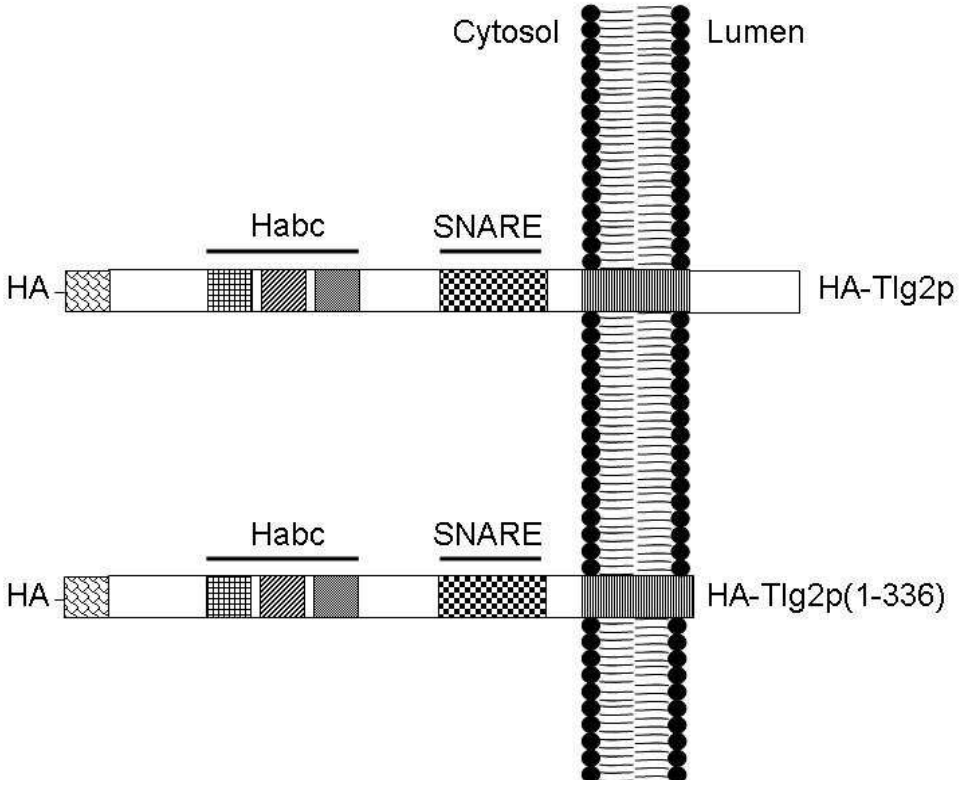

Figure 5.6 – A schematic diagram of full-length HA-tagged Tlg2p (HA-Tlg2p) and truncated HA-tagged Tlg2p (HA-Tlg2p(1-336)).
The truncated version of HA-tagged Tlg2p was generated by introducing two stop codons immediately after the TM domain of the coding sequence for HA-Tlg2p (in pMAZ006). The abbreviations in this diagram represent the HA-tag (HA), the Habc domain (Habc) and the SNARE domain (SNARE). The TM domain is embedded in the phospholipid bilayer.

The newly generated plasmid, pMAZ038 (encoding HA-Tlg2p(1-336)), the parental plasmid pMAZ006 (encoding HA-Tlg2p) and the empty vector, pNB701 were used to transform wild-type cells with (RPY10) and without (SF838-9D) active vacuolar proteases. Expression of these constructs (HA-Tlg2p(1-336) and HA-Tlg2p) was under the control of the *CUP1* promoter and hence expression was driven by the addition of 100 µM $CuCl_2$ to

the selective media, SD-ura-met, in which the transformants were grown. Whole cell lysates prepared from equal numbers of these transformants (1 OD_{600} equivalents) were subject to immunoblot analysis with an antibody specific to the HA-tag.

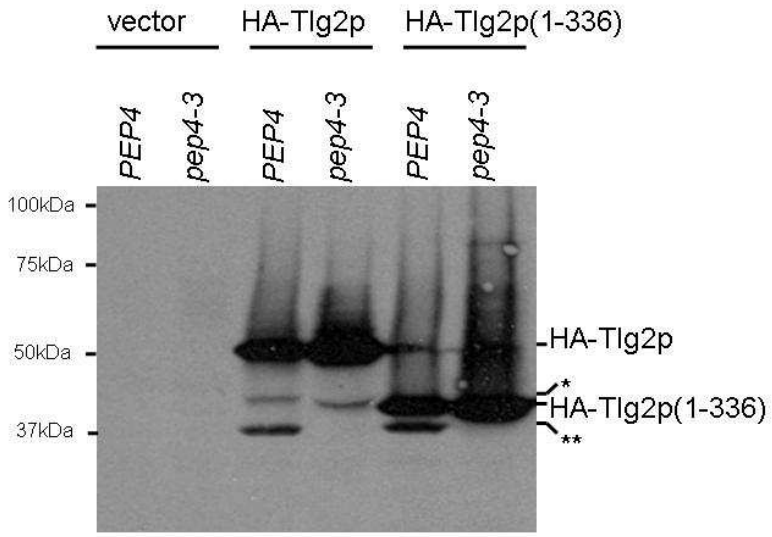

Figure 5.7 – Removal of the lumenal domain from Tlg2p does not increase the steady-state levels of Tlg2p, nor does it prevent the *PEP4*-dependent degradation of Tlg2p.
Whole cell lysates prepared from 1 OD_{600} equivalents of *PEP4* (RPY10) cells and *pep4-3* (SF838-9D) cells transformed with the plasmids pNB701 (empty vector), pMAZ006 (encoding HA-Tlg2p) or pMAZ038 (encoding HA-Tlg2p(1-336)) were analysed using immunoblot analysis with an antibody specific to the HA-tag. Expression from the *CUP1* promoter was induced by the addition of 100 µM $CuCl_2$ to the media in which the transformants were grown.

No obvious difference in the levels of Tlg2p is detectable after the removal of the lumenal domain (Figure 5.7). It is however apparent that the truncated version of Tlg2p (HA-Tlg2p(1-336)) encoded by the plasmid pMAZ038 undergoes *PEP4*-dependent degradation, as a HA-immunoreactive band of ~37 kDa (**) is still detectable in wild-type cells containing active vacuolar proteases (*PEP4*) expressing HA-Tlg2p(1-336). These results suggest that the processing event(s) that result in the generation of the 37 kDa (**) product occur in the cytosolic portion of Tlg2p.

5.3 Tlg2p is ubiquitinated in wild-type and *vps45Δ* cells

Ubiquitination is the process by which the small protein moiety, ubiquitin, becomes covalently attached to a protein (Hicke and Dunn, 2003). Ubiquitin is linked to its target protein via an isopeptide bond, connecting the carboxy group of the C-terminal glycine

residue of ubiquitin to the ε-amino group of a lysine residue in the target protein or less commonly to the amino group at the N-terminus of the target protein (Hicke and Dunn, 2003). Ubiquitination is most commonly known as the signal for degradation of a protein by the proteasome; however ubiquitination can also have a variety of different effects within the cell, for example ubiquitin can also signal for the entry of proteins into MVBs for degradation by the vacuole (Hicke and Dunn, 2003) (see Section 1.4.1.1).

As discussed previously in this chapter, Tlg2p is degraded by the proteasome in *vps45Δ* cells (Bryant and James, 2001). Taking this finding into consideration along with those presented earlier in this chapter (Section 5.2), which demonstrate that the steady-state levels of Tlg2p are, in part, regulated by the vacuole, it seemed possible that Tlg2p may be a target for ubiquitination in both wild-type and *vps45Δ* cells.

In order to investigate this, I used a GST fusion protein harbouring the ubiquitin binding (UBA) domain of the yeast protein, Dsk2p (Funakoshi et al., 2002). Dsk2p is an adaptor protein involved in the delivery of polyubiquitinated proteins to the proteasome for degradation (Funakoshi et al., 2002). Dsk2p has two key domains which are critical for this process: an N-terminal ubiquitin-like (Ubl) domain and a C-terminal ubiquitin-associated (UBA) domain (Funakoshi et al., 2002). The Ubl domain facilitates association with the proteasome, whilst the UBA domain (residues 328-373) binds ubiquitin chains (Funakoshi et al., 2002).

Structural studies indicate that the interaction between the UBA domain of Dsk2p and ubiquitin is facilitated through the main chain amide group of Gly47 of ubiquitin (Ohno et al., 2005). Two residues within the UBA domain of Dsk2p were identified as being important for its interaction with ubiquitin: a methionine residue at position 342 (Met342) and a phenylalanine residue at 344 (Phe344) which make hydrophobic contacts with Ile44 and Gly47 of ubiquitin respectively (Ohno et al., 2005). Mutation of these residues within Dsk2p, were predicted to abolish any interaction with ubiquitin (Ohno et al., 2005).

Although the UBA domain of Dsk2p has preference for binding K48-linked polyubiquitin chains, it can also associate with K63-linked chains as well as monoubiquitin (Funakoshi et al., 2002). This feature makes this domain ideal to investigate whether a protein is modified by ubiquitination, as a GST-fusion protein harbouring the UBA domain of Dsk2p (GST-UBA encoded by the plasmid pGEX-DSK$_{UBA}$) (Funakoshi et al., 2002) would serve as a convenient tool for use in pull-down assays to assess the ubiquitination status of a

protein. Hence, I utilised this to look at the ubiquitination status of Tlg2p. As a negative control for these studies, I took advantage of a mutated version of the GST-UBA fusion protein (encoded by the plasmid pCAL1; constructed by Christopher Lamb, PhD student, University of Glasgow, UK). GST-mutUBA is identical to GST-UBA except the two residues critical for ubiquitin binding, Met342 and Phe344 have been mutated to an arginine and alanine, respectively (described in Section 2.2.5).

pGEX-DSK$_{UBA}$ and pCAL1 (encoding GST-UBA and GST-mutUBA respectively), were transformed into BL21 Star™ (DE3) cells (Invitrogen). The resultant transformants were grown to mid-log phase in 500 ml Terrific Broth containing ampicillin (at a final concentration of 100 µg/ml) at 37°C before protein expression was induced by the addition of IPTG to a final concentration of 1 mM. The cultures were returned to 37°C for 4 hours with continuous shaking, after which time cells were harvested by centrifugation. GST-UBA and GST-mutUBA were purified on glutathione-Sepharose (as described in Section 2.2.20.2). The purity and amount of GST-UBA and GST-mutUBA bound to glutathione-Sepharose beads was assessed using SDS-PAGE followed by Coomassie staining (Figure 5.8).

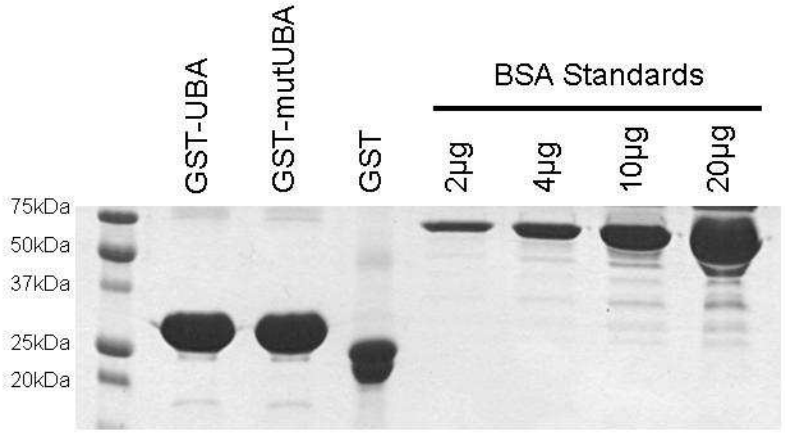

Figure 5.8 – SDS-PAGE quantification of the purified GST-fusion proteins
GST-UBA and GST-mutUBA fusion proteins were expressed in bacteria and purified glutathione-Sepharose beads. Proteins eluted from the beads were separated by SDS-PAGE (15% (v/v) polyacrylamide gel) and visualised using Coomassie Blue staining. In order to estimate the quantity of protein bound to the beads a series of protein standards (2 µg, 4 µg, 10 µg and 20 µg BSA standards) were also included. A sample of purified GST was also included to ensure that the proteins had not substantially degraded.

From Figure 5.8, I estimate that a 1 in 10 dilution of glutathione-Sepharose suspension (of which 5 µl was loaded on the gel) has approximately 20 µg GST-UBA or GST-mutUBA (with the 2 suspensions containing approximately equal amounts of their respective

GST-fusion). Therefore the concentration of GST-UBA or GST-mutUBA purified on the glutathione-Sepharose is approximately 40 µg/µl. Importantly, this gel shows that by using equal volumes of the GST-UBA and GST-mutUBA bound glutathione-Sepharose, I will be using comparable amounts of the two fusion proteins in my pull-down experiments.

Initial pull-down experiments were performed by incubating the Sepharose-bound proteins (GST-UBA and GST-mUBA) with yeast lysates prepared from SF838-9D ("wild-type"; i.e. *VPS45, TLG2*, but lacking active vacuolar proteases) and its isogenic *vps45Δ* and *tlg2Δ* derivatives NOzY1 and NOzY3, transformed with the vector p2313 (Scott et al., 2004b). p2313 encodes a GFP-tagged version of the yeast amino acid permease, Gap1p. This was included as a positive control for a protein known to be ubiquitinated under the growth conditions used (Hein and Andre, 1997, Helliwell et al., 2001, Springael and Andre, 1998, Springael et al., 1999). Following incubation with lysates prepared from equal numbers (16 OD_{600} equivalents) of the indicated strains for 2 hours at 4°C with continual mixing the amount of Tlg2p and Gap1p bound to the immobilised fusion proteins was assessed using immunoblot analysis with an antibodies specific to Tlg2p and the GFP-tag.

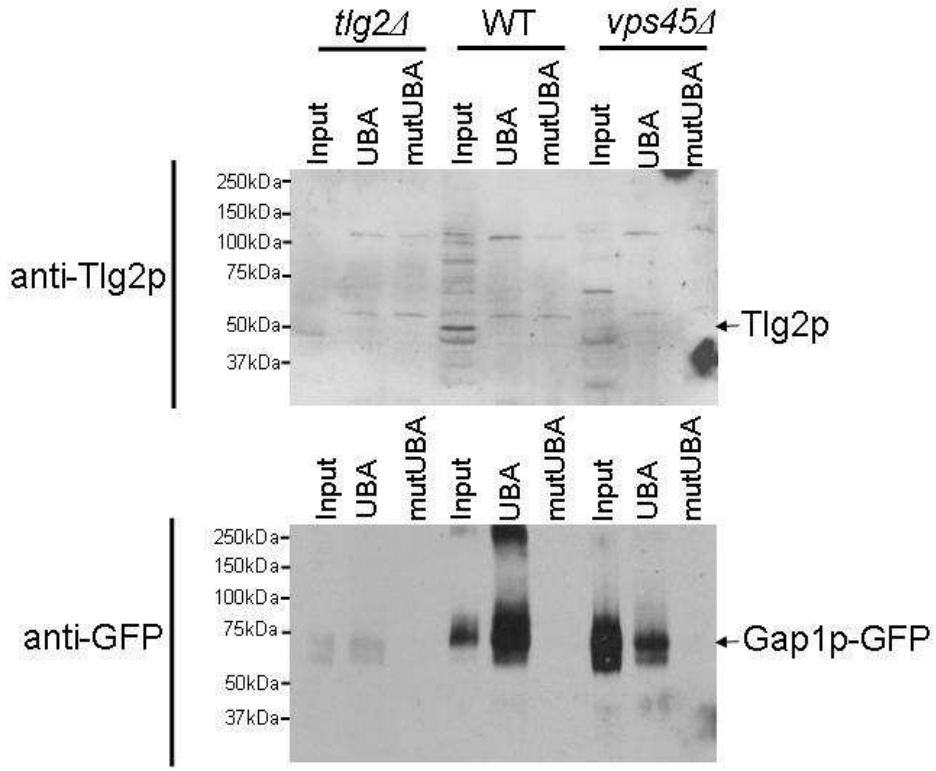

Figure 5.9 – No ubiquitinated Tlg2p is detected in wild-type or *vps45Δ* cells. Lysates prepared from SF838-9D (WT), NOzY1 (SF838-9D *vps45Δ*) and NOzY3 (SF838-9D *tlg2Δ*) cells expressing Gap1p-GFP (from p2313) were incubated with GST-UBA and GST-mutUBA prebound to glutathione-Sepharose for 2 hours at 4℃ with continuous mixing. Following extensive washing (described in Section 2.2.21.2) proteins bound to GST-UBA and GST-mutUBA were eluted and separated using SDS-PAGE prior to immunoblot analysis with antiserum specific to Tlg2p (top panel). The same filter was then probed with an antibody specific for GFP-tag (to detect Gap1p-GFP; bottom panel). 5% of lysate (input) was also included in this analysis.

This approach did not detect any ubiquitinated Tlg2p. It may be that only a small fraction of endogenous Tlg2p is ubiquitinated at any particular moment. One approach that I considered turning to, was to, utilise cells that are deficient in proteasomal activity (*pre1-1*, *pre2-2*, *cim3-1*) with the rationale that these would accumulate any ubiquitinated Tlg2p (especially in cells lacking *VPS45*). However, these cells are notoriously 'sick' and may not accumulate ubiquitinated Tlg2p, as there is only a limited pool of ubiquitin that is normally recycled (following the proteasomal degradation of ubiquitinated proteins).

As an alternative approach, I chose to use HA-tagged Tlg2p expressed from pMAZ006. My rationale was to slightly elevate the levels of Tlg2p in the hope that this would elevate the levels of ubiquitinated Tlg2p so that they would be detectable in the pull-down assay. As previously demonstrated (Figure 5.3) a copper concentration of 100 µM elevates the levels of Tlg2p to a level at which it is not fully degraded in the absence of Vps45p.

Wild-type (SF838-9D) and *vps45Δ* (NOzY1; SF838-9D *vps45Δ*) cells transformed with pNB701 (empty vector), pMAZ006 (encoding HA-Tlg2p) or p2313 (encoding Gap1p-GFP) were grown to mid-log phase in the selective media, SD-ura-met, containing 100 µM $CuCl_2$. 100 µl of lysate prepared from equal numbers of transformants (16 OD_{600} equivalents) was incubated with the Sepharose-bound proteins (either GST-UBA or GST-mutUBA) for 2 hours at 4ºC. The Sepharose was washed and eluted (as described in the Section 2.2.21.2). Proteins contained in the eluates were separated by SDS-PAGE prior to immunoblot analysis with antibodies specific to the HA- and GFP-tags.

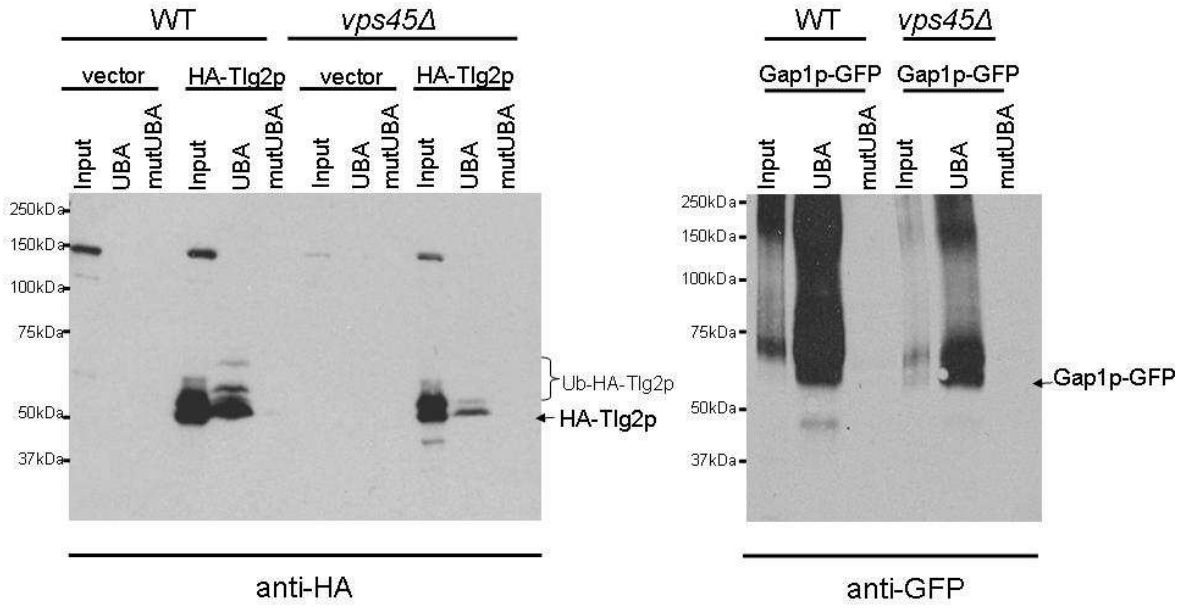

Figure 5.10 – HA-tagged Tlg2p is ubiquitinated in wild-type and *vps45Δ* cells.
Wild-type (WT, SF838-9D) and *vps45Δ* (NOzY1; SF838-9D *vps45Δ*) transformed with empty vector (pNB701), pMAZ006 (encoding HA-Tlg2p) or p2313 (encoding Gap1p-GFP) were grown to mid-log phase in SD-ura-met containing 100 µM $CuCl_2$. 100 µl of whole cell lysates prepared from equal numbers of transformants (16 OD_{600} equivalents) were incubated with either GST-UBA or GST-mutUBA prebound to glutathione-Sepharose for 2 hours at 4ºC with continuous mixing. Following extensive washes (described in Section 2.2.21.2) the Sepharose was eluted and the proteins bound to the GST-fusions analysed using SDS-PAGE and immunoblot analysis with antibodies specific for the HA- (left panel) and GFP-tags (right panel). 2.5% of the lysate (input) was also included in this analysis.

The elevated expression of HA-Tlg2p was enough to provide a pool of ubiquitinated Tlg2p detectable by the pull-down assay in both wild-type and *vps45Δ* cells (Figure 5.10). Both HA-Tlg2p and the positive control Gap1p-GFP are present in the GST-UBA pull-down, but not in the control (GST-mutUBA) (Figure 5.10). It should also be noted that there is a "ladder" of HA-immunoreactive bands (Ub-HA-Tlg2p in Figure 5.10) pulled-down by GST-UBA from wild-type cells expressing HA-Tlg2p which is not detectable in the empty vector control, suggesting that Tlg2p is polyubiquitinated and/or multi-monoubiquitinated

(monoubiquitinated on multiple sites). This is less evident in the sample prepared from *vps45Δ* cells, possibly because levels of Tlg2p are downregulated in the absence of Vps45p (Bryant and James, 2001).

5.4 Mapping the ubiquitination sites of Tlg2p

It is evident from Figure 5.10 that a fraction of HA-Tlg2p expressed from pMAZ006 in the presence of 100 μM $CuCl_2$ is ubiquitinated in both wild-type and *vps45Δ* cells. However HA-Tlg2p expressed at this level is not completely degraded in the absence of Vps45p (Figure 5.3 and 5.10). In order to map possible sites of ubiquitination involved in targeting Tlg2p for degradation in cells lacking Vps45p, I decided to express Tlg2p at levels slightly higher than endogenous Tlg2p, but low enough to be degraded in the absence of Vps45p. Hoping that, the difference in the levels of Tlg2p between wild-type and *vps45Δ* cells would be easily scorable using immunoblot analysis. This was important as it would allow me to knockout specific lysines in the cytosolic domain of Tlg2p and use immunoblot analysis to look for its recovery in *vps45Δ* cells. For this purpose I used the plasmid pMAZ001. This was constructed by subcloning the *TLG2* ORF along with 500 bp of upstream and 300 bp of downstream sequence into the plasmid, pRS416 (Sikorski and Hieter, 1989). This strategy was designed to put *TLG2* under the control of its own promoter and 3' UTR in a centromeric plasmid. By virtue of their centromere, centromeric (*CEN*) plasmids are faithfully inherited upon cell division and are maintained at a low copy number (generally 1-3 copies per cell) (Blackburn, 1984, Clarke and Carbon, 1980, Resnick et al., 1990).

In order to investigate whether or not Tlg2p expressed from the *CEN* plasmid, pMAZ001, was fully degraded in *vps45Δ* cells, I compared the level of Tlg2p expressed from the genomic *TLG2* locus to that of Tlg2p expressed from pMAZ001 in *vps45Δ* cells. For this purpose wild-type cells (RPY10) and *vps45Δ* cells (NOzY2; RPY10 *vps45Δ*) were transformed with the plasmids pRS416 (empty vector) or pMAZ001 (encoding Tlg2p). Whole cell lysates prepared from equal numbers of these transformants (1 OD_{600} equivalents) were then analysed using immunoblot analysis with an antibody specific to Tlg2p.

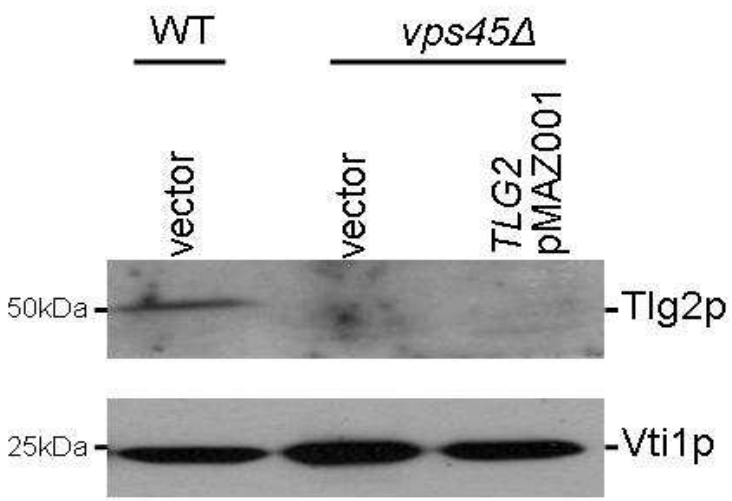

Figure 5.11 – Tlg2p expressed from pMAZ001 is fully degraded in *vps45Δ* cells. Wild-type (RPY10) were transformed with pRS416 (empty vector) and *vps45Δ* (NOzY2; RPY10 *vps45Δ*) cells were transformed with either pRS416 (empty vector) or pMAZ001 (encoding Tlg2p). Proteins contained within whole cell lysates prepared from equal numbers of these transformants (1 OD_{600} equivalents) were separated by SDS-PAGE prior to immunoblot analysis with an antiserum specific to Tlg2p. Levels of Vti1p were also assessed using immunoblot analysis to control for equal loading.

Figure 5.11 shows *vps45Δ* cells expressing Tlg2p both from their chromosomal copy of the gene and from pMAZ001, down-regulate Tlg2p to an extent that the difference between those cells and wild-type cells are easily detected by immunoblot analysis. Thus pMAZ001 is a good tool for investigating the degradation of Tlg2p in *vps45Δ* cells.

As mentioned previously in this chapter (Section 5.2) there were problems that arose with detecting Tlg2p using specific antiserum (which was in limited supply and not wholly reliable), hence as a complementary approach to detecting Tlg2p degradation by immunoblot analysis I also set out to develop a functional assay which could also be used to map possible sites of ubiquitination.

My approach was to utilise the enzyme imidazoleglycerol-phosphate dehydratase, His3p (Struhl and Davis, 1977). His3p catalyzes the sixth step in histidine biosynthesis; mutations cause histidine auxotrophy and sensitivity to Cu, Co, and Ni salts (Struhl and Davis, 1977). The rationale behind this functional assay was to produce a fusion protein made up of Tlg2p and His3p. I hypothesised that in wild-type cells (lacking endogenous His3p) this would support growth on media lacking histidine, but in cells lacking Vps45p this fusion protein would be degraded (by virtue of its Tlg2p sequences) and would no longer support growth on histidine deficient media. If this is the case, mutations could

then be introduced in the context of the fusion proteins to look for those that allow the fusion protein to support growth of *vps45*Δ cells on media lacking histidine.

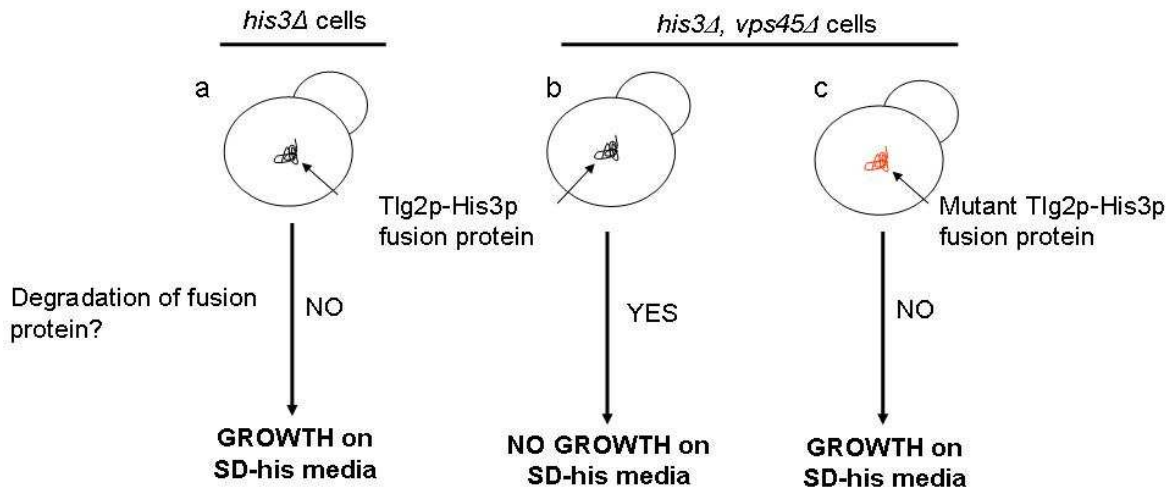

Figure 5.12 – Schematic diagram of the strategy used to develop a functional assay to monitor the degradation of Tlg2p in cells lacking endogenous Vps45p.
If the fusion protein is regulated in a similar manner to that of Tlg2p, a) wild-type cells lacking endogenous His3p (*his3Δ*) expressing the fusion protein Tlg2p-His3p should be able to grow on media lacking histidine (SD-his) where as b) *vps45Δ* cells lacking endogenous His3p (*his3Δ, vps45Δ*) expressing the fusion protein Tlg2p-His3p should not be able to grow on media lacking histidine. Introduction of mutations within the coding sequence of *TLG2* of the fusion protein, which disrupt degradation of Tlg2p in *vps45Δ* cells should c) promote the growth of *his3Δ, vps45Δ* on histidine deficient media.

Construction of the fusion protein for the assay was based around pMAZ001, as levels of Tlg2p expression are similar to that of endogenous Tlg2p, and importantly, degradation of Tlg2p is marked when Tlg2p is produced at this level (Figure 5.11). The fusion protein that was used in the assay outlined above was encoded by pMAZ017 (details of the construction of the plasmid encoding this can be found in Section 2.2.5). The first 33 residues of Tlg2p are necessary for Mode 2 binding by Vps45p (Dulubova et al., 2002, Carpp et al., 2006). This information was taken into consideration during the design of the fusion protein and this is why the *HIS3* coding sequence was fused in-frame after codon 33 of *TLG2*. A schematic diagram of the fusion protein is depicted below.

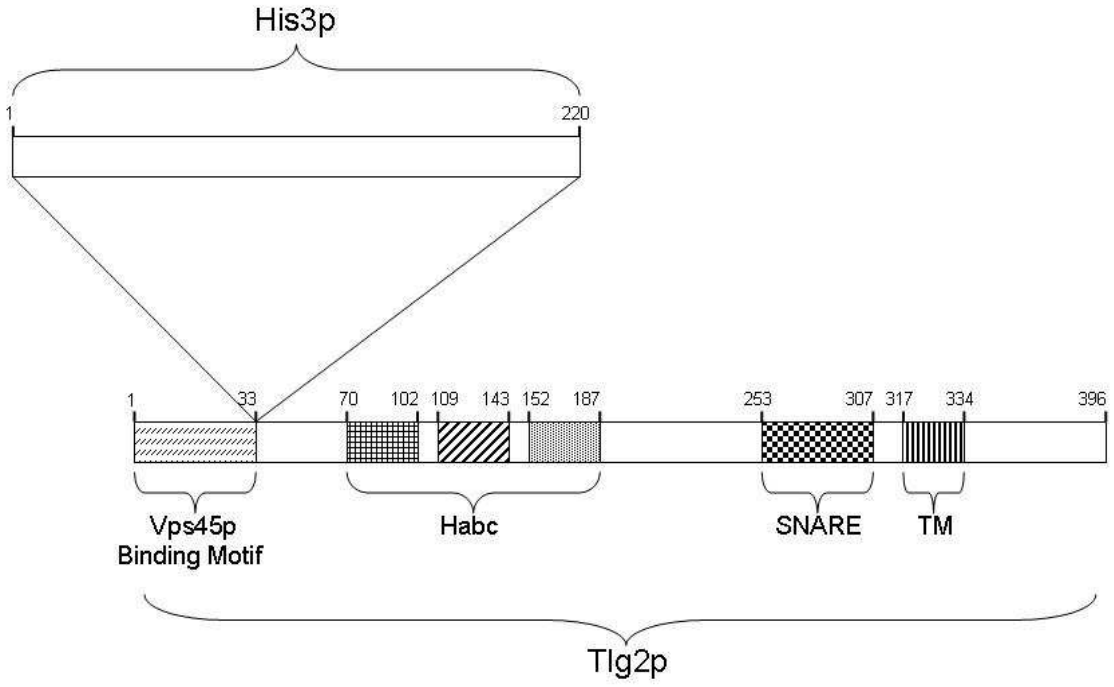

Figure 5.13 – Schematic diagram of the fusion protein encoded by pMAZ017.
This diagram is a modification of one presented by Dulubova and colleagues (Dulubova et al., 2002). The *HIS3* coding sequence was introduced in-frame after the first 33 codons of *TLG2*. The first 33 residues (Vps45p Binding Motif) of Tlg2p are necessary for Mode 2 binding (Dulubova et al., 2002). Residues 70-102, 109-143 and 152-187 represent the Habc domain (Dulubova et al., 2002). Residues 253-307 represent the SNARE domain and residues 317-334 represent the transmembrane domain (TM) (Dulubova et al., 2002).

It was important to ensure that the Tlg2p-His3p fusion protein was regulated in a similar manner to that of Tlg2p. In order to do this I monitored expression of the fusion protein from pMAZ017 in the *his3* auxotrophic strain SEY6210 and its isogenic derivatives; LCY007 (*vps45Δ*) and MSY001 (*tlg2Δ*). Wild-type (SEY6210), *tlg2Δ* (MSY001) and *vps45Δ* (LCY007) cells were transformed with either the plasmid pMAZ017 (encoding the Tlg2p-His3p fusion protein) or pRS416 (empty vector). Proteins contained within whole cell lysates, prepared from equal numbers of these transformants (1 OD_{600} equivalents), were separated by SDS-PAGE prior to immunoblot analysis with an antibody specific to Tlg2p.

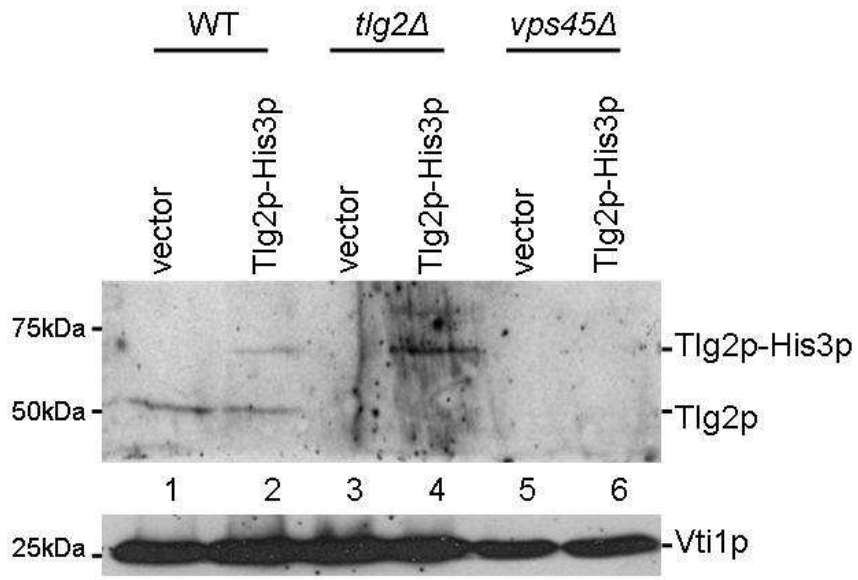

Figure 5.14 – Expression of the Tlg2p-His3p fusion protein
Wild-type (SEY6210), *tlg2Δ* (MSY001) and *vps45Δ* (LCY007) were transformed with the plasmid, pMAZ017 (encoding the Tlg2p-His3p fusion protein) or pRS416 (empty vector). Proteins contained within whole cell lysates, prepared from equal numbers of these transformants (1 OD_{600} equivalents), were separated using SDS-PAGE, after which immunoblot analysis was performed using an antiserum specific for Tlg2p. Similarly levels of Vti1p were assessed to control for equal loading.

Figure 5.14 shows that the Tlg2p-His3p fusion protein runs on SDS-PAGE as a ~70 kDa Tlg2p immunoreactive band (present in wild-type cells carrying pMAZ017 (lane 2), but not in those carrying the parent vector pRS416 (lane 1)). Interestingly, the fusion protein is present at higher levels in cells lacking endogenous Tlg2p (*tlg2Δ*) (compare lanes 2 and 4). This likely reflects the mechanisms employed by the cell to regulate Tlg2p levels. If, under the growth conditions used, the cell maintains Tlg2p at, say 50000 copies per cell this would be made up of, for example, 35000 copies produced from the endogenous gene, and 15000 molecules of the fusion protein in wild-type cells. In contrast, in *tlg2*Δ cells, the fusion protein would account for all 50000 copies, hence the more intense band. This provides some evidence that the fusion protein is folded properly in the cell and is recognised by cellular machinery as Tlg2p. Further evidence for this comes from the observation that no fusion protein is detected in *vps45*Δ cells carrying pMAZ017 (lane 6), presumably as it is subject to the same down-regulation as wild-type Tlg2p. No endogenous Tlg2p is detected in these cells (lanes 5 and 6), consistent with the finding that Vps45p is required for the stability of Tlg2p (Bryant and James, 2001).

SEY6210 is a histidine auxotroph (it carries the *his3-Δ200* mutation) and is therefore incapable of growing on histidine deficient media. In order to investigate whether or not His3p was functional within the context of the fusion protein, I monitored the growth of wild-type (SEY6210), *tlg2Δ* (MSY001; SEY6210 *tlg2Δ*) and *vps45Δ* (LCY007; SEY6210 *vps45Δ*) cells on media lacking histidine. Wild-type (SEY6210), *tlg2Δ* (MSY001) and *vps45Δ* (LCY007) cells transformed with either pMAZ017 (encoding Tlg2p-His3p) or pRS416 (empty vector) were grown in the selective media, SD-ura-met, to mid-log phase. Cells were harvested and resuspended in sterile dH_20 at an OD_{600} of 0.8. Subsequent serial dilutions were performed, generating cultures with an OD_{600} of 0.8, 0.08, 0.008, 0.0008. 5 µl from each of these cultures was spotted on to SD-ura-met and SD-his plates. Growth was monitored for 2-3 days at 30ºC.

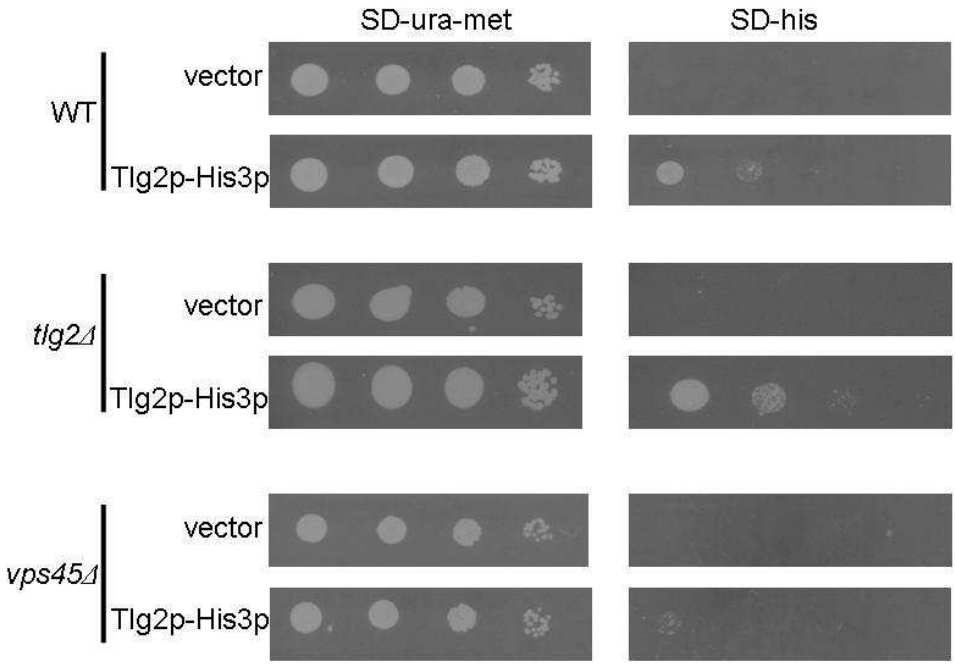

Figure 5.15 – A Tlg2p-His3p fusion protein supports growth of 'wild-type' and *tlg2*Δ but not *vps45*Δ histidine auxotrophic cells on media lacking histidine.
Wild-type (SEY6210), *tlg2Δ* (pMSY001; SEY6210 *tlg2Δ*) and *vps45Δ* (LCY007; SEY6210 *vps45Δ*) cells transformed with the plasmids, pMAZ017 (which drives the expression of the Tlg2p-His3p fusion protein) or pRS416 (empty vector) were grown in the selective media, SD-ura-met, to mid-log phase (OD_{600}=0.8). Cells were harvested by centrifugation and resuspended in sterile dH_2O at an OD_{600} of 0.8. Subsequent dilutions were performed generating cultures with an OD_{600} of 0.8, 0.08, 0.008 and 0.0008. 5 µl from each of these cultures was then spotted on to SD-ura-met or SD-his plates. Growth was monitored at 30ºC for 2-3 days.

The expression of the Tlg2p-His3p fusion protein in either SEY6210 (wild-type) or the isogenic *tlg2*Δ strain (MSY001) enables cells to grow on media lacking histidine, whereas

the same cells carrying the empty vector (pRS416) cannot grow on this media (Figure 5.15). It is noteworthy that pMAZ017 supports growth in cells lacking endogenous Tlg2p to a greater extent than it does wild-type cells. This likely reflects the higher steady-state levels of the Tlg2p-His3p fusion protein in these cells (Figure 5.14). Consistent with the data presented in Figure 5.14 showing substantially lower levels of the Tlg2p-His3p fusion protein in *vps45*Δ cells carrying pMAZ017 (compared to wild-type or *tlg2*Δ cells), pMAZ017 does not support growth of Δ*his3-200 vps45*Δ cells on media lacking histidine (Figure 5.15).

I went on to employ the assay described above to screen through lysine residues in Tlg2p to identify those whose ubiquitination may target Tlg2p for degradation. This was achieved using SDM to mutate the sequence encoding selected lysine residues to arginine residues in the background of the fusion protein. The lysine residues selected for mutation were based on published and unpublished data (Chapter 3 and 4) and the reasoning for their selection is discussed in detail below.

The first lysine residue selected resides in the N-terminal peptide of Tlg2p, Lys26. As mentioned previously, Vps45p binds to monomeric Tlg2p via Mode 2 binding (Carpp et al., 2006, Dulubova et al., 2002). One possibility is that the association of Vps45p with Tlg2p through this mode of binding could mask this lysine residue, thus preventing its ubiquitination and subsequent targeting to the proteasome for degradation.

Other lysine residues targeted include 5 lysine residues (Lys189, 193, 198, 218, 229) present in the linker region between the Habc domain and the SNARE domain of Tlg2p. These were targeted based on the assumption that Tlg2p adopts a closed conformation in the absence of Vps45p and hence exposes these residues in the linker region for the attachment of ubiquitin. It should be noted that although NMR studies performed on isolated sections of Tlg2p suggest that it does not exist in a closed confirmation (Dulubova et al., 2002), data provided in this thesis (Figures 4.6 and 4.7s) and also in (Bryant and James, 2001) contradicts these findings and as of yet no structural evidence exists to confirm that full-length Tlg2p does not adopt a closed conformation. Hence these lysine residues remain a good target for ubiquitination.

I also targeted 3 lysine residues present in the region between the SNARE domain and TM domain (Lys305, 311, 315). These lysine residues were selected as they are conserved between Sx16 and Tlg2p; data provided in Chapter 4 demonstrates that a functional

homologue of Tlg2p, Sx16 is also degraded in *vps45Δ* cells (Figure 4.4) hence these lysines also represent good targets.

Those lysine residues selected for mutation are highlighted in the following diagram.

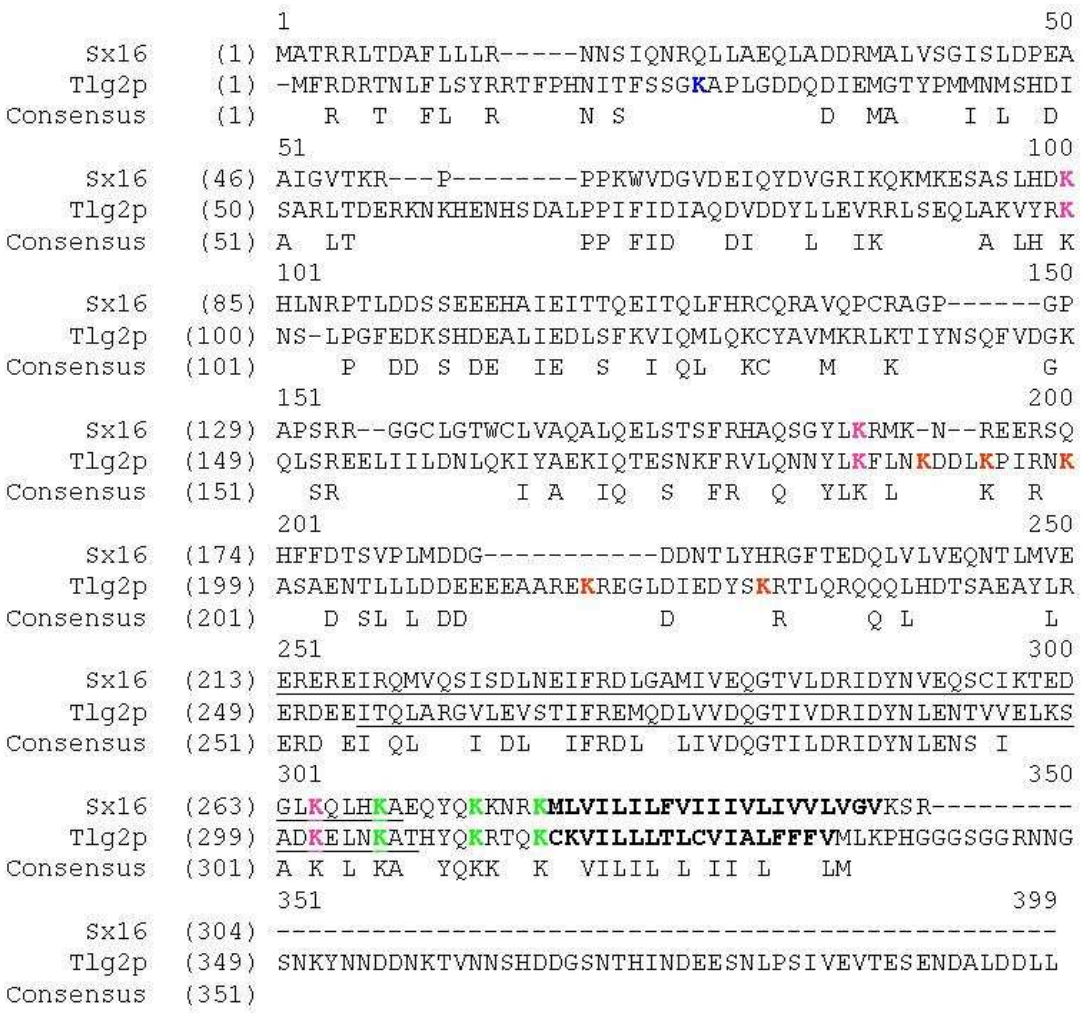

Figure 5.16 – Sequence alignment of Sx16 and Tlg2p
Vector NTI (Invitrogen) was used to align the amino acid sequence of the functional homologues Sx16 and Tlg2p in order to identify regions in which lysine residues may be conserved. Those lysine residues of Tlg2p that were mutated to arginine residues are shown in blue (K26R), red (5KR) and green (3KR). The SNARE domain is underlined and the transmembrane domain is shown in bold (the residues included in the SNARE and transmembrane domain are taken from (Dulubova et al., 2002)). Other potential lysine residues conserved between Sx16 and Tlg2p are shown in pink. There are a total of 25 lysine residues present in the cytosolic domain of Tlg2p.

Sequence encoding the lysine residues described above were mutated to sequence encoding arginine residues in the plasmid, pMAZ017 (encoding the Tlg2p-His3p fusion protein) using SDM (details of how these plasmids were generated is described in Section 2.2.5). LCY007 (SEY6210 *vps45Δ*) were transformed with the resultant plasmids, pMAZ028 (Tlg2p-His3p(K26R)), pMAZ030 (Tlg2p-His3p(5KR)), pMAZ033 (Tlg2p-

His3p(3KR)), the parent plasmid pMAZ017 (Tlg2p-His3p) or empty vector (pRS416). As a positive control for this experiment I constructed a plasmid, pMAZ027, which would represent the maximal growth achievable by those cells expressing the fusion protein. This plasmid (pMAZ027) expresses His3p under the control of the *TLG2* promoter and 3' UTR and was constructed by firstly removing the sequence encoding the first 33 codons of *TLG2* from pMAZ017 (Tlg2p-His3p) and secondly by using SDM to introduce two stop codons at the end of the *HIS3* coding sequence (this is described in detail in Section 2.2.5). LCY007 (SEY6210 *vps45Δ*) cells were also transformed with the plasmid pMAZ027. Transformants were grown to mid-log phase in the selective media SD-ura-met. Cells were harvested and resuspended in sterile dH_2O at an OD_{600} of 0.8. Serial dilutions were subsequently performed generating cultures with an OD_{600} of 0.8, 0.08, 0.008, 0.0008. 5 µl from each of these cultures was spotted on to SD-ura-met and SD-his plates. Growth was monitored for 2-3 days at 30ºC.

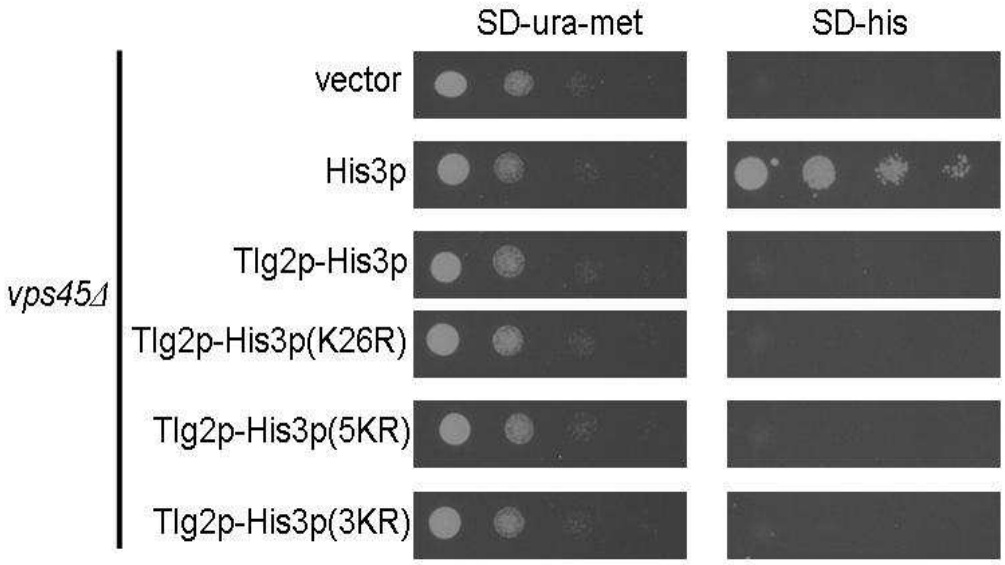

Figure 5.17 – Analysis of lysine residues in Tlg2p.
SEY6210 *vps45Δ* (LCY007) cells transformed with pRS416 (empty vector), pMAZ027 (His3p), pMAZ017 (Tlg2p-His3p), pMAZ028 (Tlg2p-His3p(K26R)), pMAZ030 (Tlg2p-His3p(5KR)) or pMAZ033 (Tlg2p-His3p(3KR)) were grown to mid-log phase in the selective media SD-ura-met, before harvesting by centrifugation. The resultant cell pellets were resuspended in sterile dH_2O at an OD_{600} of 0.8. Serial dilutions were subsequently performed generating cultures with an OD_{600} of 0.8, 0.08, 0.008, 0.0008. 5 µl from each of these cultures was then spotted onto plates containing the selective media SD-ura-met and SD-his. Growth was monitored for 2-3days at 30ºC.

None of the lysine mutants screened prevented the degradation of the fusion protein in *vps45Δ* cells as assessed by the lack of growth of these cells on histidine deficient media.

It should be noted that not all of lysine residues present in the cytosolic domain were screened (there are a total of 25) and this may be essential to prevent the ubiquitination and subsequent degradation of Tlg2p in the absence of Vps45p. Mutation of lysine residues is a complicated means to investigate ubiquitination, as ubiquitin ligases seem to select other lysine residues for modification if their favoured residue is not available (Hou et al., 1994, Lawson et al., 1999). Hence a more definitive way of mapping which residues of Tlg2p are targeted for ubiquitination would be to utilise another technique such a mass spectrometry characterisation of immunoprecipitated protein. This technique works by detecting the presence of glycine-glycine motifs present on the ubiquitinated lysine residues of the target protein after trypsin digestion (Peng et al., 2003).

5.5 Cellular levels of Tlg2p are regulated by Mode 2 binding

Vps45p interacts with its cognate syntaxin, Tlg2p, at two independent stages of the SNARE assembly/disassembly cycle, using two distinct modes of binding, Mode 2 and Mode 3 (Bryant and James, 2003, Carpp et al., 2006). In order to further understand how Vps45p functions to regulate the cellular levels of Tlg2p, Dr. Lindsay N. Carpp (University of Glasgow, UK) set out to investigate whether or not Mode 2 binding is required for the stabilisation of Tlg2p. In order to do this, she used immunoblot analysis to assess the cellular levels of Tlg2p present in *vps45Δ* cells expressing either wild-type or the 'pocket-filled' mutant version of Vps45p (Vps45pL117R); abrogated for Mode 2 binding. Her results (published in (Carpp et al., 2007)) demonstrate that there is a significant decrease in the cellular levels of Tlg2p present in those *vps45Δ* cells expressing the 'pocket-filled' mutant version of Vps45p (Vps45pL117R) compared to those expressing wild-type Vps45p. These results were intriguing as *vps45Δ* cells expressing Vps45pL117R as their only source of Vps45p correctly sort CPY (Carpp et al., 2006, Carpp et al., 2007), which suggests that these cells contain enough Tlg2p to facilitate trafficking. In order to quantify the levels of Tlg2p present in *vps45Δ* cells expressing Vps45pL117R, whole cell lysates prepared from equal numbers (1 OD_{600} equivalents) of NOzY1 (SF838-9D *vps45Δ*) cells expressing either the 'pocket-filled' mutant version of Vps45p (Vps45pL117R) or wild-type Vps45p (from the centromeric plasmids, pNB706 or pNB708 respectively) were assessed using immunoblot analysis with an antiserum specific to Tlg2p.

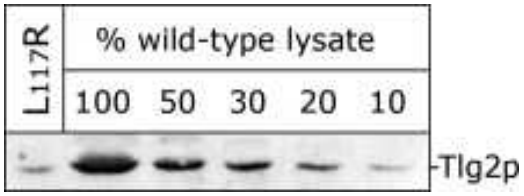

Figure 5.18 - *vps45Δ* cells expressing $Vps45_{L117R}$ contain ~15% of Tlg2p that is found in wild-type cells.
Levels of Tlg2p present in whole cell lysates prepared from equal numbers (1 OD_{600} equivalents) of NOzY1 (SF838-9D *vps45Δ*) cells expressing either the pocket-filled mutant of Vps45p (Vps45pL117R) from pNB706 were assessed using immunoblot analysis with an antiserum specific to Tlg2p. Different dilutions of wild-type lysates (NOzY1; SF838-9D *vps45Δ* cells expressing wild-type Vps45p from pNB708) were incorporated as a means of roughly estimating the levels of endogenous Tlg2p in those *vps45Δ* cells expressing Vps45pL117R.

Figure 5.18 (published in (Carpp et al., 2007)) demonstrates that *vps45Δ* cells expressing Vps45pL117R contain ~15% of the Tlg2p present in wild-type lysates. These results further support Lindsay's findings that the cellular levels of Tlg2p are reduced in *vps45Δ* cells expressing the 'pocket-filled' mutant version of Vps45p, which is unable to bind to Tlg2p via Mode 2 binding.

In order to determine whether or not Vps45p also regulates cellular levels of Tlg2p via Mode 3 binding, Lindsay also assessed the levels of Tlg2p present in *vps45Δ* cells expressing a double mutant version of Vps45p (Vps45pW244R/L117R) which can only bind Tlg2p via Mode 3 binding (Carpp et al., 2006). Her results demonstrate that cellular levels of Tlg2p in cells expressing the double mutant version of Vps45p (Vps45pW244R/L117R) are not similar to that of *vps45Δ* cells expressing wild-type Vps45p (Carpp et al., 2007). Hence Vps45p regulates the cellular levels of Tlg2p via Mode 2 binding.

Considering these findings, that Vps45p regulates the cellular levels of Tlg2p via Mode 2 binding (Carpp et al., 2007), I wondered if the N-terminal peptide of Tlg2p, required for this mode of binding, is the sole determinant that regulates the degradation of Tlg2p in *vps45Δ* cells. In order to investigate this, I used SDM to introduce two stop codons at the end of the *HIS3* coding sequence in the plasmid pMAZ017 (see Section 2.2.5). The newly synthesised plasmid, pMAZ029, encodes the first 33aa of Tlg2p fused to full-length His3p (Tlg2p(1-33)-His3p).

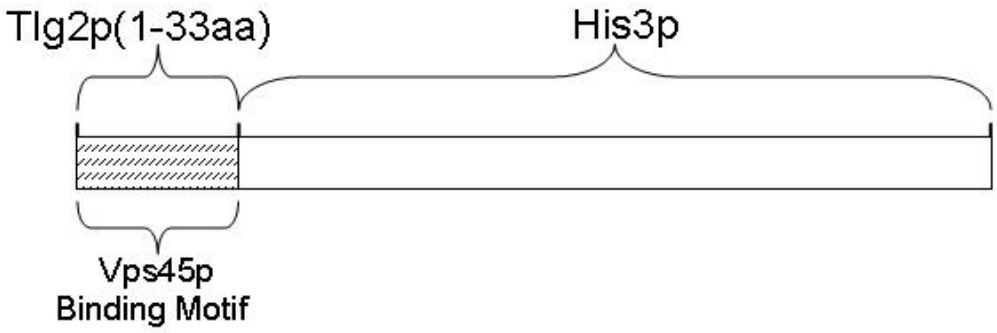

Figure 5.19– Schematic diagram of the truncated fusion protein encoded by pMAZ029. The first 33 residues (Vps45p Binding Motif) of Tlg2p, necessary for Mode 2 binding (Dulubova et al., 2002) fused to full-length His3p.

The ability of LCY007 (SEY6210 *vps45Δ*) transformed with pMAZ029 to grow in the absence of histidine was monitored on SD-his plates, using the technique described previously in this chapter (see Figure 5.15 and 5.17).

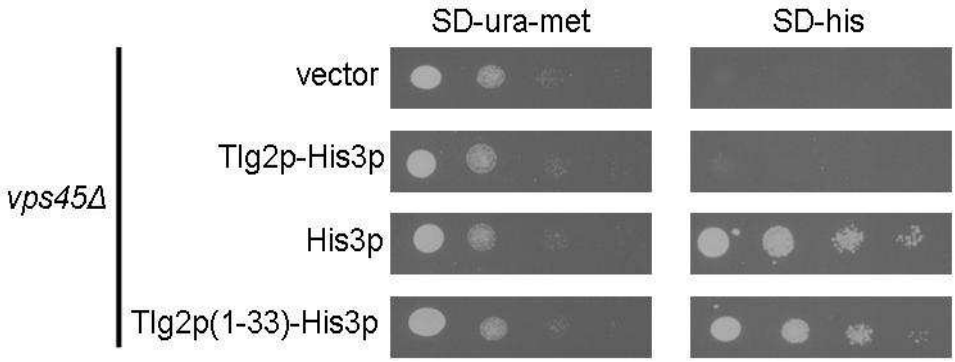

Figure 5.20 – Expression of the N-terminal peptide of Tlg2p (1-33aa) fused to full-length His3p allows the growth of *vps45Δ* histidine auxotrophic cells on media lacking histidine. LCY007 (SEY6210 *vps45Δ*) cells transformed with the plasmids pRS416 (empty vector) pMAZ017 (encoding Tlg2p-His3p), pMAZ027 (encoding His3p) or pMAZ029 (encoding Tlg2p(1-33)-His3p) were grown to mid-log phase in the selective media SD-ura-met, before harvesting by centrifugation. Cell pellets were resuspended in sterile dH_2O at an OD_{600} of 0.8. Serial dilutions were subsequently performed generating cultures with an OD_{600} of 0.8, 0.08, 0.008, 0.0008. 5 µl from each of these cultures was spotted onto plates containing the selective media SD-ura-met and SD-his. Growth was monitored for 2-3 days at 30ºC.

vps45Δ histidine auxotrophic cells expressing a truncated version of Tlg2p (residues 1-33) fused to full-length His3p (Tlg2p(1-33)-His3p) grow well on histidine deficient media (SD-his) when compared to *vps45Δ* histidine auxotrophic cells containing empty vector and the Tlg2p-His3p fusion protein (Figure 5.20). These results suggest that the N-

terminal peptide of Tlg2p alone does not contain all the sequences required to target Tlg2p for degradation in the absence of Vps45p.

5.6 Other factors that may be involved in regulating levels of Tlg2p in the cell

5.6.1 Palmitoylation of Tlg2p

Considering that both of the SNARE partners of Tlg2p, the t-SNARE Tlg1p and the v-SNARE Snc2p, are modified by palmitoylation (Valdez-Taubas and Pelham, 2005) (discussed in Section 1.4.1.2), it appeared plausible that Tlg2p may also be palmitoylated. In fact, two potential sites of palmitoylation have already been identified (Valdez-Taubas and Pelham, 2005).

As a means to detect whether HA-Tlg2p is subject to palmitoylation, yeast lysate containing 100 μg of protein (estimated using the Bradford protein assay) prepared from either wild-type (SF838-9D) or *vps45Δ* (NOzY1; SF838-9D *vps45Δ*) cells transformed with pNB701 (empty vector) or pMAZ006 (encoding HA-Tlg2p) grown in media containing 100 μM $CuCl_2$, were treated with hydroxylamine, which selectively removes thioester-linked palmitates (Chamberlain and Burgoyne, 1998). As a control for the specificity of the chemistry of hydroxylamine treatment, an equivalent amount of yeast lysate (100 μg) was also treated with the weak nucleophile Tris-HCl (as described in Section 2.2.23).

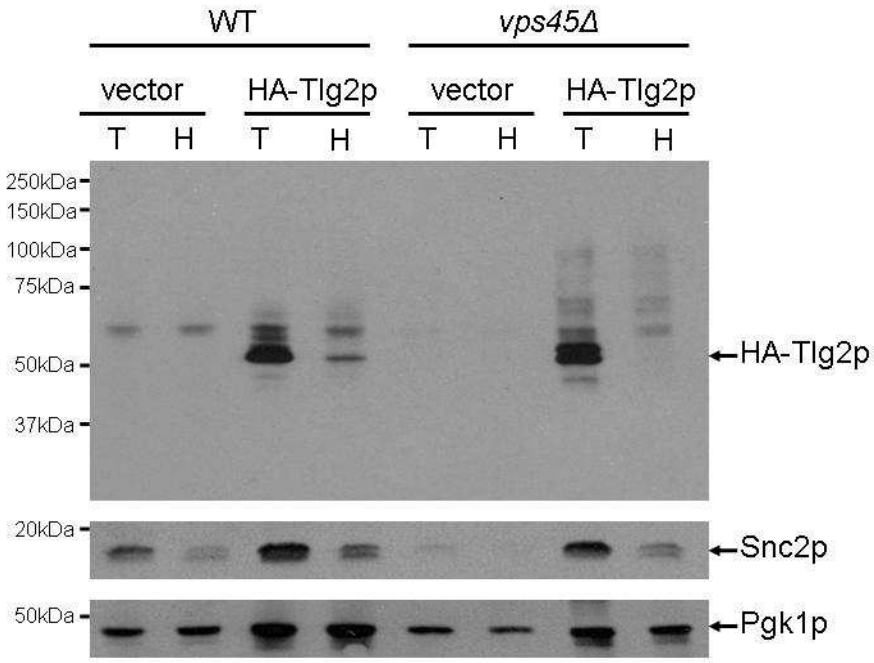

Figure 5.21 – Levels of HA-Tlg2p are reduced in wild-type and *vps45Δ* lysates treated with the compound, hydroxylamine.
Yeast lysate containing 100 µg of protein (estimated using the Bradford protein assay) prepared from either wild-type (SF838-9D) or *vps45Δ* (NOzY1; SF838-9D *vps45Δ*) cells transformed with the plasmids pNB701 (empty vector) or pMAZ006 (encoding HA-Tlg2p) grown in media containing 100 µM $CuCl_2$, were treated with either Hydroxylamine-HCl pH7.4 (H) or Tris-HCl pH7.4 (T) for 1 hour at room temperature. The lipids and associated components were separated from non-lipid contaminants using a mixture of chloroform and methanol. The proteins present in the interphase were precipitated by the addition of methanol and the resultant pellets resuspended in loading sample buffer lacking any reducing agents. The presence of HA-tagged Tlg2p was assessed in Tris (T) and Hydroxylamine (H) treated samples using immunoblot analysis with an antibody specific to the HA-tag (similarly the levels of Pgk1p were assessed to show that equal loading amounts of lysate were used in each treatment). Snc2p was also included as a positive control for a protein known to be palmitoylated (Valdez-Taubas and Pelham, 2005).

Treatment of lysates with hydroxylamine results in a reduction of the levels of HA-Tlg2p compared to those treated with Tris-HCl (Figure 5.21). It is important to note that, although levels of Pgk1p vary between transformants they are equal between different treatments (T and H). It is also clear to see that levels of Snc2p also decrease upon hydroxylamine treatment; Snc2p is known to be palmitoylated (Couve and Gerst, 1994, Valdez-Taubas and Pelham, 2005). Note that there are two Snc2p-immunoreactive bands in the hydroxylamine-HCl treated samples compared to the single band present in the Tris-HCl treated samples, this represent both the palmitoylated and depalmitoylated form of the protein.

It is not apparent why the levels of HA-Tlg2p are greatly reduced in those lysates treated with hydroxylamine, although it is noteworthy that the same phenomenon is seen for Snc2p which is known to be palmitoylated (Couve and Gerst, 1994, Valdez-Taubas and Pelham, 2005). I was, however, concerned that hydroxylamine treatment of HA-Tlg2p may alter the protein in such a way, that the protein would be separated into the upper phase rather than the interphase or lower phase following chloroform:methanol treatment. As only the lower phase and interphase were analysed, this seemed a possible explanation for the absence of HA-Tlg2p in the hydroxylamine treated samples. To investigate this, I decided to omit the chloroform:methanol separation step and perform direct methanol precipitation of the proteins following treatment with either Tris-HCl or hydroxylamine for 1 hour at room temperature.

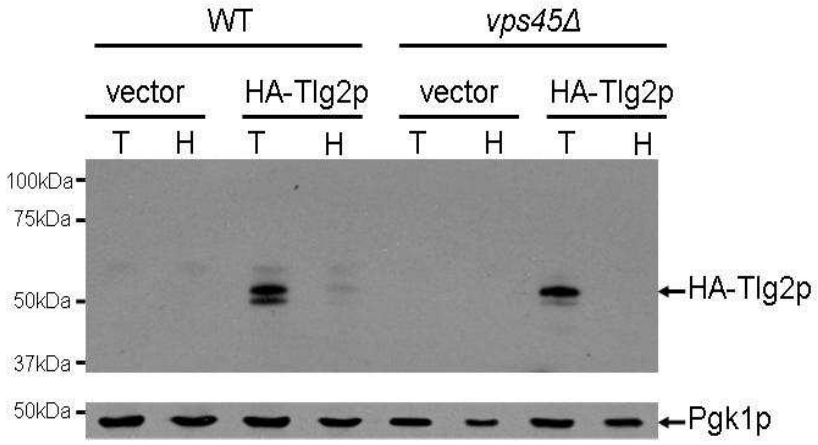

Figure 5.22 - Levels of HA-Tlg2p are reduced in wild-type and *vps45Δ* lysates treated with the compound, hydroxylamine.
Yeast lysate containing 100 µg of protein (estimated using the Bradford protein assay) prepared from either wild-type (SF838-9D) or *vps45Δ* (NOzY1; SF838-9D *vps45Δ*) cells transformed with the plasmids pNB701 (empty vector) or pMAZ006 (encoding HA-Tlg2p) grown in media containing 100 µM $CuCl_2$, were treated with either Hydroxylamine-HCl pH7.4 (H) or Tris-HCl pH7.4 (T) for 1 hour at room temperature. The proteins were precipitated by the addition of an equal volume of 100% (v/v) methanol and the resultant pellets resuspended in loading sample buffer lacking any reducing agents. The presence of HA-tagged Tlg2p was assessed in Tris (T) and Hydroxylamine (H) treated samples using immunoblot analysis with an antibody specific to the HA-tag (similarly the levels of Pgk1p were assessed to show that equal loading amounts of lysate were used in each treatment).

These results clearly indicate that the hydroxylamine treated HA-Tlg2p was not separated into the upper phase following chloroform:methanol treatment in the experiment presented in Figure 5.21 and confirms that the levels of HA-Tlg2p are greatly reduced following hydroxylamine treatment. Further work is required in order to understand the effects that hydroxylamine treatment has on HA-Tlg2p. It would be important to investigate whether or not Tlg2p is palmitoylated *in vivo*. This could be achieved using metabolic labelling

with radiolabelled palmitate. If this work confirms that Tlg2p is subject to palmitoylation an important additional step would be to investigate how this palmitoylation functions to regulate the levels of Tlg2p *in vivo*. Interestingly, palmitoylated Tlg1p is not recognised by the ubiquitin ligase, Tul1p and hence palmitoylation appears to protect Tlg1p from degradation by the vacuole (Valdez-Taubas and Pelham, 2005). It would be interesting to investigate whether or not this is also the case for Tlg2p, particularly in wild-type cells, where the vacuole appears to play a significant role in regulating the steady-state levels of Tlg2p (Section 5.2).

5.7 Discussion

This chapter describes several attempts to further investigate those findings presented in Chapter 4 and (Bryant and James, 2001), which document the degradation of Tlg2p in the absence of Vps45p.

The information provided in this chapter demonstrates that the vacuole is, in some part, involved in regulating the steady-state levels of Tlg2p (Figure 5.1 and 5.2). Vacuolar degradation is more significant in wild-type than *vps45Δ* cells (Figure 5.3), suggesting that the levels of Tlg2p are primarily regulated by a different degradative pathway in *vps45Δ* cells. This is consistent with previous findings that document the proteasomal degradation of Tlg2p in *vps45Δ* cells (Braun and Jentsch, 2007, Bryant and James, 2001). The expression of a truncated version of Tlg2p, lacking its lumenal domain (HA-Tlg2p(1-336)), previously reported to increase the expression of Tlg2p in bacterial cells (Paumet et al., 2005), did not alter the levels of Tlg2p *in vivo* nor did it prevent the *PEP4*-dependent degradation of Tlg2p (Figure 5.7). These results suggest that the processing event(s) that result in the generation of the *PEP4*-dependent product occurs in the cytosolic portion of Tlg2p.

Also documented in this chapter is the ubiquitination of Tlg2p in both wild-type and *vps45Δ* cells (Figure 5.10). However, it is unclear whether this is mono- or poly-ubiquitination or perhaps both depending on which degradative pathway Tlg2p is targeted to; the proteasome or the vacuole. This could be further determined using antibodies specific to the different types of ubiquitination (mono- or poly-) and also antibodies specific to the different linkages (e.g. Anti-Ubiquitin, Lys63-Specifc, clone HWA4C4 from Millipore). This information might provide clues as to the role of the ubiquitination of Tlg2p as different types of ubiquitination serve as a signal for different cellular processes.

For example the attachment of four ubiquitin moieties via Lys48 signals a protein for degradation by the proteasome, whereas the attachment of a single ubiquitin moiety plays and role in the intracellular transport of proteins through the late secretory and endocytic pathways (Hicke and Dunn, 2003).

Focusing solely on the degradation of Tlg2p in *vps45Δ* cells, I set out to identify those lysine residues which may undergo ubiquitination and hence target Tlg2p for degradation. This involved the development of a functional assay, which used a fusion protein made up of Tlg2p and His3p. This fusion protein was degraded in *his3-Δ200, vps45Δ* cells (by virtue of its Tlg2p sequences) and in theory would only allow the growth of this strain on media lacking histidine when I had successfully prevented the ubiquitination of Tlg2p. This was, however, unsuccessful as none of the lysine mutants screened prevented the degradation of the fusion protein in *his3-Δ200, vps45Δ* cells as assessed by the ability of these cells to grow on media lacking histidine (Figure 5.17). It should be noted that not all of the lysine residues present in the cytosolic domain of Tlg2p were screened and this may be essential to prevent the degradation of the fusion protein in the absence of Vps45p. It has also recently been suggested that the levels of Tlg2p present in *vps45Δ* cells are, in part, mediated by (Ub)-proteasome-dependent ER-associated degradation (ERAD) (Braun and Jentsch, 2007). This conclusion was reached since, in contrast to *vps45Δ* cells with a fully functional ERAD pathway, *vps45Δ* cells in which ERAD has been abolished (through deletion of the Ub-conjugating enzymes Ubc6p and Ubc7p (*ubc6Δ, ubc7Δ*) or through the expression of a temperature sensitive mutant of Ufd1p (*Ufd1-2*) which is the substrate-recruiting cofactor of the chaperone-like enzyme, Cdc48p) contain higher levels of Tlg2p detectable through immunoblot analysis (Braun and Jentsch, 2007). Hence it is possible that lysine residues not contained in the cytosolic domain of Tlg2p are also subject to ubiquitination. It is also possible that the ubiquitin moiety may become attached to a serine or threonine residue (Wang et al., 2007). Hence, a more definitive way of mapping which residue(s) are targeted for ubiquitination would be to utilise mass spectrometry characterisation (Peng et al., 2003), however immunoprecipitation of proteins can be problematic, resulting in low yields and high contamination.

It has been demonstrated that Vps45p regulates cellular levels of Tlg2p via Mode 2 binding (Carpp et al., 2007). In this chapter I further demonstrate that *vps45Δ* cells expressing the 'pocket-filled' mutant version of Vps45p (Vps45pL117R) contain ~15% of the Tlg2p that is present in wild-type cells (Figure 5.18). These results would suggest that the N-terminal peptide of Tlg2p is responsible for targeting it for degradation in the absence of Vps45p.

However expression of the first 33 amino acids of Tlg2p fused to full-length His3p, did not prevent the growth of *Δhis3-200, Δvps45* cells in media lacking Histidine (Figure 5.20), suggesting that the N-terminal peptide of Tlg2p alone does not contain all of the sequences required to target Tlg2p for degradation in the absence of Vps45p. Neither is the N-terminal peptide targeted for ubiquitination, as mutation of the only lysine residue present in this region (K26R) did not prevent the degradation of Tlg2p in the absence of Vps45p (Figure 5.17). Hence further work is required to understand how Vps45p stabilises Tlg2p through Mode 2 binding.

Treatment of Tlg2p with the compound, hydroxylamine resulted in a reduction of the levels of HA-Tlg2p compared to those treated with Tris-HCl (Figure 5.21 and 5.22). It is not apparent why the levels of HA-Tlg2p are so greatly reduced in those lysates treated with hydroxylamine-HCl, although a similar effect is seen for Snc2p which is known to be palmitoylated (Valdez-Taubas and Pelham, 2005). These results are preliminary and further work is required to investigate whether Tlg2p is palmitoylated *in vivo*. This could be performed using metabolic labelling with radiolabelled palmitate. If this work confirms that Tlg2p is palmitoylated an important additional step would be to investigate how this palmitoylation functions to regulate the levels of Tlg2p *in vivo*. For example, it would be of interest to identify which palmitoyltransferase is involved in this process. A good target would be the palmitoyltransferase, Swf1p, as a *swf1* null mutant shows synthetic sick interactions with *tlg2* mutant cells (Tong et al., 2004). Data published by (Valdez-Taubas and Pelham, 2005), indicates that Swf1p-dependent palmitoylation protects Tlg1p from ubiquitination and degradation by the vacuole. The authors demonstrate that palmitoylated Tlg1p is protected from ubiquitination by the ubiquitin ligase, Tul1p, which subsequently prevents the entry of Tlg1p into MVBs and its degradation by the vacuole (Valdez-Taubas and Pelham, 2005). It has previously been discussed, in this chapter (Figure 5.7), that a fragment greater than the lumenal domain of Tlg2p is subject to vacuolar degradation, which suggests that the cytosolic domain is also exposed to vacuolar proteases. Considering this alongside the possibility that Tlg2p may be monoubiquitinated (Figure 5.10) and also its sensitivity to hydroxylamine treatment (Figures 5.21 and 5.22), it would seem sensible to further investigate whether or not Tlg2p is degraded by the vacuole in a manner similar to that of Tlg1p (Valdez-Taubas and Pelham, 2005).

In summary, the information provided in this chapter would suggest that the vacuole is, in some part, involved in the degradation of Tlg2p. However understanding how Vps45p and

the proteasome are also involved in the degradation of Tlg2p as well as deciphering the significance of palmitoylation makes this an interesting avenue of research.

Chapter 6 – Final Discussion

Type 2 diabetes is characterised by insulin resistance caused by a deregulation of insulin action (Saltiel and Kahn, 2001, Zimmet et al., 2001). One of the major consequences of insulin binding to its receptor is the translocation of GLUT4 from its intracellular location to the plasma membrane (Bryant et al., 2002). In order to understand how insulin alters the trafficking itinerary of GLUT4 to bring about its delivery to the cell surface, it is important to understand how membrane traffic is regulated in eukaryotic cells. However, due to the experimental intractability of terminally differentiated insulin-sensitive cells, it has proven hard to gain molecular insight into this regulation. As with many areas of cell biology a lot of our knowledge about the molecular mechanism that regulates membrane traffic has come from model systems such as yeast, worms and flies (Calakos and Scheller, 1996). The overall aim of the work described in this thesis was to investigate the possibility of using the experimentally tractable yeast strain, *S. cerevisiae*, as a model organism to further investigate the molecular mechanism of insulin-regulated GLUT4 trafficking.

6.1 Sx16 is a functional homologue of the yeast t-SNARE, Tlg2p

Sx16, the syntaxin of interest in this study, and its binding partner, Sx6 (Kreykenbohm et al., 2002, Mallard et al., 2002, Perera et al., 2003) have been implicated as playing an important role in insulin-regulated GLUT4 trafficking (Perera et al., 2003, Proctor et al., 2006, Shewan et al., 2003). *In silico* analysis has demonstrated that the mammalian syntaxin, Sx16 is homologous to the yeast t-SNARE, Tlg2p (Simonsen et al., 1998). The first aim of my work was to investigate whether or not Sx16 is also a functional homologue of the yeast t-SNARE, Tlg2p.

Cells lacking Tlg2p (*tlg2Δ*) are viable, however they display a variety of different phenotypes representative of defects in endocytosis (Abeliovich et al., 1998, Holthuis et al., 1998, Seron et al., 1998). These include delayed turnover of the phermone receptors, Ste2p and Ste3p by the vacuole (Abeliovich et al., 1998, Holthuis et al., 1998, Seron et al., 1998); defects in sorting of vacuolar proteases, such as CPY, with approximately 15-20% of total CPY secreted in the late Golgi (p2) form (Abeliovich et al., 1998) and defects in the retrieval of TGN resident proteins such as Kex2p (Abeliovich et al., 1998, Holthuis et al., 1998) and less significantly DPAP A (Holthuis et al., 1998). Tlg2p is also required for recycling of the SNARE protein, Snc1p, through early endosomes (Lewis et al., 2000); the delivery of the protein aminopeptidase I to the vacuole via the cytoplasm to vacuole (CVT)

pathway (Abeliovich et al., 1999) and TGN homotypic fusion (Brickner et al., 2001). *tlg2Δ* cells are also sensitive to osmotic stress (Abeliovich et al., 1998) and have a fragmented vacuolar morphology (Abeliovich et al., 1998, Seron et al., 1998).

In Chapter 3, I described the construction of three different expression vectors which drive the expression of Tlg2p, Sx16 and the unrelated mammalian syntaxin, Sx4. Furthermore I demonstrated that the heterologous expression of Sx16, but not Sx4 complements for the loss of Tlg2p, by correcting the trafficking defects displayed in *tlg2Δ* mutant cells. These include osmotic sensitivity (Figure 3.15), incorrect trafficking of vacuolar proteases such as CPY (Figure 3.16), impaired endocytosis (Figure 3.17 and 3.18) and vacuolar morphology (Figure 3.18).

Further to these findings which demonstrate that heterologous expression of Sx16 in yeast complements for the loss of Tlg2p, I performed preliminary experiments to investigate whether or not Sx16 co-localises to the same region as Tlg2p when expressed in yeast. Confocal immunofluorescence microscopy demonstrated that these syntaxins do co-localise to the same intracellular structures (Figure 3.19), however further work is required to confirm this.

6.2 Sx16 is regulated by the Tlg2p-binding SM protein, Vps45p

A family of proteins essential for SNARE-mediated membrane fusion *in vivo* are the SM proteins. Loss of function mutations in SM genes results in a block in membrane fusion as demonstrated in the organisms *S. cerevisiae* (Cowles et al., 1994, Novick and Schekman, 1979, Ossig et al., 1991, Robinson et al., 1988, Wada et al., 1990), *D. melanogaster* (Harrison et al., 1994) and *C. elegans* (Hosono et al., 1992). SM proteins are arched-shaped peripheral membrane proteins of approximately 60-70 kDa (Bracher and Weissenhorn, 2002, Jahn, 2000, Misura et al., 2000). Most SM proteins bind to the syntaxin that is involved in the same transport step (Jahn, 2000).

Consistent with its identification as a functional homologue of Tlg2p (which binds to the SM protein, Vps45p (Bryant and James, 2001)), Sx16 has previously been shown to bind to the mammalian homologue of Vps45p (mVps45) and also to yeast Vps45p *in vitro* (Dulubova et al., 2002). However it has yet to be determined whether or not Sx16 can interact with Vps45p *in* vivo. Hence the second aim of my work was to investigate

whether or not Sx16 interacts with Vps45p *in vivo*. This was important as it would provide further confirmation that Sx16 is a functional homologue of Tlg2p by establishing whether it utilises the same molecular machinery as Tlg2p when expressed in yeast.

Vps45p uses two different modes of binding to interact with its cognate syntaxin, Tlg2p, at two different stages in the SNARE complex assembly/disassembly cycle (Bryant and James, 2003, Carpp et al., 2006). Vps45p binds to monomeric Tlg2p (Bryant and James, 2003, Carpp et al., 2006, Dulubova et al., 2002) using Mode 2 binding (Carpp et al., 2006, Dulubova et al., 2002) and also to Tlg2p containing *cis*-SNARE complexes (Bryant and James, 2003) using Mode 3 binding (Carpp et al., 2006). In Chapter 4, I demonstrated that Vps45p can interact with monomeric Sx16 *in vitro* using Mode 2 binding (Figure 4.1) and also Sx16-containing *cis*-SNARE complexes *in vivo* (Figure 4.2). I also demonstrated that levels of Sx16, like Tlg2p, are depleted in those cells lacking Vps45p (Figure 4.4).

In Chapter 4, I further demonstrated the functional homology between Tlg2p and Sx16, by demonstrating that truncated Tlg2p (Tlg2pΔHabc) and Sx16 (Sx16 ΔHabc) can bypass the requirement of the SM protein, Vps45p, and enable the vacuolar delivery of CPY (Figure 4.6). These findings are consistent the hypothesis that one function of Vps45p is to activate Tlg2p for entry into SNARE complexes. This would suggest that Vps45p interacts with Tlg2p in a mode analogous to that of Munc18a binding to Sx1a; Mode 1 binding (Bryant and James, 2001), which would require Tlg2p to adopt a closed conformation akin to that of Sx1a (Bryant and James, 2001). However evidence for and against a closed conformation of Tlg2p exists (Bryant and James, 2001, Dulubova et al., 2002). Evidence that Tlg2p can form a closed conformation is provided by the ability of a truncated version of Tlg2p, lacking its Habc domain (Tlg2ΔHabc) to partially complement the CPY trafficking defects observed in *vps45Δ* cells (Figure 4.6 and (Bryant and James, 2001)). Evidence against a closed conformation of Tlg2p comes from NMR data which suggests that a bacterially produced construct of Tlg2p (residues 60-283) is unlikely to form a closed conformation (Dulubova et al., 2002). However, it should be noted that the construct used in these NMR studies lacked residues present in the SNARE domain that may be required to form a closed conformation of Tlg2p.

In order to explain how a truncated version of Tlg2p, Tlg2pΔHabc, forms functional SNARE complexes in the absence of Vps45p (Bryant and James, 2001) with respect to their conclusion that Tlg2p does not adopt a closed conformation, Dulubova and colleagues suggested that some inhibitory factor might bind to the N-terminal portion of

Tlg2p (possibly the Habc domain) and hence prevent SNARE complex formation (Dulubova et al., 2002). They postulated that Vps45p could be involved in releasing such an inhibition and thus promote SNARE complex assembly. Tlg2pΔHabc would not be able to bind this inhibitory factor and thus would not be subject to the same regulation by Vps45p (Dulubova et al., 2002).

In order to distinguish between these two different interpretations (1) Vps45p is required for the transition of Tlg2p from a closed to an open conformation compatible with SNARE complex assembly or 2) Vps45p is required to release some inhibitory factor bound to the N-terminal portion of Tlg2p that is preventing SNARE complex assembly) we further investigated the ability of Vps45p to promote SNARE complex formation by promoting a transition of Tlg2p from a closed to an open conformation. Chris Macdonald (University of Glasgow, UK) performed GST pull-down experiments using full-length and truncated Tlg2p. He demonstrated that the truncated version of Tlg2p (Tlg2pΔHabc) was capable of forming complexes at a rate much faster than full-length Tlg2p (Figure 4.7a), suggesting that the Habc domain of Tlg2p inhibits SNARE complex formation, consistent with the hypothesis that Tlg2p forms a closed conformation. Addition of Vps45p to the GST pull-down assay (again performed by Chris Macdonald) allowed full-length Tlg2p to form SNARE complexes at a rate comparable to that of truncated Tlg2p (Figure 4.7b). These results support our hypothesis that Vps45p is required for the transition of Tlg2p from a closed to an open conformation compatible for SNARE complex assembly.

In support of our findings, it has been demonstrated using isothermal titration calorimetry (ITC) that an interaction exists between the C-terminal portion of the SNARE domain of Sx16 and Vps45, which is analogous to the interaction between Sx1a and the central cavity of Munc18a (Burkhardt et al., 2008). Consistent with the finding that Tlg2p and Sx16 are functional homologues this would suggest that the Tlg2p construct (60-283) used in NMR studies (Dulubova et al., 2002) was lacking residues required to stabilise a closed conformation of Tlg2p (Dulubova et al., 2002).

More recently, in the last couple of weeks, further evidence that Vps45p interacts with a closed conformation of Tlg2p via Mode 1 binding, has been provided using a fluorescent electrophoretic mobility shift assay (EMSA) (Furgason et al., 2009). Initially it was demonstrated that this mode of binding between Vps45p and Tlg2p is separate from Mode 2 binding, as a Tlg2p construct (residues 37-318) lacking its first 36 residues, which are required for Mode 2 binding, was still capable of interacting tightly with Vps45p

(Furgason et al., 2009). In the reciprocal experiment the 'pocket-filled' mutant version of Vps45p (Vps45pL117R) is also capable of associating with the truncated version of Tlg2p, demonstrating that the interaction is not via Mode 2 binding (Furgason et al., 2009). This mode of binding is analogous to that shared between Munc18a and Sx1a (Mode 1 binding) as it requires sites in the Habc and SNARE domain of Tlg2p. Mutation of an isoleucine residue, present in the SNARE domain of Tlg2p, to an alanine residue generated a construct (Tlg2p(37-318)-I285A) that is no longer capable of competing with Tlg2p(37-318) for binding to Vps45p (Furgason et al., 2009). Similarly mutation of three lysine residues in the Habc domain of the Tlg2p construct (37-318)-K134A, K137A, K163A that are required for Tlg2p to adopt a closed conformation, generated a construct that is also unable to compete with Tlg2p(37-318) for binding to Vps45p (Furgason et al., 2009). These three lysine residues, important in forming a closed conformation of Tlg2p, are predicted to pack tightly against residues in the C-terminal section of the SNARE domain (Furgason et al., 2009). Those C-terminal residues important for packing tightly against K134, K137 and K163 as well as the isoleucine residue at position 285 were not included in the Tlg2p construct (residues 60-283) used by Dulubova and colleagues in their NMR studies and this may explain why their structural studies did not observe a closed conformation of Tlg2p (Dulubova et al., 2002, Furgason et al., 2009). These results further support the hypothesis that Tlg2p does form a closed conformation akin to that of Sx1a and supports our model that Vps45p is required for the transition of Tlg2p from a closed to an open conformation compatible with SNARE complex assembly.

Further to their findings that Tlg2p can adopt a closed conformation, Furgason and colleagues also demonstrated that unlike Munc18a and mammalian Vps45 (Burkhardt et al., 2008), binding of Tlg2p to Vps45p via Mode 2 does not positively influence Mode 1 binding (Furgason et al., 2009). In fact Vps45p binding to Tlg2p via Mode 2 decreases the affinity of Vps45p for the closed conformation of Tlg2p (Furgason et al., 2009). This was demonstrated by the ability of the N-peptide of Tlg2p (1-33) to compete with Tlg2p (37-318) for binding to Vps45p (Furgason et al., 2009). This competition is specific to the binding of Vps45p as opposed to an intramolecular binding of the N-terminal peptide to the Tlg2p construct (37-318) as no competition was detected using the 'pocket-filled' mutant of Vps45p (Furgason et al., 2009).

SM proteins may also regulate membrane fusion via an indirect mechanism, acting as chaperone-like molecules (Toonen et al., 2005). Deletion of *VPS45* results in a decrease in cellular levels of Tlg2p by ~90% as assessed by immunoblot analysis (Bryant and James,

2001). In Chapter 4, I also detected a reduction in the cellular levels of the v-SNARE, Snc2p, in cells lacking Vps45p (Figure 4.3). As well as binding Tlg2p, Vps45p also binds directly to Snc2p (Carpp et al., 2006). However no interaction between Vps45p and the t-SNAREs, Tlg1p or Vti1p, can be detected (Carpp et al., 2006). These results suggest that the SM protein, Vps45p may play an important role in regulating the cellular levels of the syntaxin, Tlg2p and the v-SNARE, Snc2p. This may be important to control the overall trafficking of molecules *in vivo* as Snc2p is also involved in other trafficking events, such as exocytosis. For example, if levels of Tlg2p are depleted in *vps45Δ* cells this may lead to an increase in the availability of the v-SNARE, Snc2p, to participate in other fusion events. One caveat of this model is that I would have imagined it to predict that the levels of the other SNARE proteins, Vti1p and Tlg1p, should also be depleted in the absence of Vps45p, but they are not (Figure 4.3 and (Bryant and James, 2001)). One possible explanation for the unregulated levels of Vti1p and Tlg1p compared to that of Snc2p, would be the tighter regulation involved in exocytosis, which requires Snc2p, compared to that of endosomal trafficking, which requires Tlg1p and Vti1p.

6.3 Regulation of Tlg2p levels in the cell

Cells lacking Vps45p (*vps45Δ*) have reduced levels of Tlg2p (Figure 4.3 and (Bryant and James, 2001). In order to further understand the mechanism by which Vps45p stabilises this syntaxin, I set out to investigate the regulation of steady-state levels of Tlg2p in both wild-type and *vps45Δ* cells.

Considering the results provided in Chapter 5, it would appear that levels of Tlg2p are regulated by two different degradative pathways.

1) In the absence of Vps45p, levels of Tlg2p are regulated by proteasomal activity (Bryant and James, 2001), possibly via the ERAD pathway as demonstrated by Braun and colleagues (Braun and Jentsch, 2007).

2) In the presence of Vps45p, steady-state levels of Tlg2p are primarily regulated by vacuolar degradation (Figure 5.1, 5.2, 5.3 and 5.7).

Findings provided by Braun and colleagues which demonstrate that the levels of Tlg2p are restored in *vps45Δ* cells in which ERAD has been abolished (through deletion of the Ub-conjugating enzymes Ubc6p and Ubc7p (*ubc6Δ*, *ubc7Δ*) or through the expression of a

temperature sensitive mutant of Ufd1p (*Ufd1-2*) which is the substrate-recruiting cofactor of the chaperone-like enzyme, Cdc48p) (Braun and Jentsch, 2007), suggest that the SM protein, Vps45p, stabilises Tlg2p shortly after synthesis. However, stabilised Tlg2p is capable of reaching the appropriate intracellular location in *vps45Δ* mutant cells in which proteasomal degradation has been abolished (Bryant and James, 2001) arguing that Tlg2p is trafficked out of the ER in the absence of it SM protein.

Vps45p stabilises cellular levels of Tlg2p via Mode 2 binding (Carpp et al., 2007); demonstrated by the decreased levels of Tlg2p present in *vps45Δ* cells expressing the 'pocket-filled' mutant version of Vps45p (Vps45pL117R) (Figure 5.18 and (Carpp et al., 2007)). However the expression of the first 33 amino acids of Tlg2p fused to full-length His3p did not prevent the growth of *Δhis3-200, Δvps45* cells in media lacking Histidine (Figure 5.20), which suggests that the N-terminal peptide of Tlg2p alone does not contain all of the sequences required to target Tlg2p for degradation in the absence of Vps45p. Neither is the N-terminal peptide targeted for ubiquitination, as mutation of the only lysine residue present in this region (K26R) did not prevent the degradation of Tlg2p in the absence of Vps45p (Figure 5.17); demonstrating that Vps45p binding is not masking a possible ubiquitination site.

Interestingly abrogation of Mode 2 binding through mutation of the phenylalanine and leucine residue at position nine and ten of Tlg2p to alanine residues, results in increased levels of the syntaxin when expressed in *tlg2Δ* cells (Furgason et al., 2009). This is in contrast to those results presented in this thesis which demonstrate that abrogation of Mode 2 binding through mutation of Vps45p leads to the destabilisation of Tlg2p (Figure 5.18) as well as those results presented in a study involving the syntaxin Ufe1p, and its cognate SM protein, Sly1p, which demonstrate that abrogation of Mode 2 binding through mutation of Ufe1p results in decreased levels of the syntaxin (Braun and Jentsch, 2007). One possible explanation for these contrasting results could be that mutation of the N-terminal peptide of Tlg2p results in a conformation of Tlg2p that is no longer compatible with targeting Tlg2p for degradation by the proteasome. This could also be further investigated by assessing the levels of 'wild-type' and the mutant (F9A/L10A) version of Tlg2p in *vps45Δ* cells containing proteasomal activity compared to those *vps45Δ* cells in which proteasomal activity has been abolished (through mutation of either the catalytic subunits, Pre1p and Pre2p (*pre1-1, pre2-2*) or the regulatory domain, Cim3p (*cim3-1*) (Heinemeyer et al., 1993, Heinemeyer et al., 1991, Ghislain et al., 1993)). This would address whether or not this

mutant version of Tlg2p (Tlg2pF9A/L10A) is subject to the same regulation as 'wild-type' Tlg2p in *vps45Δ* cells.

The results presented in Chapter 5 also support a model in which Vps45p utilises different modes of binding to carry out its functions within the cell; regulating the cellular levels of Tlg2p and regulating membrane fusion. Vps45p binding to Tlg2p via Mode 2 binding is required for stabilisation of Tlg2p (Carpp et al., 2007) whereas Vps45p binding to Tlg2p via Mode 1 binding is involved in regulating the entry of Tlg2p into SNARE complexes (Figures 4.6 and 4.7 and (Bryant and James, 2001, Furgason et al., 2009)) and Mode 3 binding is involved in the recycling of Tlg2p following membrane fusion (Bryant and James, 2003, Carpp et al., 2006). This model is also supported by the recent finding that Mode 1 and Mode 2 binding of Vps45p to Tlg2p is non-cooperative (Furgason et al., 2009), suggesting that these modes of binding also function independently. However this model does not explain those findings which demonstrate that the introduction of the 'pocket-filling' mutation to the dominant negative version of Vps45p (Vps45pW244R/L117R) prevents the dominant negative version of Vps45p from blocking membrane fusion (Carpp et al., 2006), which would suggest that Vps45p binding to Tlg2p via Mode 2 binding is required for membrane fusion. Nor does it explain the recent findings which demonstrate that abrogation of Mode 1 and 2 binding is required to disrupt membrane fusion (Furgason et al., 2009). However it should be noted, that this later finding was demonstrated using a mutant version of Tlg2p (Tlg2pF9A/L10A) that is unable to bind to Vps45p via Mode 2 binding (Dulubova et al., 2002) as opposed to a mutant version of Vps45p (Vps45pL117R) that is unable to bind to Tlg2p via Mode 2 binding (Carpp et al., 2006). However, as discussed previously, this mutant version of Tlg2p (Tlg2pF9A/L10A) also results in elevated levels of Tlg2p rather than decreased levels of Tlg2p as detected when Mode 2 binding is disrupted through mutation of Vps45p (Vps45pL117R).

In Chapter 5, I also provided preliminary data to suggest that Tlg2p is palmitoylated (Figure 5.21 and 5.22). Palmitoylation has been proposed to increase the stability of proteins *in vivo*; this has been reported for the v-SNARE, Snc1p (Couve et al., 1995) and the t-SNARE, Tlg1p (Valdez-Taubas and Pelham, 2005). Interestingly, palmitoylated Tlg1p is thought to be protected from ubiquitination by the E3 ligase, Tul1p, which subsequently prevents its entry in MVBs and hence prevents its degradation by the vacuole (Valdez-Taubas and Pelham, 2005). In Chapter 5 (Figure 5.7), I demonstrated that in the presence of Vps45p a fragment greater than the lumenal domain of Tlg2p is subject to

vacuolar degradation, which suggests that the cytosolic domain is also exposed to vacuolar proteases. Considering this alongside the possibility that Tlg2p may be monoubiquitinated (Figure 5.10) and also its sensitivity to hydroxylamine treatment (Figures 5.21 and 5.22), it would seem sensible to further investigate whether or not Tlg2p is regulated in a manner similar to that of Tlg1p. This would primarily require investigating whether or not Tlg2p is palmitoylated *in vivo*. This could be performed using metabolic labelling with radiolabeled palmitate. If this work confirms that Tlg2p is palmitoylated an important additional step would be to investigate how this palmitoylation functions to regulate the levels of Tlg2p *in vivo*. For example, it would be of interest to identify which palmitoyltransferase is involved in this process. A good target would be the DHHC-CRD palmitoyltransferase, Swf1p, as a *swf1* null mutant shows synthetic sick interactions with *tlg2* mutant cells (Tong et al., 2004).

6.4 Future Work

This study has provided strong evidence to suggest that Sx16 is a functional homologue of the yeast t-SNARE Tlg2p. This opens up the possibility of using the model organism, *S. cerevisiae* to further investigated the role that Sx16 plays in the regulation of insulin-regulated GLUT4 trafficking. It has been demonstrated that Sx16 is dephosphorylated upon insulin binding to its receptor (Perera et al., 2003) making Sx16 an extremely attractive candidate as a regulatory node of insulin-regulated GLUT4 trafficking as phosphorylation is thought to play an important role in regulating membrane fusion (Gurunathan et al., 2002). Tlg2p is phosphorylated on Serine 90, which prevents its entry into SNARE complexes (Gurunathan et al., 2002). Sequence alignment of Tlg2p and Sx16, performed by Dr Kirsty Proctor (University of Glasgow, UK), has identified two potential sites of phosphorylation in Sx16, Serine 94 and 95. In order to further determine which of these sites is/are targeted for phosphorylation and hence is/are involved in regulating the entry of Sx16 into SNARE complexes, the complementation experiments discussed in Chapter 3 could be used. Initially mutation of both of the serine residues present in Sx16 to aspartate residues (which carry a negative charge and are mimetic of residues which have undergone phosphorylation) would allow us to determine if either of these residues are involved in regulating SNARE complex assembly by preventing this mutant version of Sx16 from correcting the trafficking defects displayed in *tlg2Δ* mutant cells. Subsequent to this mutation of each of the individual serine residues to aspartate residues would allow us to determine which, if not both of these residue(s), is/are involved in regulating SNARE complex assembly. As a control for these experiments the serine

residues should also be mutated to asparagine residues, which are equivalent in size to aspartate residue(s) but are uncharged, this would rule out the possibility that the aspartate residue(s) is/are altering the conformation of Sx16 and that the effect is specific to the negative charge of the aspartate rather than the size. A further control for this experiment would be to include phosphoresistant versions of Sx16 in which the serine residue(s) of interest is/are mutated to alanine residues and hence are unable to undergo phosphorylation, if these residue(s) is/are involved in regulating membrane fusion this mutant version of Sx16 should be capable of correcting the trafficking defects displayed in *tlg2Δ* mutant cells. One possible problem with this investigation could be the close proximity of the two serine residues, which may make it difficult to tease apart whether both of these residues are involved in regulating SNARE complex assembly or just one. Following the identification of possible phosphorylation site in Sx16 using yeast, it would be of great importance to further investigate the phosphorylation of Sx16 in mammalian cells.

With respect to the regulation of steady-state levels of Tlg2p in the presence and absence of Vps45p, a substantial amount of work is required in order to understand how Vps45p, the proteasome and/or vacuole, palmitoylation and/or ubiquitination are all involved in regulating the cellular levels of Tlg2p. This would involve identifying whether or not Tlg2p is mono and/or polyubiquitinated; which residue(s) is/are subject to ubiquitination and which E3 ligase is responsible. As well as identifying whether or not Tlg2p is palmitoylated *in vivo*; if so which palmitoyltransferase is involved in this process and also which residues are subject to palmitoylation.

The work presented in this thesis has established Tlg2p-mediated trafficking in *S. cerevisiae* as a model system for investigating Sx16 function in insulin-sensitive cells and also uncovered some of the molecular mechanisms by which these syntaxins are regulated within the cell.

Bibliography

ABELIOVICH, H., DARSOW, T. & EMR, S. D. (1999) Cytoplasm to vacuole trafficking of aminopeptidase I requires a t-SNARE-Sec1p complex composed of Tlg2p and Vps45p. *Embo J,* 18**,** 6005-16.

ABELIOVICH, H., GROTE, E., NOVICK, P. & FERRO-NOVICK, S. (1998) Tlg2p, a yeast syntaxin homolog that resides on the Golgi and endocytic structures. *J Biol Chem,* 273**,** 11719-27.

ALESSI, D. R., DEAK, M., CASAMAYOR, A., CAUDWELL, F. B., MORRICE, N., NORMAN, D. G., GAFFNEY, P., REESE, C. B., MACDOUGALL, C. N., HARBISON, D., ASHWORTH, A. & BOWNES, M. (1997) 3-Phosphoinositide-dependent protein kinase-1 (PDK1): structural and functional homology with the Drosophila DSTPK61 kinase. *Curr Biol,* 7**,** 776-89.

ANTONIN, W., FASSHAUER, D., BECKER, S., JAHN, R. & SCHNEIDER, T. R. (2002) Crystal structure of the endosomal SNARE complex reveals common structural principles of all SNAREs. *Nat Struct Biol,* 9**,** 107-11.

BANDYOPADHYAY, G., STANDAERT, M. L., GALLOWAY, L., MOSCAT, J. & FARESE, R. V. (1997a) Evidence for involvement of protein kinase C (PKC)-zeta and noninvolvement of diacylglycerol-sensitive PKCs in insulin-stimulated glucose transport in L6 myotubes. *Endocrinology,* 138**,** 4721-31.

BANDYOPADHYAY, G., STANDAERT, M. L., ZHAO, L., YU, B., AVIGNON, A., GALLOWAY, L., KARNAM, P., MOSCAT, J. & FARESE, R. V. (1997b) Activation of protein kinase C (alpha, beta, and zeta) by insulin in 3T3/L1 cells. Transfection studies suggest a role for PKC-zeta in glucose transport. *J Biol Chem,* 272**,** 2551-8.

BANKAITIS, V. A., JOHNSON, L. M. & EMR, S. D. (1986) Isolation of yeast mutants defective in protein targeting to the vacuole. *Proc Natl Acad Sci U S A,* 83**,** 9075-9.

BANTA, L. M., ROBINSON, J. S., KLIONSKY, D. J. & EMR, S. D. (1988) Organelle assembly in yeast: characterization of yeast mutants defective in vacuolar biogenesis and protein sorting. *J Cell Biol,* 107**,** 1369-83.

BASSHAM, D. C., SANDERFOOT, A. A., KOVALEVA, V., ZHENG, H. & RAIKHEL, N. V. (2000) AtVPS45 complex formation at the trans-Golgi network. *Mol Biol Cell,* 11**,** 2251-65.

BECHERER, K. A., RIEDER, S. E., EMR, S. D. & JONES, E. W. (1996) Novel syntaxin homologue, Pep12p, required for the sorting of lumenal hydrolases to the lysosome-like vacuole in yeast. *Mol Biol Cell,* 7**,** 579-94.

BENNETT, M. K. (1995) SNAREs and the specificity of transport vesicle targeting. *Curr Opin Cell Biol,* 7**,** 581-6.

BIJLMAKERS, M. J. & MARSH, M. (2003) The on-off story of protein palmitoylation. *Trends Cell Biol,* 13**,** 32-42.

BIRNBAUM, M. J. (1989) Identification of a novel gene encoding an insulin-responsive glucose transporter protein. *Cell,* 57**,** 305-15.

BLACHLY-DYSON, E. & STEVENS, T. H. (1987) Yeast carboxypeptidase Y can be translocated and glycosylated without its amino-terminal signal sequence. *J Cell Biol,* 104**,** 1183-91.

BLACKBURN, E. H. (1984) The molecular structure of centromeres and telomeres. *Annu Rev Biochem,* 53**,** 163-94.

BOCK, J. B., MATERN, H. T., PEDEN, A. A. & SCHELLER, R. H. (2001) A genomic perspective on membrane compartment organization. *Nature,* 409**,** 839-41.

BONIFACINO, J. S. & GLICK, B. S. (2004) The mechanisms of vesicle budding and fusion. *Cell,* 116**,** 153-66.

BRACHER, A. & WEISSENHORN, W. (2002) Structural basis for the Golgi membrane recruitment of Sly1p by Sed5p. *Embo J,* 21**,** 6114-24.

BRAUN, S. & JENTSCH, S. (2007) SM-protein-controlled ER-associated degradation discriminates between different SNAREs. *EMBO Rep,* 8**,** 1176-82.

BRENNER, S. (1974) The genetics of Caenorhabditis elegans. *Genetics,* 77**,** 71-94.

BRICKNER, J. H., BLANCHETTE, J. M., SIPOS, G. & FULLER, R. S. (2001) The Tlg SNARE complex is required for TGN homotypic fusion. *J Cell Biol,* 155**,** 969-78.

BRYANT, N. J., GOVERS, R. & JAMES, D. E. (2002) Regulated transport of the glucose transporter GLUT4. *Nat Rev Mol Cell Biol,* 3**,** 267-77.

BRYANT, N. J. & JAMES, D. E. (2001) Vps45p stabilizes the syntaxin homologue Tlg2p and positively regulates SNARE complex formation. *Embo J,* 20**,** 3380-8.

BRYANT, N. J. & JAMES, D. E. (2003) The Sec1p/Munc18 (SM) protein, Vps45p, cycles on and off membranes during vesicle transport. *J Cell Biol,* 161**,** 691-6.

BRYANT, N. J., PIPER, R. C., WEISMAN, L. S. & STEVENS, T. H. (1998) Retrograde traffic out of the yeast vacuole to the TGN occurs via the prevacuolar/endosomal compartment. *J Cell Biol,* 142**,** 651-63.

BRYANT, N. J. & STEVENS, T. H. (1997) Two separate signals act independently to localize a yeast late Golgi membrane protein through a combination of retrieval and retention. *J Cell Biol,* 136**,** 287-97.

BRYANT, N. J. & STEVENS, T. H. (1998) Vacuole biogenesis in Saccharomyces cerevisiae: protein transport pathways to the yeast vacuole. *Microbiol Mol Biol Rev,* 62**,** 230-47.

BURD, C. G., PETERSON, M., COWLES, C. R. & EMR, S. D. (1997) A novel Sec18p/NSF-dependent complex required for Golgi-to-endosome transport in yeast. *Mol Biol Cell,* 8**,** 1089-104.

BURGOYNE, R. D. & MORGAN, A. (2007) Membrane trafficking: three steps to fusion. *Curr Biol,* 17**,** R255-8.

BURKHARDT, P., HATTENDORF, D. A., WEIS, W. I. & FASSHAUER, D. (2008) Munc18a controls SNARE assembly through its interaction with the syntaxin N-peptide. *Embo J,* 27**,** 923-33.

BUTT, T. R., STERNBERG, E. J., GORMAN, J. A., CLARK, P., HAMER, D., ROSENBERG, M. & CROOKE, S. T. (1984) Copper metallothionein of yeast, structure of the gene, and regulation of expression. *Proc Natl Acad Sci U S A,* 81**,** 3332-6.

CALAKOS, N. & SCHELLER, R. H. (1996) Synaptic vesicle biogenesis, docking, and fusion: a molecular description. *Physiol Rev,* 76**,** 1-29.

CALDERHEAD, D. M., KITAGAWA, K., TANNER, L. I., HOLMAN, G. D. & LIENHARD, G. E. (1990) Insulin regulation of the two glucose transporters in 3T3-L1 adipocytes. *J Biol Chem,* 265**,** 13801-8.

CARPP, L. N., CIUFO, L. F., SHANKS, S. G., BOYD, A. & BRYANT, N. J. (2006) The Sec1p/Munc18 protein Vps45p binds its cognate SNARE proteins via two distinct modes. *J Cell Biol,* 173**,** 927-36.

CARPP, L. N., SHANKS, S. G., STRUTHERS, M. S. & BRYANT, N. J. (2007) Cellular levels of the syntaxin Tlg2p are regulated by a single mode of binding to Vps45p. *Biochem Biophys Res Commun,* 363**,** 857-60.

CARR, C. M., GROTE, E., MUNSON, M., HUGHSON, F. M. & NOVICK, P. J. (1999) Sec1p binds to SNARE complexes and concentrates at sites of secretion. *J Cell Biol,* 146**,** 333-44.

CHAMBERLAIN, L. H. & BURGOYNE, R. D. (1998) The cysteine-string domain of the secretory vesicle cysteine-string protein is required for membrane targeting. *Biochem J,* 335 (Pt 2)**,** 205-9.

CHARRON, M. J., BROSIUS, F. C., 3RD, ALPER, S. L. & LODISH, H. F. (1989) A glucose transport protein expressed predominately in insulin-responsive tissues. *Proc Natl Acad Sci U S A,* 86**,** 2535-9.

CHAU, V., TOBIAS, J. W., BACHMAIR, A., MARRIOTT, D., ECKER, D. J., GONDA, D. K. & VARSHAVSKY, A. (1989) A multiubiquitin chain is confined to specific lysine in a targeted short-lived protein. *Science,* 243**,** 1576-83.

CHIANG, S. H., BAUMANN, C. A., KANZAKI, M., THURMOND, D. C., WATSON, R. T., NEUDAUER, C. L., MACARA, I. G., PESSIN, J. E. & SALTIEL, A. R. (2001) Insulin-stimulated GLUT4 translocation requires the CAP-dependent activation of TC10. *Nature,* 410**,** 944-8.

CLARKE, L. & CARBON, J. (1980) Isolation of a yeast centromere and construction of functional small circular chromosomes. *Nature,* 287**,** 504-9.

COE, J. G., LIM, A. C., XU, J. & HONG, W. (1999) A role for Tlg1p in the transport of proteins within the Golgi apparatus of Saccharomyces cerevisiae. *Mol Biol Cell,* 10**,** 2407-23.

COHEN, F. S. & MELIKYAN, G. B. (2004) The energetics of membrane fusion from binding, through hemifusion, pore formation, and pore enlargement. *J Membr Biol,* 199**,** 1-14.

COUVE, A. & GERST, J. E. (1994) Yeast Snc proteins complex with Sec9. Functional interactions between putative SNARE proteins. *J Biol Chem,* 269**,** 23391-4.

COUVE, A., PROTOPOPOV, V. & GERST, J. E. (1995) Yeast synaptobrevin homologs are modified posttranslationally by the addition of palmitate. *Proc Natl Acad Sci U S A,* 92**,** 5987-91.

COWLES, C. R., EMR, S. D. & HORAZDOVSKY, B. F. (1994) Mutations in the VPS45 gene, a SEC1 homologue, result in vacuolar protein sorting defects and accumulation of membrane vesicles. *J Cell Sci,* 107 (Pt 12)**,** 3449-59.

CZECH, M. P., CHAWLA, A., WOON, C. W., BUXTON, J., ARMONI, M., TANG, W., JOLY, M. & CORVERA, S. (1993) Exofacial epitope-tagged glucose transporter chimeras reveal COOH-terminal sequences governing cellular localization. *J Cell Biol,* 123**,** 127-35.

DARSOW, T., RIEDER, S. E. & EMR, S. D. (1997) A multispecificity syntaxin homologue, Vam3p, essential for autophagic and biosynthetic protein transport to the vacuole. *J Cell Biol,* 138**,** 517-29.

DAVIS, N. G., HORECKA, J. L. & SPRAGUE, G. F., JR. (1993) Cis- and trans-acting functions required for endocytosis of the yeast pheromone receptors. *J Cell Biol,* 122**,** 53-65.

DAWSON, K., AVILES-HERNANDEZ, A., CUSHMAN, S. W. & MALIDE, D. (2001) Insulin-regulated trafficking of dual-labeled glucose transporter 4 in primary rat adipose cells. *Biochem Biophys Res Commun,* 287**,** 445-54.

DEEMS, R. O., DEACON, R. W., RAMLAL, T., VOLCHUK, A., KLIP, A. & YOUNG, D. A. (1994) Insulin action on whole body glucose utilization and on muscle glucose transporter translocation in mice. *Biochem Biophys Res Commun,* 199**,** 662-70.

DELOCHE, O. & SCHEKMAN, R. W. (2002) Vps10p cycles between the TGN and the late endosome via the plasma membrane in clathrin mutants. *Mol Biol Cell,* 13**,** 4296-307.

DICKINSON, J. R., SALGADO, L. E. & HEWLINS, M. J. (2003) The catabolism of amino acids to long chain and complex alcohols in Saccharomyces cerevisiae. *J Biol Chem,* 278**,** 8028-34.

DOBSON, S. P., LIVINGSTONE, C., GOULD, G. W. & TAVARE, J. M. (1996) Dynamics of insulin-stimulated translocation of GLUT4 in single living cells visualised using green fluorescent protein. *FEBS Lett,* 393**,** 179-84.

DULUBOVA, I., KHVOTCHEV, M., LIU, S., HURYEVA, I., SUDHOF, T. C. & RIZO, J. (2007) Munc18-1 binds directly to the neuronal SNARE complex. *Proc Natl Acad Sci U S A,* 104**,** 2697-702.

DULUBOVA, I., SUGITA, S., HILL, S., HOSAKA, M., FERNANDEZ, I., SUDHOF, T. C. & RIZO, J. (1999) A conformational switch in syntaxin during exocytosis: role of munc18. *Embo J,* 18**,** 4372-82.

DULUBOVA, I., YAMAGUCHI, T., ARAC, D., LI, H., HURYEVA, I., MIN, S. W., RIZO, J. & SUDHOF, T. C. (2003) Convergence and divergence in the mechanism of SNARE binding by Sec1/Munc18-like proteins. *Proc Natl Acad Sci U S A,* 100**,** 32-7.

DULUBOVA, I., YAMAGUCHI, T., GAO, Y., MIN, S. W., HURYEVA, I., SUDHOF, T. C. & RIZO, J. (2002) How Tlg2p/syntaxin 16 'snares' Vps45. *Embo J,* 21**,** 3620-31.

DUNN, B., STEARNS, T. & BOTSTEIN, D. (1993) Specificity domains distinguish the Ras-related GTPases Ypt1 and Sec4. *Nature,* 362**,** 563-5.

EGUEZ, L., LEE, A., CHAVEZ, J. A., MIINEA, C. P., KANE, S., LIENHARD, G. E. & MCGRAW, T. E. (2005) Full intracellular retention of GLUT4 requires AS160 Rab GTPase activating protein. *Cell Metab,* 2**,** 263-72.

EMR, S. D., SCHAUER, I., HANSEN, W., ESMON, P. & SCHEKMAN, R. (1984) Invertase beta-galactosidase hybrid proteins fail to be transported from the endoplasmic reticulum in Saccharomyces cerevisiae. *Mol Cell Biol,* 4**,** 2347-55.

ESMON, P. C., ESMON, B. E., SCHAUER, I. E., TAYLOR, A. & SCHEKMAN, R. (1987) Structure, assembly, and secretion of octameric invertase. *J Biol Chem,* 262**,** 4387-94.

FASSHAUER, D., ANTONIN, W., MARGITTAI, M., PABST, S. & JAHN, R. (1999) Mixed and non-cognate SNARE complexes. Characterization of assembly and biophysical properties. *J Biol Chem,* 274**,** 15440-6.

FASSHAUER, D., SUTTON, R. B., BRUNGER, A. T. & JAHN, R. (1998) Conserved structural features of the synaptic fusion complex: SNARE proteins reclassified as Q- and R-SNAREs. *Proc Natl Acad Sci U S A,* 95**,** 15781-6.

FERNANDEZ, I., UBACH, J., DULUBOVA, I., ZHANG, X., SUDHOF, T. C. & RIZO, J. (1998) Three-dimensional structure of an evolutionarily conserved N-terminal domain of syntaxin 1A. *Cell,* 94**,** 841-9.

FERRO-NOVICK, S. & JAHN, R. (1994) Vesicle fusion from yeast to man. *Nature,* 370**,** 191-3.

FIEBIG, K. M., RICE, L. M., POLLOCK, E. & BRUNGER, A. T. (1999) Folding intermediates of SNARE complex assembly. *Nat Struct Biol,* 6**,** 117-23.

FISCHER VON MOLLARD, G. & STEVENS, T. H. (1998) A human homolog can functionally replace the yeast vesicle-associated SNARE Vti1p in two vesicle transport pathways. *J Biol Chem,* 273**,** 2624-30.

FISK, H. A. & YAFFE, M. P. (1999) A role for ubiquitination in mitochondrial inheritance in Saccharomyces cerevisiae. *J Cell Biol,* 145**,** 1199-208.

FUKASAWA, M., VARLAMOV, O., ENG, W. S., SOLLNER, T. H. & ROTHMAN, J. E. (2004) Localization and activity of the SNARE Ykt6 determined by its regulatory domain and palmitoylation. *Proc Natl Acad Sci U S A,* 101**,** 4815-20.

FUKUMOTO, H., KAYANO, T., BUSE, J. B., EDWARDS, Y., PILCH, P. F., BELL, G. I. & SEINO, S. (1989) Cloning and characterization of the major insulin-responsive glucose transporter expressed in human skeletal muscle and other insulin-responsive tissues. *J Biol Chem,* 264**,** 7776-9.

FUNAKOSHI, M., SASAKI, T., NISHIMOTO, T. & KOBAYASHI, H. (2002) Budding yeast Dsk2p is a polyubiquitin-binding protein that can interact with the proteasome. *Proc Natl Acad Sci U S A,* 99**,** 745-50.

FURGASON, M. L., MACDONALD, C., SHANKS, S. G., RYDER, S. P., BRYANT, N. J. & MUNSON, M. (2009) The N-terminal peptide of the syntaxin Tlg2p modulates binding of its closed conformation to Vps45p. *Proc Natl Acad Sci U S A*.

GALAN, J. M. & HAGUENAUER-TSAPIS, R. (1997) Ubiquitin lys63 is involved in ubiquitination of a yeast plasma membrane protein. *Embo J,* 16**,** 5847-54.

GARCIA, E. P., GATTI, E., BUTLER, M., BURTON, J. & DE CAMILLI, P. (1994) A rat brain Sec1 homologue related to Rop and UNC18 interacts with syntaxin. *Proc Natl Acad Sci U S A,* 91**,** 2003-7.

GHISLAIN, M., UDVARDY, A. & MANN, C. (1993) S. cerevisiae 26S protease mutants arrest cell division in G2/metaphase. *Nature,* 366**,** 358-62.

GOTTE, M. & GALLWITZ, D. (1997) High expression of the yeast syntaxin-related Vam3 protein suppresses the protein transport defects of a pep12 null mutant. *FEBS Lett,* 411**,** 48-52.

GROTE, E., CARR, C. M. & NOVICK, P. J. (2000) Ordering the final events in yeast exocytosis. *J Cell Biol,* 151**,** 439-52.

GUPTE, A. & MORA, S. (2006) Activation of the Cbl insulin signaling pathway in cardiac muscle; dysregulation in obesity and diabetes. *Biochem Biophys Res Commun,* 342**,** 751-7.

GURUNATHAN, S., MARASH, M., WEINBERGER, A. & GERST, J. E. (2002) t-SNARE phosphorylation regulates endocytosis in yeast. *Mol Biol Cell,* 13**,** 1594-607.

HARRISON, S. D., BROADIE, K., VAN DE GOOR, J. & RUBIN, G. M. (1994) Mutations in the Drosophila Rop gene suggest a function in general secretion and synaptic transmission. *Neuron,* 13**,** 555-66.

HASHIRAMOTO, M. & JAMES, D. E. (2000) Characterization of insulin-responsive GLUT4 storage vesicles isolated from 3T3-L1 adipocytes. *Mol Cell Biol,* 20**,** 416-27.

HASILIK, A. & TANNER, W. (1978a) Biosynthesis of the vacuolar yeast glycoprotein carboxypeptidase Y. Conversion of precursor into the enzyme. *Eur J Biochem,* 85**,** 599-608.

HASILIK, A. & TANNER, W. (1978b) Carbohydrate moiety of carboxypeptidase Y and perturbation of its biosynthesis. *Eur J Biochem,* 91**,** 567-75.

HATA, Y., SLAUGHTER, C. A. & SUDHOF, T. C. (1993) Synaptic vesicle fusion complex contains unc-18 homologue bound to syntaxin. *Nature,* 366**,** 347-51.

HEIN, C. & ANDRE, B. (1997) A C-terminal di-leucine motif and nearby sequences are required for NH4(+)-induced inactivation and degradation of the general amino acid permease, Gap1p, of Saccharomyces cerevisiae. *Mol Microbiol,* 24**,** 607-16.

HEINEMEYER, W., GRUHLER, A., MOHRLE, V., MAHE, Y. & WOLF, D. H. (1993) PRE2, highly homologous to the human major histocompatibility complex-linked RING10 gene, codes for a yeast proteasome subunit necessary for chrymotryptic activity and degradation of ubiquitinated proteins. *J Biol Chem,* 268**,** 5115-20.

HEINEMEYER, W., KLEINSCHMIDT, J. A., SAIDOWSKY, J., ESCHER, C. & WOLF, D. H. (1991) Proteinase yscE, the yeast proteasome/multicatalytic-multifunctional proteinase: mutants unravel its function in stress induced proteolysis and uncover its necessity for cell survival. *Embo J,* 10**,** 555-62.

HELLIWELL, R. C., FERRIER, R. C. & KERNAN, M. R. (2001) Interaction of nitrogen deposition and land use on soil and water quality in Scotland: issues of spatial variability and scale. *Sci Total Environ,* 265**,** 51-63.

HERSHKO, A. & CIECHANOVER, A. (1998) The ubiquitin system. *Annu Rev Biochem,* 67**,** 425-79.

HERSKOWITZ, I. (1989) A regulatory hierarchy for cell specialization in yeast. *Nature,* 342**,** 749-57.

HICKE, L. (2001) Protein regulation by monoubiquitin. *Nat Rev Mol Cell Biol,* 2**,** 195-201.

HICKE, L. & DUNN, R. (2003) Regulation of membrane protein transport by ubiquitin and ubiquitin-binding proteins. *Annu Rev Cell Dev Biol,* 19**,** 141-72.

HOEGE, C., PFANDER, B., MOLDOVAN, G. L., PYROWOLAKIS, G. & JENTSCH, S. (2002) RAD6-dependent DNA repair is linked to modification of PCNA by ubiquitin and SUMO. *Nature,* 419**,** 135-41.

HOLMAN, G. D., KOZKA, I. J., CLARK, A. E., FLOWER, C. J., SALTIS, J., HABBERFIELD, A. D., SIMPSON, I. A. & CUSHMAN, S. W. (1990) Cell surface labeling of glucose transporter isoform GLUT4 by bis-mannose photolabel. Correlation with stimulation of glucose transport in rat adipose cells by insulin and phorbol ester. *J Biol Chem,* 265**,** 18172-9.

HOLTHUIS, J. C., NICHOLS, B. J., DHRUVAKUMAR, S. & PELHAM, H. R. (1998) Two syntaxin homologues in the TGN/endosomal system of yeast. *Embo J,* 17**,** 113-26.

HOSONO, R., HEKIMI, S., KAMIYA, Y., SASSA, T., MURAKAMI, S., NISHIWAKI, K., MIWA, J., TAKETO, A. & KODAIRA, K. I. (1992) The unc-18 gene encodes a novel protein affecting the kinetics of acetylcholine metabolism in the nematode Caenorhabditis elegans. *J Neurochem,* 58**,** 1517-25.

HOU, D., CENCIARELLI, C., JENSEN, J. P., NGUYGEN, H. B. & WEISSMAN, A. M. (1994) Activation-dependent ubiquitination of a T cell antigen receptor subunit on multiple intracellular lysines. *J Biol Chem,* 269**,** 14244-7.

HU, C., AHMED, M., MELIA, T. J., SOLLNER, T. H., MAYER, T. & ROTHMAN, J. E. (2003) Fusion of cells by flipped SNAREs. *Science,* 300**,** 1745-9.

HUA, Y. & SCHELLER, R. H. (2001) Three SNARE complexes cooperate to mediate membrane fusion. *Proc Natl Acad Sci U S A,* 98**,** 8065-70.

IKONOMOV, O. C., SBRISSA, D., DONDAPATI, R. & SHISHEVA, A. (2007) ArPIKfyve-PIKfyve interaction and role in insulin-regulated GLUT4 translocation and glucose transport in 3T3-L1 adipocytes. *Exp Cell Res,* 313**,** 2404-16.

IKONOMOV, O. C., SBRISSA, D., MLAK, K. & SHISHEVA, A. (2002) Requirement for PIKfyve enzymatic activity in acute and long-term insulin cellular effects. *Endocrinology,* 143**,** 4742-54.

IMAMURA, T., HUANG, J., USUI, I., SATOH, H., BEVER, J. & OLEFSKY, J. M. (2003) Insulin-induced GLUT4 translocation involves protein kinase C-lambda-mediated functional coupling between Rab4 and the motor protein kinesin. *Mol Cell Biol,* 23**,** 4892-900.

INOUE, M., CHANG, L., HWANG, J., CHIANG, S. H. & SALTIEL, A. R. (2003) The exocyst complex is required for targeting of Glut4 to the plasma membrane by insulin. *Nature,* 422**,** 629-33.

INOUE, M., CHIANG, S. H., CHANG, L., CHEN, X. W. & SALTIEL, A. R. (2006) Compartmentalization of the exocyst complex in lipid rafts controls Glut4 vesicle tethering. *Mol Biol Cell,* 17**,** 2303-11.

JAHN, R. (2000) Sec1/Munc18 proteins: mediators of membrane fusion moving to center stage. *Neuron,* 27**,** 201-4.

JAHN, R. & SUDHOF, T. C. (1999) Membrane fusion and exocytosis. *Annu Rev Biochem,* 68**,** 863-911.

JAMES, D. E., STRUBE, M. & MUECKLER, M. (1989) Molecular cloning and characterization of an insulin-regulatable glucose transporter. *Nature,* 338**,** 83-7.

JOHNSON, L. M., BANKAITIS, V. A. & EMR, S. D. (1987) Distinct sequence determinants direct intracellular sorting and modification of a yeast vacuolar protease. *Cell,* 48**,** 875-85.

JONES, E. W. (1984) The synthesis and function of proteases in Saccharomyces: genetic approaches. *Annu Rev Genet,* 18**,** 233-70.

KAESTNER, K. H., CHRISTY, R. J., MCLENITHAN, J. C., BRAITERMAN, L. T., CORNELIUS, P., PEKALA, P. H. & LANE, M. D. (1989) Sequence, tissue distribution, and differential expression of mRNA for a putative insulin-responsive glucose transporter in mouse 3T3-L1 adipocytes. *Proc Natl Acad Sci U S A,* 86**,** 3150-4.

KAGI, J. H., KOJIMA, Y., KISSLING, M. M. & LERCH, K. (1979) Metallothionein: an exceptional metal thiolate protein. *Ciba Found Symp***,** 223-37.

KANAI, F., NISHIOKA, Y., HAYASHI, H., KAMOHARA, S., TODAKA, M. & EBINA, Y. (1993) Direct demonstration of insulin-induced GLUT4 translocation to the surface of intact cells by insertion of a c-myc epitope into an exofacial GLUT4 domain. *J Biol Chem,* 268**,** 14523-6.

KANZAKI, M. & PESSIN, J. E. (2001) Insulin-stimulated GLUT4 translocation in adipocytes is dependent upon cortical actin remodeling. *J Biol Chem,* 276**,** 42436-44.

KATZMANN, D. J., ODORIZZI, G. & EMR, S. D. (2002) Receptor downregulation and multivesicular-body sorting. *Nat Rev Mol Cell Biol,* 3**,** 893-905.

KORNFELD, S. (1992) Structure and function of the mannose 6-phosphate/insulinlike growth factor II receptors. *Annu Rev Biochem,* 61**,** 307-30.

KREYKENBOHM, V., WENZEL, D., ANTONIN, W., ATLACHKINE, V. & VON MOLLARD, G. F. (2002) The SNAREs vti1a and vti1b have distinct localization and SNARE complex partners. *Eur J Cell Biol,* 81**,** 273-80.

KUHN, R. W., WALSH, K. A. & NEURATH, H. (1974) Isolation and partial characterization of an acid carboxypeptidase from yeast. *Biochemistry,* 13**,** 3871-7.

LAEMMLI, U. K. (1970) Cleavage of structural proteins during the assembly of the head of bacteriophage T4. *Nature,* 227**,** 680-5.

LARANCE, M., RAMM, G., STOCKLI, J., VAN DAM, E. M., WINATA, S., WASINGER, V., SIMPSON, F., GRAHAM, M., JUNUTULA, J. R., GUILHAUS, M. & JAMES, D. E. (2005) Characterization of the role of the Rab GTPase-activating protein AS160 in insulin-regulated GLUT4 trafficking. *J Biol Chem,* 280**,** 37803-13.

LAWSON, T. G., GRONROS, D. L., EVANS, P. E., BASTIEN, M. C., MICHALEWICH, K. M., CLARK, J. K., EDMONDS, J. H., GRABER, K. H., WERNER, J. A., LURVEY, B. A. & CATE, J. M. (1999) Identification and characterization of a protein destruction signal in the encephalomyocarditis virus 3C protease. *J Biol Chem,* 274**,** 9871-80.

LEE, J. & PILCH, P. F. (1994) The insulin receptor: structure, function, and signaling. *Am J Physiol,* 266**,** C319-34.

LENEY, S. & TAVARE, J. (2009) The molecular basis of insulin-stimulated glucose uptake: signalling, trafficking and potential drug targets. *J Endocrinol*.

LEVINE, R. & GOLDSTEIN, M. S. (1958) On the mechanism of action of insulin. *Hormoner,* 11**,** 2-22.

LEWIS, M. J., NICHOLS, B. J., PRESCIANOTTO-BASCHONG, C., RIEZMAN, H. & PELHAM, H. R. (2000) Specific retrieval of the exocytic SNARE Snc1p from early yeast endosomes. *Mol Biol Cell,* 11**,** 23-38.

LI, F., PINCET, F., PEREZ, E., ENG, W. S., MELIA, T. J., ROTHMAN, J. E. & TARESTE, D. (2007) Energetics and dynamics of SNAREpin folding across lipid bilayers. *Nat Struct Mol Biol,* 14**,** 890-6.

LIN, R. C. & SCHELLER, R. H. (1997) Structural organization of the synaptic exocytosis core complex. *Neuron,* 19**,** 1087-94.

LINIAL, M. (1997) SNARE proteins--why so many, why so few? *J Neurochem,* 69**,** 1781-92.

LIU, L. Z., ZHAO, H. L., ZUO, J., HO, S. K., CHAN, J. C., MENG, Y., FANG, F. D. & TONG, P. C. (2006) Protein kinase Czeta mediates insulin-induced glucose transport through actin remodeling in L6 muscle cells. *Mol Biol Cell,* 17**,** 2322-30.

LODHI, I. J., CHIANG, S. H., CHANG, L., VOLLENWEIDER, D., WATSON, R. T., INOUE, M., PESSIN, J. E. & SALTIEL, A. R. (2007) Gapex-5, a Rab31 guanine nucleotide exchange factor that regulates Glut4 trafficking in adipocytes. *Cell Metab,* 5**,** 59-72.

LORENZO, M., TERUEL, T., HERNANDEZ, R., KAYALI, A. G. & WEBSTER, N. J. (2002) PLCgamma participates in insulin stimulation of glucose uptake through activation of PKCzeta in brown adipocytes. *Exp Cell Res,* 278**,** 146-57.

LUTSTORF, U. & MEGNET, R. (1968) Multiple forms of alcohol dehydrogenase in Saccharomyces cerevisiae. I. Physiological control of ADH-2 and properties of ADH-2 and ADH-4. *Arch Biochem Biophys,* 126**,** 933-44.

MACREADIE, I. G., JAGADISH, M. N., AZAD, A. A. & VAUGHAN, P. R. (1989) Versatile cassettes designed for the copper inducible expression of proteins in yeast. *Plasmid,* 21**,** 147-50.

MAFFUCCI, T., BRANCACCIO, A., PICCOLO, E., STEIN, R. C. & FALASCA, M. (2003) Insulin induces phosphatidylinositol-3-phosphate formation through TC10 activation. *Embo J,* 22**,** 4178-89.

MAIER, V. H. & GOULD, G. W. (2000) Long-term insulin treatment of 3T3-L1 adipocytes results in mis-targeting of GLUT4: implications for insulin-stimulated glucose transport. *Diabetologia,* 43**,** 1273-81.

MALIDE, D., DWYER, N. K., BLANCHETTE-MACKIE, E. J. & CUSHMAN, S. W. (1997) Immunocytochemical evidence that GLUT4 resides in a specialized translocation post-endosomal VAMP2-positive compartment in rat adipose cells in the absence of insulin. *J Histochem Cytochem,* 45**,** 1083-96.

MALLARD, F., TANG, B. L., GALLI, T., TENZA, D., SAINT-POL, A., YUE, X., ANTONY, C., HONG, W., GOUD, B. & JOHANNES, L. (2002) Early/recycling endosomes-to-TGN transport involves two SNARE complexes and a Rab6 isoform. *J Cell Biol,* 156**,** 653-64.

MARCUSSON, E. G., HORAZDOVSKY, B. F., CEREGHINO, J. L., GHARAKHANIAN, E. & EMR, S. D. (1994) The sorting receptor for yeast vacuolar carboxypeptidase Y is encoded by the VPS10 gene. *Cell,* 77**,** 579-86.

MARETTE, A., BURDETT, E., DOUEN, A., VRANIC, M. & KLIP, A. (1992) Insulin induces the translocation of GLUT4 from a unique intracellular organelle to transverse tubules in rat skeletal muscle. *Diabetes,* 41**,** 1562-9.

MASCORRO-GALLARDO, J. O., COVARRUBIAS, A. A. & GAXIOLA, R. (1996) Construction of a CUP1 promoter-based vector to modulate gene expression in Saccharomyces cerevisiae. *Gene,* 172**,** 169-70.

MAYER, A., WICKNER, W. & HAAS, A. (1996) Sec18p (NSF)-driven release of Sec17p (alpha-SNAP) can precede docking and fusion of yeast vacuoles. *Cell,* 85**,** 83-94.

MISURA, K. M., SCHELLER, R. H. & WEIS, W. I. (2000) Three-dimensional structure of the neuronal-Sec1-syntaxin 1a complex. *Nature,* 404**,** 355-62.

MUNSON, M., CHEN, X., COCINA, A. E., SCHULTZ, S. M. & HUGHSON, F. M. (2000) Interactions within the yeast t-SNARE Sso1p that control SNARE complex assembly. *Nat Struct Biol,* 7**,** 894-902.

MYERS, M. G., JR., SUN, X. J., CHEATHAM, B., JACHNA, B. R., GLASHEEN, E. M., BACKER, J. M. & WHITE, M. F. (1993) IRS-1 is a common element in insulin and insulin-like growth factor-I signaling to the phosphatidylinositol 3'-kinase. *Endocrinology,* 132**,** 1421-30.

NAIDER, F. & BECKER, J. M. (2004) The alpha-factor mating pheromone of Saccharomyces cerevisiae: a model for studying the interaction of peptide hormones and G protein-coupled receptors. *Peptides,* 25**,** 1441-63.

NICHOLS, B. J., HOLTHUIS, J. C. & PELHAM, H. R. (1998) The Sec1p homologue Vps45p binds to the syntaxin Tlg2p. *Eur J Cell Biol,* 77**,** 263-8.

NICHOLS, B. J., UNGERMANN, C., PELHAM, H. R., WICKNER, W. T. & HAAS, A. (1997) Homotypic vacuolar fusion mediated by t- and v-SNAREs. *Nature,* 387**,** 199-202.

NICKERSON, D. P., BRETT, C. L. & MERZ, A. J. (2009) Vps-C complexes: gatekeepers of endolysosomal traffic. *Curr Opin Cell Biol,* 21**,** 543-51.

NOTHWEHR, S. F., CONIBEAR, E. & STEVENS, T. H. (1995) Golgi and vacuolar membrane proteins reach the vacuole in vps1 mutant yeast cells via the plasma membrane. *J Cell Biol,* 129**,** 35-46.

NOVICK, P. & BRENNWALD, P. (1993) Friends and family: the role of the Rab GTPases in vesicular traffic. *Cell,* 75**,** 597-601.

NOVICK, P. & SCHEKMAN, R. (1979) Secretion and cell-surface growth are blocked in a temperature-sensitive mutant of Saccharomyces cerevisiae. *Proc Natl Acad Sci U S A,* 76**,** 1858-62.

OHNO, A., JEE, J., FUJIWARA, K., TENNO, T., GODA, N., TOCHIO, H., KOBAYASHI, H., HIROAKI, H. & SHIRAKAWA, M. (2005) Structure of the UBA domain of Dsk2p in complex with ubiquitin molecular determinants for ubiquitin recognition. *Structure,* 13**,** 521-32.

OLSON, A. L., KNIGHT, J. B. & PESSIN, J. E. (1997) Syntaxin 4, VAMP2, and/or VAMP3/cellubrevin are functional target membrane and vesicle SNAP receptors for insulin-stimulated GLUT4 translocation in adipocytes. *Mol Cell Biol,* 17**,** 2425-35.

OSSIG, R., DASCHER, C., TREPTE, H. H., SCHMITT, H. D. & GALLWITZ, D. (1991) The yeast SLY gene products, suppressors of defects in the essential GTP-binding Ypt1 protein, may act in endoplasmic reticulum-to-Golgi transport. *Mol Cell Biol,* 11**,** 2980-93.

PALADE, G. (1975) Intracellular Aspects of the Process of Protein Synthesis. *Science,* 189**,** 867.

PARK, C. R. & JOHNSON, L. H. (1955) Effect of insulin on transport of glucose and galactose into cells of rat muscle and brain. *Am J Physiol,* 182**,** 17-23.

PAUMET, F., BRUGGER, B., PARLATI, F., MCNEW, J. A., SOLLNER, T. H. & ROTHMAN, J. E. (2001) A t-SNARE of the endocytic pathway must be activated for fusion. *J Cell Biol,* 155**,** 961-8.

PAUMET, F., RAHIMIAN, V., DI LIBERTO, M. & ROTHMAN, J. E. (2005) Concerted auto-regulation in yeast endosomal t-SNAREs. *J Biol Chem,* 280**,** 21137-43.

PENG, J., SCHWARTZ, D., ELIAS, J. E., THOREEN, C. C., CHENG, D., MARSISCHKY, G., ROELOFS, J., FINLEY, D. & GYGI, S. P. (2003) A proteomics approach to understanding protein ubiquitination. *Nat Biotechnol,* 21**,** 921-6.

PENG, R. & GALLWITZ, D. (2004) Multiple SNARE interactions of an SM protein: Sed5p/Sly1p binding is dispensable for transport. *Embo J,* 23**,** 3939-49.

PERERA, H. K., CLARKE, M., MORRIS, N. J., HONG, W., CHAMBERLAIN, L. H. & GOULD, G. W. (2003) Syntaxin 6 regulates Glut4 trafficking in 3T3-L1 adipocytes. *Mol Biol Cell,* 14**,** 2946-58.

PEVSNER, J., HSU, S. C., BRAUN, J. E., CALAKOS, N., TING, A. E., BENNETT, M. K. & SCHELLER, R. H. (1994a) Specificity and regulation of a synaptic vesicle docking complex. *Neuron,* 13**,** 353-61.

PEVSNER, J., HSU, S. C. & SCHELLER, R. H. (1994b) n-Sec1: a neural-specific syntaxin-binding protein. *Proc Natl Acad Sci U S A,* 91**,** 1445-9.

PILCH, P. F., WILKINSON, W., GARVEY, W. T., CIARALDI, T. P., HUECKSTAEDT, T. P. & OLEFSKY, J. M. (1993) Insulin-responsive human adipocytes express two

glucose transporter isoforms and target them to different vesicles. *J Clin Endocrinol Metab,* 77**,** 286-9.

PIPER, R. C., COOPER, A. A., YANG, H. & STEVENS, T. H. (1995) VPS27 controls vacuolar and endocytic traffic through a prevacuolar compartment in Saccharomyces cerevisiae. *J Cell Biol,* 131**,** 603-17.

PIPER, R. C. & LUZIO, J. P. (2007) Ubiquitin-dependent sorting of integral membrane proteins for degradation in lysosomes. *Curr Opin Cell Biol,* 19**,** 459-65.

PIPER, R. C., WHITTERS, E. A. & STEVENS, T. H. (1994) Yeast Vps45p is a Sec1p-like protein required for the consumption of vacuole-targeted, post-Golgi transport vesicles. *Eur J Cell Biol,* 65**,** 305-18.

POIRIER, M. A., XIAO, W., MACOSKO, J. C., CHAN, C., SHIN, Y. K. & BENNETT, M. K. (1998) The synaptic SNARE complex is a parallel four-stranded helical bundle. *Nat Struct Biol,* 5**,** 765-9.

PROCTOR, K. M., MILLER, S. C., BRYANT, N. J. & GOULD, G. W. (2006) Syntaxin 16 controls the intracellular sequestration of GLUT4 in 3T3-L1 adipocytes. *Biochem Biophys Res Commun,* 347**,** 433-8.

PUTILINA, T., WONG, P. & GENTLEMAN, S. (1999) The DHHC domain: a new highly conserved cysteine-rich motif. *Mol Cell Biochem,* 195**,** 219-26.

RALSTON, E. & PLOUG, T. (1996) GLUT4 in cultured skeletal myotubes is segregated from the transferrin receptor and stored in vesicles associated with TGN. *J Cell Sci,* 109 (Pt 13)**,** 2967-78.

REGGIORI, F. & PELHAM, H. R. (2002) A transmembrane ubiquitin ligase required to sort membrane proteins into multivesicular bodies. *Nat Cell Biol,* 4**,** 117-23.

RESNICK, M. A., WESTMORELAND, J. & BLOOM, K. (1990) Heterogeneity and maintenance of centromere plasmid copy number in Saccharomyces cerevisiae. *Chromosoma,* 99**,** 281-8.

RIBON, V., HUBBELL, S., HERRERA, R. & SALTIEL, A. R. (1996) The product of the cbl oncogene forms stable complexes in vivo with endogenous Crk in a tyrosine phosphorylation-dependent manner. *Mol Cell Biol,* 16**,** 45-52.

RIBON, V., PRINTEN, J. A., HOFFMAN, N. G., KAY, B. K. & SALTIEL, A. R. (1998) A novel, multifuntional c-Cbl binding protein in insulin receptor signaling in 3T3-L1 adipocytes. *Mol Cell Biol,* 18**,** 872-9.

RIBON, V. & SALTIEL, A. R. (1997) Insulin stimulates tyrosine phosphorylation of the proto-oncogene product of c-Cbl in 3T3-L1 adipocytes. *Biochem J,* 324 (Pt 3)**,** 839-45.

RICKMAN, C., MEDINE, C. N., BERGMANN, A. & DUNCAN, R. R. (2007) Functionally and spatially distinct modes of munc18-syntaxin 1 interaction. *J Biol Chem,* 282**,** 12097-103.

ROBINSON, J. S., KLIONSKY, D. J., BANTA, L. M. & EMR, S. D. (1988) Protein sorting in Saccharomyces cerevisiae: isolation of mutants defective in the delivery and processing of multiple vacuolar hydrolases. *Mol Cell Biol,* 8**,** 4936-48.

ROBINSON, L. J., PANG, S., HARRIS, D. S., HEUSER, J. & JAMES, D. E. (1992) Translocation of the glucose transporter (GLUT4) to the cell surface in permeabilized 3T3-L1 adipocytes: effects of ATP insulin, and GTP gamma S and localization of GLUT4 to clathrin lattices. *J Cell Biol,* 117**,** 1181-96.

ROEDER, A. D. & SHAW, J. M. (1996) Vacuole partitioning during meiotic division in yeast. *Genetics,* 144**,** 445-58.

ROTHMAN, J. E. (1994) Mechanisms of intracellular protein transport. *Nature,* 372**,** 55-63.

ROTHMAN, J. H. & STEVENS, T. H. (1986) Protein sorting in yeast: mutants defective in vacuole biogenesis mislocalize vacuolar proteins into the late secretory pathway. *Cell,* 47**,** 1041-51.

ROUILLER, I., DELABARRE, B., MAY, A. P., WEIS, W. I., BRUNGER, A. T., MILLIGAN, R. A. & WILSON-KUBALEK, E. M. (2002) Conformational changes of the multifunction p97 AAA ATPase during its ATPase cycle. *Nat Struct Biol,* 9**,** 950-7.

ROWE, J., CALEGARI, F., TAVERNA, E., LONGHI, R. & ROSA, P. (2001) Syntaxin 1A is delivered to the apical and basolateral domains of epithelial cells: the role of munc-18 proteins. *J Cell Sci,* 114**,** 3323-32.

ROWE, J., CORRADI, N., MALOSIO, M. L., TAVERNA, E., HALBAN, P., MELDOLESI, J. & ROSA, P. (1999) Blockade of membrane transport and disassembly of the Golgi complex by expression of syntaxin 1A in neurosecretion-incompetent cells: prevention by rbSEC1. *J Cell Sci,* 112 (Pt 12)**,** 1865-77.

SALGHETTI, S. E., CAUDY, A. A., CHENOWETH, J. G. & TANSEY, W. P. (2001) Regulation of transcriptional activation domain function by ubiquitin. *Science,* 293**,** 1651-3.

SALTIEL, A. R. & KAHN, C. R. (2001) Insulin signalling and the regulation of glucose and lipid metabolism. *Nature,* 414**,** 799-806.

SANO, H., KANE, S., SANO, E., MIINEA, C. P., ASARA, J. M., LANE, W. S., GARNER, C. W. & LIENHARD, G. E. (2003) Insulin-stimulated phosphorylation of a Rab GTPase-activating protein regulates GLUT4 translocation. *J Biol Chem,* 278**,** 14599-602.

SATO, T. K., REHLING, P., PETERSON, M. R. & EMR, S. D. (2000) Class C Vps protein complex regulates vacuolar SNARE pairing and is required for vesicle docking/fusion. *Mol Cell,* 6**,** 661-71.

SCHWARTZ, D. C. & HOCHSTRASSER, M. (2003) A superfamily of protein tags: ubiquitin, SUMO and related modifiers. *Trends Biochem Sci,* 28**,** 321-8.

SCOTT, B. L., VAN KOMEN, J. S., IRSHAD, H., LIU, S., WILSON, K. A. & MCNEW, J. A. (2004a) Sec1p directly stimulates SNARE-mediated membrane fusion in vitro. *J Cell Biol,* 167**,** 75-85.

SCOTT, P. M., BILODEAU, P. S., ZHDANKINA, O., WINISTORFER, S. C., HAUGLUND, M. J., ALLAMAN, M. M., KEARNEY, W. R., ROBERTSON, A. D., BOMAN, A. L. & PIPER, R. C. (2004b) GGA proteins bind ubiquitin to facilitate sorting at the trans-Golgi network. *Nat Cell Biol,* 6**,** 252-9.

SEAMAN, M. N., MARCUSSON, E. G., CEREGHINO, J. L. & EMR, S. D. (1997) Endosome to Golgi retrieval of the vacuolar protein sorting receptor, Vps10p, requires the function of the VPS29, VPS30, and VPS35 gene products. *J Cell Biol,* 137**,** 79-92.

SERON, K., TIEAHO, V., PRESCIANOTTO-BASCHONG, C., AUST, T., BLONDEL, M. O., GUILLAUD, P., DEVILLIERS, G., ROSSANESE, O. W., GLICK, B. S., RIEZMAN, H., KERANEN, S. & HAGUENAUER-TSAPIS, R. (1998) A yeast t-SNARE involved in endocytosis. *Mol Biol Cell,* 9**,** 2873-89.

SHEN, J., TARESTE, D. C., PAUMET, F., ROTHMAN, J. E. & MELIA, T. J. (2007) Selective activation of cognate SNAREpins by Sec1/Munc18 proteins. *Cell,* 128**,** 183-95.

SHEWAN, A. M., VAN DAM, E. M., MARTIN, S., LUEN, T. B., HONG, W., BRYANT, N. J. & JAMES, D. E. (2003) GLUT4 recycles via a trans-Golgi network (TGN) subdomain enriched in Syntaxins 6 and 16 but not TGN38: involvement of an acidic targeting motif. *Mol Biol Cell,* 14**,** 973-86.

SIKORSKI, R. S. & HIETER, P. (1989) A system of shuttle vectors and yeast host strains designed for efficient manipulation of DNA in Saccharomyces cerevisiae. *Genetics,* 122**,** 19-27.

SIMONSEN, A., BREMNES, B., RONNING, E., AASLAND, R. & STENMARK, H. (1998) Syntaxin-16, a putative Golgi t-SNARE. *Eur J Cell Biol,* 75**,** 223-31.

SOLLNER, T., WHITEHEART, S. W., BRUNNER, M., ERDJUMENT-BROMAGE, H., GEROMANOS, S., TEMPST, P. & ROTHMAN, J. E. (1993) SNAP receptors implicated in vesicle targeting and fusion. *Nature,* 362**,** 318-24.

SPRINGAEL, J. Y. & ANDRE, B. (1998) Nitrogen-regulated ubiquitination of the Gap1 permease of Saccharomyces cerevisiae. *Mol Biol Cell,* 9**,** 1253-63.

SPRINGAEL, J. Y., GALAN, J. M., HAGUENAUER-TSAPIS, R. & ANDRE, B. (1999) NH4+-induced down-regulation of the Saccharomyces cerevisiae Gap1p permease involves its ubiquitination with lysine-63-linked chains. *J Cell Sci,* 112 (Pt 9)**,** 1375-83.

STEPHENS, L., ANDERSON, K., STOKOE, D., ERDJUMENT-BROMAGE, H., PAINTER, G. F., HOLMES, A. B., GAFFNEY, P. R., REESE, C. B., MCCORMICK, F., TEMPST, P., COADWELL, J. & HAWKINS, P. T. (1998) Protein kinase B kinases that mediate phosphatidylinositol 3,4,5-trisphosphate-dependent activation of protein kinase B. *Science,* 279**,** 710-4.

STEVENS, T., ESMON, B. & SCHEKMAN, R. (1982) Early stages in the yeast secretory pathway are required for transport of carboxypeptidase Y to the vacuole. *Cell,* 30**,** 439-48.

STOKOE, D., STEPHENS, L. R., COPELAND, T., GAFFNEY, P. R., REESE, C. B., PAINTER, G. F., HOLMES, A. B., MCCORMICK, F. & HAWKINS, P. T. (1997) Dual role of phosphatidylinositol-3,4,5-trisphosphate in the activation of protein kinase B. *Science,* 277**,** 567-70.

STRUHL, K. & DAVIS, R. W. (1977) Production of a functional eukaryotic enzyme in Escherichia coli: cloning and expression of the yeast structural gene for imidazole-glycerolphosphate dehydratase (his3). *Proc Natl Acad Sci U S A,* 74**,** 5255-9.

STRUTHERS, M. S., SHANKS, S. G., MACDONALD, C., CARPP, L. N., DROZDOWSKA, A. M., KIOUMOURTZOGLOU, D., FURGASON, M. L., MUNSON, M. & BRYANT, N. J. (2009) Functional homology of mammalian syntaxin 16 and yeast Tlg2p reveals a conserved regulatory mechanism. *J Cell Sci*.

SUTTON, R. B., FASSHAUER, D., JAHN, R. & BRUNGER, A. T. (1998) Crystal structure of a SNARE complex involved in synaptic exocytosis at 2.4 A resolution. *Nature,* 395**,** 347-53.

TANG, B. L., LOW, D. Y., LEE, S. S., TAN, A. E. & HONG, W. (1998) Molecular cloning and localization of human syntaxin 16, a member of the syntaxin family of SNARE proteins. *Biochem Biophys Res Commun,* 242**,** 673-9.

TELLAM, J. T., JAMES, D. E., STEVENS, T. H. & PIPER, R. C. (1997a) Identification of a mammalian Golgi Sec1p-like protein, mVps45. *J Biol Chem,* 272**,** 6187-93.

TELLAM, J. T., MACAULAY, S. L., MCINTOSH, S., HEWISH, D. R., WARD, C. W. & JAMES, D. E. (1997b) Characterization of Munc-18c and syntaxin-4 in 3T3-L1 adipocytes. Putative role in insulin-dependent movement of GLUT-4. *J Biol Chem,* 272**,** 6179-86.

TENGHOLM, A. & MEYER, T. (2002) A PI3-kinase signaling code for insulin-triggered insertion of glucose transporters into the plasma membrane. *Curr Biol,* 12**,** 1871-6.

THROWER, J. S., HOFFMAN, L., RECHSTEINER, M. & PICKART, C. M. (2000) Recognition of the polyubiquitin proteolytic signal. *Embo J,* 19**,** 94-102.

TONG, A. H., LESAGE, G., BADER, G. D., DING, H., XU, H., XIN, X., YOUNG, J., BERRIZ, G. F., BROST, R. L., CHANG, M., CHEN, Y., CHENG, X., CHUA, G., FRIESEN, H., GOLDBERG, D. S., HAYNES, J., HUMPHRIES, C., HE, G., HUSSEIN, S., KE, L., KROGAN, N., LI, Z., LEVINSON, J. N., LU, H., MENARD, P., MUNYANA, C., PARSONS, A. B., RYAN, O., TONIKIAN, R., ROBERTS, T., SDICU, A. M., SHAPIRO, J., SHEIKH, B., SUTER, B., WONG, S. L., ZHANG, L. V., ZHU, H., BURD, C. G., MUNRO, S., SANDER, C., RINE, J., GREENBLATT, J., PETER, M., BRETSCHER, A., BELL, G., ROTH, F. P.,

BROWN, G. W., ANDREWS, B., BUSSEY, H. & BOONE, C. (2004) Global mapping of the yeast genetic interaction network. *Science,* 303**,** 808-13.

TOONEN, R. F., DE VRIES, K. J., ZALM, R., SUDHOF, T. C. & VERHAGE, M. (2005) Munc18-1 stabilizes syntaxin 1, but is not essential for syntaxin 1 targeting and SNARE complex formation. *J Neurochem,* 93**,** 1393-400.

TOONEN, R. F. & VERHAGE, M. (2003) Vesicle trafficking: pleasure and pain from SM genes. *Trends Cell Biol,* 13**,** 177-86.

TRIMBLE, R. B., MALEY, F. & CHU, F. K. (1983) GlycoProtein biosynthesis in yeast. protein conformation affects processing of high mannose oligosaccharides on carboxypeptidase Y and invertase. *J Biol Chem,* 258**,** 2562-7.

TSUI, M. M. & BANFIELD, D. K. (2000) Yeast Golgi SNARE interactions are promiscuous. *J Cell Sci,* 113 (Pt 1)**,** 145-52.

VALDEZ-TAUBAS, J. & PELHAM, H. (2005) Swf1-dependent palmitoylation of the SNARE Tlg1 prevents its ubiquitination and degradation. *Embo J,* 24**,** 2524-32.

VALLS, L. A., HUNTER, C. P., ROTHMAN, J. H. & STEVENS, T. H. (1987) Protein sorting in yeast: the localization determinant of yeast vacuolar carboxypeptidase Y resides in the propeptide. *Cell,* 48**,** 887-97.

VEIT, M., SOLLNER, T. H. & ROTHMAN, J. E. (1996) Multiple palmitoylation of synaptotagmin and the t-SNARE SNAP-25. *FEBS Lett,* 385**,** 119-23.

VERHAGE, M., MAIA, A. S., PLOMP, J. J., BRUSSAARD, A. B., HEEROMA, J. H., VERMEER, H., TOONEN, R. F., HAMMER, R. E., VAN DEN BERG, T. K., MISSLER, M., GEUZE, H. J. & SUDHOF, T. C. (2000) Synaptic assembly of the brain in the absence of neurotransmitter secretion. *Science,* 287**,** 864-9.

VERNET, T., DIGNARD, D. & THOMAS, D. Y. (1987) A family of yeast expression vectors containing the phage f1 intergenic region. *Gene,* 52**,** 225-33.

VIDA, T. A. & EMR, S. D. (1995) A new vital stain for visualizing vacuolar membrane dynamics and endocytosis in yeast. *J Cell Biol,* 128**,** 779-92.

VOLCHUK, A., WANG, Q., EWART, H. S., LIU, Z., HE, L., BENNETT, M. K. & KLIP, A. (1996) Syntaxin 4 in 3T3-L1 adipocytes: regulation by insulin and participation in insulin-dependent glucose transport. *Mol Biol Cell,* 7**,** 1075-82.

VOLDSTEDLUND, M., TRANUM-JENSEN, J. & VINTEN, J. (1993) Quantitation of Na+/K(+)-ATPase and glucose transporter isoforms in rat adipocyte plasma membrane by immunogold labeling. *J Membr Biol,* 136**,** 63-73.

WADA, Y., KITAMOTO, K., KANBE, T., TANAKA, K. & ANRAKU, Y. (1990) The SLP1 gene of Saccharomyces cerevisiae is essential for vacuolar morphogenesis and function. *Mol Cell Biol,* 10**,** 2214-23.

WANG, X., HERR, R. A., CHUA, W. J., LYBARGER, L., WIERTZ, E. J. & HANSEN, T. H. (2007) Ubiquitination of serine, threonine, or lysine residues on the cytoplasmic tail can induce ERAD of MHC-I by viral E3 ligase mK3. *J Cell Biol,* 177**,** 613-24.

WEBB, G. C., HOEDT, M., POOLE, L. J. & JONES, E. W. (1997) Genetic interactions between a pep7 mutation and the PEP12 and VPS45 genes: evidence for a novel SNARE component in transport between the Saccharomyces cerevisiae Golgi complex and endosome. *Genetics,* 147**,** 467-78.

WEBER, T., ZEMELMAN, B. V., MCNEW, J. A., WESTERMANN, B., GMACHL, M., PARLATI, F., SOLLNER, T. H. & ROTHMAN, J. E. (1998) SNAREpins: minimal machinery for membrane fusion. *Cell,* 92**,** 759-72.

WEISSMAN, A. M. (2001) Themes and variations on ubiquitylation. *Nat Rev Mol Cell Biol,* 2**,** 169-78.

WICKNER, W. & HAAS, A. (2000) Yeast homotypic vacuole fusion: a window on organelle trafficking mechanisms. *Annu Rev Biochem,* 69**,** 247-75.

WILLIAMS, A. L., EHM, S., JACOBSON, N. C., XU, D. & HAY, J. C. (2004) rsly1 binding to syntaxin 5 is required for endoplasmic reticulum-to-Golgi transport but does not promote SNARE motif accessibility. *Mol Biol Cell,* 15**,** 162-75.

WILSON, D. W., WILCOX, C. A., FLYNN, G. C., CHEN, E., KUANG, W. J., HENZEL, W. J., BLOCK, M. R., ULLRICH, A. & ROTHMAN, J. E. (1989) A fusion protein required for vesicle-mediated transport in both mammalian cells and yeast. *Nature,* 339**,** 355-9.

WOOLFORD, C. A., DANIELS, L. B., PARK, F. J., JONES, E. W., VAN ARSDELL, J. N. & INNIS, M. A. (1986) The PEP4 gene encodes an aspartyl protease implicated in the posttranslational regulation of Saccharomyces cerevisiae vacuolar hydrolases. *Mol Cell Biol,* 6**,** 2500-10.

YAMAGUCHI, T., DULUBOVA, I., MIN, S. W., CHEN, X., RIZO, J. & SUDHOF, T. C. (2002) Sly1 binds to Golgi and ER syntaxins via a conserved N-terminal peptide motif. *Dev Cell,* 2**,** 295-305.

YANG, B., GONZALEZ, L., JR., PREKERIS, R., STEEGMAIER, M., ADVANI, R. J. & SCHELLER, R. H. (1999) SNARE interactions are not selective. Implications for membrane fusion specificity. *J Biol Chem,* 274**,** 5649-53.

YIK, J. H. & WEIGEL, P. H. (2002) The position of cysteine relative to the transmembrane domain is critical for palmitoylation of H1, the major subunit of the human asialoglycoprotein receptor. *J Biol Chem,* 277**,** 47305-12.

ZERIAL, M. & MCBRIDE, H. (2001) Rab proteins as membrane organizers. *Nat Rev Mol Cell Biol,* 2**,** 107-17.

ZIMMET, P., ALBERTI, K. G. & SHAW, J. (2001) Global and societal implications of the diabetes epidemic. *Nature,* 414**,** 782-7.

ZWILLING, D., CYPIONKA, A., POHL, W. H., FASSHAUER, D., WALLA, P. J., WAHL, M. C. & JAHN, R. (2007) Early endosomal SNAREs form a structurally conserved SNARE complex and fuse liposomes with multiple topologies. *Embo J,* 26**,** 9-18.

Publications

STRUTHERS, M. S., SHANKS, S. G., MACDONALD, C., CARPP, L. N., DROZDOWSKA, A. M., KIOUMOURTZOGLOU, D., FURGASON, M. L., MUNSON, M. & BRYANT, N. J. (2009) Functional homology of mammalian syntaxin 16 and yeast Tlg2p reveals a conserved regulatory mechanism. *J Cell Sci*.

CARPP, L. N., SHANKS, S. G., STRUTHERS, M. S. & BRYANT, N. J. (2007) Cellular levels of the syntaxin Tlg2p are regulated by a single mode of binding to Vps45p. *Biochem Biophys Res Commun,* 363**,** 857-60.